CRANFIELD UNIVERSITY

A. C. STITT

A PHYSICS-BASED MAINTENANCE COST METHODOLOGY FOR COMMERCIAL AIRCRAFT ENGINES

SCHOOL OF AEROSPACE, TRANSPORT AND MANUFACTURING
Propulsion Centre

EngD
Academic Year: 2013–2014

Supervisor: Dr P. Laskaridis and Prof. R. Singh
August 2014

CRANFIELD UNIVERSITY

SCHOOL OF AEROSPACE, TRANSPORT AND MANUFACTURING
Propulsion Centre

EngD

Academic Year: 2013–2014

A. C. STITT

A physics-based maintenance cost methodology for commercial aircraft engines

Supervisor: Dr P. Laskaridis and Prof. R. Singh
August 2014

Executive Summary

A need has been established in industry and academic publications to link an engine's maintenance costs throughout its operational life to its design as well as its operations and operating conditions. The established correlations between engine operation, design and maintenance costs highlight the value of establishing a satisfactory measure of the relative damage due to different operating conditions (operational severity). The methodology developed in this research enables the exploration of the causal, physics-based relationships underlying the statistical correlations in the public domain and identifies areas for further investigation.

This thesis describes a physics-based approach to exploring the interactions, for commercial aircraft, of engine design, operation and through life maintenance costs. Applying the "virtual-workshop" workscoping concept to model engine maintenance throughout the operating life captures the maintenance requirements at each shop visit and the impact of a given shop visit on the timing and requirements for subsequent visits. Comparisons can thus be made between the cost implications of alternative operating regimes, flight profiles and maintenance strategies, taking into account engine design, age, operation and severity.

The workscoping model developed operates within a physics-based methodology developed collaboratively within the research group which encompasses engine performance, lifing and operational severity modelling. The tool-set of coupled models used in this research additionally includes the workscoping maintenance cost model developed and implements a simplified 3D turbine blade geometry, new lifing models and an additional lifing mechanism (Thermo-mechanical fatigue (TMF)).

Case studies presented model the effects of different outside air temperatures, reduced thrust operations (derate), flight durations and maintenance decisions.

The use of operational severity and exhaust gas temperature margin deterioration as physics based cost drivers, while commonly accepted, limit the comparability of the results to other engine-aircraft pairs as the definition of operational severity, its derivation and application vary widely. The use of a single operation severity per mission based on high pressure turbine blade life does not permit the maintenance to vary with the prevalent lifing mechanism type (cyclic / steady state).

Acknowledgements

This work would not have been completed without the help and support received from friends, family and colleagues both near and far. Particularly Panos, Jan and Hari, fellow members of the project team, and our many skilled and enthusiastic MSc students.

Many thanks to my supervisors Dr. Panagiotis Laskaridis and Prof. Riti Singh at Cranfield. Thanks for Dr Peng Ho for continuing to support the project inspired by Naaval Ramdin and to Alan Leclerc for taking on the challenge.

I am extremely grateful to Matt and Clive for being willing to proof read and interpret my ramblings when I couldn't quite get down on paper the thoughts I had mulling at the back of my mind.

I am in debt to the many Cranfield University administrative staff, in the department and the library for their continuing help. Especially Maria, Gill and Nicola. This would all have been so much harder without you.

Keywords

Severity; Lifing; Jet Engine; Aero gas Turbine; Aging; Creep; Fatigue; Oxidation; Thermo-mechanical Fatigue; Cost; Maintenance; Through life; Shop Visit; Workscope; Physics-based; Virtual Workshop; Life Limited Part; Restoration; EGT Margin

Contents

List of Figures

List of Tables

Acronyms

ACQ Acquisition . . . 111
AMT Accelerated Mission Test . . . 50
AROC Airplane Related Operating Cost . . . 96
ATA Air Transport Association of America . . . 110
BC Boundary Condition . . . 183
BOM Bill of Material . . . 111
CAROC Cash Airplane Related Operating Cost . . . 96
CC Conventional Casting . . . 26
CDM Continuum Damage Mechanics . . . 27
CER Cost Estimating Relationship . . . 212
CER Cost Estimating Relationship . . . 212
CFD Computational Fluid Dynamics . . . 66
CROC Cargo Related Operating Cost . . . 96
DISP Disposal . . . 8
DMC Direct Maintenance Cost . . . 209
DMM Design Mission Mix . . . 54
DMTrade Design and Maintenance Trade Study Tool . . . 128
DOC Direct Operating Cost . . . 96
DS Directional Solidification . . . 26
EB-PVD Electron-Beam Physical Vapour Deposition . . . 38
EFH Engine Flight Hour . . . 98
EGT Exhaust Gas Temperature . . . 208
EGTM Exhaust Gas Temperature Margin . . . 240

EMCWG Engine Maintenance Cost Working Group 242
ENSIP Engine Structural Integrity Program 61
EROC Engine Related Operating Cost 96
FC Flight Cycle 242
FE Finite Element 209
FH Flying Hours 242
FL Flight Length 182
FOD Foreign Object Damage 103
GB Grain Boundary 26
HCF High Cycle Fatigue 67
HPC High Pressure Compressor 212
HPT High Pressure Turbine 209
LCC Life Cycle Cost 109
LCF Low Cycle Fatigue 66
LLP Life Limited Part 253
LMP Larson Miller Parameter 27
LPC Low Pressure Compressor 147
LPT Low Pressure Turbine 253
LTFC Life to First Crack 63
LTO Landing and Take-Off 31
MRO Maintenance, Repair and Overhaul 95
MTBF Mean (operating) Time Between Failures 62
MTBR Mean Time Between Removals 129
MTBSV Mean Time Between Shop Visits 99
NASA National Aeronautics and Space Administration 110
NDT Non Destructive Testing 58
NFF No Fault Found 114
NGV Nozzle Guide Vane 80
NPV Net Present Value 98
OAT Outside Air Temperature 256
OCM On Condition Maintenance 103
OEM Original Equipment Manufacturer 94

Chapter 1

Introduction

1.1 Research aims and objectives

Aim Develop a physics-based engine related maintenance costs methodology for commercial aircraft/engine combinations using only public domain information.

Objectives

1. Review public domain cost models, assess their sensitivity to operational and technological variables. Identify and assess the relative importance of significant physics-based cost drivers.

2. Develop and implement maintenance work-scope and cost methodology.

3. Develop and implement tool kit functionality to better capture damage mechanisms and facilitate use of methodology for newer technologies, e.g implementation of Thermo-mechanical fatigue (TMF) to better account for lifing of single crystal super alloy turbine blades.

4. Investigate the relationship between operational decisions and engine related operational costs for commercial aircraft, and the impact of planning decisions on maintenance costs.

1.2 Contribution and Novelty

The novelty and contribution of this research comes from the derivation of engine related operating costs from first principles using physics-based modelling of engine operational performance and life. This removes the dependency of cost modelling on large commercially sensitive, and airline, airframe dependent databases of cost and operation.

The key challenge inherent in this research is the necessity to bridge multiple technical disciplines in order to link engine design choices and operational decision with through life maintenance costs. These include aircraft and engine performance, lifing mechanism modelling, Finite Element (FE) modelling, engine maintenance and operational costs.

At each step of the multidisciplinary methodology developed a balance has been sought between physics-based constituent of a model and the number of variables required, which may, if unavailable have to estimated or assumed. Given a choice, a preference is made for models which reflect the physical reality of the situation best. However, this option is sometimes not available, when models considered are either not reproducible using public domain inputs, or an unreasonably large number of assumptions would have to be made for variables and inputs which would not usually be available at the conceptual design stage of engine development.

The purpose of the methodology developed is two-fold. To further the un-

derstanding of the effect of engine design and operation on costs, through the development of cost trends due to design, operation(cockpit) and planning decisions. To provide a methodology, which uses only public domain data, and which uses physics-based modelling, for the verification of regressive big data tools.

Novelties, inherent in this research, include: the use of engine and aircraft performance modelling to generate the cost driver inputs to maintenance and cost model, and further development of lifing tools implementing simplified yet representative geometries for High Pressure Turbine (HPT) blades, enabling the study of multiple failure mechanisms, for the purpose of a physics driven “virtual workshop” cost model.

The aim of this research, to the sponsor, was to develop and provide an independent physics-based methodology and constituent models, based only on public domain data which would be used to validate an in-house, commercial data driven model. As a result this methodology has been developed independently and isolated from that commercial model. This requirement has led to one of the key constraints on this research programme, which has, as a result been obliged to prioritise physics-based models and use only public domain data.

Tools such as this one, are important at the technical sales stages for large scale engineering equipment, such as gas turbines, with extended operational lives. Purchase decisions for such systems are no longer based primarily on acquisition cost, but increasingly through life operation costs form a more important part of the decision making process. In this context, potential clients are not interested in how much a system would nominally cost to operate (under design or ideal conditions), but instead, they are focused on how much it will cost them to operate it given their expected operational regime and resulting constraints.

As such the methodology to be developed could conceivably be used by the

purchaser to benchmark potential systems that they are considering purchasing. It could also be used by the manufacturer to demonstrate or support predicted operational cost forecasts.

While the purchase decision is an obvious point for operational cost forecasts, increasingly, the lease market for engines and aircraft mean that this is also assessed continuously through the life of a lease component, at each successive lease agreement negotiation.

1.3 Thesis structure

This thesis is structured so as to address thematically the topics considered and addressed within the project. The multidisciplinary project described attempts at all stages to balance the desire of the researcher to model accurately the phenomena concerned and the need to rely solely on public domain information set out in the research specification.

This first introductory chapter has introduced the aims and objectives of this project and its contribution. The subsequent chapters in turn address:

Chapter 2. Presents a summary of background literature addressing and describing the need for this research and its scope, in the context of the research programme history and context within a larger sponsored project. The methodology developed is introduced in outline form describing the framework linking engine design and performance to operational maintenance costs within which the rest of the thesis develops.

Chapter 3. Introduces the concept of lifing and its application in gas turbines as a key link between engine operation, component failure and maintenance cost. Key lifing mechanisms are considered and presented along with selected lifing models.

Chapter 4. The concept of Operational Severity (S) as a relative measure of operational damage is introduced. A summary of current literature on severity is reviewed. The important link between Operational Severity and physics-based lifing methods is explored, and the methodology linking engine performance to operational severity is developed in more detail.

Chapter 5. Presents a brief summary of literature on engine related operating costs, introduces common cost classifications and considers their respective applicability to a physics-based methodology. Reviews available public domain engine maintenance models and their sensitivity to operational parameters. Outlines the key physics-based cost drivers, including Operational Severity, engine aging and maturity.

Chapter 6. Introduces the workscoping methodology developed in this research to link engine operation and gas turbine performance to through life engine maintenance cost in operation. The model developed is presented conceptually, then the method functionality is described in more detail. Key verification cases are presented which apply the workscoping model developed to standalone simplified cost cases.

Chapter 7. Develops on the overall methodology first introduced in section 2.2, including the models selected and choices made in the intervening chapters. This chapter demonstrates the modular nature of the methodology developed, the choices made in this project and the scope to use different models within the methodology.

Chapter 8. Presents case studies reflecting the capabilities and scope of the methodology as a tool for understanding the effect of operating and management decisions on engine maintenance costs, for a selection of applications.

Chapter 9. Considers the scope and applications of the methodology developed in relation to the initial goals. Considers the opportunities for further development and presents a descriptive summary of the project. Developed conclusions thematically and proposes opportunities for further work and development.

Chapter 2

Background and Method Outline

This chapter will address the need for the research, the background to the research project and introduce in outline the methodology developed and followed.

2.1 Background

The commercial airline industry operates primarily in a high cash flow, low margin market. Financial tools and methods employed within the industry have developed to better meet its demands.

As airlines have moved from primarily state owned and operated flag-carrying high cost operations towards an open competitive market, other aspects of the business have also changed and adapted. There has been movement away from the operator also being the equipment owner, and maintainer, toward significant roles for financiers in an active leasing environment. Outsourcing has become widespread, particularly in Maintenance, Repair and Overhaul (MRO) services, and some products previously considered capital investments have been developed into a “servitized” offering, including propulsion.

In this environment, the fine control of day to day costs has become significant, with some commentators [19] considering that Specific Fuel Consumption (SFC), weight and noise will no longer be the key market drivers for commercial aircraft operators, but that, instead, through-life cost of ownership will be the leading driver of aircraft selection. Commercial aircraft, SFC, weight, noise and through life operating costs are in great part driven by the engine, its operation and maintenance but also its design. Roskam [1] considers four broad phases in the life cycle: Research, development, test and evaluation (RDTE), Acquisition (ACQ), Operation (OPS) and Disposal (DISP), and declares that the following hierarchy of costs exists between them:

$$C_{OPS} \gg C_{ACQ} \gg C_{RTDE}$$

.

Operational costs are considered within the framework of the system life cycle. It is commonly asserted that the Pareto Principle applies here, such that 80% of the costs are fixed during the first 20% of the life cycle. The numbers in the “80:20” rule must be considered arbitrary, with quoted ranges of 70-80% [20], but the message that significant costs are determined early in planning and conceptual design is significant and illustrated in Figure 2.1 [1]. Operational costs can not only be affected by decisions made years before operation, but they are also financially significant, accounting for between 70%to 85% [20, 21, 22, 23] of total Life Cycle Cost (LCC).

While acquisition costs are important, their impact on the airline industry has changed. No longer do governments invest capital in their flag-carrying airlines. Increasingly operators lease aircraft, so spreading the acquisition cost can be-

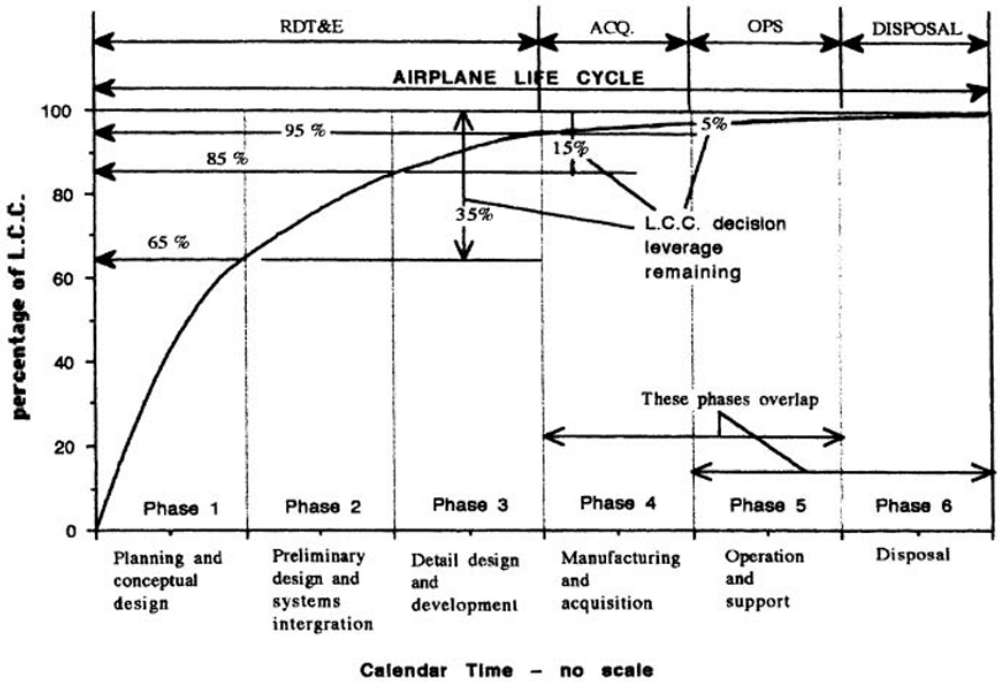

Figure 2.1: Roskam's [1] schematic relating programme phase and life-cycle cost

come spread over the usable life of the aircraft and its engines. Such leasing and financing agreements also mean that the cost of a new aircraft and engines to an operator is dependent on the airline's credit history, cash flow, and capital position as well as on the financier's best guess at the airlines' future profitability and risk, and not just the cost or the value of the aircraft and engines purchased.

Operating costs are significant in the assessment of LCC, as they are directly related to design and operation, and as such can be reduced through good design and decision making. Significant through life operating costs for airlines include fuel, crew, fees, taxes, maintenance, passenger handling and back office overheads. Of these, fuel, maintenance and fees can all be related to engine operation and design.

These engine-related costs can be significantly influenced by market trends and changes. It is unreasonable to expect to predict these costs accurately at

the early stages of RDTE, which might be up to 20 years before operation in the case of new engine systems. It is reasonable, however, to expect trends in costs related to the physics of the engine design and operational choices to remain valid and significant.

Significant work was conducted by the military in the 1980s, to both understand the cause for significantly increased rates of Unplanned Engine Removal (UER) events in their engine fleets, and to determine accurately the relationships between design choices and operational costs. The increased rates of UERs were attributed to the significant difference between actual engine operation and the engine design missions on which the Accelerated Mission Tests (AMTs) used for certification had been based.

Severity (S) was developed as a measure to compare the effect of missions on engine damage [6], and was subsequently applied to component redesign to increase usable life [24]. The history and development of severity models is discussed further in chapter 4. The severity models developed were integrated in to an LCC approach [25, 26], which was used successfully to demonstrate that considering LCC at the component design stage could enable the trade-off of “higher initial component costs for lower maintenance overhaul costs (greater durability)” [27] and facilitate a more cost effective engine development process [28].

While these studies identified the need to link operating costs, and in particular maintenance demand and cost, to engine design and operation, they relied on historic cost data bases and empirical relationships to drive the operational severity calculations.

In this research, the link between design, operation and cost, is to be physics-based, relying solely on public domain data, with the aim of developing a method-

ology to determine the trend relationships involved, for the two-fold purpose of understanding the relationships, and validating a commercial, database dependent model of engine maintenance costs.

This has lead to the development in this research of the “virtual workshop” or work-scoping model, which first establishes the maintenance need driven by the selected engine operation, by integrating a physics-based severity calculation, and then calculates the resulting costs throughout the engine’s operational life.

2.2 Project history and method outline

This project is part of a larger research program whose goal is to develop a tool kit capable of assessing the relative technical and economic performance of different aircraft/engine combinations through implementation of the following key elements:

- Aircraft Model
- Gas Turbine Transient Model
- Life Consumption Estimator
- Maintenance Cost Estimator

Phase one of this research was conducted by two PhD students [18, 29] and several MSc students. Phase one resulted in the development of a lifing, severity and aging tool linked with an engine and aircraft performance tool capable of transient modelling represented schematically in Figure 2.2.

Phase two is, like phase one split primarily between two doctoral students responsible for planning and conducting research including several cooperative

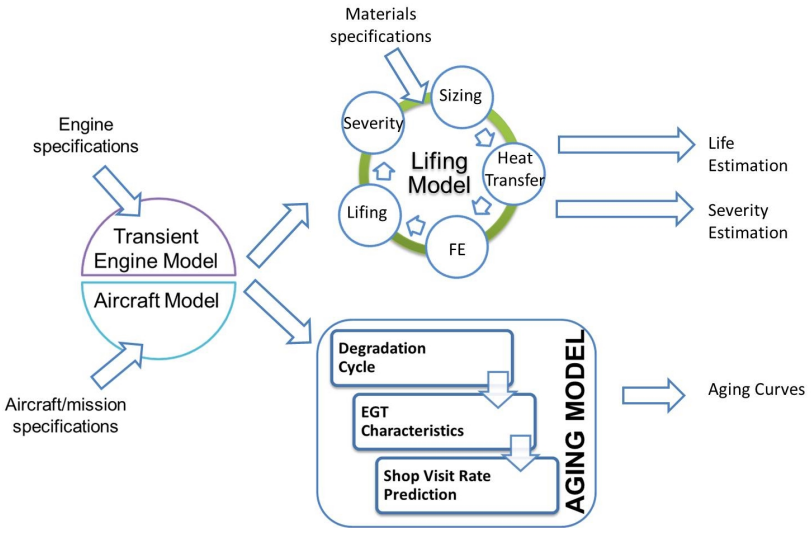

Figure 2.2: Schematic of phase one modelling tools

studies conducted with MSc students. The following elements form the core of the Phase two work:

- Improved Aircraft Model with novel engine capability
- Maintenance Cost Estimator

Expanding the engine and aircraft modelling capability to include the capacity to model novel technologies, represented schematically in Figure 2.3. This was conducted by Panos Giannakakis including collaboration with MSc students and is summarised in his thesis [30].

This research project encompasses the second phase-two component. It has at its core the development of a maintenance cost estimator, but also includes the further development of the lifing model tools developed in phase-one, including the implementation of a different simplified three dimensional geometry, new lifing models and new lifing mechanisms (Thermo-mechanical fatigue (TMF)). It is presented schematically in context with the other work involved in this research

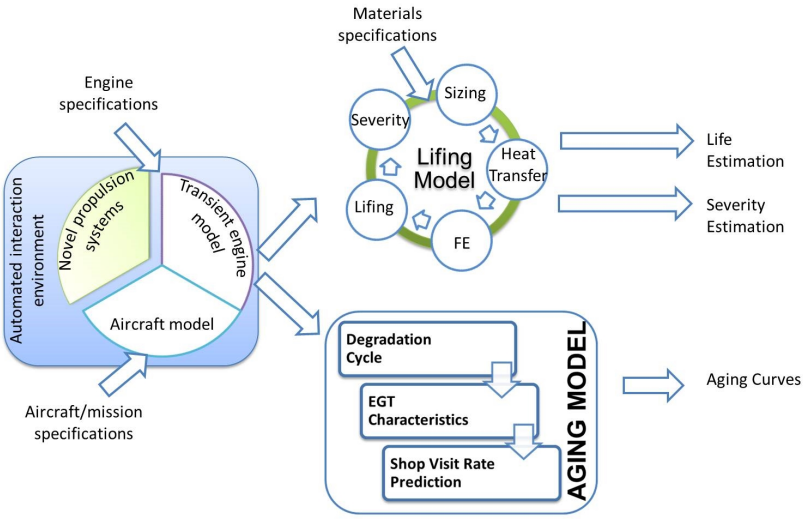

Figure 2.3: Expanded novel engine technology capability

program in Figure 2.4. This multi disciplinary research project would not have been feasible without the collaborative effort involved in work conducted with multiple MSc students and other doctoral researchers.

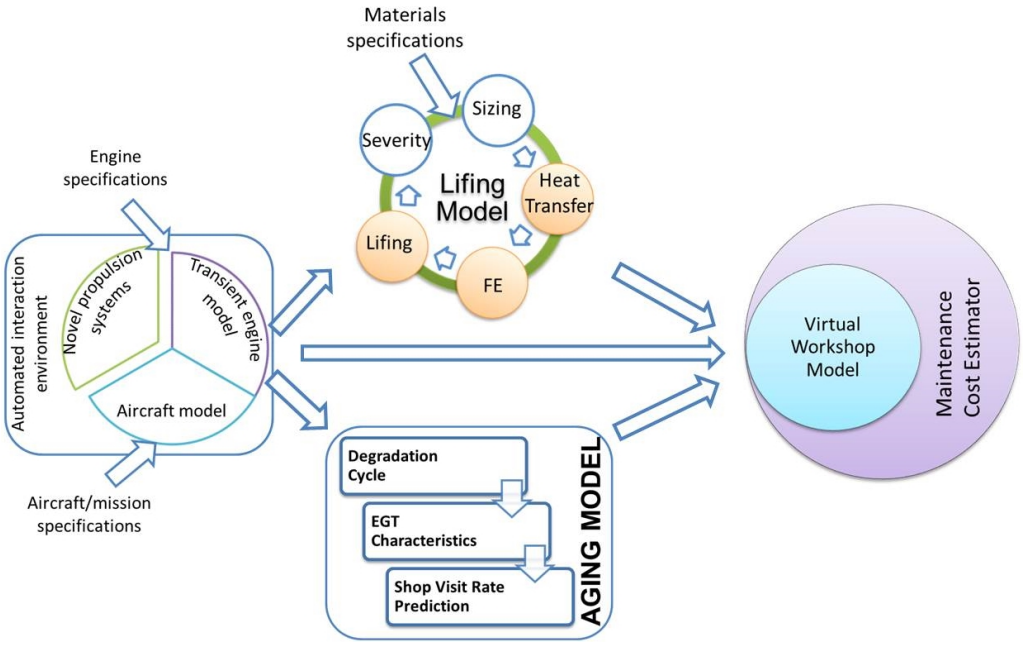

Figure 2.4: Research project in context

The handover period between doctoral students responsible for phases one and two, included a number of case studies demonstrating the tool-set capabilities as well as two co-authored publications.

Research Report [16] investigating the effects of mission profile and engine rating strategy on fuel and life consumption.

A.C. Stitt, P. Giannakakis, and P. Laskaridis. The effect of mission profile and rating strategies on the fuel and life consumption of commercial aircraft engines. Technical report, Department of Power and Propulsion, Cranfield University, Dec. 2009.

Paper [7] reporting the final configuration of the phase one tool set.

H. Hanumanthan, A. Stitt, P. Laskaridis, and R. Singh. Severity estimation and effect of operational parameters for civil aircraft jet engines. Proceedings of the Institution of Mechanical Engineers, Part G: Journal of Aerospace Engineering*, 226(12):1544–1561, 2012.*

The methodology developed in this project, extends and improves that developed during phase one. The result is a large tool-set of coupled models following broadly the format developed by Hanumanthan and Janikovic. An overview of the tools used is presented in Figure 2.5.

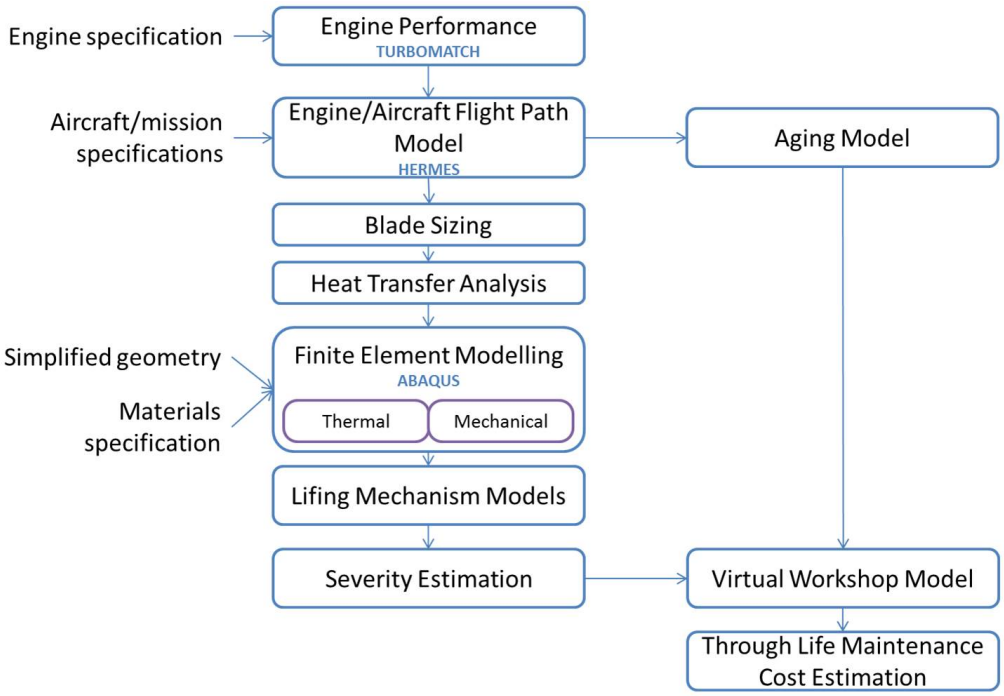

Figure 2.5: Overview methodology and tools

Chapter 3

Life estimation

3.1 Fundamentals

Hot section gas turbine components operate in a hostile gaseous environment under high and oscillating temperatures and loads. In these difficult conditions many mechanisms contribute to wear and damage. While mechanisms can be considered separately it has been established that mechanisms also frequently interact. This highly loaded high temperature environment restricts hot section component lives. Progress in material development and component design (including cooling) has progressively increased the available life of hot section components and increased possible operating temperatures. Under these loading conditions several damage mechanisms are considered relevant including creep, fatigue and oxidation. Some authors would also consider erosion, fretting and wear in the list of failure mechanisms [31], whereas, to others [32], oxidation, corrosion, erosion, fouling and abrasion are instead defined as degradation mechanisms as they tend to affect surface roughness and geometry, including clearances, of flow path components, thus degrading the component performance. Components subject

to high temperature operations, such as high pressure turbine blades, can be subject to several of these mechanisms interacting to reduce life. Schematically, the relation between the mechanisms and the overall component life envelope can be considered, as shown in Figure 3.1. While this sketch assumes that the mechanisms act independently, it is clear that at high temperatures failure could be indicative of multiple relevant modes and possible interactions.

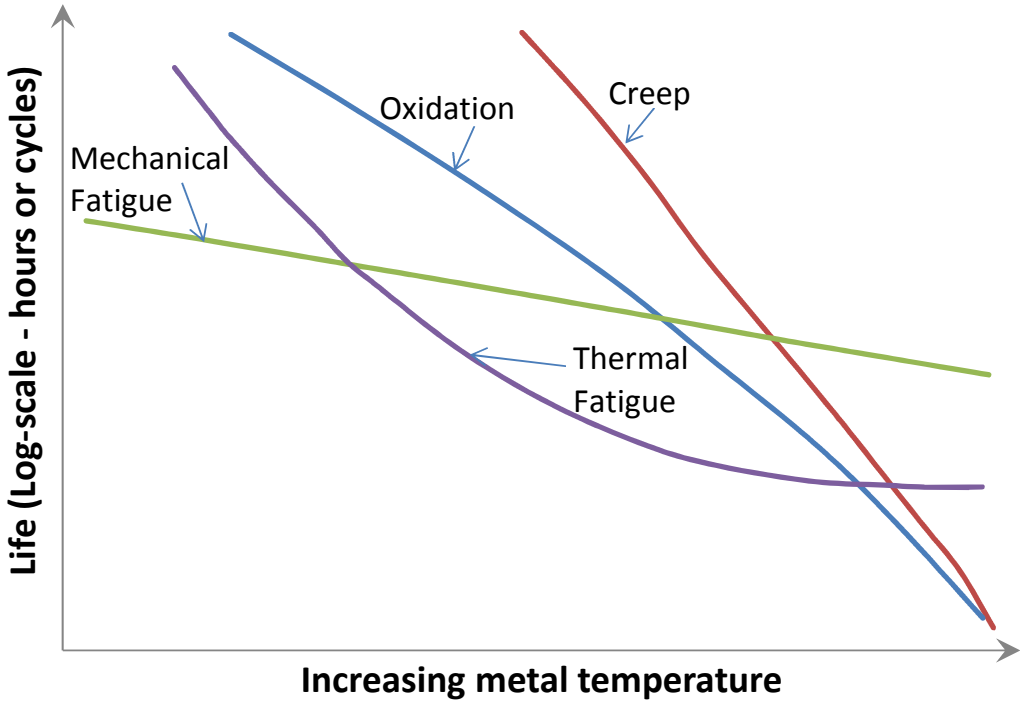

Figure 3.1: Schematic available life envelope for HPT components adapted from [2]

3.2 Approaches

Lifing models are developed to predict failure of materials due to specific mechanisms caused by defined loading profiles. The best models are validated against experimental or operational data. Experimental test data, using validated test-

ing techniques, is frequently for material billets or samples of predefined shape, which may not be representative of in-service components.

The scatter of materials failure data leads to a preference for use of large sample numbers in testing, although, this in turn limits the use of expensive full system or component tests.

Much research into lifing is conducted by materials scientists involved with material or manufacturing process developments. Engineers, both design, and maintenance focused are also interested in failure prediction.

Two groups of lifing models can therefore be distinguished: those which consider the observable effect of a damage mechanism (including material loss, geometry change or rupture) and those concerned with the micro structural changes occurring within the material causing these observable effects (including cavitation, dislocation motion, nucleation and growth of voids or crystal structure realignment). These two groups will be referred to as phenomenological [31], more common in engineering applications, and micro-mechanical, more common in materials science, respectively [33].

In the following sections each of the lifing mechanism considered relevant to Low Pressure Turbine (LPT) blade applications (creep, Low Cycle Fatigue (LCF), oxidation and TMF) will be considered in turn, including a brief review of models available.

3.3 Mechanisms

3.3.1 Creep

Introduction

Creep The time-dependent permanent deformation that occurs under stress; for most materials it is important only at elevated temperatures. [3]

Creep becomes a significant lifing mechanism at elevated temperatures. Specification of elevated temperature vary depending on material composition and manufacture: $T > 0.4T_m$ [3], $T > 0.45T_m$ [34], $T > 0.5T_m$ [31], however it is evidently important for most hot section gas turbine components. According to [10, p. 392], the components in a gas turbine engine most liable to creep are: shafts, combustor and hot section (turbine) disks and blades.

Loading of a constrained body causes displacements within the material due to strain. When these induce dimensional changes to the component, failure due to brittle fracture can ensue [34]. Phenomenological laws of creep are derived which relate creep strain rate ($\dot{\varepsilon}$) to stress (σ), temperature (T), time(t), accumulated creep strain (ε) and internal material structure (s), such that $\dot{\varepsilon} = f(\sigma, T, s, t, \varepsilon)$.

In High Pressure Turbine (HPT) applications, blade deformation in extension under creep conditions might lead to contact with the turbine casing, causing significant damage to the turbine and casing. Increasing blade tip gaps to account for blade deformation under creep would significantly reduce turbine efficiency due to tip gap losses. The development of creep resistant materials has been essential to this high temperature application. In parallel, many gas turbines have abradable materials fitted in the casing to further reduce in service tip gaps and resulting losses.

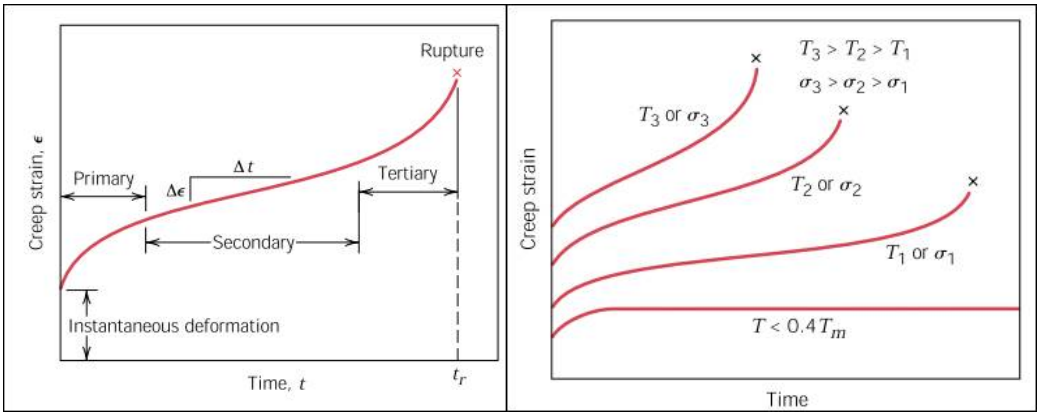

(a) Phases of Creep

(b) Effect of temperature and stress on creep curve

Figure 3.2: Schematic creep behaviour [3]

Review

Creep is considered to be a multi-stage mechanism, with each stage characterised by its strain rate and scematically represented in Figure 3.2.a.

Primary phase is considered as transient, sees increasing strain hardening resulting in a reducing creep rate

Secondary phase, also referred to as steady state creep, is characterised by a constant creep rate as strain hardening and recovery balance

Tertiary phase is characterised by an increasing strain rate to rupture

Though creep is stress dependent (Figure 3.2.2), sufficient thermal activation energy must also be present. Below approximately $0.4T_m$ creep does not develop beyond a secondary phase characterised by constant creep strain and null creep rate into a tertiary phase. The standard creep curve, is represented in Figure 3.2.b by the T_1 or σ_1 curve, in this schematic, the T_3 or σ_3 curve exhibits a

very short secondary phase. For some materials the secondary phase may be insignificant .

Frost and Ashby [4] consider creep to be either diffusional or dislocational because of the mechanisms within the material which are driving and controlling the creep rate: flow of vacancies by diffusion or the movement of disclocation by glide or climb.

Methods and models describing creep consider principally the type of creep and the mechanism or parameters which limit the associated creep strain rate ($\dot{\varepsilon}$).

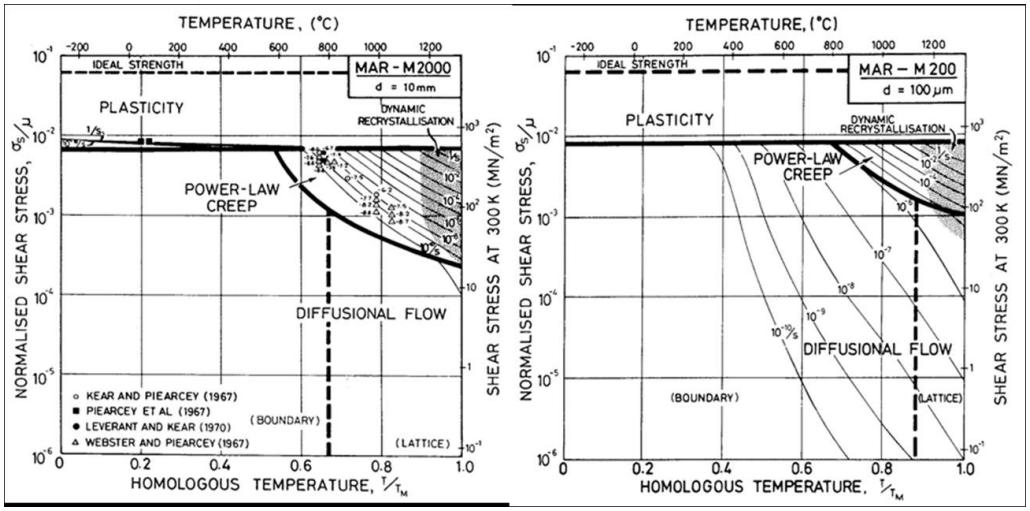

Figure 3.3: Effect of grain size on Ni-based super alloy according to Ashby [4]

Creep mechanism and rate vary depending on the crystal structure of the component, temperature and load, such that for a given material and grain size: stress-temperature deformation maps can be generated. Failure, or creep rupture generally finally occurs due to metallurgical changes in the material[1] which result in a reducing effective cross-sectional area and an exponentially increasing strain rate. Comparing two Ashby deformation maps for the same material (MAR-M200) as in Figure 3.3 shows the expected effect of grain size change, such that

[1] including crack, cavity and void formation, necking or grain boundary separation

reducing grain size would increase the envelope in which power law and lattice diffusion creep was relevant.

Creep-rupture (or strain-temperature) tests are conducted under either constant-load (Isostress) or constant strain conditions. Generally 2-D specimens are used including cruciform, thin walled tubes and notched bars [34, 35]. These inform the generation of log strain-temperature based deformation maps.

The strain hardening in polycrystalline materials during primary phase creep is evidence of dislocation strain field interactions aggravated by the formation of new dislocations. In this process ductile metals trade strength for ductility. Increasing dislocation density and the repulsive nature of dislocation strain interaction leads to increased load required for deformation, hence material strengthening.

Recovery during secondary phase creep is characterised by a reduction in the internal strain built up during strain hardening, due to a reduction in dislocation density or the re-configuration of dislocations.

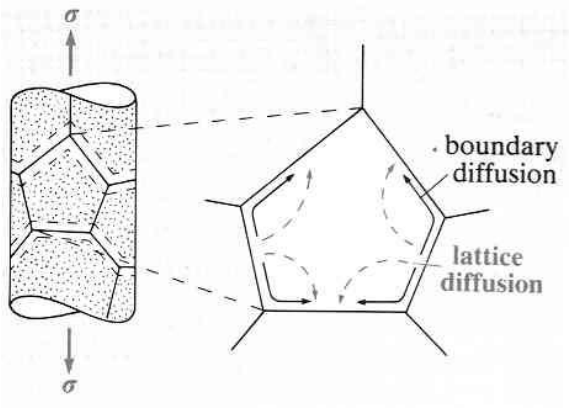

Figure 3.4: Schematic representation of diffusional creep types adapted from [4]

Diffusion in creep can be considered as either the migration of vacancies (“a normally occupied lattice site from which an atom or ion is missing” [3]) or the transfer of mass [36]. Both are interchangeable as, for the motion to be possible

a vacancy must be adjacent to an atom (or ion) with sufficient energy (activation energy) to break existing bonds and distort the lattice [3]. Diffusion can also be interstitial such that the migration is between interstitial sites rather than vacancies. Diffusion creep is significant at low stress and in the presence of small grains, atoms diffuse from lateral grain boundaries to transverse grain boundaries thus elongating the grains in the direction of the applied stress. Diffusion can be either through the grains (variously called: diffusion, lattice diffusion and Nabarro-Herring creep) where many paths exist but the rate of creep is reduced, or along the grain boundaries (grain boundary diffusion, cobble creep) where increased creep rates are possible in the presence of small grains, these are identifyable in Figure 3.4. Diffusional creep, which tends to be characterised by strain rates with a linear stress relationship ($\dot{\varepsilon} \propto \sigma$) is limited by lattice diffusion at high temperatures and grain boundary diffusion at lower temperatures.

At higher stresses, dislocation motion becomes more significant than diffusion. Harper-Dorn Creep, is characterised by strain rates proportional to stress and independent of grain size, though approximately a thousand times faster than diffusion creep [36]. As stresses increase further (above Peierls Stress) creep tends to Power-law creep ($\dot{\varepsilon} = \dot{\varepsilon}_0.\sigma_e^n$) characterised by rapid extension then decreasing creep rates.

Nabarro classes both diffusion creep mechanisms and Harper-Dorn creep as constant rate creep mechanisms. Under power law creep regimes creep strain is characterised by Andrade term ($\beta.t^{(\frac{1}{3})}$) and a logarithmic term ($\ln(1+t\tau)$) as the material becomes subject to work hardening, exhaustion and phase transitions. Steady state creep would only be maintained in situations where dislocation multiplication and annihilation were in balance.

Materials developments can change the mechanisms of creep and their respective relations. In materials with solid solutions, the diffusion coefficients of the solutes (D_s) must be considered ($\dot{\varepsilon} \propto D_s\sigma^3$), whereas for precipitation hardened materials the resulting resistance to dislocation motion (σ_0) also becomes relevant ($\dot{\varepsilon} \propto D_s(\sigma - \sigma_0)$) [36].

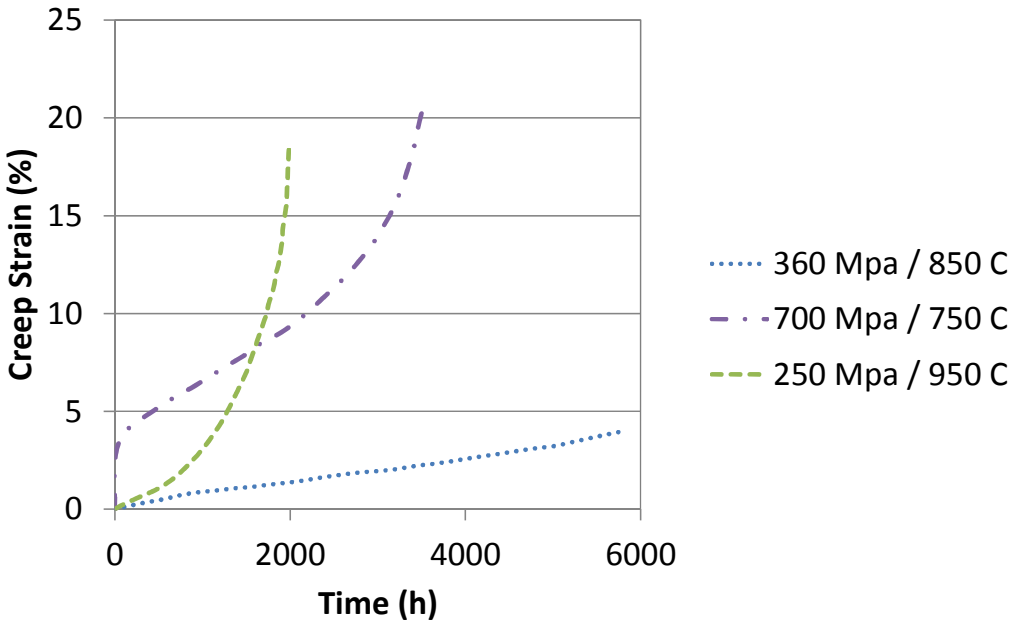

Figure 3.5: Typical Ni-base superalloy creep curves adapted from McLean [5]

The key driver of material development for creep resistance has been the reduction of operational and maintenance costs of components subject to creep through the extension of inspection intervals and reduction of inspection costs [35]. Since the 1960s, materials development in HPT materials have been driven by the desire to operate at increasing gas temperatures to improve engine efficiency, with some authors considering temperatures approaching $0.8T_m$ [5]. Nickel based super-alloys are the common choice for gas turbine HPT applications, but even within this group of materials there has been significant development. Early developments in cast and wrought alloys produced creep resistant materials due

to the addition of an inter-metallic γ‘ phase, but were limited in creep ductility. The development of Directional Solidification (DS) alloys with with columnar grains to reduce transverse Grain Boundarys (GBs) in the 1960s provided components with significantly improved ductility $(25-30\%)$ for materials that were brittle after Conventional Casting (CC). The alignment of the crystal structure with the component loading direction also reduced thermal stresses in blades [5]. The growth of Single Crystals (SCs) using these nickel based alloys during the 1980s provided scanty improvement over DS components, however, int he 1980s alloys were developed specifically for SC applications. The specially formulated second and third generation SC alloys demonstrate interesting creep performance as seen in Figure 3.5, including a direct transition from primary to tertiary creep without a (secondary) steady state creep phase. For these SC alloys, creep is important above a homologous temperature of $T/T_m = 0.07$ [37]. According to McLean [5] they also do not conform to the power law equation, indicating that creep deformation in SC alloys is not controlled by recovery, but rather by rate kinetics which are considered consistent with dislocation movement through γ phase. Anisotropic effects are also significant in SC super-alloys. Kassner and Perez-Prado [38] identify the key mechanisms in high temperature creep of SC to be the formation of dislocation networks at the γ/γ' interfaces and subsequent rafting which “ continue[s] even after the external stress is removed” at an apparently unchanged rafting rate [38].

Modelling

Micro-mechanical models of creep are widespread and focus on a specific creep mechanism, they are therefore limited int heir applicability to a specific region

of the deformation map and material. Many specific models exist, Kassner and Perez-Prado [38] review and categorise nearly 900 models. Many of these models, given their specific focus on a single creep mechanism, could be included in a Continuum Damage Mechanics (CDM) framework or micro-mechanical approach, such as that described by Dyson [39] who contrasts this “metalurgy trained researcher” approach, to those “phenomenological” or “empirical” models common in engineering.

Dyson summarises the application of CDM by considering creep damage to be either strain induced, thermally induced or environmentally induced, and due to one or a combination of eight creep mechanisms. CDM has been applied severally as an empirical approach and a physics-based approach, more recently also coupled increasingly with Finite Element (FE) analysis tools. The creep mechanisms considered by Dyson include: cavity nucleation and growth, GB cavitation, dynamic sub-grain coarsening, mobile dislocation multiplication, particle coarsening, solid solution element depletion, internal oxidation and the cracking of products of surface corrosion, though the method is extendible to further mechanisms when appropriately defined.

The phenomenological approach, describing creep in terms of observable phenomenon, and predicting it based on operational parameters using empirically derived formula, has been the common approach in engineering. These methods are primarily log-linear and consider stress, temperature and time to derive strain and time at rupture.

The Larson Miller Parameter (LMP) is the most commonly used parametric method. It uses short term test data to predict service lives, and is sometimes referred to as an Accelerated Mission Test (AMT) method. LMP derivation assumes that the minimum creep rate ($\dot{\varepsilon}_m$) is proportional to a stress dependent

activation energy (A_1) defined by an Arrhenius equation (Equation 3.1), and inversely proportional to a second activation energy (A_2) related to rupture life (t_r)(Equation 3.2).

$$\dot{\varepsilon_m} = A_1 \exp -\frac{f(\sigma)}{T} \tag{3.1}$$

$$\dot{\varepsilon_m} = \frac{t_r}{A_2} \tag{3.2}$$

The resulting LMP is defined as:

$$P_{L-M} = T(C_{L-M} + \log t_r) \tag{3.3}$$

where,

$$C_{L-M} = \log\left(\frac{A_1}{A_2}\right) \quad \text{and} \quad P_{L-M} = \frac{f(\sigma)}{2.303} \tag{3.4}$$

Larson and Miller assumed C_{L-M} to be a constant independent of material and "satisfactory for all alloys considered" [40], though even in the discussion published with their 1952 paper, peer reviewers questioned the applicability of this constant at high temperatures and in high Cr content alloys. This assumption has not persisted and C_{L-M} is now considered material dependent, though it may appear constant for a limited range of materials, as A_2 is related to fracture strain, and A_1 is considered a kinetic parameter [39]. Dyson [39], considers LMP model as derived from CDM and notes that the following assumptions (restrictions) are applied to the alloy behaviours considered: particles do not age, only constant ductility behaviour is considered and primary creep is saturated such that essentially, "any damage mechanism [...] cannot be allowed to evolve", though Dyson notes that test data uncertainty is likely to have a greater impact on the reliability

of LMP than the degree of damage evolution. LMP is commonly presented as straight line plots on a $\log t_r$ vs. $1/T$ where the y-axis intercept represents C_{L-M} and the gradient of the plot, the LMP (P_{L-M}).

Other common log-linear parametric approaches to creep characterisation, sometimes referred to a Time -Temperature Parameter (TTP), include:Orr-Sherby-Dorn, Goldhoff-Sherby, Manson Haferd and Manson Succoup [41].

Other approaches include empirical models, where test data are used to refine a generalised solution, so as to limit the number of coefficients and constants required such as the Harrison modification [42] to the Graham and Walles method for total creep strain (ε), considered "useful" by some authors [37] over a wide range of temperatures (T) and stresses (σ):

$$\varepsilon = \Sigma C \sigma^{\beta} t^{\kappa} e^{Q/RT} \tag{3.5}$$

This study has established that while a multitude of creep models are available, selecting one for a modelling application is fraught with risks. As such a methodology for selecting a furhter creep model to supplement the Lifing models chapter 3 has been developed and is represented graphically in Figure 3.6. This process requires that the model be selected so as to confirm with both the material and the application. In the case of gas turbine blades the plan is to overlay the loads experienced by the components throughout the mission (generated by Turbomatch and Hermes) onto an Ashby [4] deformation map to identify which mechanisms of creep should be present. By identifying the mechanism of creep prevalent in the application methods can be selected based on criteria associated with implementation.

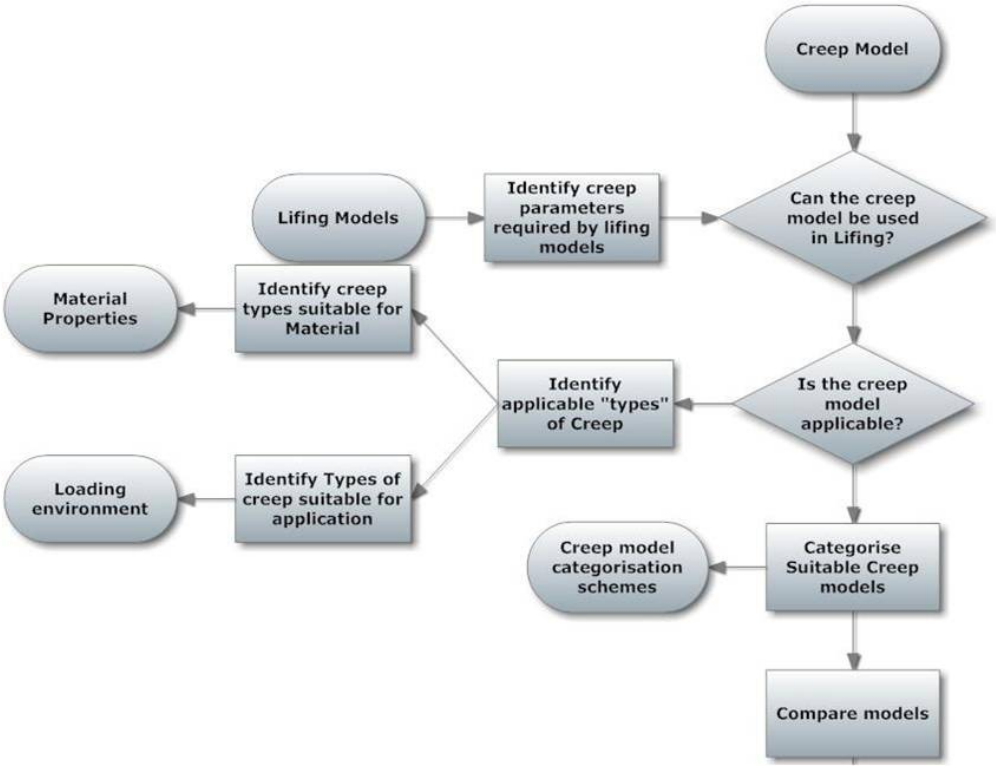

Figure 3.6: Creep method selection flow diagram

3.3.2 Fatigue

Introduction

Fatigue is a failure mechanism of great importance to all applications which contain a source of unsteady loading. Under fatigue, failure can occur much earlier and at a significantly reduced load, than would be expected under steady load conditions.

Three stages of fatigue are identified and distinguished:

1. crack initiation (or nucleation)

2. crack growth (or propagation)

3. fracture (or brittle rupture)

A component's fatigue limit is very dependent on the specifics of the load conditions, and load cycle definition, but fatigue is also influenced by the speed at which cracks can initiate or nucleate, and therefore all sources that create or induce stress concentrators are of importance in fatigue, including but not limited to surface finishing and roughness, the presence of machined holes and corner radii in the geometry of the part.

Three types of fatigue are widely acknowledged:

1. Low Cycle Fatigue (LCF)

2. High Cycle Fatigue (HCF)

3. Thermo-mechanical fatigue (TMF)

The distinction between low and high cycle fatigue is often set at 10^4 cycles, however this division can vary by application. HCF occurs at lower stress but higher load frequencies than LCF. Gas turbine components are subject to significant cyclic loading, both thermally and mechanically, while the thermal and mechanical load cycles are not always aligned, and can act "out of phase" further increasing shear stresses and strain within components. While both HCF and LCF are very important in gas turbine applications, HCF which is associated with resonant loading states is usually designed out as HCF failure tends to be abrupt (90% crack initiation and 10% crack growth) and sometimes catastrophic, and is therefore less common as an in service failure mechanism than LCF (10% crack initiation and 90% crack growth) . LCF in gas turbines is often considered in reference to flight cycles or Landing and Take-Off (LTO) cycles, but thermal cycles (of which there may be several in each LTO cycle) must not be neglected.

Many Life Limited Parts (LLPs) are subject to LCF related hard life limits determined through modelling and testing.

The third form of fatigue, TMF captures the effect of thermal loading cycles as well as mechanical loading and is addressed in more detail in subsection 3.3.4. When TMF is considered, some phases of gas turbine operation which would not usually be considered as highly damaging come to the fore-front, including cool-down phase where localised high levels of strain become significant.

Review

Fatigue modelling varies, depending on application, but is often heavily reliant on empirical models derived from large sets of sample tests. Though these sample tests can be heated or performed in a furnace, it is common for tests to vary either the mechanical loads applied, or the temperatures, but it is unusual to find tests varying both temperature and load. Fatigue modelling can be considered to be split into three broad groups. Stress methods are primarily applied to HCF and consider strain to be limited to the ellastic range. Strain methods are primarily applied to LCF and considerhigh levels of cyclic loads and resulting strain in the plastic range. Fracture mechanics models are also increasingly common, (linear-elastic and elasto-plastic) which consider the rate of crack propagation caused by local plastic deformation at an existing crack or flaw and calculate life to critical crack size.

The status quo approach to fatigue adopted in this research program, assumed that HCF was designed out of the High Pressure Turbine (HPT), and that LCF was the primary mode of fatigue. A Method of Universal Slopes was adoped [18] following the Coffin-Manson relation [43] [44], where by total strain ampli-

tude (ε_a) is considered as the sum of elastic ($_e$) and plastic($_p$) strain amplitude components:

$$\frac{\Delta\varepsilon}{2} = \varepsilon_a = \frac{\Delta\varepsilon_e}{2} + \frac{\Delta\varepsilon_p}{2} = \frac{\sigma'_f}{E}(2N_f)^{bf} + \varepsilon'_{ff}(2N_f)^{cf} \tag{3.6}$$

where:

ε'_{ff} =fatigue ductility coefficient

^{cf} = fatigue ductility exponent

σ'_f = fatigue strength coefficient

^{bf} = fatigue strength exponent

E = modulus of elasticity (Pa)

N_f = cycles to failure

This type of approach to LCF ignores the interactive effect of oxidation and creep on crack initiation and propagation. While this limits the approach, it does enable these mechanisms to be combined using linear summation rules, for though the mechanisms are known to be coupled, the modelling approaches used for each assume independence.

3.3.3 Oxidation

Oxidation is the time and temperature dependent process through which a metal surface, like a blade, exposed to an oxidising environment, such as combustion gas flow, forms a scale or surface growth. Callister [3] considers oxidation to be a form dry form of corrosion.

The chemical process, reaction kinetics and type of oxide scale produced are a function of the oxidising environment and the oxidised item, both in terms of

chemical or material composition, as well as temperature and any complex structures (such as a Thermal Barrier Coating (TBC)).

Introduction

Oxide layer formation on a metal substrate (M) is an electrochemical process in which, during oxide scale (MO) growth, electrons (e^-) are conducted through the oxide layer to the scale-gas interface, M^{2+} ions diffuse away from the metal-scale interface and O^{2-} ions diffuse toward it. The oxide layer or scale formed can serve as a protective layer against further rapid oxidation.

Oxidation can be considered holistically:

$$M + \frac{1}{2}O_2 \longrightarrow MO \tag{3.7}$$

Or as two separate halves as illustrated in the schematic Figure 3.7:

$$M \longrightarrow M^{2+} + 2e^- \tag{3.8}$$

$$\frac{1}{2}O_2 + 2e^- \longrightarrow O^{2-} \tag{3.9}$$

In gas turbines, oxidation can occur at the blade surface, at grain boundaries and internally. Though increasingly hot section blades in gas turbines are protected by a TBC which serves as protection against hot temperatures as well as against the corrosive environment. In the presence of a TBC, though the substrate may be protected to a certain extent from oxidation, the TBC bond coat is often liable to oxidation growth, which can in turn induce spallation of the external TBC. However, the complex layers TBC can induce shear stresses at materials bond layers, and oxidation damage can be displaced from the metal substrate to

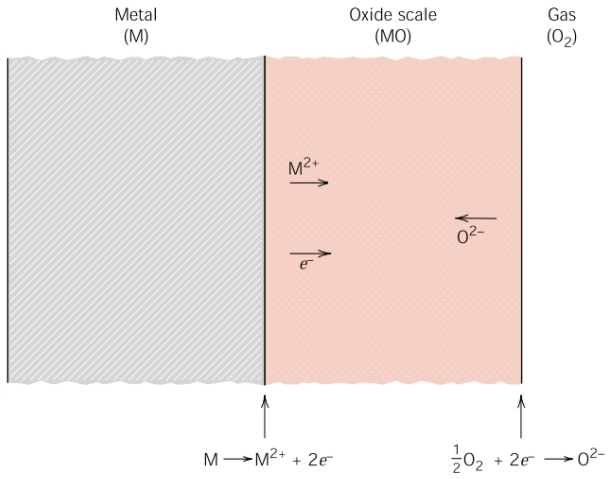

Figure 3.7: Schematic two part oxidation process according to Callister [3]

the Boundary Condition (BC), where oxidation layer growth can cause increased stress to the TBC which in turn can spall.

Damage from oxidation varies, but can include surface deterioration, mechanical integrity, spallation and γ' depletion in Nickel based super-alloys. Surface deterioration affecting localised surface roughness in turn affects the gas flow path geometry and performance. Spallation of the blade surface or TBC can expose the substrate to higher temperatures and oxidation attach, which can reduce the materials mechanical integrity and resistance to the aggressive conditions at which it operates. Spallation can also be coupled with the initiation of cracks at the blade surface. These may develop due to other mechanisms such as creep and fatigue. The presence of an oxidizing environment, tends to modify the crack growth mechanisms and crack growth rates, at surface cracks irrespective or their original cause.

The severity of oxide damage is a function of many factors, including the metal and gas flow temperatures, time, the chemical composition of the gas flow, the material properties of the coatings and substrates.

The characteristic nature and rate of oxide growth formation varies. Initial oxidation tends to be linear and primarily consists of transport based growth. As oxidation changes into a diffusive process, it oxide growth tends to a more parabolic form. The parabolic growth law is most common in oxide models, though linear and logarithmic models also exist.

The established model used initially within this project is that developed by Swaminathan [45], which considers oxide growth rate to be parabolic and conforms to the relationship between time (t) and temperature (T) identified by Arrhenius:

$$[logC - log(d^2/t)][T + 460] = Q/R \tag{3.10}$$

where oxide depth (d) is assessed as a function of material constant (C), activation energy (Q) and gas constant (R), which are measured experimentally in furnace tests for Rene 80 by Chang [46].

Establishing a reasonable and realistic reaction rate is an essential step in characterising the oxidation mechanism, and a pre-requisite of assessing the effect of oxidation on component life.

Review

A review and assessment study was developed to determine the possibility of replacing oxidation model [45] in the Lifing Module [18] with a more suitable model mathematically representing the effect of oxidation on blade failure in gas turbines.

The study, summarised here, was conducted collaboratively with two MSc students and is reported in more detail in their theses [47] and [48].

An initial literature review of available oxidation models was conducted. Due to the wide range and large number of models available, a systematic assessment and comparison of models was conducted. Models reviewed were classified by approach and considered to be: mechanical, coupled, experimental (data fitting), coatings or thickness evolution models. Models were compared and ranked, depending on the material considered, its published application (gas turbine or otherwise), failure mechanism, failure criterion, number of input parameters required and their availability in the public domain. The models were marked qualitatively, so as to assess their applicability, to this study and the feasibility of finding the required inputs in the public domain. Of twenty models assessed, twelve were deemed reproducible and three models were selected for further study, representing two types of TBC and in the bulk metal substrate [49, 50, 51, 52, 53]. These models source temperature as an input from the engine/aircraft performance model and consider oxidation damage due to spallation, scintering and thermal expansion coefficient miss-matches between TBC layers. Each of the three models was then assessed independently.

This study highlighted the need to consider oxidation as a factor in creep and fatigue lifing, rather than solely as a stand alone lifing mechanism, due to the effect of oxidation on the nature of crack growth at the surface. It demonstrated that fatigue and creep failure, in an oxidising environment, result in shorter lives than in a non-oxidising environment. The accurate modelling of oxidation is dependent on the accuracy of the thermal models adopted and the temperature field imposed on the Finite Element (FE) model used. While oxidation is accepted to be a high temperature phenomenon, it is noted that when considered in the context of a flight cycle, the choice for the ”cold” temperature (whether ambient temperature or idle temperature for example) in the cycle has a significant effect

on the resulting oxidation life calculated.

Implementation

Following the review, the primary model retained and sued for further study is that of Meier et al. [54] [49] [55].

It considers the failure of a Electron-Beam Physical Vapour Deposition (EB-PVD) TBC and focusses on the growth of the Thermal Growth Oxide (TGO) on the bond coat joining the substrate metal to theEB-PVD ceramic coating. The model uses Temperature and Strain inputs from the FE model. Two failure cases are available using this model: Oxidation (with failure determined by a critical oxide growth thickness) or Fatigue with Oxidation (where failure is determined by a strain range damage term).

The oxide layer thickness (δ) is considered as:

$$\delta = e^{Q(\frac{1}{T_0}-\frac{1}{T})} t^n \tag{3.11}$$

Where:

$Q =$ ratio of apparent activation energy to gas constant (R)

$T_0 =$ temperature constant

$n = 0.332$

$T =$ Temperature (K)

$t =$time (s)

It is considered that TGO mechanical strain is induced by the mismatch in thermal expansion. The free elongation of the TGO is defined as:

$$\frac{L(T)}{L} = \alpha_0(T - T_{sf}) + \frac{1}{2}\alpha_1[(T - T_{amb})^2 - (T_{sf} - T_{amb})^2] \tag{3.12}$$

where: $T =$ temperature at the metal -ceramic EB-PVD interface

$T_{sf} =$strain (or stress) free temperature for the oxide

$\frac{L(T)}{L} =$ free thermal elongation of the TGO

$\alpha_0, \alpha_1 =$ thermal expansion coefficients

Failure is defined in cycles (N), following a power law relationship such that:

$$N = \left(\frac{\Delta\varepsilon_{ff}}{\Delta\varepsilon}\left(1 - \frac{\delta}{\delta_c}\right)^c + \left(\frac{\delta}{\delta_c}\right)^c\right)^b \tag{3.13}$$

where: $\Delta\varepsilon =$ TGO strain range

$b, c =$ model constants

$\Delta\varepsilon_{ff} =$ static failure mechanical strain range (leading to N=1)

$\delta_c =$critical thickness that would lead to fail in one cycle

The implementation followed is that coded by Izquierdo [47] as part of this research programmed and further developed in collaboration with Corbo [48] for use witht eh simplefied geometry adopted (subsection 4.3.3).

3.3.4 Thermo-mechanical Fatigue

Through the development of components especially in gas turbines, but also in other high temperature and load applications it has become apparent that creep, fatigue and oxidation considered independently were insufficient to explain and characterise the rates of failure in service which were found to be caused by the

coupled effect of superimposed mechanical and thermal loading cycles which could be either in-phase or out-of phase with each other. Such loading conditions become increasingly important in thin walled structures subject to cooling where the through thickness thermal gradients induce additional strains especially at material boundaries (for example on the presence of a Thermal Barrier Coating (TBC)).

Introduction

Thermo-mechanical fatigue (TMF) modelling and life prediction attempts to capture the interaction between simultaneous thermal and mechanical load cycle. Which combined produce damage similar to fatigue damage.

High Pressure Turbine (HPT) blades are subject to both mechanical loads inducing primarily tensile mechanical strain. As well as thermal loads in the form of thermal transients and thermal gradients. Thermal transients (changes of temperature with time) occur during changes in the engine operating state, such as start up and shut down procedures, but also with lower amplitudes during take-off, at top of climb, during descent, and on the application of thrust reversal at landing. Thermal gradients also exist through the blade material thickness during operation. Thermal gradients increase in amplitude int he presence of blade internal cooling. Thermal transients and gradients induce thermal strains which can be both tensile and compressive, sometimes simultaneously. As such, the current load state of an HPT blade is a function not only of the current boundary temperatures and mechanical loads, but also of the temperature history and temperature distributions both through the blade and along its surfaces [56].

A key factor in TMF is the nature of the coupled thermal-mechanical load

cycle [57, 58]. This is often described in terms of phasing, where a blade load cycle would be considered in phase where maximum strain at peak temperature coincide, but out of phase when minimum strain and peak temperature coincide. The nature of gas turbine engine cycles is such that both types of TMF cycle are likely to happen during a mission cycle. Thermal loads can induce simultaneous compression at the hot -side surface and tension at the cold-side surface of a blade. When superimposed on tensile mechanical loads, these thermal loads act to reduce the tensile stain at the hot side surface, but increase the tensile loads at the root of the cold side.

Review

A review of available public domain TMF models was carried out in collaboration with Blanchard [59] and the findings are summarised here. This study compared nineteen models and asesed their applicability to this and other similar applications given the constraints that they should be reproducible from and required a manageable number of input variables, that their inputs might be generated from cycle information and Finite Element (FE) modelling and that they were suitable for gas turbine applications in terms of mechanism and material definitions.

TMF testing procedures have developed rapidly and not “standard method” has as yet been adopted [60, 61, 62]. Test types can vary, often depending on the equipment available. Though all attempt to capture the coupled effect of mechanical and thermal loading, it is common for tests to vary either mechanical or thermal loads, but rare for both to vary. Common types of testing include:

- Isothermal, high temperature fatigue testing
- Two-level testing

- Bi-thermal tests
- Multi-axial testing

Two level testing, improves on isothermal testing in that the component is cyclically loaded mechanically at two different temperatures, usually high temperature followed by low temperature [44]. However, inverted Low-High tests have established clearly that damage accumulation in these conditions is both non-linear and sequence dependent, therefore limiting the applicability of two level tests and models to gas turbine applications subject to complex mechanical and thermal loading cycles. In bi-thermal testing the temperature of the component is changed using the mechanical load cycle, though the samples are usually not loaded mechanically and thermally simultaneously these tests and models are more representative of damage under operational conditions [63, 44]. Developments in multi-axial testing allowing simultaneous loading in bending, rotation and by hot and cost heat sources is allowing TMF testing at higher load frequencies [64, 65].

TMF damage can be considered as the effect of coupled interaction between creep fatigue and oxidation. It is commonly modelled as two independent mechanism interactions creep-fatigue and fatigue-oxidation.

Creep-fatigue interaction is acknowledged as being more damaging than the addition of creep and fatigue damage calculated separately [37, 66]. Creep-fatigue interaction is commonly considered the following ways:

- Linear damage summation
- Strain range partitioning
- Ductility exhaustion

Linear damage summation is the most common approach, possibly because it is the simplest to implement requiring commonly available data such as S-N and stress rupture curves. However, this approach is phenomenological and material dependent. It is also limited by the assumption that tensile and compressive dwell periods are equally damaging.

Strain range partitioning considers four different types of strain, classified depending on the stress being tensile or compressive,and the strain being creep or time independent plasticity. This approach is limited by the amount of testing required for the assessment of any arbitrary cycle including the failure limits from independent testing under each strain condition.

Ductility exhaustion uses a strain based rule to sum the fractional strain damage due to fatigue and creep. While some of the inputs can be sourced from pure fatigue and creep tests, selection of appropriate input values can be arbitrary and therefore limit accuracy [37].

The inclusion of creep-fatigue in TMF testing and modelling is openly debated, given that the influence of creep in modern gas turbines (with directionally solidified or single crystal blades) is unlikely to cause failure [67], and satisfactory results have been claimed without it [68], others consider that it should not be ignored [69].

Fatigue-oxidation interaction has grown in importance as a focal area of TMF research for while failure due to oxidation alone is unlikely, an oxidising environment has been found to significantly reduce the fatigue life of components.

Implementation

The key factors influencing the selection of an TMF model were its applicability to gas turbine operating conditions, the availability of appropriate materials data, and the capacity of the model to capture the arbitrary strain-temperature histories common in aero engine operations.

The selected model, is that of Neu and Sehitoglu [70, 71] adapted by Boismier and Sehitoglu [72, 73] to Mar-M247 a Ni-based super-alloy is described briefly here.

The Neu-Sehitoglu (NS) model is a crack nucleation and early growth model which considers fatigue in the context of of oxide growth and rupture at crack tip zones, the inter-granular damage related to creep when components are exposed to arbitrary strain temperature histories which result in a phasing effect.

The NS model considers that at high temperature fatigue life is a function of both oxidation-fatigue and creep-fatigue interactions. As all these mechanisms are strain, temperature, strain rate, and phase dependent, the strain-temperature histories determine which of the mechanisms is most damaging under a given loading cycle for a given material.

The NS model considers each mechanism (creep, fatigue and oxidation) separately, then calculates a total damage term assuming that linear damage is unity at failure. Where D indicates the per cycle damage from each mechanism (superscript):

$$D^{tot} = D^{fat} + D^{ox} + D^{creep} \tag{3.14}$$

Or, where damage is considered as the inverse of the number of cycles to failure (N_f):

$$\frac{1}{N_f} = \frac{1}{N_f^{fat}} + \frac{1}{N_f^{ox}} + \frac{1}{N_f^{creep}} \tag{3.15}$$

Fatigue is considered using a strain -life relation assuming that that fatigue is governed by mechanical strain range ($\Delta\varepsilon_{mech}$). This approach consider fatigue by dislocation slip and crack formation and initial growth by localised deformation and slip in the plastic region surrounding a crack tip. Boismier and Sehitoglu [72] further assume that inelastic strain is negligible when Nickel based super alloys are subject to lower temperature isothermal fatigue loading.

Creep is considered stress based. The creep model considers the growth of voids and inter-granular cracks due to creep loading, which are primarily functions of tensile loading and therefore asymmetric. It relies on a unified constitutive equation to relate the inelastic strain rates, stresses, thermo-mechanical loads, and hold times.

Oxidation damage is considered to be a function of oxide layer growth as a cause of crack initiation and initial crack growth. Both continuous and stratified oxidation is considered. The NS model considers the cyclic effect of the oxidising environment where:

1. a material surface is exposed to an oxidising environment
2. an oxide layer starts to form
3. the oxide layer growth to a critical thickness (which is not constant but may vary with strain range, temperature and strain rate)
4. the oxide layer ruptures

5. new material surface is exposed to the oxidising environment
6. $\rightarrow$ continue at step 2

The crack is considered nucleated the first time an oxide layer ruptures at which point the oxide growth can no longer be considered parabolic due to a localised increase in oxidation rate at the exposed material surface.

Key to the NS approach is the inclusion of phasing parameters in both the creep and oxidation mechanism life terms. The cycle dependent phasing factors (Φ^{ox} and Φ^{creep}) are related the ratio of thermal to mechanical strain rates ($\dot{\varepsilon}_{th}/\dot{\varepsilon}_{m}$) present during the cycle load history.

The NS model captures bulk and micro-structural effects and therefore requires a combination of materials constants and variables. While at initial publication, the NS model required a large number of material and model input parameters. Sensitivity studies by Amaro [68] and more recently by [12] have identified that when applied to a Nickel base super-alloy, the NS TMF model is sensitive to only five parameters.

The significant drawback of the NS model, is the large number of material and model variables required (19), many of which require access to testing results which are not available for all desired materials.

The implementation of the NS model used in this research is that coded by Blanchard [59] for this research programme is illustrated in Figure 3.8 has since been used and validated by Abdullahi [12] who completed a sensitivity study on the model and material parameters identifying five oxidation damage parameters which have a significant effect on the total TMF life. Four of these parameters had previously been identified by Amaro [68] as significant in a previous sensitivity study applied to out-of-phase TMF lives. The NS model as implemented

by Blanchard allows three cycle counting variables to be used, however, as per Abdullahi's [12] application and verification case, Temperature is selected as the cycle counting variable in this study.

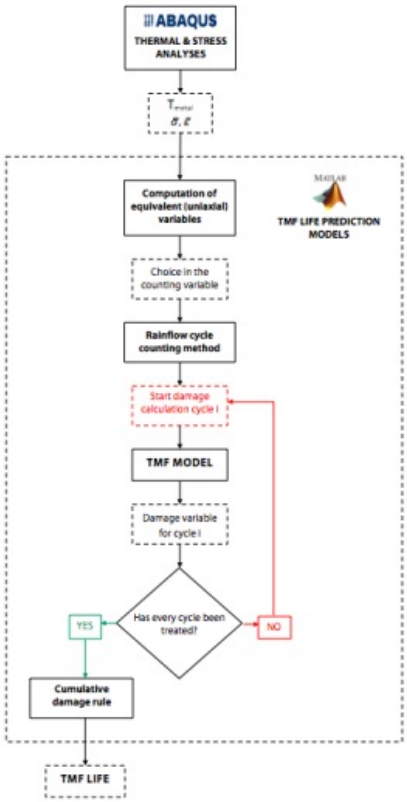

Figure 3.8: NS TMF model implementation

Chapter 4

Operational Severity

Severity (S) has been used, as a conceptual tool, over the past 40 years, during which time its meaning and application has evolved. At its core, it is a measure of the impact of varying operational conditions on the damage (D) incurred in a normalised reference framework. It is therefore a measure of variability of damage due to engine operations.

When comparing the effect of different operating regimes and conditions on an engine, the operational severity is considered as a measure of damage incurred relative to the damage that would have occurred had the same system been subjected instead to a defined reference operation.

$$S = \frac{D}{D_{ref}} \tag{4.1}$$

Severity (S) has been used as an input to operational cost models to deepen understanding of the impact that different operational regimes have on maintenance requirements and thus on operational costs.

This chapter introduces the concept of operational severity and an overview

of the available academic literature. Key choices made in the modelling of operational severity for this project are then considered and justified.

Recent research publications on operational severity are limited as recent research on this topic has been conducted by the aviation industry and results are rarely published. When referred to in publications it is common for a severity value to be given, without detail of either the method, tools or mechanisms used or considered.

4.1 The concept of operational severity

Early interest, primarily military, in severity arose from the need to determine appropriate and representative rapid testing methods, which led to improved Accelerated Mission Tests (AMTs). In this context, the use of severity enabled the development of more accurate AMT profiles, reflecting the expected operational damage incurred over an extended service period involving a mix of missions which might include training, fighting and tanking, as well as transfer flights.

Severity is usually applied to a mix of mechanisms (see equations Equation 4.2 to 4.5), in which case it is often considered as being composed of both steady-state and cyclic elements. Because the proportion of steady-state to cyclic severity reflects the failure mode, it is essential to keep both elements in mind when using total severity to compare mission profiles. Considering only total severity can lead to misinterpretations: not all missions with the same total severity are subject to the same damage, as this damage could be driven by different mechanisms.

The outcome of a severity analysis can also be represented as the degree of life consumed by a given operational regime [18, 6]. This offers the possibility

of using severity analyses to “predict[...] the relative effect of changes in aircraft mission profiles on the damage rates of major engine components”. In this context “it can also be stated as the number of new mission usage hours required to cause the same amount of damage as the reference mission usage” [6, p.2]. This application is schematically represented in Figure 4.1.

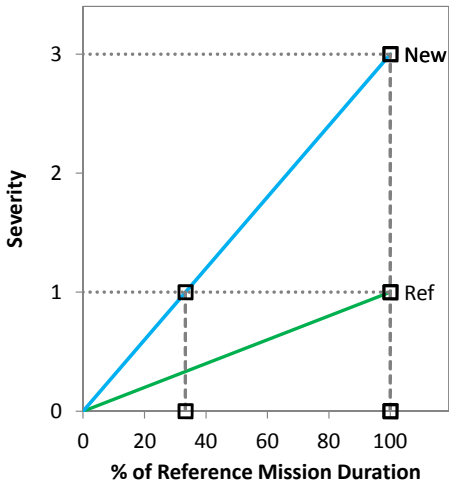

Figure 4.1: Schematic of severity flight duration relationship adapted from [6, Fig.13]

One of the more common graphic representations of severity in literature is the severity curve, notably the derate-severity curve: an example is shown in Fig-

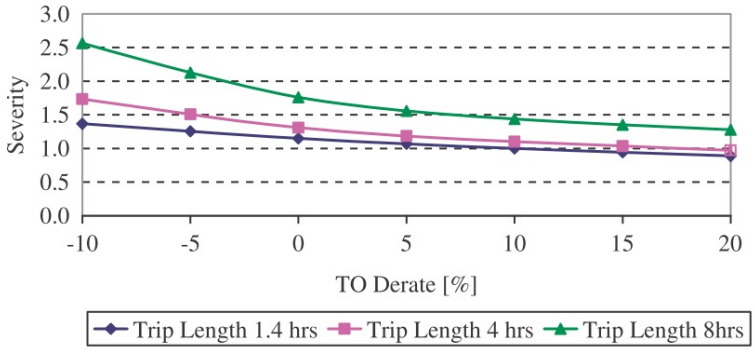

Figure 4.2: Example of a derate severity curve for lower thrust engine HPT blade [7]

ure 4.2. Derate (thrust setting) is a significant factor in engine lifing and severity estimation, because it can incorporate the effect of several operational conditions including outside air temperature, runway length and payload.

Stabrylla and Troha [6] derive Severity (S) using damage rate fractions (γ) and distinguishing between cyclic and steady-state modes for reference and new cases:

$$(\gamma_t)_r = (\gamma_c)_r + (\gamma_s)_r \tag{4.2}$$

$$(\gamma_t)_n = (\gamma_c)_n + (\gamma_s)_n \tag{4.3}$$

where

γ	damage rate fraction (failures/time)	$_t$	total
$_r$	reference case	$_c$	cyclic
$_n$	new case	$_s$	steady

normalising Equation 4.2 and Equation 4.3 by the total reference damage fraction $(\gamma_t)_r$ generates the following identities for reference and new mission severities

$$(S_t)_r = 1 = (S_c)_r + (S_s)_r \tag{4.4}$$

$$(S_t)_n = (S_c)_n + (S_s)_n \tag{4.5}$$

Severities calculated in this way, and schematically represented in Figure 4.1 can be used to determine the amount of time an engine would be able to operate at the new mission conditions before it experienced the same amount of damage

as the reference mission.

$$S_{total} = \frac{\gamma_{total}}{(\gamma_{total})_{ref}} = \frac{\gamma_{cyclic}}{(\gamma_{total})_{ref}} + \frac{\gamma_{steady}}{(\gamma_{total})_{ref}} \tag{4.6}$$

The cyclic and steady-state severity elements as defined above can capture a mix of failure mechanisms. Severity can also be calculated considering individual mechanisms explicitly [18]:

$$S_{total} = S_{creep} + S_{fatigue} + S_{oxidation} \tag{4.7}$$

4.1.1 Initial context

In the late 1970s and early 1980s several newly developed engine systems fitted to aircraft delivered lower than expected levels of operational readiness and increased operational costs. These trends led engineers to study the effect of aircraft operation on engine life (or durability). A joint commercial-military study was published by Stabrylla and Troha [6]. They present a single methodology (applying the OPSEV tool), validated for two engine types (J79 and CF6) and applied across civilian and military applications. This method was used to develop operational cause and severity effect trends, which they deem to be indicative of more complex interactions between operation and failure mechanisms and thus consider to be a tool for decision making as well as potentially for problem analysis. The authors do not however explicitly identify the lifing mechanisms they considered.

They [6] studied the two engine types (CF6 and F101 - using the the model as validated for the J79) and four aircraft mission sets, using data from flight recorders where available as well as collated removal, damage and shop visit

data. This allowed them to compare the effects of the different operating regimes to those assumed or specified in the Design Mission Mixes (DMMs) and Accelerated Mission Test (AMT) profiles set during the design and test phases of the engine life cycles. Types of damage considered include, cracks to several hot section components as well as turbine blade coating deterioration. The Operating Severity Analysis Program (OPSEV) tool analyses flight profiles either defined or recorded, to link operation with damage rates incurred by 26 major engine components. The tool and method are however not described in detail. “Trade-off curves [are used] to predict the relative severity for each mission profile as seen by each component”. These curves are “derived from experience” and from “basic failure equations” and are “related to the specific engine parameters that influence [the] failure [of each major component]”. The engine parameters, failure modes, models and equations used are not set out in the paper. OPSEV uses operational inputs (speed, pressure, temperature, stress, strain, and strain rate) to generate “cyclic (power transients) and steady state (time at power condition) damage fractions as well as their sum”.

For the CF6 engine they were able to compare recorded military use to commercial operations. They report that shorter flights lead to increased cyclic severity and increased Unplanned Engine Removals (UERs). As part of their validation, they compare predicted to actual removals for flights grouped by duration. Predicted removal rates are accurate to between 3 and 19% of actual removal rates. Accuracy reduced for longer flight durations. Analysis of CF6 UER and Shop Visit Rate (SVR) data to identify the failed component and the OPSEV severity analysis separately identified the High Pressure Turbine (HPT) rotor as the component most likely to result in engine removal.

Analysis of 32 military sortie types for a total of 189 sorties, including 614

hours of flight data and 3 commercial flights enabled them to consider the possibility of using averaged severities for aircraft engine types. Each flight was compared to a reference mission of 4.43 hours and 7.5% Take Off Derate. Total severities for all the missions were near the nominal reference mission severity of 1 and mean total severity across the missions was 1.103. However, the cyclic content of the military missions varied widely (0.48 to 3.589).

The authors deem this variation to indicate the need to study missions individually rather than collectively. Such a wide range of cyclic severities could also indicate a change of severity mode from a steady-state failure mechanism such as creep to a cyclic failure mechanism such as fatigue. The dominant severity mode varied between mission sets, illustrated in Figure 4.3 which shows the loci within which the military and commercial flight severities fell. The analysis identified cyclic severities as dominant in flight test mission severity whereas steady state severity was predominant in commercial usage. This distinction was attributed to the different power settings used in the Short Take-off and Landing (STOL) military application of the engine and the commercial flights. Touch and go cycles and low altitude cruise were identified as particularly severe military flight segments. It would be reasonable by analogy to assume that commercial training flights which include touch and go circuits and manual throttle operations are also likely to be the most severe flight segments in commercial operation.

The F101 engine was evaluated in both bomber and fighter roles using the OPSEV tool validated for the similar J79 engine. Data from flight recordings showed a wide range of severities for nominally similar missions. This was attributed to the influence of individual pilots and also to terrain-following flight segments. However as these flight segments are terrain dependent, it is unclear whether the terrain or the pilot is primarily responsible.

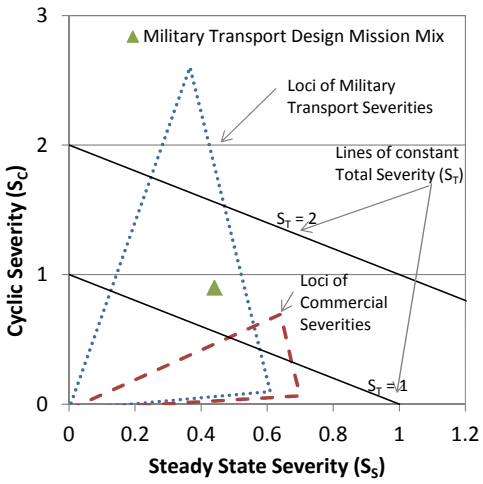

Figure 4.3: Schematic of cyclic and steady state severities for CF6 adapted from [6]

Stabrylla and Troha [6] were able to use their severity methodology to suggest as design goals for military turbine engines, increased flying hour and cycle targets. They consider that the balance of cost, life, performance and weight should continue throughout engine development and operation of the engines. While the trade-off decisions made will vary from system to system, they consider their method to be universal.

In summary their findings include:

- severity tended to be higher in service usage than predicted at the design stage
- severity tended to be higher during AMT cycles than predicted at the design stage
- in tactical usage cyclic severity predominates

While Stabrylla and Troha [6] do not give details of mechanisms, or lifing estimation methods used in the OPSEV programme, they do establish the case for

operational severity as a measure of relative damage for the purpose of comparing the effect of varying operations on engine maintenance costs. Generalising the process to other engines or missions will require damage fractions related to appropriate lifing mechanisms, applied to the full mission profile.

4.2 Approaches to applying severity

Practical application of operational severity as a link between operation and maintenance requires the development of appropriate lifing estimations methods. For a predictive severity model, component life must be estimated for varying operational profiles.

Currently life estimation methods are used throughout the life cycle of a component. At the design stage they can be used to enable the selection of appropriate materials and to understand the effect of different design decisions, including geometry and loading, whereas during operation they can contribute to decisions relating to part retirement or removal and repair. Continued use of life estimation models in service is increasingly common in systems designed using the damage tolerance approach or managed under Retirement for Cause (RFC) processes [74]. They are used by Maintenance, Repair and Overhaul (MRO) entities to develop and validate new maintenance processes, or might be used by the Original Equipment Manufacturer (OEM) to support applications for certification extensions. At each stage, decisions based on lifing data can lead to reduced operational costs. Sapsard [75] even argues that operational factors can be more important than design choices . As a result, a plethora of methods exist from varying sources, and for the operational severity calculation to be viable, the selection of suitable lifing models is critical.

Several different categorisations are used to describe lifing methods and related maintenance procedures. Some distinguish between “hard-life” or certified limits and “on condition” maintenance. Previously, hard life limits have been used after the application of safety margins for all “critical” engine components. Militaries started to monitor components with periodic inspections using Non Destructive Testing (NDT) methods to detect incipient cracks, allowing operation beyond hard life limits, or reduction in the safety margins applied on top of the predicted usable lives to reduce maintenance costs and increase lives. This tendency to look for damage fed into the “damage tolerance” philosophy of lifing, which contrasts with the “safe life” philosophy. These differ both in their initial assumptions about the components and their definition of “failure” or end of life.

Safe life assumes that all components are perfect (without impurities or flaws) when they start operation, and that end of life is determined by the initiation and growth of a crack to a detectable size. Under safe life, components should be removed before crack initiation. Safe life can result in removal of components with significant remaining usable lives, and can be overly conservative leading to increased maintenance demand and costs. Damage tolerance however, considers that flaws (just below detectable size) exist in components, and that end of life occurs when these crack grow to a “critical” size. With correct determination of critical size, components should be removed before cracks become unstable and approach rupture. Manufacturing and material variability is accounted for under both “design methodologies” by the addition of sometimes large safety margins, especially on components deemed critical to aircraft safety such as turbine disks.

More simply, Beres [37] defines failure as any change resulting in a component’s inability to perform its design function satisfactorily. The failure mode is the physical or mechanical process which results in component failure.

Tinga et al. [76] also group lifing models into two categories, “total life” and “crack growth”. They consider total life models to be those models only concerned with the determination of the end of life point and consider these to conform to the safe life philosophy, while crack growth models also consider how the part fails: these they consider to conform with the damage tolerance philosophy.

Sapsard [75] considers the safe life approach to be commensurate with the life to first crack method. This approach assumes failure at the point of crack detection, aims to retire components before incipient cracks are detected and applies a safety margin which aims to ensure that an acceptably low number of components will fail in service. Commonly, this is arbitrarily set at three sigma or one in one thousand components. He considers the damage tolerance approach also referred to as two-thirds dysfunction method to incur an automatic component weight penalty and significantly increase inspection costs. The damage tolerance approach assumes that the component has been designed and its material selected in such a way that any incipient cracks grow sufficiently slowly, following a predictable growth pattern, such as linear elastic crack growth in order to enable detection through non-destructive monitoring.

Holmes [77] reviews safe life and damage tolerance approaches and their application in military and civil operations of gas turbine engines. As the design, maintenance, and retirement policies and approaches have developed gradually, the methods tools and techniques used to set, monitor and test them have also evolved. Variously these have included test failure, coupon testing, spin pit testing, accelerated mission testing, and analytical techniques including structural and mechanical modelling and finite element method. Safety limits set for each component and operational application depend in part on the component classification. This varies by country and operator (military and civilian), with the most

high risk parts being classified as critical (safety or mission) or uncontainable (in case of failure). Holmes [77] states that commonly the most critical components, while designed using damage tolerance approach and incurring the associated weight and cost penalties, are in practice managed to first crack initiation through on-condition and preventative maintenance. As such, he identifies a common misalignment between design philosophy and maintenance management approaches in operational engine systems.

The advantages of the safe life approach according to Holmes [77] include the minimisation of maintenance requirement, the maximisation of time on wing without inspection and a reduced requirement for facilities and equipment. This widely practised approach is however subject to certain disadvantages. These include fewer options available to fleet management, a poorly defined inspection process, a significant requirement for replacement parts and significant premature retirement of components (depending on margin up to 99.9% for a one in one thousand in service failure rate). Further Holmes [77] asserts that extending the life of safe life designed components through the application of fracture mechanics offers only a small margin of benefit when compared to the damage tolerance approach: at best one additional usable cycle for every two cycles justified through testing.

The damage tolerance which is common in newer engines especially those containing highly stressed components is beneficial as it enables the use of components with inspection beyond low cycle fatigue limits. It requires improved design, test and verification procedures and significantly improved inspection capacity to detect incipient cracks. Therefore it is costly to implement, incurs a weight penalty, requires significant levels of infrastructure and an increase in part handling. Holmes [77] concludes that there is no obvious preferred approach to

critical component design. Before a choice between safe life and damage tolerance approaches should be made, a thorough comparison of life cycle costing is needed which considers availability of suitable facilities and non-destructive testing capacity as well as expected utilisation rates.

Davenport [78] considers that coupling the safe life, hard time and hard life methods offers a conservative approach to gas turbine plant management given its significant dependence on estimated operational histories, material properties and safety factors and margins. Noting that irrespective of whether the engine structural integrity programs (such as Engine Structural Integrity Program (ENSIP)) and retirement for cause applications of damage tolerance implementing monitoring systems are applied, in most cases (in practice unless there is a part shortage) components are still retired eventually either at crack detection, or at a hard time limit. He further states that the key to successful life management is the successful classification of component type by criticality and the selection of the appropriate selection of damage mechanism.

He considers that one of the key factors in hindering the uptake of damage tolerance methods is the formulation of the RFC hypothesis in which crack initiation sites are assumed to be present in all manufactured components, with the resulting implication that all manufactured components are either flawed or defective. Micro porosity, lattice vacancies and grain boundary inclusions are however inevitable and a component's quality should only be judged on the size and frequency of flaws present. He argues that the interval used between non-destructive inspection through testing or examination should be based on the largest possible undetected crack rather than the smallest detected such that the largest missed crack being detected at the end of the next inspection interval would still be stable. As a result it is common for inspection intervals to be set

at approximately half of crack growth life. While coupled damage tolerance and inspection processes can lead to significant reduction in the removal of components with remaining usable life, he considers that it is ”preferable to retire at a fraction of population before actual life consumed to preclude any in-service critical component failure”.

Though the damage tolerance approach is intended to reduce waste and increase component usable life, Grooteman [79] considers both design philosophies to be inherently wasteful and conservative. The dependence of these philosophies on the accurate determination of a suitable safety factor and their deterministic nature means that they are both simple and widely used although their reliability has been questioned and their suitability for novel concepts is questioned.

He suggests the addition of a stochastic model overlying the deterministic one enabling the assessment of Probability of Failure (PoF) alongside a life estimation, which once coupled with NDT methods and their associated Probability of Detection (PoD) forms the Retirement for Cause (RFC) maintenance philosophy. This would tend to reduce waste by only retiring those parts containing cracks likely to become unstable before the next inspection. He thus replaces safety margins applied to critical sizes and life values with two probabilistic measures.

Crocker [80] considers PoD determination to be critical to the use of stochastic models such as these, especially as human factors intervene in the fallibility of inspection and repair processes. Not only is it likely that not all cracks of a critical size present will be detected, but there will be variability in the repairs, which will not be of the same resilience as the original components, evidenced by a reduction in Mean (operating) Time Between Failures (MTBF) with successive repairs.

Design Philosophies	Safe Life	Damage Tolerance
Alternative Names	Life To First Crack total life	Crack Growth, 2/3 dysfunction
Initial Assumption	Flawless component	Undetectable material flaws, design subject to predictable and slow crack growth phase
Failure point	Detectable Crack	Unstable or critical Crack
Management Policy		Inspection at 1/2 crack growth life intervals
Retirement Policy	Hard-life	On Condition, Retirement for Cause or Hard Life
Safety Margin Target	1 in 1000 in service failure	10% in service failure
Note		component weight penalty increased infrastructure requirement and inspection related costs

Table 4.1: Summary of common deterministic lifing philosophies

Vittal et al. [81] offer an alternative classification which can be considered as deriving from the life management perspective, as opposed to design. Their classification intends to facilitate life extension programmes. They propose a distinction between Life to First Crack (LTFC) models derived from the safe life philosophy and depending on significant amounts of sample test data, and RFC models. They suggest that while the RFC models are less conservative than LTFC models, because despite their popularity in industry, and use in validating probabilistic approaches to lifing as suggested by Grooteman [79], their relative simplicity does not allow them to account fully for the stochastic nature of crack growth.

They identify that one of the critical decisions required in lifing is to combine time-scales which differ not only between failure mechanisms, but also in engine health monitoring systems.

It is essential to distinguish between design philosophies including safe life

and damage tolerance, maintenance approaches including hard life and condition monitoring and removal policies such as hard life limits and retirement for cause. While all of these philosophies and approaches concern the determination of the point at which components should be removed and therefore the risk associated with their continued operation or the cost incurred in their removal while useful life remains, they are each applicable at different stages in the system's life-cycle, and have varying impact on system life, maintenance requirement, reliability and durability.

4.2.1 Physics-based methodologies

Integrated lifing approach methodologies have been developed within industry and research institutions for the purpose of understanding and quantifying the physics-driven links between operational decisions and component lifing. These are sometimes referred to as physics-based methods or integrated lifing approaches. In each case, a balance has to be struck between the use of high fidelity models requiring a large number inputs and simpler, lower accuracy models requiring fewer inputs. The use of assumed inputs in high fidelity models, when actual inputs are not available, can undermine the validity of their results.

Eady [31] considers the choice of failure mechanism to be essential. Stabrylla [6] has shown that changing operations can cause failure mechanisms to change. A balance needs to be found between capturing a sufficiently wide range of failure mechanism to cover the spread of failures in operation and the limited number of inputs likely to be available at the preliminary design stage. He argues that even minor changes in operating conditions leading to negligible operational impact can significantly lower, life usage rates and therefore reduce life cycle costs. Many

authors integrate these mechanisms, by using a single set of inputs for each mechanism, derived from a process of mission definition, geometry selection, material selection and Finite Element (FE) modelling to establish the stress, strain and temperature profiles required for lifing.

Methods of gas turbine usable life estimation that consider multiple mechanisms have been developed previously, and fall into two categories, models intended to predict engine lives intended for use at an early design stage (which are sometimes referred to as physics-based lifing methods), and models intended for use in monitoring engine performance during testing or operation.

Most of these methods have followed a common process:

- determination of component loads (thermal and mechanical) either analytically or using FE modelling
- application of damage models to stress strain and temperature profiles

Multi-mechanism models tend to focus on the creep/fatigue interaction. Some authors [76, 82, 83, 84] combine the different failure mechanism lives using Miner's rule, linear summation, ductility exhaustion, linear damage rule and Robinson's life fraction, while others consider each mechanism completely independently [85, 86, 87].

Gyekenyesi et al. [88] present a method for integrated lifing under cyclic thermo-mechanical loading due to Thermo-mechanical fatigue (TMF) and creep rupture. The key factors they identify as necessary to enable the process are: capturing multi-axial loading, accounting for variable load cycles, capturing cyclic effects and selection of appropriate stress counting variables and suitable step sizes. They consider multi-axial loading by using Von Mises stresses, and count varying loads using the rainflow counting technique. They use damage cycle

counting, in order to capture the most damaging conditions (low stress-high temperature). They use Miner's Rule to accumulate Low Cycle Fatigue (LCF) damage with step sizes in time or stress. For creep rupture, they use a Larson Miller Parameter modified by Conway [89] and a time step defined by Zuo [90].

Bagnall et al. [91] consider integrated lifing methodology for the purpose of understanding the effect of operation on the cost effectiveness of "Power by the Hour" contracts. They consider creep, LCF, TMF and oxidation, but note that many models could be chosen. The methodology is applied to both 2D and 3D geometries. The 3D geometry is preferable where stress concentrations on detailed geometries are to be considered, or where the thermal gradients are to be considered. Different levels of detail in geometry can be considered at different stages in the system life cycle. Simple lifing algorithms are endorsed, especially when coupled by matching and calibrating bench tests, enabling them to rival more complex approaches in accuracy but with a far reduced burden of calculation.

Tinga et al. [76] present an integrated lifing tool for high pressure turbine blades with the declared purpose of supporting On Condition Maintenance (OCM) or enabling comparison of flight mission effect on life. Their coupled multi-tool model uses recorded data for the mission profile followed by FE analysis on a detailed 3D geometry using Computational Fluid Dynamics (CFD)-supported heat transfer calculations to supply thermo-mechanical load histories to multi-mechanism lifing models. Though they do not define the mechanisms considered or models used, they do consider time and cycle dependent mechanisms and declare their lifing methods to be their greatest source of error in the process due to the restricted nature of this approach and the inherent errors associated with material definitions required.

Turbine blades are primarily subject to TMF, creep, hot corrosion, LCF, and High Cycle Fatigue (HCF). The load cycles to which high-pressure turbine blades are subject can be analysed through coupled thermal and stress analysis.

Lifing mechanisms as seen in chapter 3 enable the assessment of specific load conditions. These then need to be accumulated to account for the variation in cyclic thermal and stress load patterns throughout an aircraft or engine mission. Damage from each cycle in the form of damage fractions contribute to the overall flight cycle (mission) damage.

Damage rate fractions, γ , are required as inputs to the severity estimation calculations described previously in in equations 4.2 and 4.3. By definition, when based on operational accumulated mission data, damage rate fractions are assessed such that:

$$\gamma = \frac{N_{\text{failures}}}{t_{\text{flying hours}}} \tag{4.8}$$

This data is not however available to predict severity for defined modelled operations rather than analysing in service failures. Instead it is common to consider a single flight cycle in terms of cyclic and steady state accumulated damage.

Cyclic damage is accumulated using Miner's Rule, also referred to as Palgrem-Miner linear damage theory, such that the cyclic damage of a mission is considered to be the sum of the damage rates incurred during each successive damaging load condition (i) defined as the number of cycles at a given load condition (n_i) experienced during the mission relative to the number of cycles to failure (N_i) at that condition:

$$D_{\text{cyclic}} = \Sigma \frac{n_i}{N_i} \tag{4.9}$$

Under Miner's hypothesis of cumulative damage, fatigue damage is consid-

ered to accumulate neglecting the effect of previous damage on the component. Inherent in the formulation is the assumption that once the sum of damage fractions considered becomes unity, the component is considered to have failed.

Similarly damage due to time dependent mechanism is accumulated using Robinson's rule, which cumulates for each damage condition (i), the ratio of time at condition (t_i) during the mission relative to the time to rupture under that loading state ($t_{\text{rupture},i}$):

$$D_{\text{steady}} = \Sigma \frac{t_i}{t_{\text{rupture},i}} \tag{4.10}$$

It is considered that, as both Equation 4.9 and Equation 4.10 consider a single operational flight mission, they can be combined to estimate the total damage following a similar approach to that seen previously in equations 4.2 and 4.3, such that for a given flight/mission, subject to j mechanisms whether cyclic or steady:

$$\frac{1}{D_{\text{total}}} = \Sigma \frac{1}{D_j} \tag{4.11}$$

otherwise, where one cyclic and one steady state mechanism are considered:

$$\frac{1}{D_{\text{total}}} = \frac{1}{D_{\text{steady}}} + \frac{1}{D_{\text{cyclic}}} \tag{4.12}$$

There is as yet no universal approach to damage accumulation. The Palmgren-Miner damage rule is commonly used, as, though it is a simplified approach to the problem, its limitations are widely known and understood. Non-linear adaptations have been added by some authors to capture the effects of high temperature effects and mechanism interaction. All cumulative methods are limited by the availability of relevant material properties at the loading conditions.

Most damage accumulation rules assume independence of the damage factors. Damage accumulation used both within a flight cycle as a means to agglomerate the effects of each subsequent thermal or load cycles [18, 12] but also to combine the effect of different mechanisms into a general life estimation [92, 70, 71, 93, 94]. The use of a combination of accumulation methods, including Robinson's Rule, Miner's Rule and the Linear Damage Theory, is common in publications considering integrated lifing methods of components subject to multi-mechanism damage [91, 95, 96].

4.3 Modelling approaches

The accuracy of a lifing method for an operational component is most dependent on the valid selection of the lifing mechanism. This selection is difficult when assessing the lifing implications of flight missions: different lifing mechanisms are pre-eminent at different phases of the flight profile. It is reasonable to expect creep to be significant during the cruise phase of a long haul flight (constant load at elevated temperature) for example.

The severity estimation process illustrated in Figure 4.4 conforms in many ways to the integrated lifing approach presented by Bagnall et al. [91] with the addition of a severity estimation step and preceded by engine and aircraft performance calculations required to generate the Boundary Conditions (BCs) for the FE problem. The process is also similar to those presented by Tinga [76] and Suarez [97, 98]. Bagnall considers that this process could be applied at various stages in the life cycle, with varying levels of accuracy.

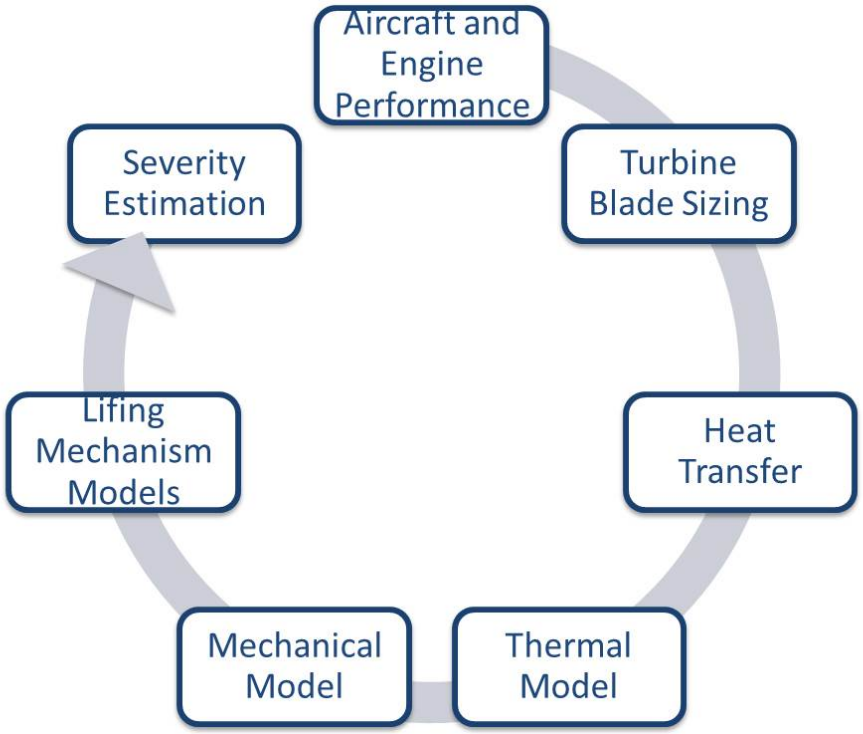

Figure 4.4: Severity estimation process

4.3.1 Overview of the Severity estimation approach

Engine and aircraft performance modelling. In this research, the TURBOMATCH and HERMES codes developed at Cranfield University are coupled and used to generate mission time histories including gas and cooling flow temperatures, mass flows, pressures and rotational speeds, throughout the flight profile. These require prior definition of the reference and study missions, as well as an acceptable engine model. The engine performance code TURBOMATCH is used to assess the design point and off-design performance of the engine. The design point is set at take-off conditions, and modelled using suitable engine design parameters from open literature. Off-design performance is assessed throughout the flight profile generated by

the aircraft performance code HERMES which determines the overall aircraft performance throughout the various flight segments for a given aircraft defined in terms of shape, geometry and required performance, and coupled with the design point engine performance data generated by TURBOMATCH, along with defined climb and descent schedules, cruise speed and altitude. For each flight segment, duration, and engine performance including rotational speeds, temperatures and cooling flows are calculated. These serve either directly or indirectly as inputs for the thermo-mechanical structural analysis.

Turbine blade sizing is conducted for a single stage HPT blade using the engine performance as defined at the design point. Steps in the sizing process [10, 99, 100] include calculation of: inlet and outlet annulus geometries, stage efficiencies, rotor inlet velocity leading to preliminary blade design at root, mid-span and tip blade locations, given an initial estimation of rotational speed, inlet Mach number and hub-to-tip ratio. Key assumptions of the calculation include: constant nozzle angle, 50% degree of reaction, constant axial velocity and constant mean diameter.

Bulk stress due to centrifugal loading is calculated analytically and used during the verification of FE analysis. Given the blade height(h) derived during the sizing process and angular speed(ω) from the engine performance calculation, and assuming that centrifugal load acts through blade centre of gravity (defined in terms of its distance d_{CG} from the rotational axis), constant span-wise cross-sectional blade area and flow velocity, the centrifugal stress is calculated along the blade span such that $\sigma_{CF} = \rho.h.\omega^2.d_{CG}$.

Heat transfer calculation is conducted to derive the bulk material and flow tem-

peratures as well as associated heat transfer coefficients along the blade span. The analytical process followed assumes that the blade can be considered as a heat exchanger subject to heating by hot gas flow, and subject to cooling. The model is capable of assessing a range of coatings and cooling methods. This process is described in more detail in subsection 4.3.2.

Two step FE modelling (thermal and mechanical) is implemented in order to capture some of the coupled thermo-mechanical effects present in the gas turbine. The first step involves transient thermal analysis of a simplified turbine blade leading edge profile. The through blade thermal distributions, and their variations throughout the flight mission are then loaded by superposition of the static stress analysis as a function of angular velocity throughout the flight profile, blade height and disk radius. The key areas under investigation are the blade hot-side which is subject to heat transfer from the combustor exhaust flow and the blade cooling hole which additionally is subject to internal cooling by compressor bleed air. A simplified blade leading edge geometry is defined in the FE package with temperature dependent materials properties. In the thermal step, the blade is formed of linear heat transfer elements. Boundary conditions for the thermal analysis are principally the outputs of the heat transfer process described above, including hot side blade metal temperatures, and cold side surface film temperature and heat transfer coefficients.

The flight profile is considered in four segments: ground idle and taxi, take-off and climb, cruise, and, descent and landing. An initial temperature field equivalent to ground idle is set throughout the model. The boundary conditions are set as span-wise analytical fields along the blade span, and calcu-

lated for design point take-off conditions, and are then modulated throughout the flight profile by the application of varying amplitude factors.

In the mechanical stress analysis step of the FE modelling, the model elements are set as linear stress elements. Mechanical loads are implemented as a uniform rotational body force, that varies through the mission, by the application of amplitude factors, and the blade root is constrained so as to restrict both rotation and translation. This is superimposed on a "heated" blade generated by the thermal analysis step which captures the effect of thermal loads and specifically the stresses due to thermal gradients. Throughout the FE analysis process, the geometry, materials definition and mesh sizes are held constant. Post-processing of the FE analysis is conducted for verification and data extraction of through mission stresses, strains and temperatures.

Lifing analysis. The coupled thermal and mechanical loads determined at the preceding step are used to estimate component life. Mechanisms considered include creep, fatigue, oxidation and TMF (coupled creep-fatigue in an oxidising environment).

Severity estimation is possible once lifing has been completed for two mission profiles, including a reference mission, considering the relative damage incurred by the blade subject to the relevant damage mechanisms.

The pre-requisites of severity estimation are :

- mission definitions (for both the mission under analysis and the reference mission for that engine)
- component loading throughout the mission profile

Engine	Aircraft	Take Off Derate (%)	Trip Length (hrs)	OAT(Outside Air Temperature) (˚C)
Lower Thrust	Narrow Body	10	1.4	18
Higher Thrust	Wide Body	10	4	18
CF6 [6]	Commercial	7.5	4.4	†

†Outside Air Temperature (OAT) not defined by Stabrylla [6]

Table 4.2: Reference Mission definition

- component life based on selected lifing mechanisms

All of the lifing mechanisms studied previously require some level of component data including stresses strains and temperatures.

In this research, severity is used to compare operational regimes related to flying engine/aircraft combinations on missions other than the reference mission.

It is common for aircraft and their power plant to operate primarily under conditions and on missions which differ than those for which they were designed [6]. Many narrow bodied aircraft are designed for short-medium length flights, though many, especially in Europe will primarily operate on short intercity hops with little or no cruise segment. While this may be ”economically viable”, it will result in different load patterns than the design mission, with resulting differences in deterioration rates and damage. The effect of such operational changes can be predicted and analysed through a severity calculation such as this.

In this research, an industry standard engine reference mission is adopted, as used by [18] , see Table 4.2. This defines the reference missions in terms of flight duration, take off derate and outside air temperature. The reference mission used in severity estimations is not generally the engine design mission.

Severity analysis enables a mission to mission comparison for a given aircraft, collating and incorporating the varying effect of operating conditions and mission definitions as well as the consequential differences in importance of each lifing

mechanism considered.

Severity can be used for a single, or for multiple lifing mechanisms. In assessing the combined effect of multiple lifing mechanisms, the assumption is made that each mechanism can be considered as independent, to enable the use of linear damage theory.

This research uses a three step process, of FE component modelling, life estimation and severity estimation.

The finite element modelling gathers inputs from aircraft engine performance simulation. These are then used in turbine sizing and heat transfer calculations to generate the inputs required for FE modelling. This considers thermal and mechanical loads. The principal loads experienced by gas turbine blades are centripetal, gas bending and thermal. The key modelling decision at this stage is to define the blade geometry, balancing accuracy and model size or computational effort. In this project, Bagnall's [91] interpretation, that 3D models are required in order to enable the capture of thermal gradients within the blade, is followed. As a full 3D geometry is not however accurately defined at the preliminary design stage, a simplifying decision is made to focus on a simplified leading edge.

Gas bending forces are sometimes accounted for in turbine design through "hot forming", or otherwise through the structural design of the blade. Modelling gas bending loads, which tend to be small relative to centripetal and thermal loads, requires significant CFD modelling.

Two generalised approaches are therefore followed in blade lifing, the extremely detailed approach combining looped use of CFD and FE emulating the hot forming and working of components seen during the operational stages of components generally for the purposes of life extension programmes, and the certification of alternative parts or maintenance procedures. In these cases accu-

racy is key, with detailed models often produced by laser scanning actual parts. This approach is very accurate and detailed, but not feasible at the early stages of design.

The critical decisions required to enable severity modelling are:

- definition of functional simplified geometry
- suitable material selection
- sufficient thermal analysis to generate representative boundary conditions for finite element modelling
- damage mechanism selection

Having reviewed the key steps in the severity estimation process, the heat transfer calculation, simplified geometry implementation and materials selection are addressed in more detail in the following subsections.

4.3.2 Heat transfer

An HP Turbine blade is heated by the gaseous flow exiting the combustor. This is a convective heat transfer which depends on the velocity and temperature distributions of the flow as well as on the nature of the blade's boundary layer [101] and the blade's geometry (wetted surface area). Heat transfer through the blade is conductive and depends on the blade's design including the presence or not of a thermal barrier coat. Heat transfer away from the blade through cooling can be complex and might include film cooling, impingent cooling and convective cooling by means of a multitude of internal voids and micro pores throughout the blade material. The presence of cooling allows the blades to operate in an higher temperature environment while maintaining a minimum of blade life required to make

operation economically viable. Increased efficiency in the turbine gained by operating at increased temperature must be balanced at the design stage against the reduced efficiency of the compressors, from which the cooling flow is extracted as bleed air in sufficient quantities, to provide suitable velocity of cooling flow.

In this research a balance is sought between the requirement to capture adequately the effect of transient temperatures and thermal gradients through the turbine blade for the purposes of TMF damage modelling, with the complexity and computational cost of detailed CFD models. With the paucity of detailed geometric data available at the initial design stage, this would result in a geometry dependent on assumption. Where an existing blade geometry is used, the benefit of a generic physics-based approach would be lost through the adoption of all the design choices in the chosen blade geometry.

In initial design several analytical semi-empirical approaches have been developed which attempt to capture the effect of heat transfer on the blade without the need for detailed CFD modelling. These approaches vary from 1-D to 3-D and in the detail of the geometry considered.

Heat transfer modelling in gas turbines can be detailed, including use of CFD [102] or an analytical [9, 103, 104, 105, 12] approach. Due to the computational cost associated with high fidelity CFD, much of the development undertaken in detailed heat transfer methods which have been developed by OEMs or licensed MRO establishments has not been published. A set of standard published correlations for different parts of the blade and disk assembly can however be used as a substitute for extensive CFD analysis. This method is reported in [7]; where it is considered that circular cylinder approximations would account for the leading edge heat transfer, while the trailing edge could be considered to be a flat plate and the tip gap could be considered channel flow. Heat transfer flows consid-

ered include the heating of the blade by the hot flow gases by convection , the convection through the multi-material blade and the cooling of the blade.

The results of the analytical approach are however more widely published, and generally use the standard blade model and assumptions developed by Ainley [103]. Early work on the standard blade model [103] assumed constant metal temperatures in the chord-wise direction, and radially constant inlet gas temperatures. Subsequent developments, both serial and parallel, extended the applicability by adding increased flexibility and variability of temperatures and flow profiles of combustion gas and cooling flows [104, 105], and thermal distributions though both metal [106, 107] and multi-layered blades including Thermal Barrier Coatings (TBCs) [104, 105, 108, 109]. Eshati [9] later introduced variation in flow properties of cooling air to his implementation and used his heat transfer model to link design and technology parameters to an assessed creep life. Eshati's model generates span-wise temperature distributions and heat transfer coefficients, for a multi-layered blade with TBC for both external and internal wetted surfaces. Abdullahi [12] applied Eshati's method to a flight path, by linking heat transfer input parameters to engine performance.

In this research, a simplified analytical heat transfer model is adopted, considering blade leading edge (hot side) and cooling hole (cold side). This method, originally developed by Eshati [9] for industrial gas turbines, and later modified by Abdullahi [12] for aero engine applications and validated against NASA E3 engines, uses an approach which considers a modified heat exchanger subject to heat flux [8], schematically represented in Figure 4.5. The method consists of a two part calculation, identifying the heat transfer between the blade and the coolant separately to the heat transfer between the hot gasses and the blade before combining them to determine the blade metal temperature. The model

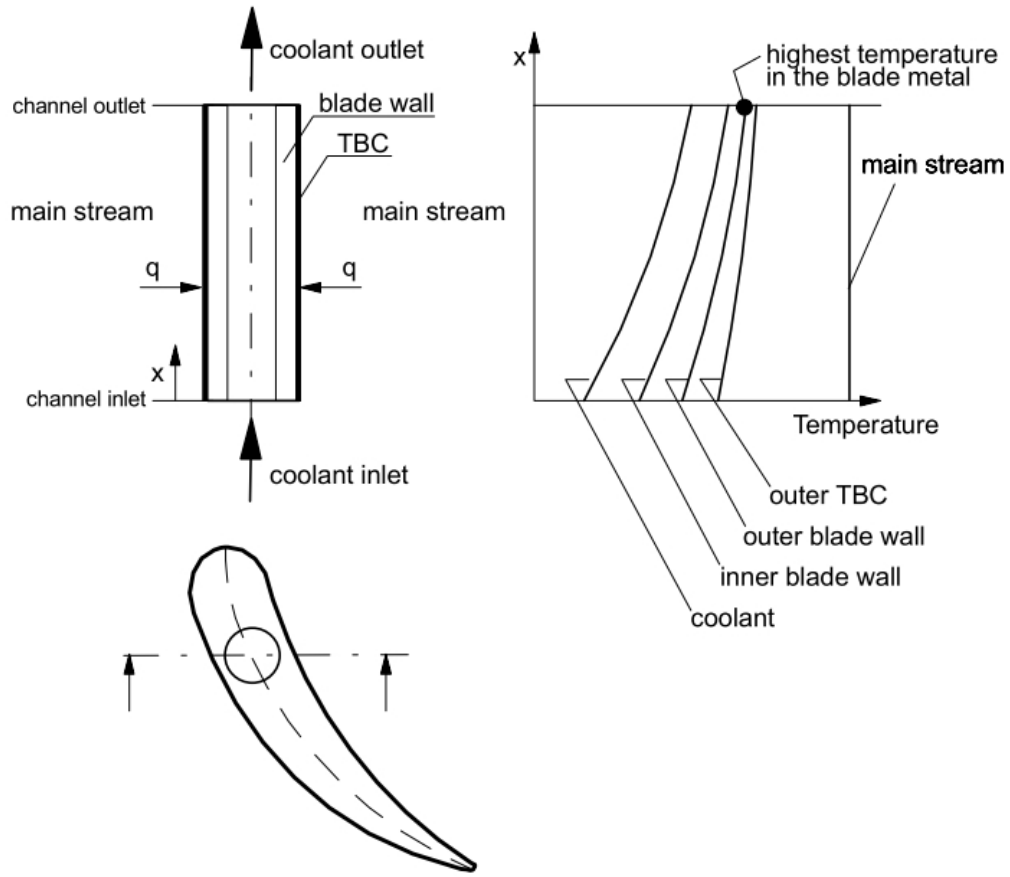

Figure 4.5: Schematic of simplified heat exchanger approach from Chiesa [8]

combines aero thermal parameter inputs from TURBOMATCH with blade geometry and material data to generate temperature distributions along the hot-side and cold-side blade spans. To facilitate the calculation while allowing for varying temperature along the blade span, the blade is subdivided into sections visible in Figure 4.7a.

The heat exchanger concept followed [8] defines the blade as subject to heat flux defined by the heat transfer coefficient of the gas flow (h_g) and the temperature difference between the gas and the blade hot side (T_{b_h}). The changing temperature profile through the blade wall is represented schematically in Fig-

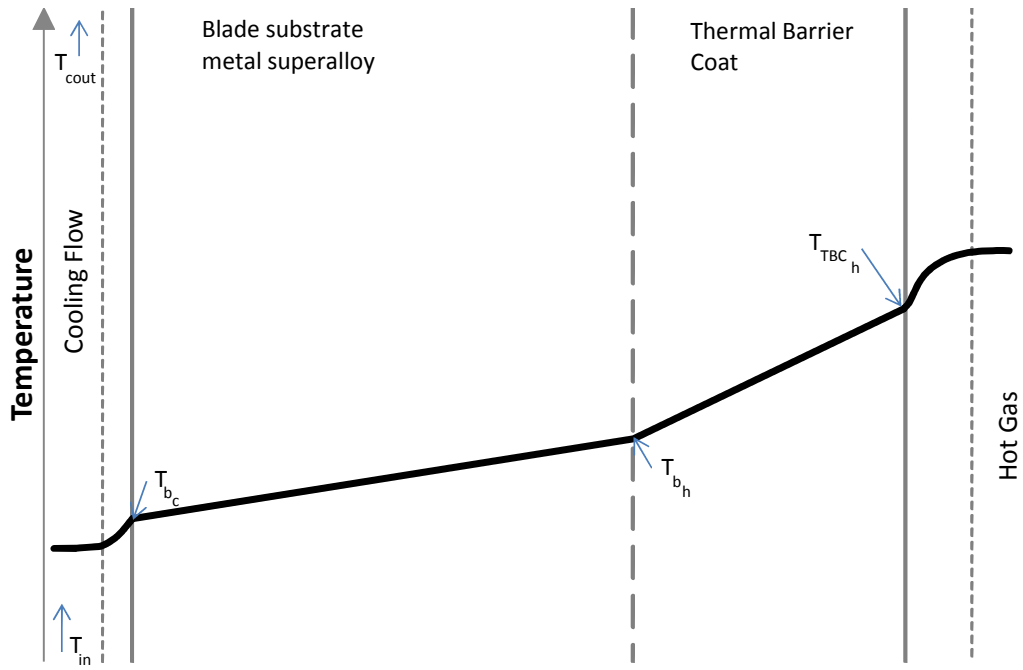

Figure 4.6: Temperature profile through coated blade wall, adapted from [9, Fig. 6-1] and [10, Fig. 8.18]

ure 4.6. Temperatures are assumed to vary span-wise but not chord-wise, thus capturing the inlet gas temperature variation due to flow mixing between the combustor exit row and Nozzle Guide Vane (NGV) cooling flow outlet, whose radial distribution is accounted for by the inclusion of a Radial Temperature Distribution Factor (RTDF). Cooling channel area is assumed constant. The coolant flow properties are functions of temperature and humidity. The gas flow temperature is considered as the gas recovery temperature (T_{gr}) to account for the irreversible conversion of kinetic energy to thermal energy in the turbulent boundary layer.

$$q_g = h_g.(T_{gr} - T_{b_h}) \tag{4.13}$$

The heat transfer of the blade is considered in four steps (Figure 4.5): between the gas and the hot side of the TBC, through the TBC, through the blade and

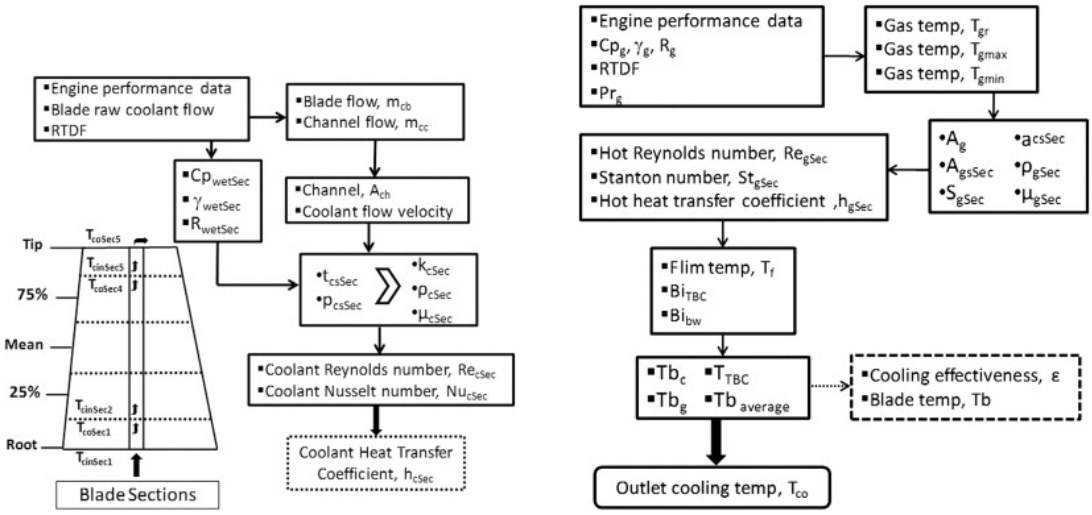

(a) Cold Side (b) Hot Side

Figure 4.7: Heat transfer processes defined by Eshati [11]

finally between the blade and the cooling flow. Following Ainley's assumption that the total rate of heat flow into an element is zero, the following set of energy equations can be applied:

From the gas to the hot side of the TBC considering the wetted area of the blade (A_g), giving heat flux (dq),

$$dq = h_g.A_g.(T_{gr} - T_{TBC_h}) \tag{4.14}$$

for the heat flux through the TBC, considering the TBC thickness (t_{TBC}) and thermal conductivity (k_{TBC}),

$$dq = \frac{k_{TBC}}{t_{TBC}}.A_g.(T_{TBC_h} - T_{b_h}) \tag{4.15}$$

again for the heat flux between the blade hot side (T_{b_h}) and the blade cold side

(T_{b_c}) considering its thickness (t_b) and thermal conductivity (k_b),

$$dq = \frac{k_b}{t_b}.A_g.(T_{b_h} - T_{b_c}) \tag{4.16}$$

and lastly for the heat flux between the blade and cooling flow ($T_{c_{out}}$) given the cooling wetted area (A_c) and coolant heat transfer coefficient (h_c)

$$dq = h_c.A_c.(T_{b_c} - T_{c_{out}}) \tag{4.17}$$

The heat transfer process followed is fully described by Eshati and Abu [11]. The key steps and assumptions can be summarised as follows.

Cold side heat transfer

The cooling system is defined in terms of its internal geometry and cooling flow properties given by the engine performance model TURBOMATCH (Figure 4.7a). The coolant blade flow (m_{cb}) and channel flow (m_{cc}) are calculated from the blade raw coolant flow, given the number of blades and cooling channels present. Coolant channel wetted area (A_c) is calculated as a function of hydraulic diameter (D_h) Coolant flow velocity calculation follows a process defined by Eshati [9, Appendix C], which iterates a non-dimensional mass flow ($1000Q$) and Mach number to determine absolute gas velocity (V_{Abs}). This is then used to determine coolant flow Reynolds (Re_c) and Nusselt (Nu_c)numbers given cooling flow density (ρ_c), and viscosity (μ_c), which combined with coolant flow thermal conductivity (k_c) and hydraulic diameter (D_h) permit the calculation of coolant heat transfer coefficient(h_c). Equations 4.18, 4.19 and 4.20 are applied to each section ($_{Sec}$) of the blade di-

vided as seen in Figure 4.7a.

$$Re_c = \frac{\rho_c . V_{Abs} . D_h}{\mu_c} \tag{4.18}$$

$$Nu_c = 0.15(Re_c)^{0.7} \tag{4.19}$$

$$h_c = Nu_c \frac{k_c}{D_h} \tag{4.20}$$

Hot side heat transfer

The hot side heat transfer process is then considered (Figure 4.7b), assuming the hot side gas flow to be dry. Radial gas temperature distribution is estimated using an RTDF and assuming that the gas flow minimum temperatures are at the blade root and tip, with a maximum at 75% span given a shift from mid span at combustor exit due to flow rotation and mixing with NGV coolant outlet flow, that gas flow temperature variations to maximum are linear and that rotor inlet temperature should equate to the mean temperature of the defined temperature points. The external Stanton number (St_g) for each blade section is used to enable the estimation of an average heat transfer coefficient (h_g) is calculated using Chiesa's [8, eq.22] empirical relation for turbulent flow, Equation 4.22, given flow Reynolds Number (Re_g) and the blade chord (c). Sutherland's Law is used to calculate the viscosity of the gas flow (μ_g).

$$Re_g = \frac{\rho_g . V_{Abs_g} . c}{\mu_g} \tag{4.21}$$

$$St_g = 0.285 Re_g^{0.37} Pr^{-\frac{2}{3}} g \tag{4.22}$$

$$h_g = St_g . Cp_g \left(\frac{m_g}{A_g} \right) \tag{4.23}$$

4.3.3 Simplified geometry

The exact design of gas turbine blades has a significant effect on engine performance, weight and balance. Increasingly detailed 3-D hot formed designs have been used to further reduce weight, and increase component lives.

While detailed blade design undoubtedly influences engine performance by changing heat transfer, losses, boundary layer and the effect of gas bending stressed, the specifics of the eventual design are unknown at the preliminary design stage [110].

Given the intention of establishing the effect of intended operational conditions on lifing at the preliminary design stage, a choice has to be made between implementing a detailed 3-D model for an incorrect blade, and adopting a simplified generic geometry.

For the purposes of a generic method, a simplified representative geometry with reduced detail is preferable: it reduces the required computational burden of FE calculations and minimises the required input data. Using a representative geometry for modelling is not considered beneficial. The principal benefits of a simplified geometry are the reduction in CPU time required for FE calculations, the ability to link back all inputs to the FE model to open data or previous model outputs (gas turbine performance, sizing and heat transfer) and the ability to avoid the requirement for full fidelity CFD modelling, further reducing the computational burden. This approach will however not be able to assess the detailed impact of stress concentrations.

Various approaches to simplified geometries have been considered. Hanumanthan et al. [7] considered a 2D geometry supplemented by a thickness profile, while Abdullahi [12] focused on 3D leading edges with cooling hole. The leading

edge is considered to be significant as it experiences the greatest heat transfer coefficients, and is a common source of failure. From the simplified generic perspective the leading edge also has the advantage of having the best defined gas properties derived from gas turbine performance modelling.

This 2D+Thickness was also used by Izquierdo [47] who confirmed the findings of Hanumanthan [18, 7] that failure (in Izquierdo's case, oxidation failure) being highly temperature dependent, occurred first at the hottest blade section: the leading edge.

The simplified geometry is to be used within the FE thermal and stress models, where it will be subjected to centrifugal and thermal loading. Given that gas bending stresses are to be ignored, simplified geometries are viable so long as constant cross sectional areas are maintained. This gives sufficiently accurate mechanical loading and thermal boundary conditions to emulate heat transfer conditions at the leading edge.

Blanchard [59] compared two forms of simplified geometry, a simplified semi-circular leading edge and a simplified turbine blade formed of a closed circular leading edge and with a flat plate blade, as seen in Figure 4.8(b & c). Given his assumption that there would be no heat transfer between the leading edge and the flat plate blade and considering the maximum Von Mises equivalent stress in each case, a difference of 1.5% was observed. This confirms the effect of constant cross sectional area on centrifugal stresses.

Corbo [48] compared the results from the 2D+thickness geometry to the simplified 3D leading edge geometry used by Blanchard [59] and found that where temperature was the only variable considered the two geometries generated surprisingly similar oxidation lives. When mechanical loads were also considered, lives of the 2D geometry were smaller than the 3D, and it was determined that the

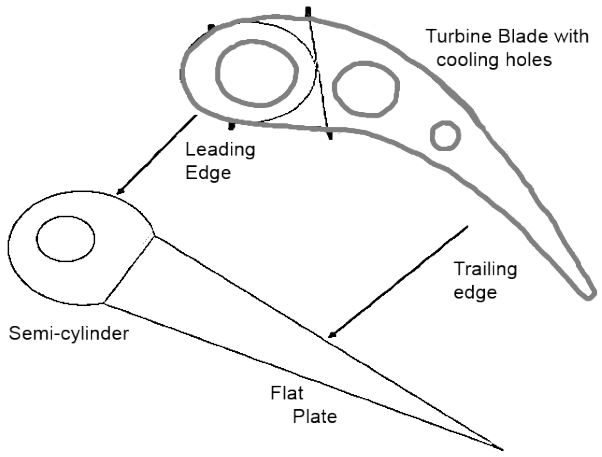

(a) Idealisation concept

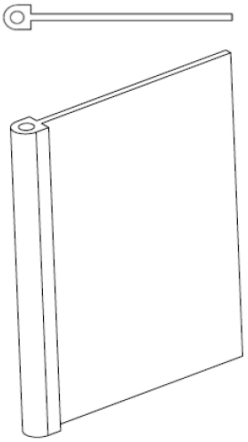

(b) Two part blade

(c) Simplified Leading Edge

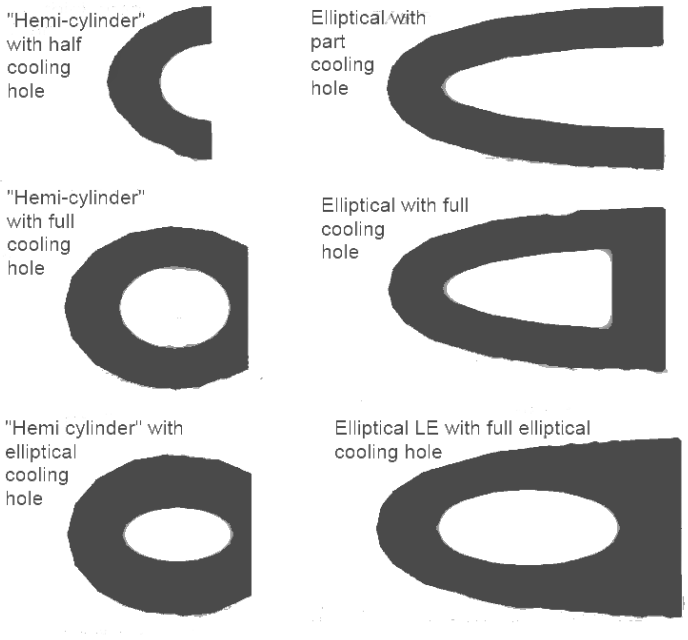

(d) LE geometries

Figure 4.8: Steps considered in geometry simplification

2D geometry tended to overestimate centrifugal loads at the leading edge.

Bagnall et al. [91] also consider the relative merits of 2D+thickness and simpli-

fied 3D geometries. They consider that, while the enhanced 2D methods benefit in terms of computational demands, 3D methods are necessary to capture the effects of temperature gradients, especially when considering cooled blades where thermal gradients induced by cooling can significantly affect component loading and lives.

Abdullahi [12] considered six variations of leading edge shapes (open/closed, circular/elliptical) for his simplified geometry and compared them against a fully detailed 3D geometry, sketched in Figure 4.8d. It was found that each geometry accurately captured temperatures and centrifugal loads, while stress concentrations were generated at sharp edges. In general the effect of geometry selection resulted in less than 7% variation in thermo-mechanical stress. This in turn resulted in a variation of predicted blade lives between 1.3 and 0.9 relative to the reference shape (a hollow semi-circle). When compared to a high fidelity 3D model, the simplified geometries were found to accurately predict temperatures and maximum stresses, but were not able to capture the stress reduction at mid-span due to the 3D nature of the blade (taper and stack angle). The simplified geometries provided conservative but accurate estimates of temperature and maximum stresses. Within the study it was also established that the accuracy of boundary conditions used within the FE stress and thermal models was a more important contributor to the resulting stresses and lives than the accuracy of the geometry.

4.3.4 Materials Selection

Davenport [78], identified the selection materials property definitions as one of the three key drivers of life estimation accuracy, alongside service history and

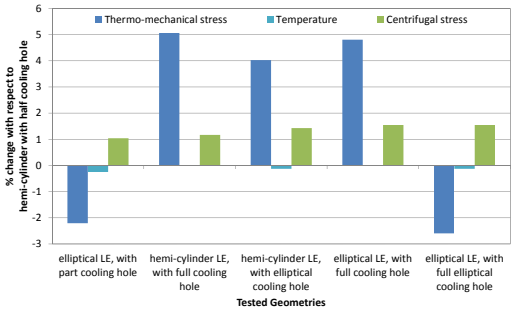

(a) Simplified geometries compared with selected geometry simplification

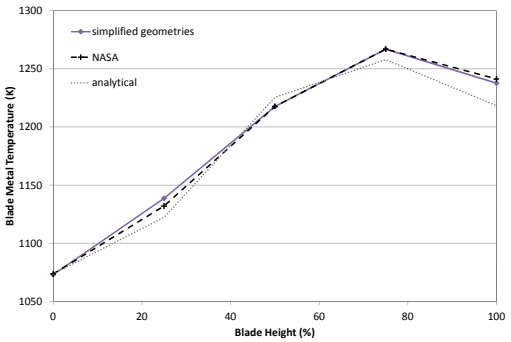

(b) Blade metal temperature

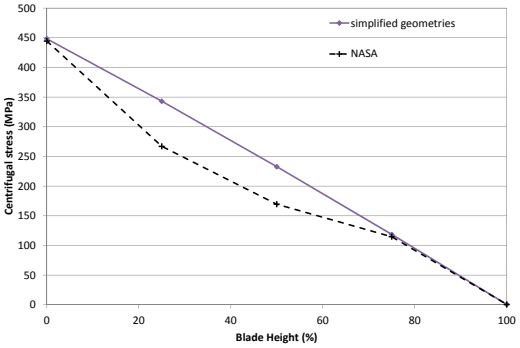

(c) Centrifugal stress

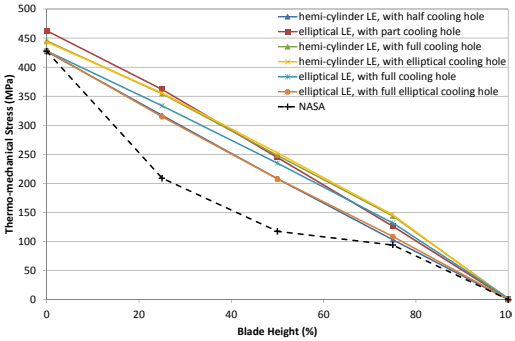

(d) Thermo-mechanical Stress

Figure 4.9: Simplified geometry selection and validation based on [12]

safety margin definitions. Materials definition can be considered on several levels, including how they accurately reflect the “real” material installed by capturing manufacturing processes, micro-structural flaws and handling, and whether they are sufficient to allow life estimation at the load conditions considered, given the material property requirements of the mechanism models employed.

Tinga [96] identifies materials data scatter as the key contributor to inaccuracy in his integrated lifing analysis method due to the scatter in the experimental material data used. Where necessary he endorses the use of isotropic alloy data when single crystal super-alloy materials data are not available. This is frequently the case in the application of models using only public domain data as the spe-

cific anisotropic materials definition of single crystal materials are dependent on the crystal growth process as well as the alloy used: this is usually considered commercially sensitive and therefore remains unpublished.

Materials properties defined for thermal and mechanical FE analysis of gas turbine blades must be temperature dependent, and should include thermal conductivity, density, thermal expansion, specific heat, Young's Modulus, Poisson's Ratio, and yield strength. It is essential that the range of temperatures over which these materials are defined is larger than the range of temperatures at which the FE analysis will be conducted so as to avoid significant extrapolation errors.

In his review of TMF models, Blanchard considered materials properties definitions to vary and classified them in terms of material type for each "designated material" (conventionally cast, directionally solidified and single crystal). He also considered materials constants unique to each material and lifing model. Some models might require material specific constants, derived from experimental testing, which are not available in public literature for a material of interest.

Further work has however determined that in spite of the fact that, in some cases, models can require a significant number of materials constants, not all of these are significant to the model result. For example, the Neu and Sehitoglu TMF model [70, 71] originally required 20 materials constants, however, work by Amaro [68], and later by Abu [111] identified that only four or five of the parameters were significant. (The fifth parameter was identified by Abu, as being specific to the the impact of a flight mission profile on environmental damage phasing. This was missing from the Amaro analysis, which considered only out-of-phase load conditions.) In the studies by Abu [111] and Alia [112], oxidation (environmental damage) was the limiting mechanism. Use of the four or five critical parameters, with optimised values for the other 15 constants assumes that this the relative

damage incurred in the blade remains limited by oxidation. Were the damage to become fatigue limited for example, other parameters would become significant [112, Appendix C].

Although in-service analysis of lifing would permit experimental testing of components, or test samples of appropriate materials, some compromises must be made in the determination of materials for modelling for estimation at the design stage, prior to material and manufacturing process selection. The following factors are therefore considered essential in the selection of material for integrated lifing and severity analysis:

- availability of suitable range of temperatures (greater than operational range to be studied) for temperature dependant material properties

- availability of model specific, significant material constants

- consideration of material of suitable type, such as nickel-based super alloys

Due to these restrictions, at least at this stage of proof of methodology, the materials available for modelling are limited by those for which significant public domain data is available. These tend to be older materials, which will tend to result in lower, more conservative lives.

The limited availability of significant materials constants for the Neu Sehitoglu TMF model, when applied to nickel-based super alloys, has determined the selection of MAR-M247, as the base substrate metal in the FE and subsequent life and severity modelling conducted.

4.4 Implementation

While severity or relative damage estimation has been established as a useful tool for comparing the effect of operations on gas turbine component life, degradation and therefore maintenance requirement and operational costs, it is important to consider the combined effect of the assumptions and limitations inherent to the methodology.

In combining the series of tools necessary for severity estimation, including aircraft and engine performance models, heat transfer methods, FE modelling and post processing, lifing and damage accumulation, the method is limited in its accuracy by that of the least accurate tool or method employed in the series. Each tool will tend to amplify the errors and inaccuracies present in the previous steps of the process.

Tinga et al. [76] who follow a similar integrated analysis process to determine lifing for OCM or mission comparison, consider that the lifing step will be responsible for the greatest error in accuracy (between 20 and 50%), though they attribute this not to the lifing methods themselves, but to their dependence on materials data from experimental sources, and the lack of data available for the desired materials leading to analysis of simpler materials.

The accuracy of the lifing results, in this research, is also limited by by the availability of materials data, which imposes the requirement to study materials for which sufficient data is available and is subject to the accuracy of that materials data. Where possible, the number of material data variables has been limited, following the adoption of parametric study results identifying the material parameters which are significant to the lifing models employed.

Common to the damage accumulation methods employed is the assumption

that the effect of stress distributions throughout the component due to existing damage or previous missions can be neglected. In other words each damage increment is independent of previous missions. This assumption leads to a conservative estimation of life. Further, it is generally assumed that the interaction between failure mechanisms can be neglected (except in the application of some TMF models).

While these primary assumptions could be deemed to limit the accuracy of the lifing results generated, it is considered that they have only a peripheral effect on the trends of relative damage and severity calculated and used for further analysis. The limitations resulting from the use of simplified material property inputs are only a constraint to the proof of methodology cases described here, and not a limitation of the methodology itself.

Chapter 5

Engine-Related Operating Costs

In this chapter, a brief summary of the open literature will be presented to establish the principal engine-related operating costs, by considering the commonly used cost classifications and their respective links to operation, and to present an overview of the cost models available in the public domain. Engine aging and maturity and their effect on engine maintenance requirements, and resulting costs will be considered.

5.1 Cost definitions and classification

In this research certain commonly used terms are used for specific purposes. In particular cost, value and price represent distinct concepts. Price is deemed to represent the amount paid at acquisition by the purchaser. Different purchasers of the same product may pay different prices depending for example on purchase volume, and other negotiating factors including multinational political effects. In the private, business and military aircraft markets, cost-based (or cost $+$) pricing

is common (though not universal), such that a

$$\text{Price} = \text{Cost} + \text{Profit} \tag{5.1}$$

relationship would be common. In the commercial transport market however a market value approach is more common [113] such that:

$$\text{Market Value} = f(\text{Performance}, \text{Operating Cost}, \text{Competition}, \text{Passenger Appeal}) \tag{5.2}$$

Pricing is of primary importance at system acquisition, although part pricing can be significant through life and the relative prices of Original Equipment Manufacturer (OEM) replacement parts and Parts Manufacturer Approval (PMA) replacement parts can contribute to differences in maintenance costs through life. “Book price” or “list price” is rarely the actual cost paid for parts, especially as many parts are supplied under contract, accruing a bulk or contractual discount, and all prices and costs are subject to the variability of the raw material markets, foreign exchange markets and inflation.

While, simply, cost might be considered to be the amounts expended and declared in tax returns or company accounts, in the case of engine-related costs not all expenditure will be made by the operator. During an engine’s serviceable life several entities may contribute to the engine-related operating costs. The manufacturer will be responsible for certain costs during the warranty period and during any recall programmes. In the case of leased engines, the distribution of payments between the owner and operator will also vary specifically with respect to upgrade programmes. Cost is also used to define the sums expended in Research, development, test and evaluation (RDTE) and manufacture.

5.1.1 Cost classification

In literature, several classification frameworks are applied to costs. The key differences are based on:

- the position of the engine in its life-cycle
- the position of the engine type in its development cycle
- the relative position of the engine within its operating fleet
- the author's role or business function

For a given engine/aircraft pair, it would be feasible that the operator, owner, manufacturer and Maintenance, Repair and Overhaul (MRO) provider of both the engine and the aircraft would be studying the operating costs, simultaneously, but using different classification frameworks.

Common classification frameworks distinguish between costs that are:

direct	or	indirect (burden/overhead)
fixed	or	variable
recurring	or	non-recurring
sunk	or	reserved
capital	or	operating

Even where authors agree on a classification vocabulary, it is common for costs to be attributed differently within them. For example, an operator who owns, staffs and manages their own maintenance facility will have significant overheads due to staffing, and maintaining the facility and its equipment, whether or not it is in use. An operator who outsources the same work, may either consider these costs to be direct and attributed to the engine operating period prior to or

subsequent to overhaul, or they may divide the contractual cost into direct and indirect portions.

Operating costs are sometimes grouped into a Cash Airplane Related Operating Cost (CAROC) measure, and may distinguish between crew, fuel, maintenance, landing fees, ground handling, equipment depreciation and maintenance as well as control and communications systems costs. These costs can be subdivided into Airplane Related Operating Costs (AROCs), Passenger Related Operating Costs (PROCs), Cargo Related Operating Costs (CROCs) and Systems Related Operating Costs (SROCs) such that:

$$\text{CAROC} = \text{AROC} + \text{PROC} + \text{CROC} + \text{SROC} \tag{5.3}$$

The CAROC measure is commonly used by operators and manufacturers as a means of evaluating the relationship between predicted and actual operating cost for in-service fleets, as well as an input to market value predictions such as that produced by Markish [114], which links market value of commercial transport aircraft to range, payload and a function of CAROCs:

$$Price = k_1(\text{Seats})^{\alpha} + k_2(\text{Range}) - f(\text{CAROC}) \tag{5.4}$$

where the constants k_1, k_2 and α are vary depending on the aircraft type and are determined through data set regression.

In this research, the cost focus is on those costs which can be directly attributed to the engine and vary with engine operation: maintenance and fuel.

Fuel is a significant contributor to Engine Related Operating Costs (EROCs), but its relative importance to the Direct Operating Cost (DOC) varies significantly.

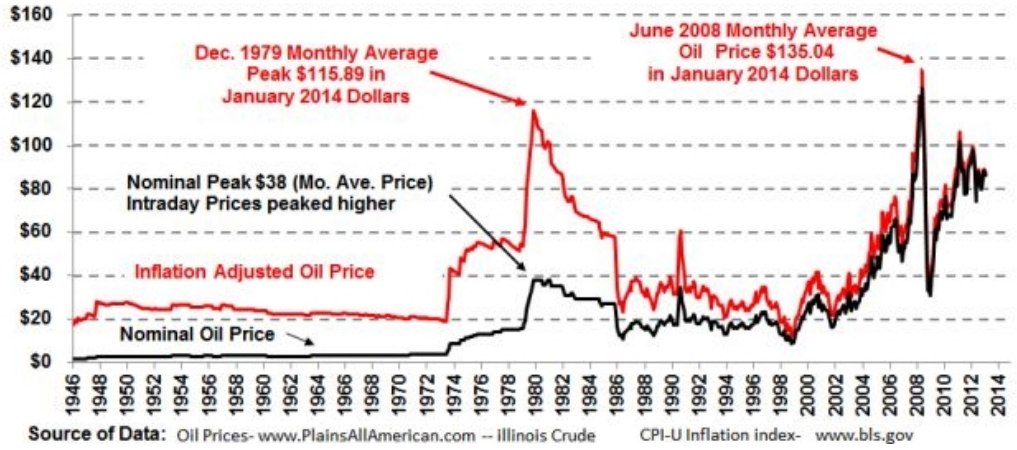

Figure 5.1: Historical variation of monthly average crude price including inflation adjustment [13]

Sefarty [115] concluded that the effect of a variation of between 60 and 100 $/barrel in fuel price would change the fuel share of DOCs from 36% to 48%. The actual impact of fuel price variation on DOC is likely to be greater than that considered by Sefarty given actual variations in fuel prices (Figure 5.1). Fuel price also varies daily depending on the airport and provider of each fuel uplift. As the cost of fuel is so significantly influenced by the trading markets and the global economy, in this research it will be considered in terms of weight/volume rather than price.

Maintenance costs and Specific Fuel Consumption (SFC) are therefore identified as the key EROC components.

5.2 Engine Maintenance

5.2.1 Measures of engine maintenance

Engine maintenance costs are commonly defined as a function of cost and Engine Flight Hours (EFHs): $\frac{\$}{EFH}$. This formulation simplifies the integration of maintenance costs into accounting assessments using tools such as Net Present Value (NPV).

An NPV calculation permits the determination of the net present value of future cash flows associated with a given project, such that for a project running over a period T broken down into time steps $t = 0, 1, 2, \ldots T$ (commonly years or months), subject to cash flows C_t in each time step and given a discount rate r to account for the opportunity cost of capital, had it been spent on another (often lower risk) project .

$$NPV = \sum_{t=0}^{T} \frac{C_t}{(1+r)^t} \tag{5.5}$$

In practice published values of Direct Maintenance Cost (DMC) presented as $\frac{\$}{EFH}$ are not always comparable as the costs and timescales applied vary significantly in number and meaning. Shop Visit Rates (SVRs) are used in association with DMC in an attempt to clarify the applicability of the DMC measure under consideration, however, while in the concept of a SVR is simple: either the number of Shop Visits (SVs) in a set period or the interval between successive SVs, in practice, when applied to a fleet or derived from aggregated data sets, it's actual derivation and therefore source can lead to it being miss-used and confusing.

SVR is accepted as a measure of engine reliability and is commonly expressed in two ways:

SVR is often referred to as diluted-SVR or popular-SVR, and is defined as the

ratio between the number of shop visits in a fleet and the total fleet flying time within a set time period (T). It is often annualised, or calculated as a rolling 12-month average. It is a measure deemed representative of the aging process of the whole fleet under consideration, but, it ignores the mix of age and usage within the fleet.

$$SVR(kEFH^{-1}) = \frac{\sum_{t=0}^{T} SV_{fleet}}{\sum_{t=0}^{T} EFH_{fleet}/1000} \tag{5.6}$$

The Mean Time Between Shop Visits (MTBSV) of such a fleet, in EFHs, is frequently calculated from this SVR such that:

$$MTBSV(EFH) = \frac{1}{SVR}.1000 \tag{5.7}$$

and is then considered to be a measure of the engine fleet average Time On Wing (TOW). The DMC can be considered a function SVR such that it is frequently though simplistically presented as:

$$ShopDMC(\$/EFH) = SVC(\$).SVR(kEFH^{-1}).1000 = \frac{SVC(\$)}{MTBSV(EFH)} \tag{5.8}$$

rSVR is referred to as non-diluted-SVR or Restored-SVR and is used as a mean of assessing on-going costs of maintenance. It is defined as the ratio between the total number of SVs having occurred during a set time period and the number of hours flown by the overhauled engines since the last SV. It is considered that rSVR more closely represents an average measure of TOW between removals than does SVR.It is only applicable within a fleet, and is

smoothed by the fleet mix of age and utilisation.

$$rSVR(kEFH^{-1}) == \frac{\sum_{t=0}^{T} SV_{fleet}}{\sum_{t=0}^{T} EFH_{fleet_{since\,SV}}/1000} \tag{5.9}$$

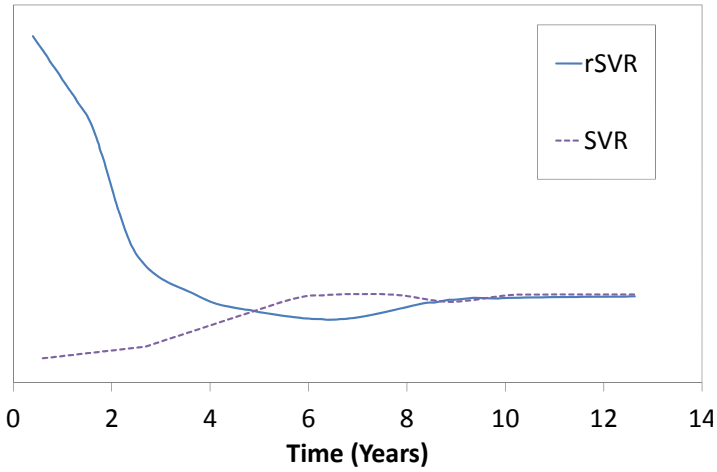

Figure 5.2: Sketch showing effect of fleet age on shop visit rates, adapted from [14]

Studies that use SVR and rSVR commonly define and engine fleet to be mature once $SVR = rSVR$. This definition is only applicable in fleet studies as the rSVR calculation is not valid for single engine studies. Other definitions exist for maturity, such as those considered by Dixon [116, 117] and discussed further in section 5.4.3. Maturity is intended, whatever its derivation, to identify the operating phase in which SV Costs and Intervals are relatively constant, however, it is definition dependent and maturities should not be compared unless it can be clearly established that they follow the same definition and derivation.

Both shop visit rate measures (SVR and rSVR) are often presented as representative of TOW, though as can be seen from Figure 5.2, the discrepancies between them, lead to their use primarily to assess a so-called mature TOW related to a mature SVR (mSVR), which once combined with an average ma-

ture Shop Visit Cost (SVC) allows the application of Equation 5.8 to calculate a average mature maintenance cost per engine flying hour. By definition, engine maintenance costs derived in this way are not capable of determining the effects of age or operation on the resulting bulk aggregated fleet mixed costs.

Inherently, while defining engine maintenance costs as DMC($\$/EFH$) might appear straightforward, several DMC values are unlikely to be comparable. While DMC is clearly a measure of cost per unit time:

Costs considered could be shop visit costs, but may also include other maintenance actions. Where it is restricted to SV costs, these may be for a specific SV, or an average SV, or an average mature SV, the last also depending on the definition of maturity used. Otherwise, the cost could be a through life total cost, or a fleet average (with inherent age and utilisation mix), or it may be a fleet expenditure during a given interval.

Time considered will usually be EFH, but may also be aircraft rather than engine based. It is often a measure of TOW, but this can be an average, a mature average, a fleet average, or a utilisation rate for a give period.

While it is accepted that both the cost of shop visits and the intervals between them affect the overall costs, reducing SV cost alone is insufficient. Decreasing the cost of a shop visit can lead to significant reduction in the subsequent shop visit interval, and thus to an overall reduction in TOW increasing costs when assessed per flying hour, as represented by the sketch in Figure 5.3. While increasing time on wing increases shop visit costs, it tends to decrease the cost per flying hour.

In this research, to fulfil the intention of allowing all cost measured to be traced back to engine operation, it is deemed that the SVR and rSVR measures are sig-

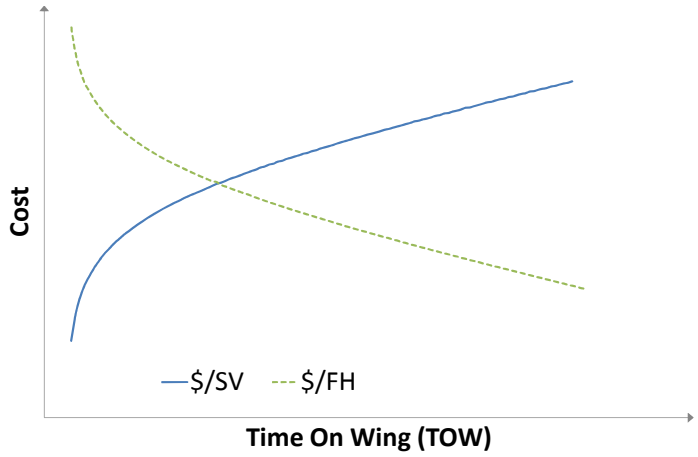

Figure 5.3: Effect of TOW on Cost when considered per SV or per FH

nificantly limited by their derivation from aggregated fleet data without accounting for fleet age and utilisation variations. While these measures are undoubtedly useful for accountancy and financing studies, they do not offer the option of distinguishing between operating effects and aging effects. As such they are not used as inputs to this research.

However, much understanding of the linked relationships can be gained from considering the key principles that lead to the use of SVRs. Specifically, that the cost of maintenance should not be considered in isolation, but must instead be coupled with the TOW or SV Interval, if an understanding of through life cost of maintenance is to be achieved.

5.2.2 Types of engine maintenance

Aircraft engines undergo regular and planned servicing, maintenance, repair and overhaul as well as unscheduled maintenance due to failure or accidents.

Each of these tasks may occur, to a certain degree, with the engine either installed (on wing) or removed to an engine maintenance facility (off wing), though

some MRO tasks can only be completed on un-installed engines. They may also be either scheduled or unscheduled.

In this project the following definitions are adopted:

Inspection assesses the condition of parts following established plans, schedules and methods and triggers certain maintenance tasks using non-destructive techniques.

Monitoring refers principally to the inspection of electronic systems and their data caches. Increasingly, monitoring is continuous and carried out remotely. Monitoring is also used to refer to the process of assessing On Condition Maintenance (OCM) parts for incipient cracks.

Servicing includes the replenishment of consumables and cleaning.

Maintenance, Repair and Overhaul (MRO) is both a service industry supplying the aviation market, and a reference to the services that they provide, though these are also frequently managed by airlines themselves.

Maintenance actions can be scheduled and unscheduled as well as preventative or corrective and include all actions required to maintain operability.

Repair involves the re-working of deteriorated or damaged parts, for example the replacement of Thermal Barrier Coatings (TBCs), or work required after failure.

Overhaul of engines involves removal from the aircraft for tear-down, maintenance and repair, also referred to as SV

Models exist in the public domain which account statistically for Unplanned Engine Removals (UERs). These are primarily attributed to Foreign Object Dam-

age (FOD), and bird strikes as well as equipment failure. These rates tend to be relatively low and can be accounted for statistically as a risk parameter if required, but their random nature does not allow them to be usefully correlated with engine operating regimes. In some models they are included in a bulk low incidence constant failure rate parameter [26].

To assess the effect of engine operation and maintenance planning decisions on the through life maintenance costs of an engine, this work focuses on MRO carried out during the planned Shop Visits (SVs) of commercial aircraft engines. In this case planned Shop Visits (SVs) include maintenance due to performance deterioration and Life Limited Part (LLP) replacements. These are sometimes considered by other authors to be unscheduled [6, 26].

This research therefore focuses on scheduled or planned engine removal and shop visit, sometimes called overhaul, and the maintenance, repair and replacement tasks which each such visit requires.

5.3 Engine Shop Visits

Modern gas turbine engines are only infrequently removed from the aircraft to an engine shop for overhaul. The tasks carried out during a shop visit are identified on the SV Workscope. These task broadly fall into two categories: component replacement (including LLPs) and performance restoration.

Increasingly modern engines are formed of modules, which can be maintained, restored or repaired individually without the need to tear down the rest of the engine. Replacement of LLPs within a module will often be accompanied by restoration of that module, since the LLP replacement will require the removal and tear down of the module.

The workscopes of successive shop visits will vary in terms of which parts and LLPs are replaced and the level of restoration conducted. These will vary with the age of the engine, its utilisation and operating environment, amongst others.

Broadly, a shop visit can be considered as containing six stages:

1. Induction and inspection
2. Disassembly
3. Piece part inspection
4. Repair
5. Reassembly
6. Testing and inspection

These stages, presented graphically in Figure 5.4, are not necessarily linear and may overlap, especially when modular engines are considered. Modules and components which are repaired are often replaced on the engine by comparable units so that the shop visit does not stall waiting for the return of repaired parts. This and the availability of new spares are significant considerations for those organising SVs.

A workscope identifying the tasks to be completed at a given shop visit is not final, as it may be supplemented by tasks, the need for which is only identified during maintenance. Tasks on the workscope can therefore be considered in terms of two cost parameters, the cost of parts and materials required for the task, and the cost (in hours) of the labour required to carry it out.

The costs of this task will vary over time, as raw material costs and labour rates vary, by geography (logistics, availability of spares and labour rates) and by

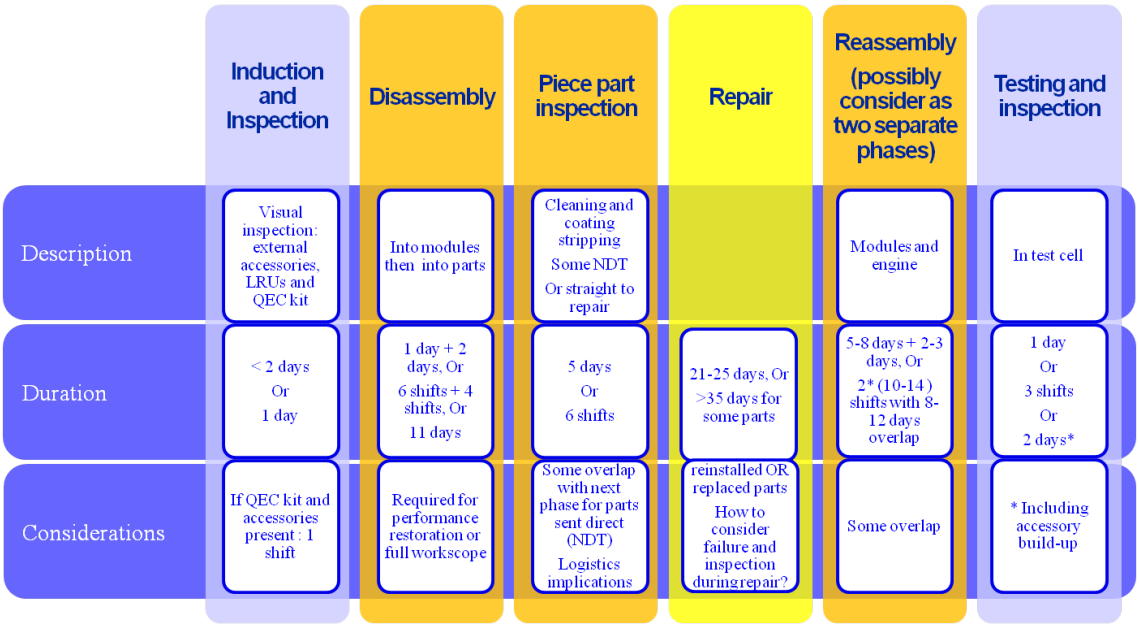

Figure 5.4: Shop visit process and tasks based on [15]

maintenance facility (in house or outsourced). Further, the cost of the maintenance to the operator will be affected by the length of the period during which the engine/module/component is unavailable. This interval will be correlated with the labour required, but may be determined by other organisational factors such as spare supply logistics and the availability of maintenance facilities.

Shop Visits (SVs) can be triggered by in-flight shut down of the engine, component failures, fixed inspection or service intervals, hard-time limits (such as those applied to LLPs), and deterioration of operating performance margins (temperatures and efficiencies). Whatever the SV trigger, it determines the minimum workscope required during the SV.

Considering the SV trigger alone and the ensuing minimum worskcope can lead to additional SVs and maintenance costs as the subsequent shop visit my be prohibitively soon after the engine returns to service. The effect of dealing only with the minimum maintenance need became apparent in the 1980s with

the introduction of quick change modules, which, when managed independently without consideration of incipient maintenance need in other modules, led initially to increased engine removal rates [118].

The principal factor that must be considered when determining additions to the minimum workscope is the desired interval to the next SV, referred to as the "build goal". Setting the build goal is a planning decision and may be influenced by availability of and demand for the engine and/or aircraft within the fleet or the maintenance facility. Once a build goal has been set, any maintenance due prior to build goal will be added to the current SV work-scope.

The build goal decision will both increase the cost of the current shop visit, and result in additional costs when maintenance is considered on a $/EFH basis over the preceding interval. For example, if an LLP set is removed before it reaches its life limit (L_{LLP}) then the cost per EFH of this LLP set will be deemed to have increased by a factor of $\frac{n}{1-n}$ where the stub life (L_{stub}) "lost" by pre-limit removal is defined as a function of the life limit such that $L_{stub} = n.L_{LLP}$, where $0 < n < 1$. However, the actual cost of early removal is mitigated by the costs saved in not having to remove the engine from service again later: namely, the costs of the additional shop visit, and of the loss engine availability. A further SV just to replace this LLP set will be disproportionately costly, as a significant portion of the SV costs, including those related to induction, inspection, reassembly, test and re-inspection , are incurred irrespective of the work carried out. In practice, within a larger engine fleet, this stub life may not be lost at all, as LLP sets are moved between engines so as to synchronise the life limits installed on each.

A similar loss is associated with restoration work carried out before its associated performance margin has been exhausted. Workscopes and build goals are commonly managed, where possible, so as to synchronise LLP replacement and

restoration work, but final decisions can be driven by organisational and contractual demands rather than minimum cost considerations.

Each shop visit therefore is both dependent on previous operation and maintenance, and will affect future maintenance and operational capacity. While the cost of a given shop visit might be minimised, it might, by its effect on future maintenance, increase the through life shop visit costs. The impact of engine maintenance choices on future costs results in lease contracts that are particularly stringent in terms of maintenance standards, part supply (OEM or PMA) and subcontract, given that engines hold their value better than airframes, especially when maintained with OEM parts [119]. This relationship is illustrated in Figure 5.5 which compares the value of a narrow bodied airframe to the two engines with which it is fitted.

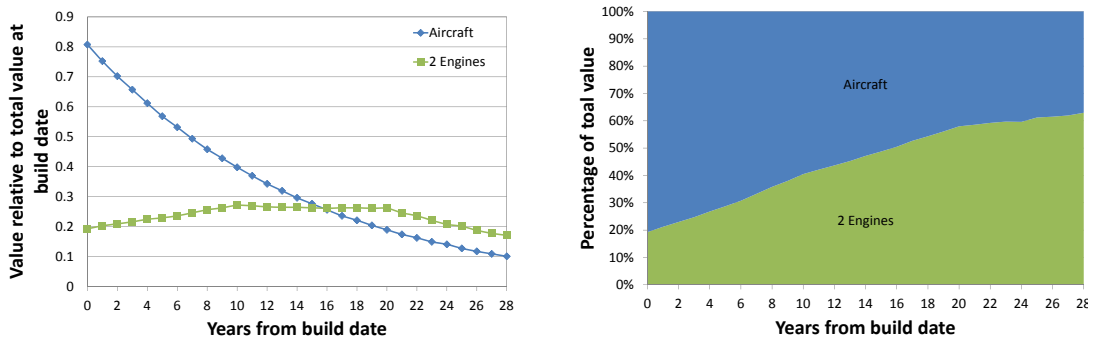

(a) Expected change in value with age (b) Expected relative values

Figures adapted from data [17, (2009)] for a narrow body aircraft (2007 build date) and its two engines using 2.5% inflation base for future values.

Figure 5.5: Effect of age on aircraft and engine values

These considerations give rise to the two most common goals or policies in work-scope planning:

- minimising the cost of this Shop Visit (SV) (SVC)
- minimising the lifetime Direct Maintenance Cost (DMC).

Given that DMC is a function of both SVR and SVC, and considering that Time On Wing is of value to an operator, as it reduces the number of spare engines required, the following workscope planning goals are also common:

- maximising lifetime availability
- maximising next interval on wing

It has been demonstrated that focusing solely on on the costs of the shop visit rather than the through life cost of maintenance considering SV Cost and TOW can increase the cost of maintenance per hour by approximately 14% [120, 121]. Optimising individual SV Costs is considered in this context to be only of short-term benefit (cash flows) rather than term longer term benefits in terms of availability offered by maximising TOW.

5.4 Engine maintenance cost model review

A review of engine maintenance cost models was conducted in collaboration with MSc students within the research group [122] [123] [124]. The purpose of the review was to identify key maintenance cost drivers and to assess the sensitivity of public domain models to technological and operation parameters.

Key factors considered during the cost model review include the purpose of the model, specifically the business function for which they were developed and the Life Cycle Cost (LCC) during which they are intended to be applied, and the data inputs that they require. These in turn determine their applicability to use within a physics-based framework aimed at assessing the effect of engine operations and the basis on which they can be compared with each other.

Maintenance cost models are sometimes self-contained, but are also often included as part of DOC, financing, leasing, CAROC or LCC models. Eden [125] considered that all shop visits, whether scheduled or un-scheduled affected "economy", whereas in-flight shut-downs and delays affected "reliability", and further that these two measures alone were sufficient to assess the operational performance of aircraft engines. Conversely, Willis and Sewall [26], consider that "reliability" is a function of failures due to lifing mechanisms not integrated into LLP limits (referred to a "new-mode" failures), while LLP lives determine "durability". Because these terms are used diversely for different purposes in the literature. This can lead to confusion and they will be avoided where possible.

Many publications address the estimation of engine related maintenance costs. They can be considered early (1950s-1990s) or more recent.

The early publications are primarily commercial, originating from airlines [126, 127, 128] and industry associations [129, 130, 131]. Some are from research bodies including National Aeronautics and Space Administration (NASA) [132]. They generally depended on databases of industrial data with restricted availability in the public domain [131, 1]. On closer consideration however, most of these models can be traced back to a single cost model published by the Air Transport Association of America (ATA) [130]. In the 1980s, there was a surge in studies of military engine costs conducted by manufacturers [6, 25, 28, 26, 27, 24] related to unexpectedly high maintenance requirements. These lead to the development of the Operation and Support Cost Analysis Program (OSCAP) LCC model, which integrates the Operating Severity Analysis Program (OPSEV) severity codes described previously, and focused on the link between specific mission profiles, severity and resulting costs. More recently, there is a significant trend toward large data and its analysis in publications, considering both military and commer-

cial aviation. These models often develop Cost Estimating Relationships (CERs) [133], which are then used for cost prediction.

Considering the models reviewed, the following categories were identified to support discussion and comparison:

Bottom-up methods [134, 135, 136], referred to as "analytical" methods in the review by Yee May Goh et al. [20], are used by manufacturers during the Acquisition (ACQ) and Operation (OPS) phases of engine life cycles to calculate operation and supports cost predictions, often within the context of warranty of full service costing. The methods require detailed knowledge of the engine systems and components including full Bill of Materials (BOMs) as well as life and predicted usage data, maintenance, repair and replacement costs in terms of labour and materials contributions.

Conceptual methods [129, 137] are applied at the initial design stage, require a minimum of inputs and apply statistical methods to generate high level trends. These methods can be similar to those categorised by Yee May Goh et al. [20] as "intuitive" or "expert opinion approaches".

Analogue methods [137, 138] can be applied by manufacturers and operators at the design or acquisition phases of new systems that are part of closely related product families. Where a bottom-up method exists for a previous variant, which does not differ significantly in technology level or performance, these methods can be very reliable.

Parametric methods [130, 131, 132, 128, 1, 138] represent the majority of public domain models, and are sometimes referred to as "empirical", "statistical" or CER methods [133]. They rely on large databases of aggregated usage

and cost data, some of which may be publicly available. They are primarily used by operators and their trade bodies, throughout the operational phase of engine life cycles, but are also used during preliminary design to compare design options. Their dependence on large data sets limits their applicability to engine types with similar performance and technological levels as those within the data set.

The aggregated nature of the usage data considered, often by airline fleet, leads to models which can identify correlations between trends in operating patterns and cost. It would be unreasonable to determine causation from such data. Additionally, much of the cost data in such models is derived from aggregated maintenance expenditure reported by commercial operators for tax purposes (for example in a CAB form 41 return). As such, this data does not consider expenditure by manufacturers under warranty, or recall, and the expenditure on maintenance in a given tax year, is also not necessarily representative of the maintenance need accrued due to operations in that year. Lacey [139] warns that such uses of these data sets are commonly mis-uses, and unqualified conclusions drawn from these sources can therefore be highly misleading. Where these models use aggregated data for the engine under evaluation at previous life cycle phases, these are considered by Yee May Goh et al. [20] to be further identifiable as “extrapolation models”. Some authors who generate CER go so far as to consider their models explanatory rather than predictive due to the limitations of the data sources available and the regressive nature of the analysis [140].

There is clearly some significant overlap between these classifications. Both conceptual and parametric methods use statistical tools including regression.

While the bottom-up methods require a large set of data inputs for the engine to be assessed, the analogue approach will often require similar data for a previous engine in the family, and additionally will require definition of changes.

Overall the classifications established in this study align well with those determined by Yee May Goh et al. [20] during their review which included cost modelling throughout engineering literature. Data required by these models can be broadly labelled as cost, schedule and technical inputs.

Yee May Goh et al. note that the uncertainty in these models is primarily epistemic data input uncertainty, caused by the lack of knowledge about the behaviour of the system and the true values of parameters, variability in the data, linguistic vagueness in definitions, data source ambiguity and imprecision. They also suggest that scenario uncertainty must be considered when these models are applied to the prediction of future costs.

The ”virtual workshop” approach developed in this research, is intended to combine the deterministic nature of the bottom-up method, with the use of a limited input data set, commensurate with that available at the early design stage.

5.4.1 Engine-Related Cost Drivers

The review of engine-related cost models also identified the key cost drivers from literature and published models. For this purpose, cost drivers are deemed to be any decisions made during the Research, development, test and evaluation (RDTE), Acquisition (ACQ) and Operation (OPS) life cycle phases which influence engine related operating costs.

The cost drivers identified are categorised in this research depending on when during the life cycle they are set, how they are determined and who made the

decision.

Technical drivers include engine design choices including materials selections, implementation of novel technologies, and the resulting gas turbine performance and individual components design [21] as well as the overall design choices which determine ease of access and maintenance [118]

Operational drivers include decisions during operations by the pilots, operations planners and air traffic control which affect the engine loading such as the application of derate, and the flight path definition (climb and descent rates, cruise speeds and altitudes, flight length, payloads, ...) [138]

Environmental drivers include the effects resulting primarily from local ambient conditions at take off and landing [138, 21, 141]

Regulatory drivers include taxes and fees applied, the cost of which are functions of engine emissions, or SFCs.

Organisational drivers become most influential when considering fleet based maintenance cost data and models and include fleet diversity in terms of age, utilisation and commonality, outsourcing levels, subcontracting, maintenance policies, local labour rates, and maintenance standards and rates of fault diagnosis (No Fault Found (NFF) rates). [138, 21, 141]

Regulatory drivers of engine-related operating costs are considered relevant, in terms of their effect on the scenario considered when maintenance cost models are applied, though they are not actually drivers of engine maintenance costs themselves. The other cost drivers identified are relevant to both engine maintenance cost calculations and fuel consumption. Other categorisations exist in literature [138].

Some publications list as cost drivers factors which, though correlated with maintenance costs, and which might be identified in CERs as a significant variable in regression analysis, are not necessarily causative. For example, engine list or sale price is listed as a maintenance cost driver and justified by the notion that engines that cost more to purchase will contain components which are more expensive to replace [118]. However, it is also possible that more expensive components may have longer replacement intervals, or might be repairable, such that the cost of the components, their design and operation determining their usable life would be the drivers of maintenance cost, not the list price of the engine.

5.4.2 Sensitivity of maintenance cost models to physics-based cost drivers

A review of public domain maintenance cost models was planned then completed in collaboration with Marrero [122]. The purpose of the study was to collate and compare available public domain models, identifying those models which might be considered “physics-based” and then assess their relative sensitivities to known physics-based cost drivers as identified in subsection 5.4.1. Three models were selected for sensitivity analysis:

1. Liebeck [142] assesses Labour and Materials costs and considers maximum take off thrust as a key cost driving parameter

2. Sallee [128] assesses Labour and Materials costs and considers cost as a function of opterating temperatures and pressures, flight length, and blade tip speed.

3. BEA [143] assesses labour costs and considers thrust as a function of Take-

off thrust and block time.

These models were compared using three flight routes between airport pairs at summer (hot) and winter (cold) ambient conditions. For each route, the full mission performance assessment was conducted, so while some models only took a limited number of specific inputs, these did vary in accordance with the specific mission description, and available derate for the conditions.

The effect of ambient conditions were captured, with winter flights operating at increased derate, resulting in lower maintenance costs than the summer flight on the same route. Model 3 is most sensitive to take off thrust variation, but as a result, when compared to the other models appears to undervalue the influence of flight duration. Model 2 is more conservative, showing lower sensitivity to derate and thrust, though this is still the most important parameter, and is found to be more significant than the other parameters considered and stated in decreasing order of sensitivity: take-off altitude, ambient temperature and flight length. Model 1, similarly to model 3, is limited to take off thrust as the “physical” cost driver. This is the least sensitive model.

Overall assessment was continued with the comparison of relative labour and materials costs from the three models, with each mission severity. In each model it was found that costs increased with increasing severity as expected. Though the rate varied. Materials costs being more sensitive to severity than labour costs (except for model 3 where labour costs were very sensitive)

5.4.3 Effect of key cost drivers on engine maintenance costs

It is generally accepted in the literature that Time On Wing (TOW) can be considered as a function, such that:

$$\mathrm{TOW} = f\left(\begin{array}{l}\text{Thrust rating, Derate, EGTM and payload,}\\ \text{Operational Severity}\left[\begin{array}{l}= f\left(\begin{array}{l}\text{Flight length (FH:FC),}\\ \text{Thrust rating, Derate, EGTM and payload,}\\ \text{Ambient and environmental conditions}\end{array}\right)\end{array}\right],\\ \text{Engine Age (and maintenance history)}\end{array}\right) \tag{5.10}$$

given that, as previously established, Operational Severity can be considered as a function of flight length (FH:FC), thrust rating and derate applied, ambient conditions, payload, and environmental factors, and that the rate of performance deterioration reflected in the aging calculation is also correlated with mission severity, it is clear that some engine performance factors affect several steps in the maintenance cost calculation process.

This section will present briefly the expected impact of each so-called cost driver on maintenance cost and TOW.

Ambient air temperature affects both the internal gas temperatures and available thrust c. Increasing ambient temperature tends to decrease the available thrust from an engine. Most high by-pass ratio engines are flat-rated, such that, below a corner point, as ambient temperature increases, Turbine Entry Temperature (TET) increases to maintain the output thrust, above the corner point, often identified for a given Outside Air Temperature (OAT) but set by TET, the thrust reduces, as illustrated in Figure 5.6.

Increasing OAT and the resulting higher TET are also reflected in increased operational severity, reflecting the harsher operating environment. Engines op-

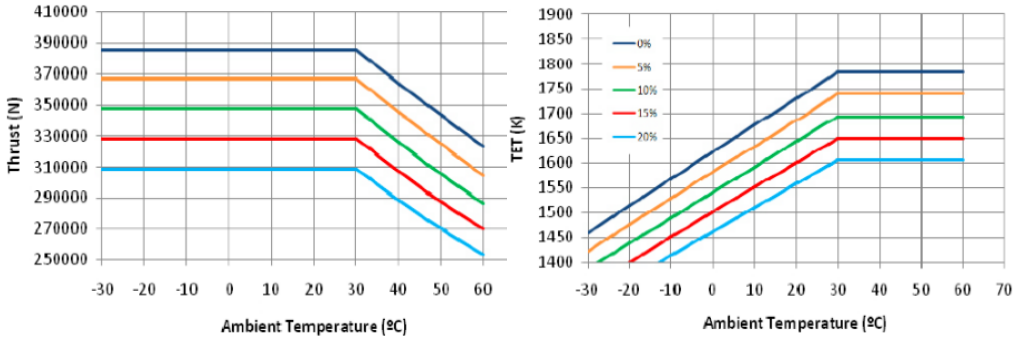

(a) Thrust (N) (b) TET(K)

Effect presented schematically for varying fixed thrust derates, with corner point at 30(°C).

Figure 5.6: Effect of ambient temperature (OAT in °C) on engine performance [16]

erating at higher temperatures tend to have reduced Exhaust Gas Temperature (EGT) margins resulting is shorter TOW between performance overhauls.

Flight Duration affects the FH:FC ratio, and has a significant effect on the balance of lifing mechanisms and failure mechanism as considered in the operational severity calculation. Shorter flights will tend to have the same number of thermal (fatigue) cycles as longer flights, so that fatigue life expended by mission will be relatively constant irrespective of flight length, such that shorter flights will tend to shorter TOW intervals measured in hours (Figure 5.7) .

Thrust Rating accounts for both the maximum rated thrust at which an engine in certified, and the thrust setting below that at which it is operated. Operating below rated thrust, or applying a de-rate, is not always possible, but might be available to pilots when operating at reduced flight range, payload, ambient temperatures, or on longer runways. Some airlines mandate the use of reduced thrust through either take off derate, or climb derate, or both.

From a performance perspective, operating a given engine and payload at

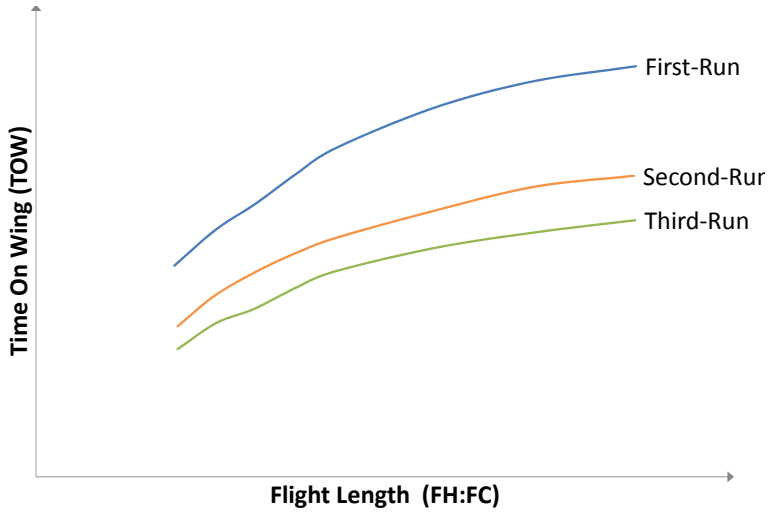

Figure 5.7: Sketched effect of Flight Duration on Time On Wing, adapted from [17]

fixed ambient and environmental conditions, increasing derate tends to longer ground roll lengths at take-off associated with slower aircraft acceleration, lower engine speeds and temperatures. By decreasing the amplitudes and peak values of the thermal and load cycles present in the engine, applying derate where available tends to decrease engine operating severity.

Considering deterioration in engines, operating below maximum rated thrust increases the margin available (EGTM, before performance overhaul is required) and slows the rate at which the margin reduces.

Some regressive cost models have established statistically significant correlations between certified rated thrusts and maintenance costs. While it is clear that higher rated engines can operate at higher temperatures, such models often fail to decorrelate in-service date and technology level, which also correlate with rating to generate higher operating temperatures.

Other engine performance factors. Engine technology level, and performance, as well as engine operating variable such as, but not limited to, cruise altitude, climb speed are considered during the engine and aircraft performance, lifing and operational severity calculation phases of this methodology and affect cost and time on wing, through their impact which is captured as part of the operational severity and aging calculations.

Maturity and aging. An aging fleet of equipment is often cited in literature as a key driver of maintenance costs, to the extent that several studies have focussed solely on the effect of 'age' on costs. Again, clarity of nomenclature is of primary importance. Much heavy equipment is referred to as either "new", "mature" or "aging", while others consider "aging" to be the process by which the equipment reaches "maturity". Aging is a term which is also applied to the process of developing new product families, where the product family is deemed mature once the causes of "infant mortality" failures have been resolved and the product is operating under predicted service and cost goals [118].

Irrespective of the terminology applied, studies of aggregated usage data and cost have found correlations between the age and maintenance cost of aircraft and engines. The explanations frequently include: that older systems need more maintenance and that performance margins after restoration are smaller than new margins. Less frequently, reference is made to the annual increase in the cost of replacement components (5% to 8% per annum) [21] otherwise called price escalation [144]. The costs considered in these studies are primarily listed as DMC and measured in $\frac{\$}{FH}$. It is often not clear whether the cost increases are related to an increase in the cost of maintenance or to the increase in maintenance frequency. The consideration of 'age' rather than operating hours or cycles will tend

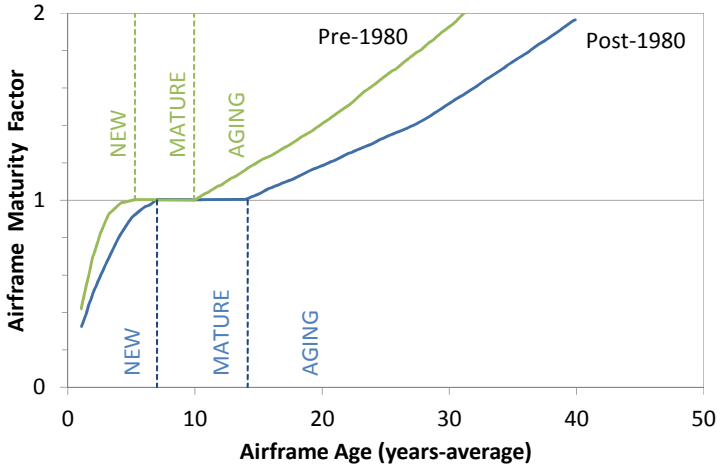

Figure 5.8: Commercial aiframe maturity curve from Dixon(2005)

to aggregate into a single ‘age’ group equipment with a range of utilisations and actual operation.

Predicting the cost of operating aging fleets has been of primary interest to militaries who may operate fleets for upward of 70 years [145] in changing operating environments. For military operators, data is required to justify the choice between operating increasingly expensive fleets, or replacing them with new fleets, which will be expensive to source and have unpredictable maintenance costs at the decision making stage. This obsolescence decision is key.

A significant study on aging was conducted by Dixon [117, 116]. He reported a common commercial approach to aging, presented in Figure 5.8 for airframe costs, which considers through life operating costs are belonging to one of three phases (new, mature or aging) separated by heavy aircraft maintenance checks (D-checks). In this approach a “maturity curve” of cost change over time is formed by normalising the costs with respect to the mature phase costs which have

	Slope $\frac{\delta(Maturity)}{\delta(Age)}$	Slope Change $\frac{\delta^2(Maturity)}{\delta(Age)^2}$
New	$+$	$-$
Mature	0	0
Aging	$+$	$+$

Table 5.1: Changing effect of aging on Maturity according to Figure 5.8

been set such that mature rate cost growth rate is zero. Significant technological changes present in the fleet analysed are accounted for by considering early fleet (pre-1980) and newer fleet (post-1980) separately. Dixon notes that this approach is "not yet proven": neither the statistical model or basis of analysis is either given or described.

Dixon proceeded to conduct his own analysis of available cost data (including CAB form 41 breakdown of spending on maintenance by aircraft type) and fleet inventory and age data (from the SEC, individual airlines and manufacturers). His model also identifies three phases, but his phase intervals are fixed at six and twelve years. He considered maintenance costs as a total measure, but also split into overhead and direct costs associated with either the airframe or the engines. He generates an empirical relationship linking maintenance cost (y) to age for a given fleet and airline:

$$log(y_{itr}) = \alpha + \beta * Age_{itr} + \mu_t + \delta_r \tag{5.11}$$

where

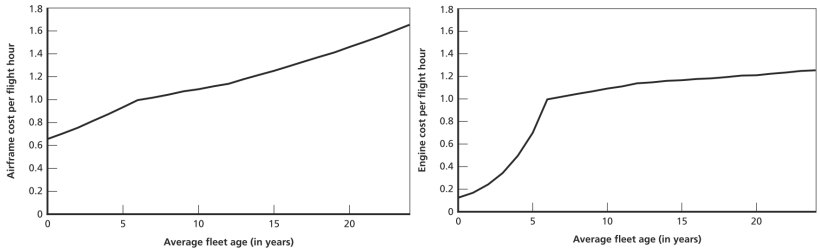

(a) Airframe (b) Engine

Figure 5.9: Maintenance costs per flying hour, normalised with respect to cost at Year 6 from Dixon

Cost	Total		Airframe		Burden		Engine	
	β	σ	β	σ	β	σ	β	σ
New	0.152	0.017	0.061	0.013	0.118	0.025	0.38	0.030
Mature	0.035	0.008	0.023	0.009	0.067	0.018	0.022	0.014
Aging	(0.007	0.007)	0.031	0.006	(0.007	0.012)	(0.008	0.018)

Numbers in brackets indicate where Null Hypothesis [that age does not influence cost] cannot be rejected

Table 5.2: Summary of Dixon's Age effect analysis

μ_t aircraft type fixed effects

δ_r year fixed effects

i airlines

β age effect

α intercept

y total maintenance cost per flight hour

$100 * \beta$ approximately the percent change in the costs (y) due to one year increase in age.

Dixon notes that the shape of the commercial aging curve (Figure 5.8) is similar to that which he has produced for airframe cost (Figure 5.9a) given that he has not set the growth rate in the mature phase to zero. The engine costs do not follow the same pattern in (Figure 5.9b). Statistical analysis of the age effect

conducted by Dixon, and reported in Table 5.2, clarifies that distinct aging phases can only be confirmed for the airframe costs.

The sharp increases in cost during the "new" phase are attributed by Dixon to the end of warranty periods and the transfer of maintenance costs from manufacturers to operators. As Dixon's cost data contain only costs expended by operators, OEM warranty costs are not apparent.

Hanumanthan [18] adopts the Engine Maintenance Cost Working Group (EMCWG) approach to aging, and determines that a Weibul curve with shape parameter of 1.5 can be used effectively to generate an aging curve given engine specific scaling to account for the effect of degradation on the mature shop visit rate.

Engine aging must be considered in order to to capture the changes in maintenance costs through life. Considering an engine, and calculating its maintenance requirement through life, including successive shop visits through the "virtual workshop" approach, will offer more clarity on cost causation than has been gained previously from empirical, correlative, models.

5.4.4 Effect of severity on engine maintenance costs

A measure of operational severity is commonly used to aggregate the combined effects of these key cost drivers. Aging and severity are often considered together as a means of capturing the effects of operation and time respectively on engine maintenance costs.

An accepted relation is that of the EMCWG presented by Hanumanthan [18] and reproduced in section B.1, where:

$$\text{Shop material cost} = f(\text{Maturity factor}, \text{Severity Factor}, \text{Material DMC}) \tag{5.12}$$

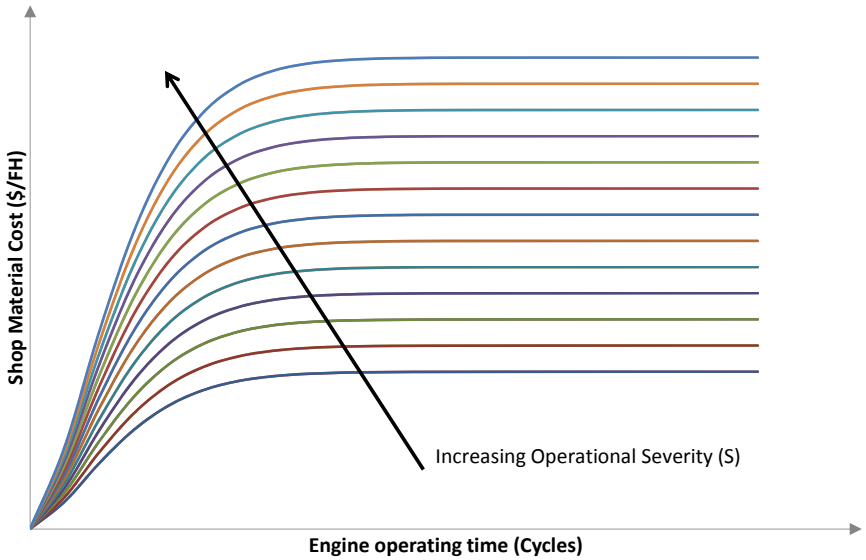

Figure 5.10: Accepted effect of aging and severity on shop materials cost.

So described, engine maintenance cost are expected to increase until the engine reaches maturity, at a rate commensurate with the increasing maturity factor, until a level set by the standard maintenance cost rate. While missions with increased operational severity follow the shape cost profile, the maximum cost is increased. The expected shape of shop material costs is presented in Figure 5.10.

Conclusions The need for operational cost of engines, specifically through life maintenance cost has been established. The limitations of large data regression studies have been considered, and while these offer significant glimpses into the some of the parameters which are important through correlation. It is considered that further insight may be gained into the causative nature of these correlated relationships through the development and use of deterministic analysis. And, that

so doing, greater clarity can be gained of the physics-based causes of engine maintenance cost variations due to operational decisions. It is therefore considered that, to establish a physics-based link between operational choices, engine technology levels (design decisions) and operational through life maintenance costs, the concept of associating cost with operational severity and aging must be developed further, to couple the engine operation with cost with increased physics-basis using a well defined and clearly derived operational severity measure.

Chapter 6

The workscoping approach

This section presents an overview and description of the methodology developed during and used in this research.

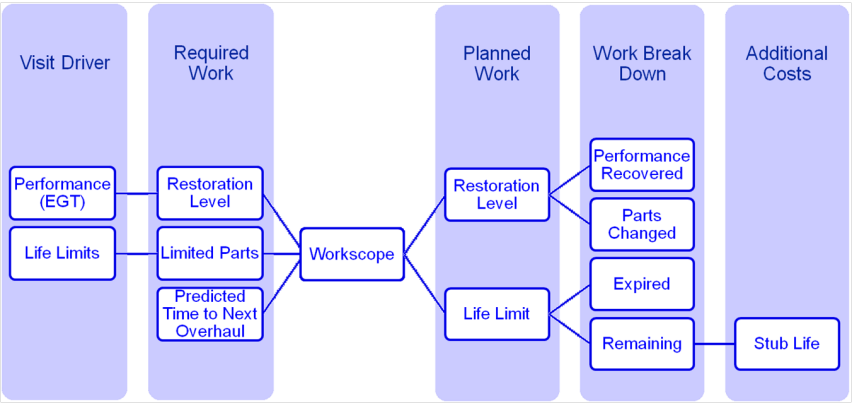

Figure 6.1: Single shop visit workscope overview

The workscoping approach developed in this research is deterministic and aims to link the operation of the engine with its maintenance costs. The multi-step approach considers a planned workcsope (described by a work breakdown of planned work) as presented in Figure 6.1 which is determined as a function of the visit driver, the required work, and the predicted time to next overhaul. This enables the distinction between cost drivers which correlate with maintenance

cost changes to be distinguished from those that cause them.

The methodology is multi-step, and follows a similar process to both the Design and Maintenance Trade Study Tool (DMTrade) [135] and OSCAP [27] cost models which are summarised in Table 6.1.

Each shop visit in an engine's life is considered separately. For each SV, the shop visit driver is established considering previous usage and life limits. The actual work-scope of a given shop visit is determined considering both the shop visit driver (minimum work-scope) and the expected or desired interval to the next shop visit. The engine's LLP limits and performance margins are updated based on the maintenance carried out. The costs for the shop visit are accounted for. This workscoping stage is repeated for each shop visit of the engine's life. The costs of all the shop visits are distributed over the engine life to determine costs on a per hour or per cycle basis. The considerations for each shop visit workscope definition are illustrated in Figure 6.1.

DMTRADE [135]	**OSCAP [27]**
Predictions:	**Process:**
When will the product fail?	Engine Removal Generator (ERG)
What failure mode will cause the failure?	Resultant maintenance action calculator
What repairs will be needed?	(REMAC)
What proactive repairs will be performed?	Maintenance Event Processor (MEP)
The cost of those repairs?	Life cycle cost post processor (LCCPP)
Outcomes:	**Output:**
Shop Visit Rates (SVRs)	LCC Report
Shop visit causes	
Shop Visit Costs (SVCs)	
Maintenance cost per operating hour	

Table 6.1: Public Domain Maintenance Cost Model Processes

The aim of this approach is to produce a cost model capable of capturing the effect of engine operation, by considering the effect of operation on component life and aging of the engine and determining the resulting maintenance requirements

thus enabling an estimation of maintenance cost.

The challenge is to capture the physics-based effect of operation, using the minimum number of inputs, to make the model suitable for use in considering early design stage engines, for which full geometries and designs are not yet established.

The purpose of the model is to enable trend analysis, considering changes in flight path and operation, to enable a skilled user to ask the right questions about proposed early design stage engines.

Considering the engine throughout its operational life is considered essential in order to capture the change in maintenance requirements through life as the system ages, and to account for the effect of maintenance decisions on future costs.

Managing a single, imminent SV in isolation, leads to the possibility of a shorter interval to the next SV than might be possible in considering both the maintenance immediately required, and that which is possible. Bringing maintenance tasks forward can lead to increased costs as a LLP part removed before its declared life will incur increased hourly costs ($\$/FH$) over its lifetime, or performance restoration conducted before it's required can be considered to result it lost margin. These costs must however be balanced against an increased interval to the next SV, thus increasing TOW and the Mean Time Between Removals (MTBR), which can outweigh the increased costs when considering overall hourly costs for the engine ($\$/FH$).

6.1 Model

6.1.1 Concept

The virtual workshop methodology considers for a given engine each successive shop visit individually. At each shop visit the maintenance actions completed are determined and their costs accrued. Simplistically this can be considered as a three step process for each shop visit.

Figure 6.2: The workscoping shop visit approach

1 - When? A shop visit interval (or time to next shop visit) is determined by the minimum remaining interval of all maintenance actions considered. When an engine is new, and the first shop visit is being considered, all the elapsed times on wing are null, and lives remaining equal life limits. Once the interval to shop visit has been determined each maintenance action is updated with a corresponding time on wing since maintenance and life remaining.

Such that, given n possible maintenance actions (A) , each with an available life (A_{life}) and elapsed operating period in service $(A_{elapsed})$, the next shop visit interval $(SV_{interval})$ is:

$$SV_{interval} = \min_{x=1,...n} (A(x)_{life} - A(x)_{elapsed}) \tag{6.1}$$

$$\text{for} x = 1, \ldots n \qquad A(x)^{new}_{elapsed} = A(x)_{elapsed} + SV_{interval} \tag{6.2}$$

2 - What? The work to be completed at this shop visit is determined such that any maintenance action with remaining life smaller than the maintenance planning margin set will be completed. Any maintenance action identified as due at this shop visit will be updated to reflect this with a zeroed time on wing since maintenance and life remaining re-set.

$$\text{for} x = 1, \ldots n \qquad A(x)_{due} = \begin{cases} 1 & \text{if} A(x)_{life} - A(x)_{elapsed} \leq SV_{planning\,margin} \\ 0 & \text{if} A(x)_{life} - A(x)_{elapsed} > SV_{planning\,margin} \end{cases} \tag{6.3}$$

3 - How much? The cost of all maintenance actions completed is then accumulated to determine the Shop Visit Cost (SVC) ($) and the shop visit is deemed complete.The process continues with the calculation of the next shop visit interval.

$$SVC(x) = \sum_{x=1,\ldots n} (A(x)_{due}.A(x)_{cost}) \tag{6.4}$$

While each shop visit is considered individually, by considering them in sequence as illustrated in **??**, the maintenance completed at each shop visit affects both the interval to and maintenance actions required at the subsequent shop visits.

The status of each available maintenance item is updated at each successive shop visit to reflect the increased elapsed time since maintenance and the

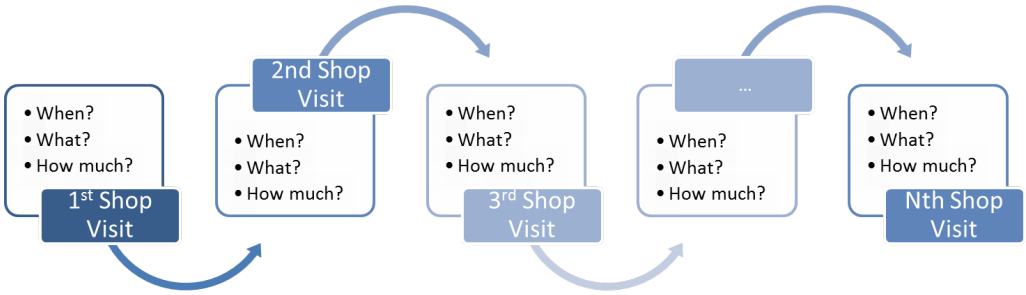

Figure 6.3: The repeating three step process for successive shop visits

remaining available life.

Two types of maintenance action considered: life limited parts and restoration. Maintenance actions are specified in terms of costs and intervals.

6.1.2 Approach

Each successive shop visit is considered as described in subsection 6.1.1, within the context of the whole engine life.

The overall workscoping approach consists of the following steps:

- Define and initialise Input Structures
- Identify Case Inputs
- Define and initialise working structures
- Load case inputs
- For each shop visit
  - Determine Shop Visit Workscope
  - Calculate Shop Visit Cost and DMC

  - Output Shop Visit Description and Cost

- Repeat until last shop visit determined by life limiting rule.
- Calculate aggregate operating period
- Calculate aggregate Shop Visit Cost and DMC
- Output summary Shop Visit history and costs
- Save working structures
- (Optionally) Output cost curves

The resulting saved case working structures can be further post processed as required depending on the case application.

6.1.3 Key considerations

Each Shop Visit (SV) is considered alone but in sequence, thus the elapsed intervals and margins are passed between them (Figure 6.3, Figure 6.4). Therefore each shop visit is dependent on the prior maintenance completed and the subsequently remaining performance margins and LLP lives.

The planning rule can be set either using a fixed shop visit interval called the build goal with a maximum number of shop visits, or as a fixed number of shop visits with varying build goal. Both can use a margin interval to account for bringing forward maintenance that would cause an imminent return to shop after return to service.

The Shop Visit (SV) driver. Given the focus on planned (scheduled) shop visits rather than shop visits that follow engine removal due to in-flight shut-down,

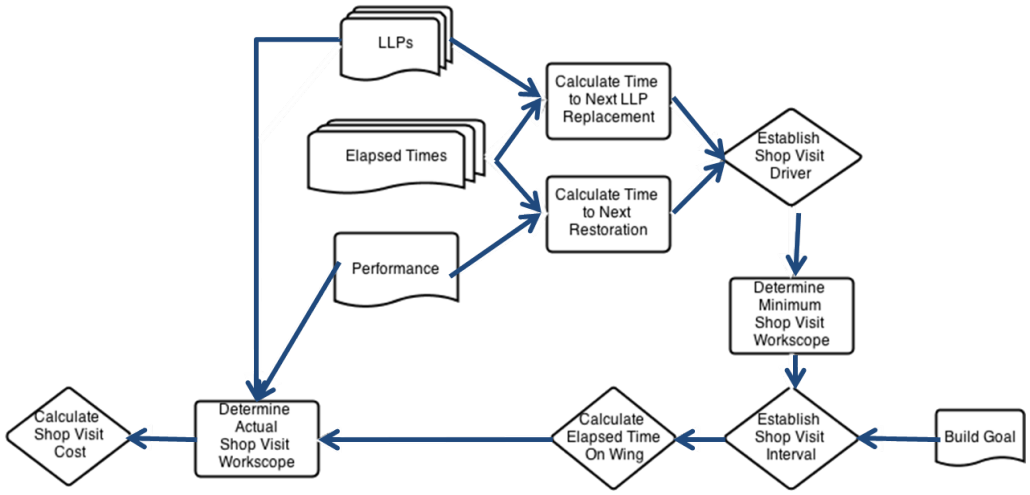

(a) Process

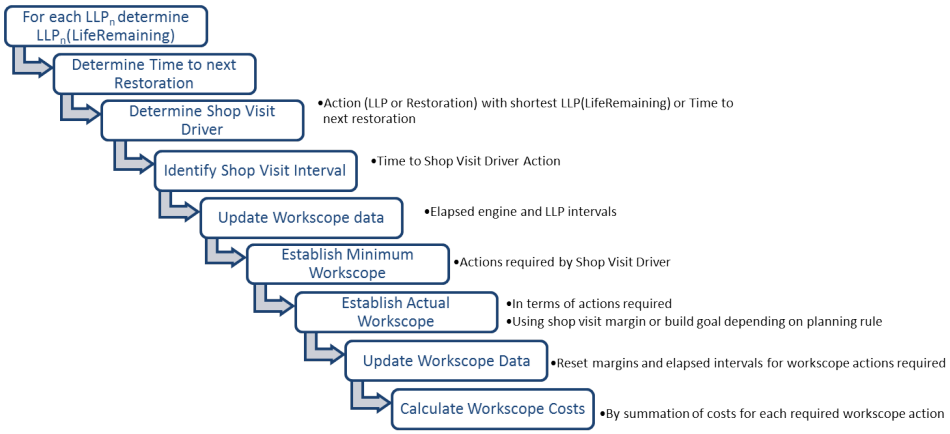

(b) Description

Figure 6.4: Determining a shop visit workscope.

bird-strike or other failures, two types of shop visit driver are considered: life limits, and performance margin exhaustion. Shop visits are triggered by either a LLP reaching its certified life, a performance variable reaching its limiting or ‘red-line’ value. The performance variable considered in the case studies completed as part of this research is the Exhaust Gas Temperature

Margin (EGTM), though other variables such as shaft speed might also be implemented in the same way if desired. To determine the shop visit driver, the time to next maintenance action is calculated for each LLP and performance margin considered. The shortest time to next maintenance action, belongs to the “shop visit driver”.

The Shop Visit (SV) minimum work-scope. For a LLP driven shop visit, the minimum work-scope will include both the replacement of the expired LLP or LLP set, and any restoration work carried out on that module at the same time.

For a performance driven shop visit, the minimum workscope will be restoration work, though the level of restoration carried out may be a function of the SV number. For example, the restoration carried out at SV(1) may be lighter than at subsequent SVs.

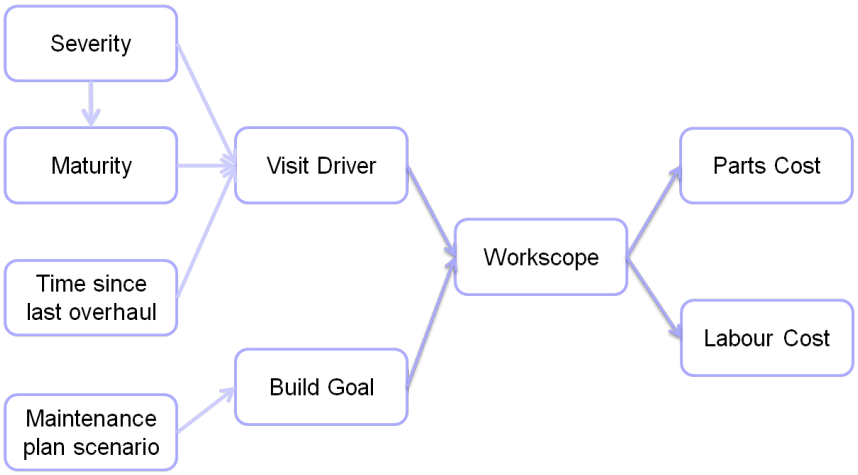

Figure 6.5: Single SV workscope considerations

Actual work-scope The actual work-scope is determined by combining all maintenance actions required by the shop visit driver, and all maintenance actions that would otherwise become due during the interval margin period

after shop visit (Figure 6.5).

Once the work to be completed at this shop visit is established, elapsed lifing intervals and performance margins are reset for LLPs and Restoration actions conducted.

Elapsed intervals are accumulated and stored for each LLP, restoration item subject to aging deterioration and for the overall engine. The engine elapsed life is used in the calculation of overall costs when presented per flying hour.

Cost attribution and distribution follows a simple accountancy process, for each shop visit, costs associated with each action are accumulated both overall and in categories (LLP, Restoration, Labour, Material, Subcontract) along with the relevant elapsed shop visit interval.

The through life maintenance plan and costs are compiled from aggregating all the shop visits identified during its usable life.

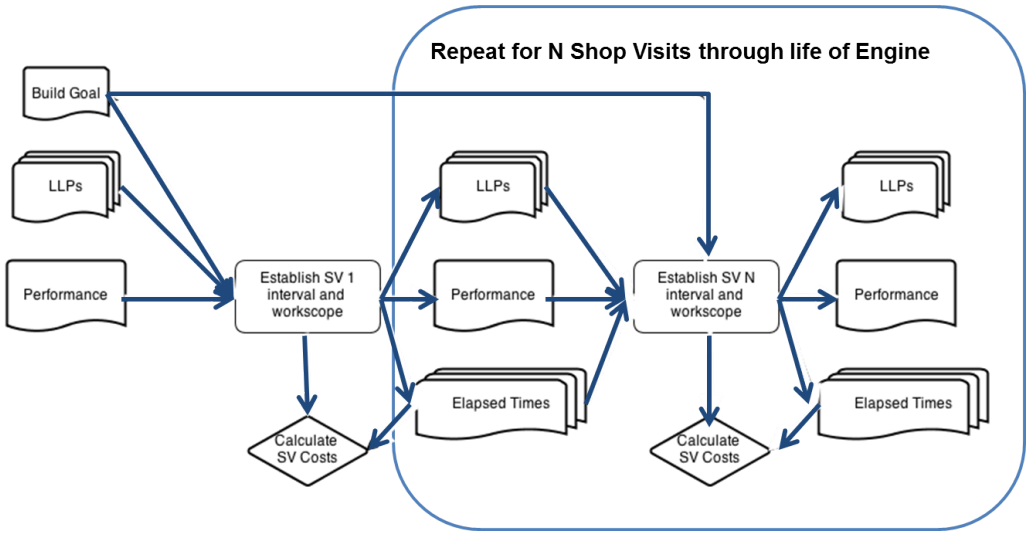

Figure 6.6: Through life maintenance workscope process

Through life maintenance plan is assembled by combining, workscope actions, costs, intervals and margins for each shop visit workscope (Figure 6.6) during the case study period (defined by either a maximum number of shop visits or a maximum service life). The through life plan, also includes the time on wing available after the last shop visit.

Through life hourly costs are calculated from the accumulated costs of all workscopes over the engine usable life including the time on wing following the last shop visit. In so doing, the method developed and presented here accounts implicitly for lost margins and stub lives due to maintenance intervals and management decisions.

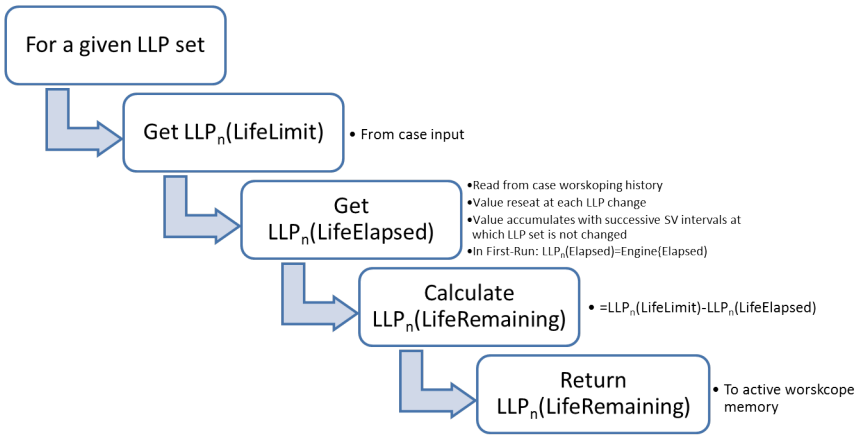

Figure 6.7: Determining time to next LLP replacement

6.2 Inputs

Inputs to the model are defined by the user in an input file and loaded in to structures that are predefined during model initialisation.

The following input structures are defined:

- Case inputs describing the mission, costs, planning rules and identifying the engine to be analysed.
- Engine structures (one per engine defined) identify the engine in question by number, name and rating, and defines for that engine the performance deterioration method, profile and limits.
- Maintenance actions are defined in two types:
  - LLPs
  - Restoration

6.2.1 Case Inputs

The `Inputs` structure defines the case to be analysed by the model. Inputs defined by the user include:

- Mission description (EFH, OAT, derate and severity)
- Cost definitions (Labour rate)
- Model Options (Planning rule, limit and margin, aging method selection and Engine ID)

Engine ID is an input to the Case definition as the input file contain several engine definitions.

6.2.2 Engine Inputs

Each engine defined in its own `Engine` structure is identified by Engine ID, name and rating. The `Engine` structure(s) contain inputs determining the engine performance deterioration leading to performance based restoration actions. For both

first-run and mature-run operations the engine EGT margin is defined. Depending on the aging method selected by the user in the `Inputs` structure, either the EGT margin deterioration is defined, or the performance based maintenance interval as calculated by the separate aging methodology identified.

6.2.3 Maintenance actions

Each maintenance action is identified by ID number and name, with one structure per maintenance action.

The `LLP` structure(s) require inputs of:

- LLP replacement cost
- Life limit (cycles)

The `Restoration` structure(s) require inputs of:

- Trigger type and rule
- Cost in terms of man hours and materials both in the shop and optionally for subcontract work.

Given that the design of the model was required to operate solely on public domain data, the cost definition requirements are not restrictive. The onus is on the user to ensure that all costs defined in the input structures are coherent in terms of currency and date for a given case, so as to limit errors due to inflation and foreign exchange variations.

6.2.4 Planning Rules

Three planning rules are available to frame the through life workscoping case for an engine-aircraft-mission set. These are:

nSV in which a total number of SVs is set by the user. In this case the overall usable life of the engine and the SV intervals are outputs of the workscoping method.

build goal in which a minimum SV Interval is set. The the overall usable life of the engine is an output of this approach.

engine life in terms of ultimate usable engine life cycles can also be set as the planning rule. In this case the number of SVs and their intervals are outputs of the model.

6.2.5 Restoration Triggers

Three types of restoration maintenance action are accounted for in the model. They are principally distinguished by the method by which they invoked or triggered.

- Performance margin depletion (EGTM)
- Associated with a LLP change
- Fixed to happen (or not to happen) at a specific numbered Shop Visit

Performance margin depletion Two methods are available for performance maintenance interval calculation. The maintenance interval due to EGT margin

depletion, can follow either a bi-linear book method in which the initial and mature EGT margins are defined (with margin and temperature), and a deterioration rate is set, or uses input EGT aging intervals calculated separately following the operational aging method developed by Hanumanthn [18].

Bi-linear book method calculates the interval following the simplified approach described by Ackert [14]. This approach is very simplified and used a bi-linear simplification for the rate of margin depletion. This method is included as it enables the use of the workscoping model independently of the full performance-lifing-severity-aging method if required. It was also implemented as a means of functional verification for the workscoping model using published cases. The minimum data required for this method are: an initial EGT margin and associated OAT, an installation loss in terms of initial loss and period, and a deterioration rate after installation loss. Where available, each of these data items can also be supplied for ”mature” operations, where two deterioration data sets are supplied, they are applied respectively to ”new” (prior to first SV) and ”mature” (subsequent to first SV) interval calculation.

EGT margin deterioration through performance aging calculation is a more complex method. The performance driven shop visit intervals defined by EGT margin deterioration are inputs to the workscoping model. These are calculated externally to the workscoping model, following the method developed by Hanumanthan [18].

Hanumanthan’s process is illustrated in Figure 6.8, and involves the use of engine and aircraft performance modelling to simulate deteriorated gas path and performance to estimate average SVR throughout engine life assuming that maintenance is caused only by performance deterioration.

For the purposes of this project, as the performance driven maintenance ac-

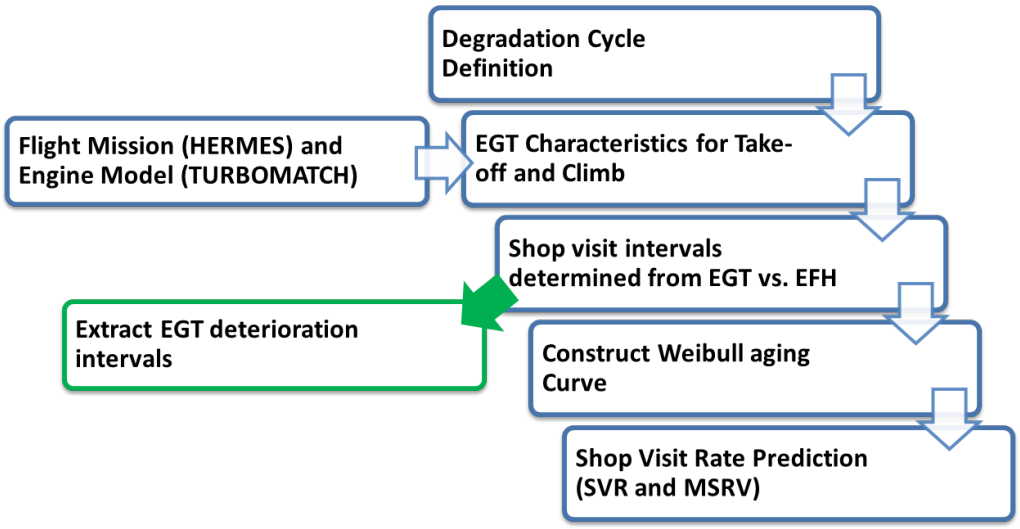

Figure 6.8: Hanumanthan's aging process [18]

tions are only one of the causes for engine removal considered, Hanumanthan's process is considered incomplete. Instead it is followed to the intermediate step and the shop visit intervals determined by EGT reaching red-line temperatures is calculated and output for use in the workscoping model.

The degradation cycles applied in the method follow a typical pattern defined by Litt and Aylward [146] and used by Hanumanthan.

6.2.6 Severity and aging

Operational severity and aging is captured in several ways in the model. Though engine aging is captured implicitly by the "through life" nature of process adopted, in which the maintenance required at any shop visit is a function of the previous operation and maintenance, three additional calculation methods are considered and available to explicitly link severity and aging to shop materials costs. In each case the method used for calculating the cost of restoration maintenance is varied such that:

MATSEV as per EMCWG Equation B.1 Shop Materials Cost is a function of Engine Maturity and Mission Severity

MAT Shop Materials Cost is a function of Engine Maturity

Arithmetic Shop materials cost is constant for each maintenance activity

6.3 Outputs

Two types of output are produced, text reports and Matlab data structures. Text reports are produced for each individual shop visit, and output as a report for a single engine mission through life maintenance case detailing each shop visit as well as a through life DMC summary of costs. An example of such a summary is presented in Figure 6.9 (a) Where several cases are assessed, an additional summary version is produced such as that presented in Figure 6.9 (b). In this version the through life cost summary is presented for each case studied, but not the detail of each shop visit. The data structure produced during calculation is also output, containing details of costs and intervals for each shop visit. This output is then available for further post-processing as well as calculation verification.

The main output report generated and presented in Figure 6.9(a) is structured following workscoping concept described in subsection 6.1.1: when, what, how much.

For each shop visit costs are presented in two ways:

- Shop Visit Total Cost with sub-total values for restoration tasks and LLP costs required during this shop visit. Where given i possible LLP replacements (LLP) and j possible restoration actions ($REST$):

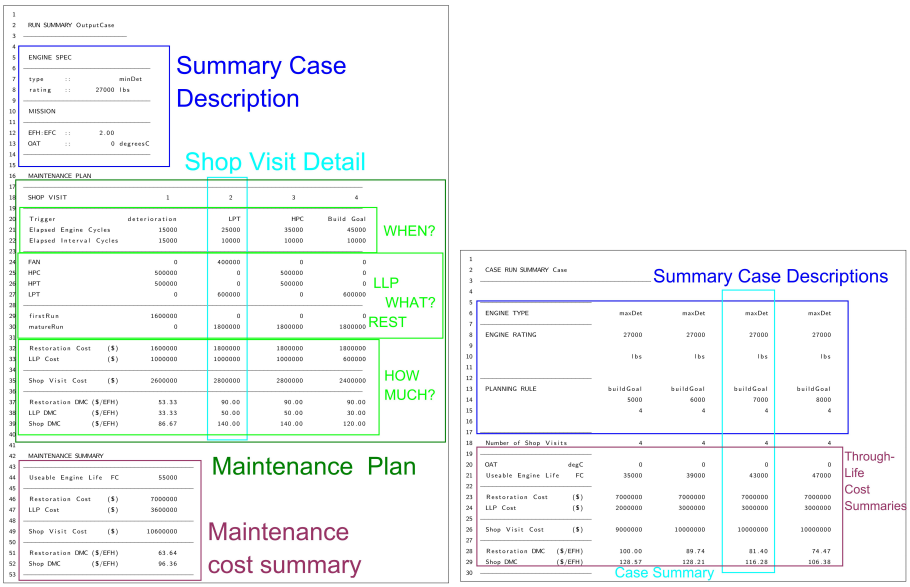

(a) Case Detail (b) Multi Case Summary

Figure 6.9: Structure of output reports generated

$$\text{ShopRestorationCost}(\$) = \sum_{x=1,\ldots i} REST(x)_{due} \tag{6.5}$$

$$\text{ShopLLPCost}(\$) = \sum_{x=1,\ldots j} LLP(x)_{due} \tag{6.6}$$

$$\text{ShopVisitCost}(\$) = \text{ShopLLPCost} + \text{ShopRestorationCost} \tag{6.7}$$

- DMCs, where the shop visit costs calculated in total for the shop visit is distributed over the shop visit interval so as to determine the cost per flying hour ($\$/EFH$)

6.3.1 DMC calculations

The key to distributing shop visit costs into a DMC value assessed per engine flying hour, once the maintenance actions and therefore the maintenance cost have been established is the selection of the time period over which to calculate it.

In calculating DMCs a choice must be made as to which operating period a replacement cost is attributed.

For a given maintenance action such an an LLP replacement, the “when” is determined by the old component removal, whereas the “how much” is related to the cost of the replacement LLP installed. One possibility would be to assess the DMC of that LLP set over its own operating period. However, at the point that the LLP set is installed, its operating period is not yet known. At the point that the new part is installed, the operating period of the part removed is known.

If the cost of the new components is distributed over the service interval of the old component, there is a discrepancy, but the calculation can be completed. Whereas if the cost of a new component were to be distributed over its expected usable life, then the effect of operational parameters and planning decision would be lost.

Were each component to be costed against its own service life, negligible values of DMC would be calculated for the initial shop visit interval, which is unreasonable, as the DMC value is intended to reflect hourly cost of operation.

This project focuses on the through life DMC values, so the final operating interval must also be accounted for. DMCs outputs are calculated over the whole usable engine life and are also calculated at each shop visit as follows:

$$\text{ShopRestorationDMC}(\$/\text{EFH}) = \frac{\text{ShopRestorationCost}}{ElapsedIntervalHours} \tag{6.8}$$

$$\text{ShopLLPDMC}(\$/\text{EFH}) = \frac{\text{ShopLLPCost}}{ElapsedIntervalHours} \tag{6.9}$$

$$\text{ShopVisitDMC}(\$/\text{EFH}) = \frac{\text{ShopVisitCost}}{ElapsedIntervalHours} \tag{6.10}$$

For the cost summary calculations, the service interval considered is the Us-

able Engine Life (FH) which is calculated for a maintenance life including n Shop Visits:

$$\text{UsableEngineLife(FH)} = (EFH : EFC) \sum_{x=1,\ldots n+1} SV(x)_{interval} \tag{6.11}$$

$$\text{ShopDMC(\$/EFH)} = \frac{\sum_{x=1,\ldots n}(SV(x)Cost)}{\text{UsableEngineLife}} \tag{6.12}$$

$$\text{RestorationDMC(\$/EFH)} = \frac{\sum_{x=1,\ldots n}(SV(x)RestorationCost)}{\text{UsableEngineLife}} \tag{6.13}$$

Note that the LLP DMC values are not presented by default in the case summary outputs as the cost outputs considered key are the Restoration DMC and Total LLP costs as these values allow the quickest most meaningful comparisons between engine cases.

In this way the full service life of the engine is considered. This process utilises the built in structure of the workscoping model, which assess the interval remaining until the next shop visit at each shop visit, so that though only the number of shop visits completed is presented in the maintenance detail, the remaining useful life after the last shop visit is also considered.

The workscoping method is applied to case studies of engine-aircraft applications. The initial case studies presented in this chapter are considered verification and validation cases and are limited by the availability of comparative data available. Further cases are presented in chapter 8, these further demonstrate of the capabilities of the methodology through the application of more complex operational conditions and decisions that are of interest to the project.

6.4 Verification Cases

Two simplified engine studies are presented here. They allow the workscoping model to be verified against published cases and demonstrate some of the models capabilities. Further studies, which integrate the workscoping model, into the full workscoping methodology are presented separately in chapter 8.

6.4.1 Initial Verification Cases

Simplified cases derived from Ackert [14] are used for initial functional verification of the code. These cases consider a two-spool engine with four Quick Change Modules (QCMs) containing LLPs (fan, Low Pressure Compressor (LPC), Low Pressure Turbine (LPT), High Pressure Turbine (HPT)) for which life limits and replacement costs are defined. They are considered as two variants of the same engine distinguished by their performance deterioration rates and referred to as "minDet" and "maxDet" respectively.

The nominal mission considered is a two hour flight, in temperate conditions using 10% derate with a nominal defined severity of 1[1].

The primary planning variable considered in this case is the build goal, which can be used as the model handle to illustrate the effect of maintenance planning.

Performance maintenance interval calculation

Ackert defines two deterioration cases as follows:

The engine is projected to have an initial EGT Margin of 85°C, and installation loss of 10-15 degrees Celsius per 1,000 flight cycles.

[1] note the reference mission in this case differs from that generally considered under EMCWG guidelines and used in the rest of this research.

Thereafter, rates of deterioration will stabilize to 4-5 degrees Celsius per 1,000 flight cycles. – Ackert [14, Appendix 1 - p23]

These are implemented in the workscoping model as two engine cases, with separate engine input blocks in the input file. The complete engine blocks are reproduced in Appendix C (Listing C.1 and Listing C.2), but the key functional lines are extracted in Listing 6.1

Listing 6.1: Extract from engine Input Block

```
1  Engine(1).type = 'minDet';
2  Engine(1).EGT(1).margin=85;
3  Engine(1).EGT(1).deterioration=[1000, 10, 0.004];
4  Engine(2).type = 'maxDet';
5  Engine(2).EGT(1).deterioration=[1000, 15, 0.005];
```

The performance based maintenance interval driven by these deterioration rates is assessed in the workscoping model by calculating a base case as described by Ackert [14, Ex8. B], assuming a build standard goal of 10,000 FC. This case is repeated for both engine deterioration cases. The full case results are presented in Listing 6.3 and Listing C.3. In both cases the first shop visit is driven by deterioration alone. The first shop visit output detail for each case is reproduced in Listing 6.2.

The deterioration intervals are 15,000FC and 19,750FC respectively for the “maxDet” and “minDet” cases, as defined. This matches the solutions given by Ackert [14, Example 1 - p.23] for Theoretical TOW Low and Theoretical TOW High.

In Listing 6.2, it can be seen that the deterioration rates set do more than merely change the SV interval. In line with the workscoping concept of “When? - What? - How Much?”, while both cases are subject to the defined “First-Run” restoration cost, the LLPs sets to be replaced change. In the “minDet” case

Listing 6.2: Extract of first Shop Visit for both deterioration cases

type ::	maxDet	minDet
Trigger	deterioration	deterioration
Elapsed Engine Cycles	15000	19750
Elapsed Interval Cycles	15000	19750
FAN	0	0
HPC	500000	500000
HPT	500000	500000
LPT	0	600000
firstRun	1600000	1600000
matureRun	0	0
Restoration Cost ($)	1600000	1600000
LLP Cost ($)	1000000	1600000
Shop Visit Cost ($)	2600000	3200000
Restoration DMC ($/EFH)	53.33	40.51
LLP DMC ($/EFH)	33.33	40.51
Shop DMC ($/EFH)	86.67	81.01

subject to a longer first SV interval, the LPT module is changed in addition to the High Pressure Compressor (HPC) and HPT changed in the “maxDet” case.

These LLP replacement choices, are functions of the next interval to the second shop visit, in this application, these are defined by the build goal which was set at 10,000 cycles.

Though more work is carried out in the “minDet” case, increasing the Shop Visit cost, Total Shop DMC is lower due to the increased TOW outweighing the increased cost of maintenance.

Through life maintenance costs

Two cases are considered, with 9,000 FC and 10,000 FC build goal limits respectively.

For each a complete workscoping process is completed and through life maintenance plan and costs determined. The outputs from the workscoping model are presented in Listing C.4 and Listing 6.3 respectively.

Listing 6.3: Results maxDet with 10000FC Build Goal

ENGINE SPEC

type ::	maxDet
rating ::	27000 lbs

MISSION

EFH:EFC ::	2.00

Planning Mode

Rule ::	buildGoal
Limit ::	10000
(SV) ::	4

MAINTENANCE PLAN

SHOP VISIT	1	2	3	4
Trigger	deterioration	LPT	HPC	Build Goal
Elapsed Engine Cycles	15000	25000	35000	45000
Elapsed Interval Cycles	15000	10000	10000	10000
FAN	0	400000	0	0
HPC	500000	0	500000	0
HPT	500000	0	500000	0
LPT	0	600000	0	600000
firstRun	1600000	0	0	0
matureRun	0	1800000	1800000	1800000
Restoration Cost ($)	1600000	1800000	1800000	1800000
LLP Cost ($)	1000000	1000000	1000000	600000
Shop Visit Cost ($)	2600000	2800000	2800000	2400000
Restoration DMC ($/EFH)	53.33	90.00	90.00	90.00
LLP DMC ($/EFH)	33.33	50.00	50.00	30.00
Shop DMC ($/EFH)	86.67	140.00	140.00	120.00

MAINTENANCE SUMMARY

Useable Engine Life FC	55000
Restoration Cost ($)	7000000
LLP Cost ($)	3600000
Shop Visit Cost ($)	10600000
Restoration DMC ($/EFH)	63.64
Shop DMC ($/EFH)	96.36

These are then compared to the reference case published by Ackert [14] and reproduced[2] in section C.2. A summary of the results, allowing comparison between the workscoping methodology and the published reference case is presented in Table 6.2.

Both build goal cases produced by the workscoping method conform to the published pattern of maintenance expected which are illustrated in the corrected

[2]subject to the correction of typographical errors

Build goal	9,000 FC		10,000 FC	
	Workscoping Listing C.4	Reference Figure C.2	Workscoping Listing 6.3	Reference Figure C.3
Restoration Cost		$7,000,000		
LLP Cost		$3,600,000		
Total Shop Visit Cost		$10,600,000		
Usable Engine Life (or total FH (*))	102,000	84,000*	110,000	90,000*
Restoration DMC ($\$/FH$)	68.63	83.33(68.63)†	63.64	77.78(63.64)†
Shop DMC ($\$/FH$)	103.92	126.19(103.92)†	96.36	117.78(96.36)†

† re-calculated with Total FH adjusted to include usable period equal to build goal after final shop visit

Table 6.2: Summary of through life maintenance case results

reference cases (Figure C.2 and Figure C.3). The costs of each shop visit (restoration, LLP and total) also match the published reference. However the DMC values do not match.

Investigation of the differences in DMC find them to be attributable to the assumptions made in the premise of cost attribution. The reference case [14] assumes that the cost of maintenance over the engine life is distributed across the service life prior to the final shop visit, but does not account for any service life subsequent to the final shop visit. Under this assumption, the period after the final shop visit would be “free” in terms of DMC charges.

One of the premises of the workscoping method developed and implemented in this research is, however, to account for the full service life, therefore the usable engine life includes the service life available after the final shop visit. As such, the usable service life used in the workscoping DMC calculations is longer and the resulting DMC values are lower than the reference case as published. This is a however an artefact of the usable life definition used in each model rather than a fault in either.

The difference in usable life between the published case [14] and the workscop-

ing model, is one shop visit interval, which in both cases would be determined by the build goal setting. When the published case DMC is re-calculated with an adjusted usable life (including the life after the final shop visit and before retirement), the DMCs values match.

These cases reinforce the conceptual design of the workscoping methodology, where “what” maintenance is carried out is considered alongside “when” it is carried out and the knock on effect of both “what” and “when” on the overall cost of maintenance through life.

Life Limited Part (LLP) costs

Considering the “maxDet” case presented above and detailed in Listing 6.3, the through life cost of LLP can be considered further. Over the engines usable life, each LLP set is replaced at least once. Stub lives are therefore lost at each LLP replacement as well as at engine retirement.

Lost stub life due to premature removal of LLPs can add considerably to the cost of maintenance over its life. Many operators and MRO providers reduce LLP stub life losses by using removed LLP sets together, to produce “streamlined” engine builds, where all the LLPs would have the same remaining usable life even if this is lower than would usually be ideal.

The stub lives discarded and considered lost in the “maxDet” with 10,000FC build goal across all the LLP sets is 13.73% (varying between 8.33% and 26.67%). However, this stub life calculation includes the remaining usable life of 15,000FC of the LLP set which could easily be used on another engine, and would in practice not be “lost”. If the remaining usable life of the LPT is not included in the stub life calculation it results in a 7.84% stub life lost.

A LLP DMC of $32.72\$/FH$ over a usable life of 55,000FC and 110,000FH is calculated by the workscoping methodology. For comparison the Hourly and Cyclic EMCWG cost methods are applied to this case as described in section B.2, using both the default EMCWG calculation period of 25 years, and the usable life calculated by the workscoping method. For all of these calculations an annual utilisation of 3000 hours and a flight length of 2 EFH:EFC are applied as per the published case metrics (Table C.1).

When the workscoping result is assessed over 25 years, including the first three shop visits presented in Listing 6.3 and a remaining usable life following the last shop visit of 2500 Flight Cycle (FC), the shortened period after final shop visit results in elevated levels of usable LLP life remaining, which could in a fleet application be re-used. If the remaining usable life of the LLP sets at the end of the engine life are considered re-used (not lost) then the stub life lost is 6.52%, however, if these remaining lives are considered lost, then the stub life lost is 39.13%. Either way, the LLP DMC to this engine would be 40 $/FH, unless a proportion of its cost were allocated to its next host engine were it reused. Said allocation might be pro-rata to either the life used or life remaining, but additional costs would also be incurred on fitting this re-used part to its new host . However, at the point that the QCM is removed from its first host upon retirement, it would not be known whether or not the part would be re-used, so at least initially its full cost must be accounted for.

This range of lost stub life values is important, because it is commonly used as an input to LLP cost models and is often assumed to be 10%.

In each case, except for the calculation over 25 years with 39.13% stub life lost, the result of the workscoping methodology is in between the results from the hourly and cyclic LLP DMC methods. While, like the hourly method, the

Calculation period	55,000 FC (36.67 years)			25 Years		
Stub Life (%)	10	13.73	7.84	10	39.13	6.5
Hourly LLP DMC ($/EFH)	30.34	32.43	29.20	21.85	45.07	20.04
Cyclic LLP DMC ($/EFH)	48.52	50.61	47.38	48.52	71.74	46.70
Workscoping Method LLP DMC ($/EFH)		32.72			40	

Table 6.3: Comparison of LLP DMC calculations

workscoping method assumes that the initial LLP set is fully capitalised, it is observed that the hourly method result is not always closest to the workscoping result.

Effect of performance margin deterioration on through life maintenance

The two 10,000FC build-goal cases presented for the “minDet” and “maxDet” engine deterioration cases (Listing C.3 and Listing 6.3) can also be compared side-by-side. The only difference between these cases is the initial shop visit interval due to the variation in rates of deterioration. This impacts on the order and shop visit at which some of the LLPs are replaced, though not on the overall shop visit costs.

The through life cost attribution pattern changes. The costs in the “minDet” are accrued at earlier shop visits than in the “maxDet” case, due to the longer 1SV operating period. And, because the “minDet” benefits from an extended usable engine life incurred at the initial shop visit, where the performance deterioration is the shop visit driver, the overall through life DMCs are also reduced by 8% when compared with “maxDet”.

The effect of performance deterioration on through life maintenance cost is investigated further in chapter 8 in cases that consider the effect of operational conditions and decisions which affect the rate of EGT margin deterioration and

therefore the resulting shop visit intervals.

Effect of Build Goal on through life maintenance costs

The effect of build goal choice, a planning decision, is assessed, for the two engine deterioration cases already defined “minDet” and “maxDet”. For each engine deterioration case, a full through life workscope is planned with build goal varying between 5000 and 12000 FC. The engine “end of life” is set at 4 SVs. Summary outputs are reproduced in section C.3, and represented graphically in figures 6.10 and 6.11.

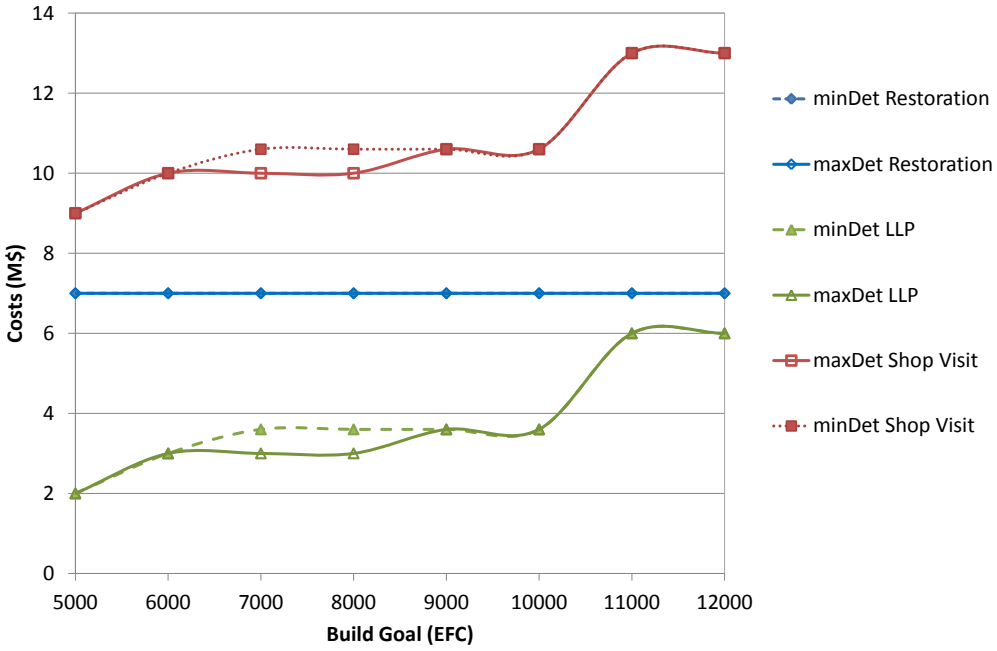

Figure 6.10: Effect of varying build goal on total through life maintenance costs

The engine usable lives increase with increasing build goal. The total restoration cost is constant (due to the case definition - as per Table C.1), therefore the restoration DMC reduces with increasing build goal (Figure 6.11).

LLP costs incurred are not constant (Figure 6.10), with increasing build goal

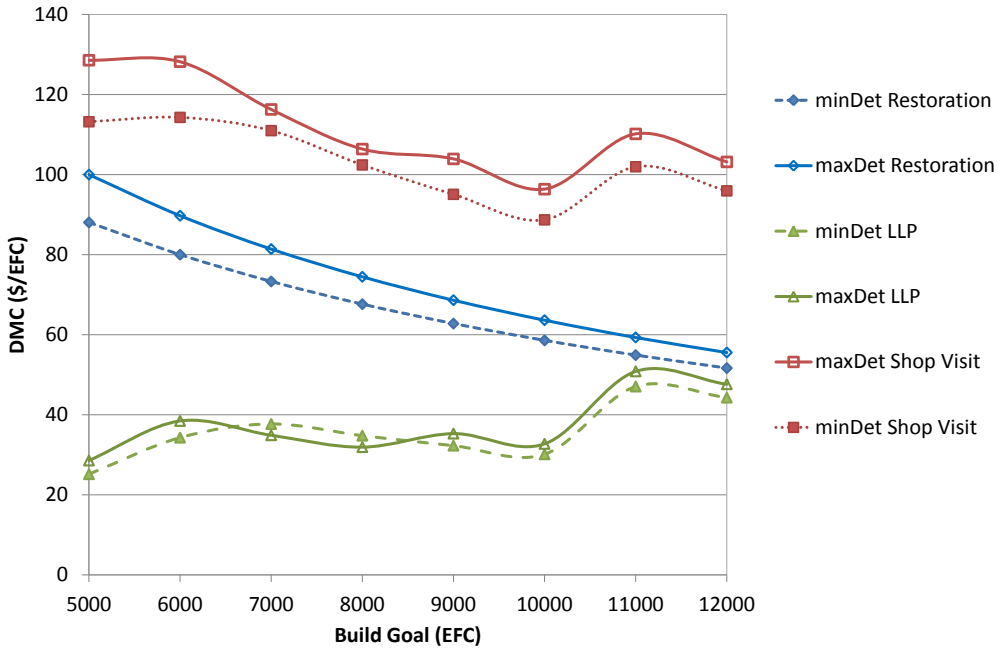

Figure 6.11: Effect of varying build goal on DMCs ($/EFC)

the total cost of LLPs increases gradually in a stepped manner. However LLP costs tend to increase at a greater rate than the usable flying hours such that theLLP DMCs also increase with increasing build goal.

Combined, the LLP and Restoration costs produce a total shop visit cost that increases with build goal. This in turn results in a total Shop Visit DMC which reduces gradually to a minimum at 10,000FC build goal, then steps up.

The pattern is repeated in both deterioration cases although the deterioration rate affects the usable engine life such that the DMCs for the “minDet” are reduced proportionately. A curiosity of the cases is that at Build Goals of 7000 and 8000, the interaction between the performance deterioration interval and the LLP lives, is such that the LLP costs are higher for the “minDet” case than for the “maxDet” case as the LPT LLP set is replaced twice instead of once during the engine life when compared to the same build goals for the “maxDet” case, but as

such these two cases have an LLP change requirement resembling that of the "maxDet" cases with increased build goals.

These studies demonstrate the key importance of the build goal choice in maintenance planning. Different engine operating regimes will result in a variation of optimal build goal.

Two assumptions set by the verification case are that usable life is determined by four shop visits an the remaining interval thereafter and that restoration actions occur at each shop visit, with the restoration at the first shop visit being cheaper than thereafter. These have artificially determined some of the results. It is reasonable to assume that in operational cases with extremely short maintenance intervals, performance restoration would not necessarily be conducted at each shop visit, and may be deferred to subsequent shop visits nearer the performance deterioration limit, though some tear-down and inspections tasks would still necessary, so the man hours and materials costs would not be null.

6.4.2 Lower Thrust Engines

These cases relate to a lower thrust engine type fitted to a narrow body airframe. A family of engines is considered, containing four engines of varying ratings. The available maintenance actions (LLP and restoration) are the same for each engine in the family. These engines differ in "soft" rating, as is now common for certain families of engines which have become commoditized allowing the operators to re-rate engines between operating intervals otherwise identical engines.

The workscoping inputs for this lower thrust engine family is presented in Appendix D.

This soft rating allows engines that have exhausted their EGT margin at a

higher rating (E4) to be re-rated to a lower thrust category and continue to operate until the margin at the lower thrust rating is also exhausted, thus extending the possible TOW between restoration driven shop visits.

In these initial cases, the engines labelled E1, E2, E3 and E4 represent engines with increasing “soft” ratings. These soft ratings are reflected initially in the core workscoping model inputs by way of distinct book deterioration profiles and EGT margins for each engine.

Cost of engine aging

This study is to consider the effect of workscoping over an engine' usable life and seeks to compare the through life cost trends developed with those described by Dixon and reproduced in section 5.4.3.

This case initially considers considers a four shop visit planning rule which conforming to an expected operational life of approximately 40,000FC applied to the E1 engine in the lower thrust engine family. The E1 engine is the lowest rated of the engine family with only 0.79 of the E4 engine thrust.The mission studied is 1.4 hours with 20$^{\circ}C$ OAT .

The shop visits are driven by LLP removals rather than performance deterioration as expected for short haul operations at moderate thrust ratings. The workscoping output produced is summarised in Listing D.12.

If, as discussed in section 6.4.1, it is assumed that the SVC incurred can be entirely attributed to the preceding shop visit interval then DMCs values can be distributed throughout the operating period producing $ / FH outputs, which are presented in Figure 6.12.

The process is repeated for different engine ratings (using a different `Engine`

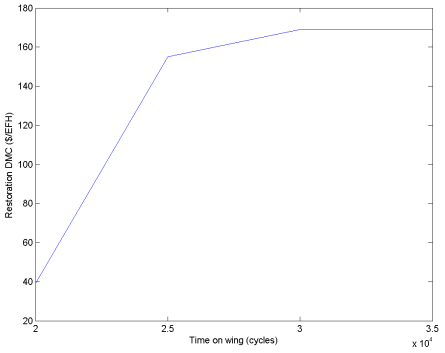

(a) Restoration DMC ($/EFC)

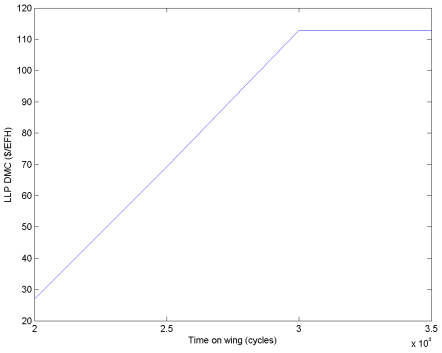

(b) LLP DMC ($/EFC)

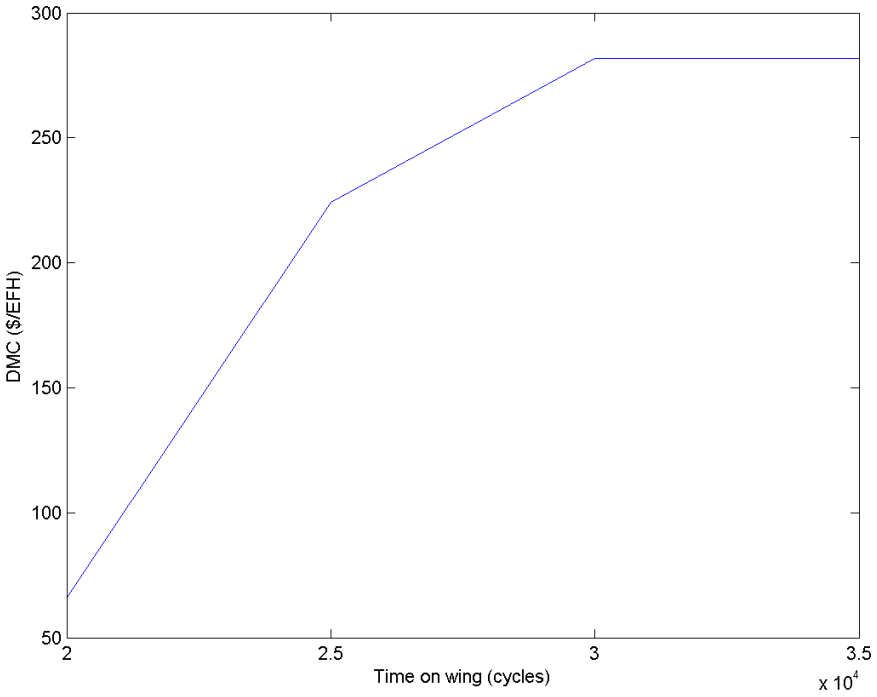

(c) Total DMC ($/EFC)

Figure 6.12: Effect of aging on DMC variation through engine life for E1 engine type operating at 20°C

input structure for each rating) and different OATs.

The corresponding output from the second example considered using the higher rated engine type E3 operating at 35°C is presented in Listing D.13 and

the DMC profile is plotted in Figure 6.13 . Engine E3 has a rated trust of 0.94 of E4 rated thrust and 1.18 of E1 rated thrust.

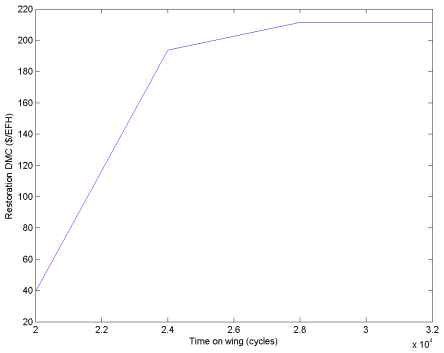

(a) Restoration DMC ($/EFC)

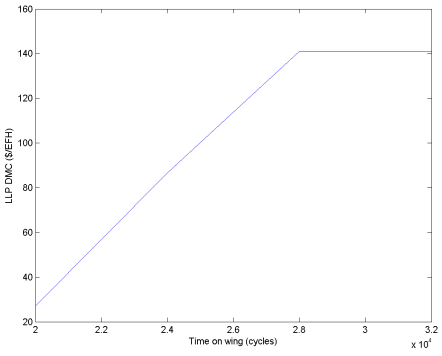

(b) LLP DMC ($/EFC)

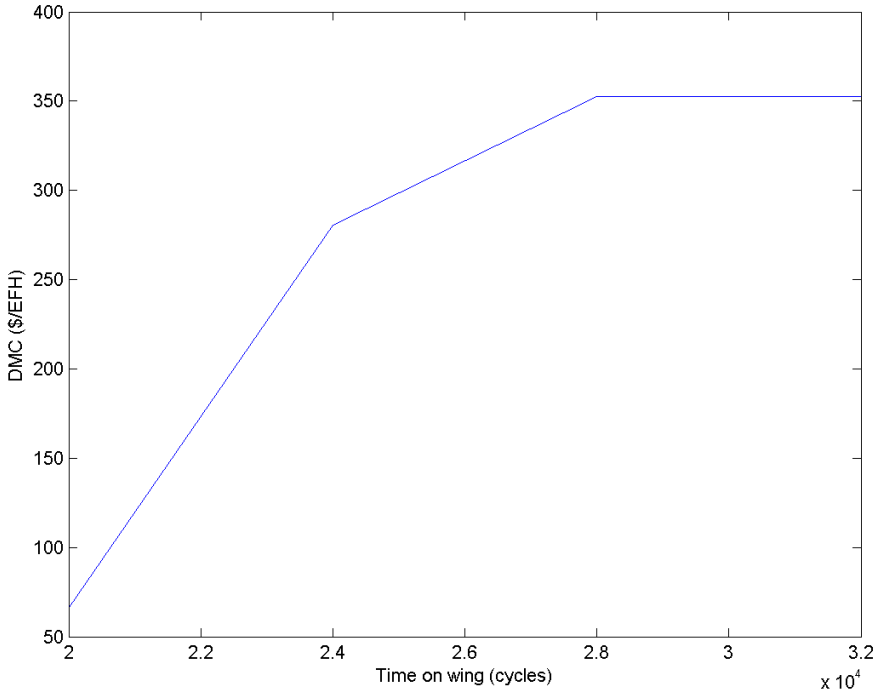

(c) [Total DMC ($/EFC)

Figure 6.13: Effect of aging on DMC variation through engine life for E3 engine type operating at 35$^{\circ}C$

From the Maintenance summaries presented in Listing D.12 and Listing D.13,

it can be seen that harsher operating regimes (OAT and Thrust) change the resulting engine maintenance profile.

The E3 engine (D.13),operating at increased OAT and at a higher thrust rating has shop visits driven by performance related limits (EGTM) requiring performance restoration, whereas workscopes on the lower rated E1 engine are primarily LLP related.

Both engine cases considered show aging of the DMCs conforming to Dixon's [117] results in that there is a distinct "new" phase up to the first (or second) shop visits and an identifiable "mature" phase. Like Dixon these engine maintenance costs do not exhibit an "aging" phase, but rather an extended mature period. However, were price escalations (due to inflation or otherwise) to be included in the cost calculation they would have an effect which might be interpreted as aging.

Over their usable lives, the effect of operating these similar engines at different thrust ratings, and therefore temperatures and loads, has the effect of reducing the available life of the higher rated engine by 4000 EFC or 10% when compared to the lower rated E1 engine and increasing direct maintenance costs ($/EFH) when accounted for over the engine life by a commensurate 11%.

The distinct phases of engine aging expected are identifiable in the cost outputs of the workscoping model. Changing engine ratings has produced different shop visit drivers and costs as expected.

Varying Outside Air Temperature (OAT)

The effect of varying OAT and the resulting EGTM deterioration are considered in terms of their affect on performance related shop visit drivers. For this study

published relationships between OAT and EGTM deterioration are used to determine performance based shop visit intervals through the application of the “book” deterioration method used previously.

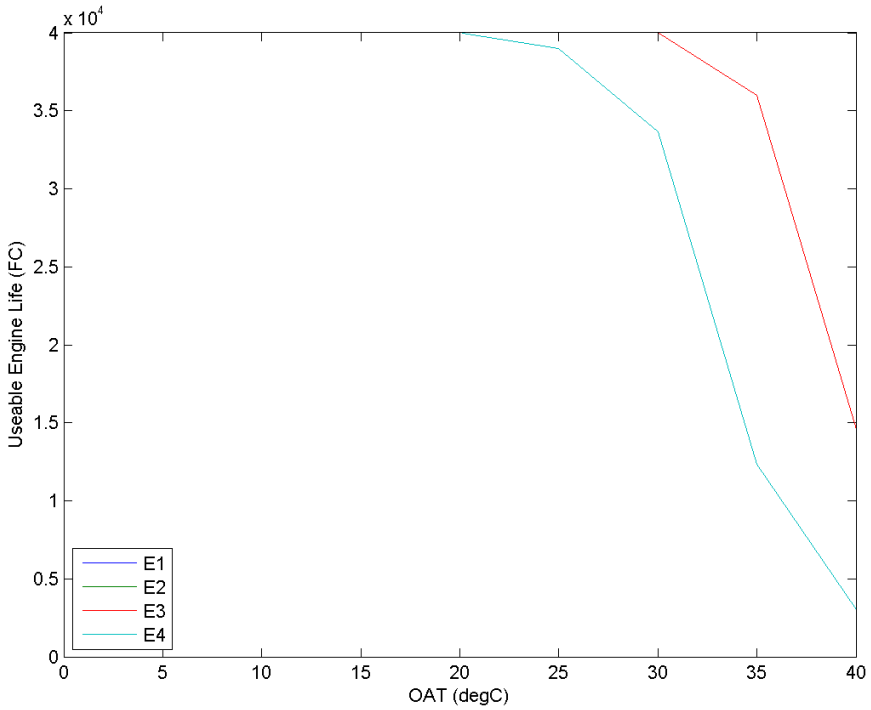

(a) Change in usable life

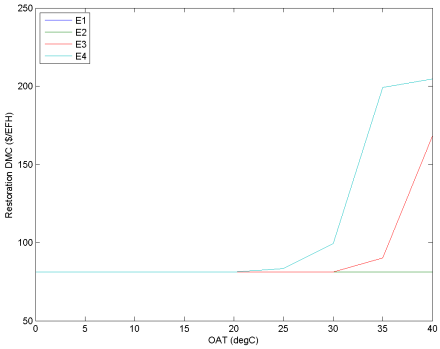

(b) Varying restoration DMC

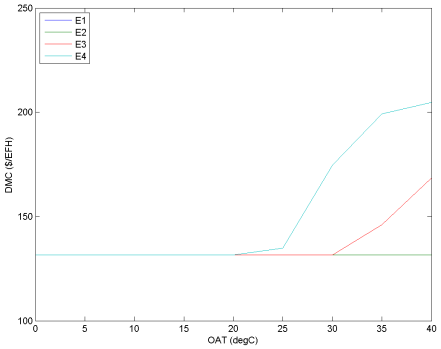

(c) Varying total DMC

Figure 6.14: Effect of OAT on through life DMC variation

Summary outputs from the cost model are presented in Appendix D.3 and are

presented graphically in Figure 6.14. Engine usable life reduces for the higher rated engines E3 and E4 at elevated OATs while the usable lives for the lower rated engines (E1 and E2) do not reduce from 40,000FC (Figure 6.14(a)). Consistent with the reduction of usable engine life seen in Figure 6.14, the engine maintenance costs increase for the higher rated engines at elevated OAT (Figure 6.14(b) and (c)). The usable life and maintenance costs of the highest rated engine (E4) are affected by smaller increases in OAT than the more moderately rated engine (E3).

Increasing OAT is found to reduce usable engine life especially for higher rated engine types, while also increasing the cost of restoration.

The initial results presented conform with expected trends, in higher rated engines operating at higher temperatures the burden of performance restoration during shop visits will increase and the usable life (for a fixed number of shop visits) as in this case will decrease. This conforms with previously published results from this research programme [7, 18] which determined that increasing OAT, would increase the severity of engine operation and decrease engine life, while increasing the rate of aging.

6.4.3 Summary

This chapter has described the decisions and choices made during the development of the workscoping model designed to assess engine maintenance costs following the "When? $\Rightarrow$ What? $\Rightarrow$ How much?" concept which is considered important when maintenance costs are to be physics-based.

The case studies presented in the verification section of this chapter represent demonstrations of the model capabilities and verification of model results

where available. Each of these cases, reflects the use of the workscoping model independently. Further cases, coupling the workscoping model with the engine performance, lifing and severity stages of the workscoping methodology are presented later in chapter 8.

Chapter 7

Model definition and methodology

This chapter presents methodology developed in this multidisciplinary project. Each stage of the methodology presented initially in section 2.2 will be presented in turn. The methodology has been developed so as to allow for individual tools and methods to be changed or replaced to suit a given case.

The methodology can be considered in terms of the following steps:

- Mission performance modelling of engine and aircraft
- Component load analysis
- Severity and aging modelling
- Operational cost modelling through the virtual workshop approach

7.1 Mission performance modelling

Engine and aircraft performance through a flight path or mission is simulated using two coupled tools: TURBOMATCH and HERMES. These are FORTRAN

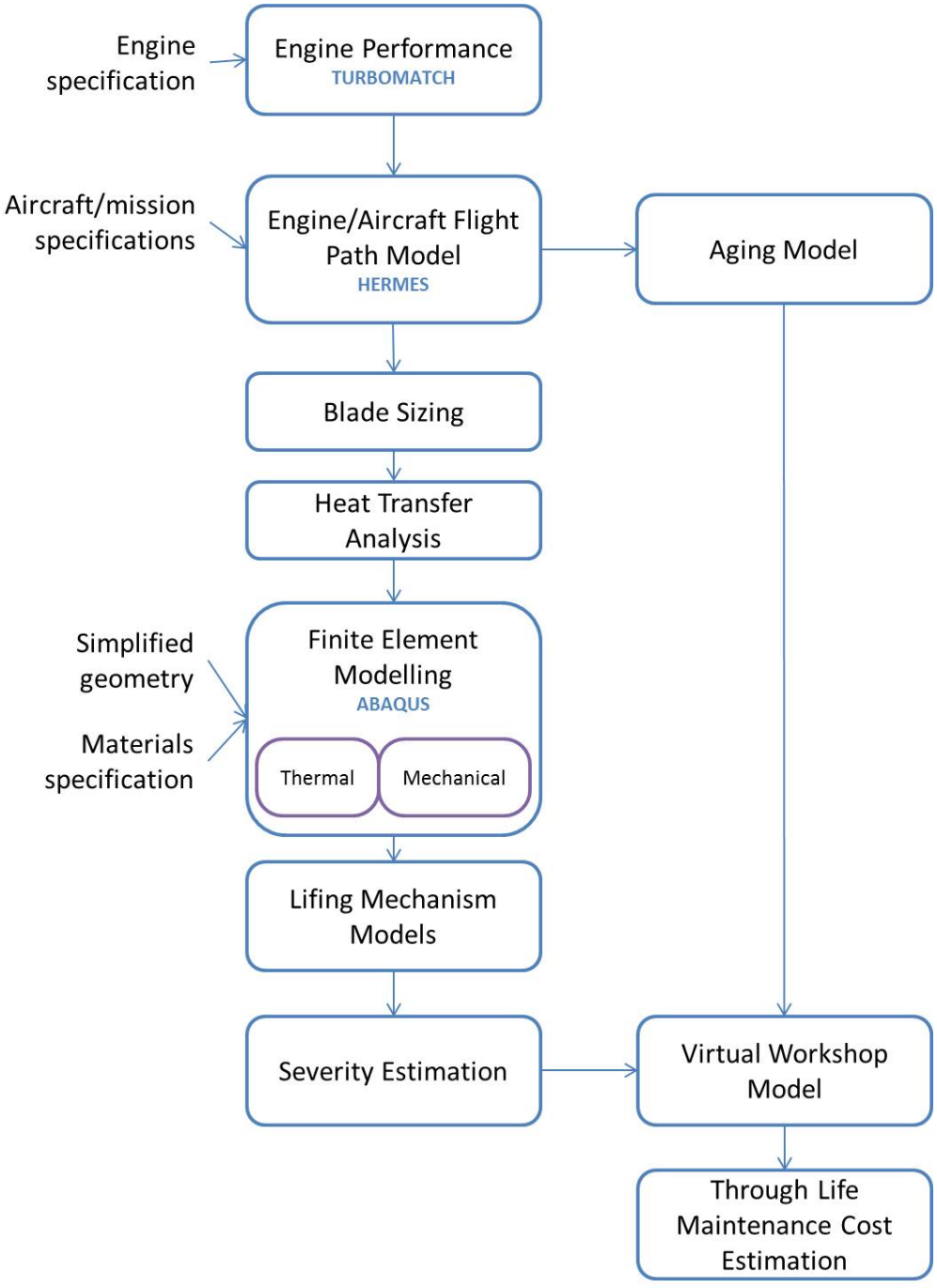

Figure 7.1: Method overview

codes developed at Cranfield University.

Engine modelling is required in order to provide inputs to the later stages in

the methodology. Key requirements of the selected engine performance model include the calculation of off design performance conditions (temperatures, pressures, ...) at a module level (turbine stage), throughout the flight envelope determined by a suitable payload range envelope for the application.

7.1.1 TURBOMATCH - Gas Turbine Performance Model

TURBOMATCH is a modular code that allows an engine model to be built module by module, with computational BRICKS representing physical engine modules (compressor, turbine, ...). It allows engine performance to be assessed for design point and off design conditions.

Requirements

The engine performance model used should be capable of:

- design point and off design performance calculations
- modelling different engines
- allow for bleed and off-takes including cooling flows

Outputs required from the engine performance model, given a focus in this research on the High Pressure Turbine (HPT), include:

- inlet and outlet gas temperatures for the HPT
- temperature of cooling flows to the HPT

The combination of BRICKS that describe and calculate module performance and stations identifying the points between subsequent modules and their interconnections is presented schematically in Figure 7.2 for the two spool lower thrust engine used in the case studies in chapter 8.

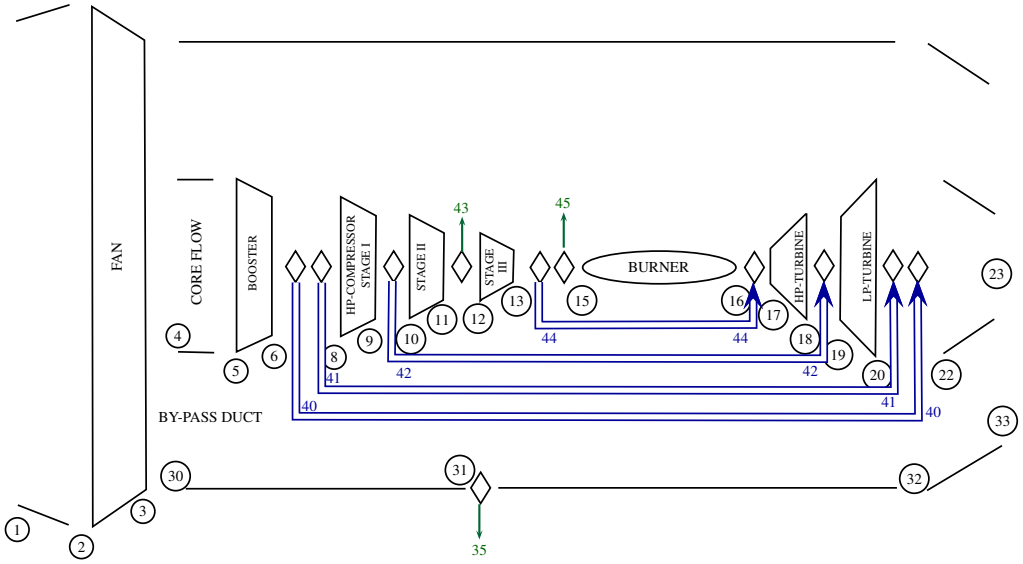

Figure 7.2: Schematic of TURBOMATCH engine model layout for two spool turbofan

7.1.2 HERMES - Aircraft Performance Model

HERMES uses weight, engine and aircraft geometry (wing, tailplane, fin and fuselage) inputs and consists of six modules:

- Inputs
- Mission profile
- Atmospheric model
- Engine data
- Aerodynamic model
- Aircraft performance module

HERMES considers a mission in terms of segments (Taxis & Take-Off, Climb, Cruise, Descent, Approach). HERMES requires two input sources, a primary

input defining aircraft, mission and engine specifications and a secondary input containing formatted engine data. In this application of these tools the formatted engine data are generated using TURBOMATCH.

HERMES outputs data in two formats, one containing aircraft performance data including fuel burn, duration and distance flown for each flight segment and the overall mission, the other output collates engine performance data for each flight segment and includes temperatures, pressures, mass flows and shaft speeds.

The engine and aircraft model produced is verified by comparing the results for the engine and aircraft modelling to those expected from published data. A key check is to verify that the model produced is capable of flying the flight envelope expected for its type and configuration. For the engine presented in Figure 7.2, this check has been completed assuming use in a narrow-body twin engine short haul aircraft, the resulting payload-range diagram is presented in Figure 7.3.

At the extreme operating corners of the flight envelope, the range and break release weights generated from the HERMES & TURBOMATCH coupled models match the published data to within -0.66% and -0.21% respectively.

7.2 Component load analysis

Once the engine and aircraft missions performance has been modelled, several steps are required to determine the HPT blade loads.

While the key stage of this phase of the methodology is the Finite Element (FE) modelling preliminary steps are required to derive suitable inputs and boundary conditions. These are:

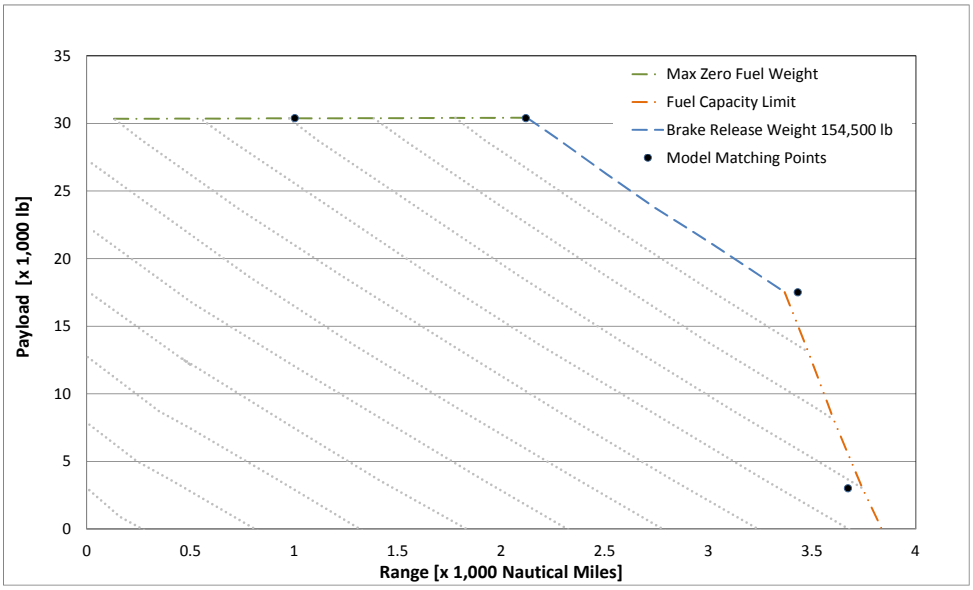

Figure 7.3: Payload range diagram

- Turbine sizing
- Heat transfer analysis

7.2.1 Turbine sizing

A generalised simplified approach to turbine sizing is adopted given an absence of known component dimensions [10, 99, 100]. Sizing is carried out using TURBOMATCH **DP!** (**DP!**) engine performance data including turbine inlet and outlet mass flow, temperatures, and required power output.

Assumptions

- nozzle angles are constant

- axial velocity is constant
- degree of reaction set at 50%

Outputs

This simplified sizing procedure defines the outline of the blade geometry, in terms of blade height as well as hub and tip radii.

These are inputs used by the FE modelling to adapt the simplified geometry (introduced in subsection 4.3.3) model selected to the specific engine and aircraft case under evaluation.

7.2.2 Heat Transfer analysis

The FE modelling requires blade material temperatures. These must be determined from the gas flow temperatures calculated in the previous stages.

Requirements

Thermal boundary conditions for the FE modelling are defined differently on the external (hot-side) surface and on the internal (cooling hole) surface. But in both cases,

- a span-wise distribution of temperatures at the design point, and
- a time history amplitude of temperatures throughout the mission

are defined. These are calculated analytically following the method introduced in section 4.3.2 and section 4.3.2 respectively which consider the effect of a Radial Temperature Distribution Factor (RTDF) on the blade hot side (external surface) and heat transfer due to:

- cooling air by convection
- conduction through a Thermal Barrier Coating (TBC) if present

Examples of the analytical temperature and heat transfer coefficient radial distributions are shown in Figure 7.4 and Figure 7.5.

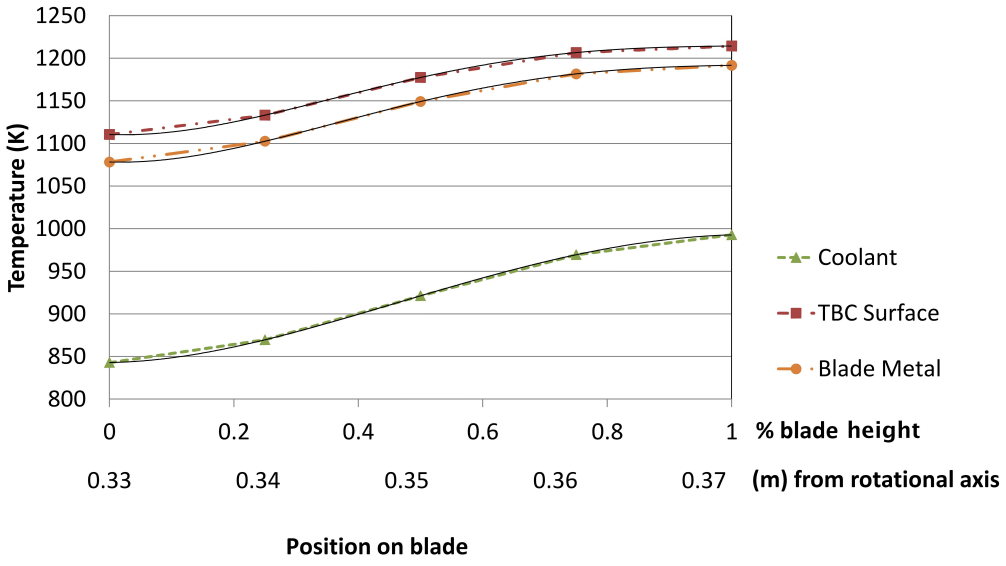

Figure 7.4: Radial temperature distributions

The radial temperature and heat transfer distributions are used as inputs to the FE model in the form of polynomial functions ($T = f(z)$, where z is the axis applied in the radial direction).

7.2.3 ABAQUS - Finite Element analysis

The FE modelling carried out forms a key link between the engine operation captured by the performance modelling and the lifing and costing which is the intended outcome.

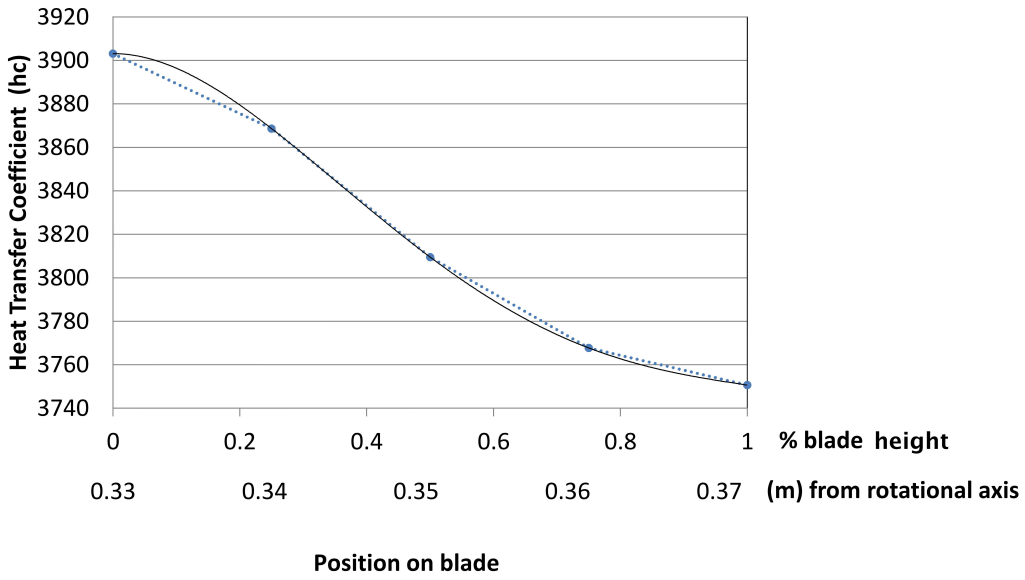

Figure 7.5: Radial heat transfer coefficient distribution

Several stages and versions of FE modelling have been used throughout this project, including two principle simplified geometry forms.

The FE process and models focused on here are the latest iteration of a process which developed from the starting point established by Hanumanthan [18] and reported in a co-authored publication [7] which consisted of a simplified 2D model with addition of element thickness built in ANSYS and described previously in subsection 4.3.3.

Requirements

The FE process developed is required to produce load output required for further lifing analysis (including nodal temperatures, element temperatures, heat flux vectors, stress components and variants, total strain, plastic strain and thermal strain at each time-step).

Method

The FE is carried out in two steps:

1. Thermal analysis

2. Mechanical analysis of hot blade

Prior to the thermal analysis, a certain amount of pre-processing is required. The baseline simplified geometry verified by Abu [12] must be adjusted to suit the specific engine modelled using inputs calculated during blade sizing and the time steps for the mission defined during the engine performance calculations. Once the case geometry has been established, it can be re-used with different boundary conditions to study subsequent flight mission cases for the same engine and aircraft.

The FE geometry is meshed prior to simulation. The mesh quality is checked for excessive warp, skew and aspect ratio and a grid dependency study varying mesh seed size is conducted to establish the range of reasonable mesh densities given a maximum output file size determined by storage constraints, and computational time limits.

The thermal analysis produces a heated blade geometry representative of the blade subject to the temperature gradients and time histories calculated during heat transfer analysis and aircraft engine performance modelling in the form of an FE object file. This heated blade consists of the simplified geometry, subject to varying time-dependent temperature throughout the mission studied.

Boundary condition inputs to the thermal analysis are verified by comparison to the desired metal temperatures calculated during the heat transfer analysis, an example verification result is presented in Figure 7.7.

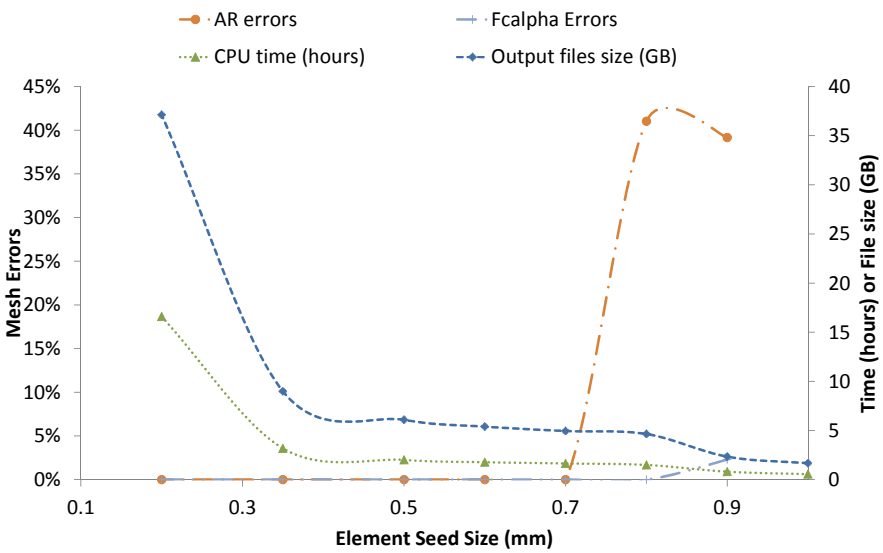

Figure 7.6: Grid dependency study results

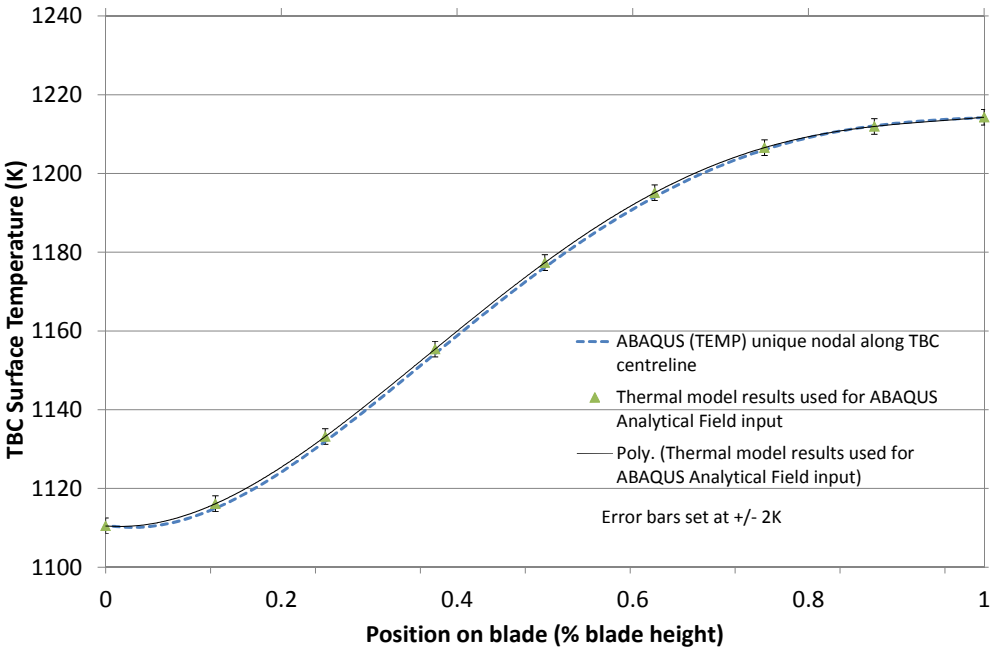

Figure 7.7: Example of thermal boundary condition verification

The heated blade, is then subjected to additional centrifugal loading with the blade root constrained. Centrifugal loading is applied in the form of an angular velocity which is applied about the rotational axis determined during blade sizing.

$$\sigma_{CF} = \rho.h.\omega^2.d_{CG} \tag{7.1}$$

Given:

h blade height

ω angular speed of axial rotation

d_{CG} distance of blade centre of gravity from rotational axis

ρ blade density

Outputs

For the purposes of verification checks outputs are produced from the thermal model, mechanical model and the coupled thermo-mechanical model. Though it is these last results which are carried forward for lifing analysis. Data is extracted from the FE modes in the form of text based ".rpt" files. Eight variables are selected for output (strain (E), thermal strain (THE), plastic strain (PE), temperature (T), stresses (S1, S2, S3) and SigPress). These are output for each calculation node of the area of interest as a time history throughout the mission. The data is primarily extracted for further study from the hot and cold side surfaces at the centre of the curved surface. However, cuts through the material are also output for interpretation and verification of the thermal gradients present. These are analysed to assess the usability of the FE results, and to check for discontinuities

in the thermal and mechanical load gradients through the leading edge which may identify errors in the FE model structure or implementation.

7.3 Operational Severity and Aging

Physics-based Lifing-Aging-Severity tool developed at Cranfield University as part of this research program by Hanumanthan [18] uses data from the combined aircraft-engine models (thrusts, altitudes, Mach numbers, mass flow rates, temperatures, pressures and shaft speeds) at each flight segment. Focusing on HPT blades which are sized following a one dimensional equivalent cross section approach at design point. Heat transfer coefficients are estimated for use in Finite Element thermal and mechanical analyses at each flight segment. Temperatures, load histories and material properties are then combined to calculate lifing considering several failure mechanisms (creep, fatigue and oxidation). Life values are converted into damage fractions following linear damage theory which enables severity estimation for the mission.

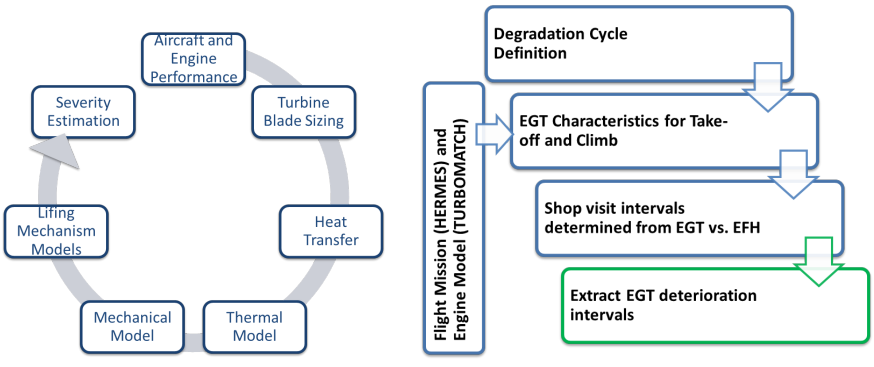

(a) Severity (b) Aging

Figure 7.8: Process schematics

Requirements

A lifing method is required which derives inputs to selected lifing mechanisms from engine and aircraft performance modelling. The methods applies should be physics-based and rely on simplified geometries, allowing the models to be applied to a range of aircraft engines and minimising the number of input parameters required which would not usually be available at the preliminary design stage. The process should be able to capture thermal gradients through the blade leading edge induced by cooling flows, enabling the study of in and out of phase load cycles. The initial method couples creep, fatigue and oxidation, while this has been expanded and further developed to account for Thermo-mechanical fatigue (TMF). The methodology is however adaptable to multiple lifing mechanism models.

The aging method applies scaled deterioration profiles based on definitions published by Litt and Aylward [146] who attribute them to Sallee [147].

Outputs

The outputs required of this step of the process are mission dependent operational severity measures for the modelled engine and aircraft performance cases. These measures of relative damage are either coupled creep-fatigue-oxidation as per Hanumanthan or TMF derived as per Blanchard [59] and Abdullahi [12].

The aging method develops in parallel to the lifing tool, the Exhaust Gas Temperature (EGT) characteristics for an engine-aircraft performance model subject to degradation. These EGT characteristics serve as input to the performance deterioration steps of the workscoping model.

7.4 Work-scoping

Requirements

The method adopted is required to capture the physics-based needs for maintenance as cost drivers. It relates maintenance costs incurred to operation. Maintenance actions should be triggered by life limits or performance deterioration. The impact of maintenance actions completed at one shop visit should affect and change the required maintenance actions and resulting costs at subsequent shop visits.

Method

The workscoping methodology assesses each shop visit during an engine's service life sequentially. Thus capturing the shop visit intervals, maintenance actions completed and resulting costs following the $When? > What? > How much?$ concept outlined in subsection 6.1.1.

Inputs

The workscoping model requires inputs defining the available maintenance actions, their triggers and associated costs for each defined engine.

Maintenance actions can variously be triggered by performance deterioration, life limits, or specific shop visits. Performance deterioration can be input by so-called "book" deterioration relationships, or, as performance intervals input as a vector of performance based intervals due to Exhaust Gas Temperature Margin (EGTM) exhaustion generated from the previous aging model.

Outputs

The workscoping model generated output reports summarising the through life

maintenance requirement of each engine-aircraft-mission case (Figure 6.9). Outlining the maintenance conducted at each shop visit and summarising overall total maintenance costs and Direct Maintenance Costs (DMCs). The model outputs are described in more detail in section 6.3

Assumptions

This approach assumes that all Shop Visits (SVs) are planned (rather than due to unexpected failures). That shop visits consist of maintenance actions which can be pre-defined and costed. Which care triggered either by life limits or deterioration of EGTM.

Chapter 8

Case studies

In considering the physics-based cost of engine operation, we distinguish between operating decisions and operational conditions. Operational conditions are considered to be those operational parameters (such as Outside Air Temperature (OAT) and flight duration) which are outside the control of the operator once the route has been established. Whereas operational decisions include operational parameters which are at least nominally within the control of the operator such as derate and maintenance planning. Applying the full workscoping methodology from engine performance modelling through to maintenance cost assessment as described in chapter 7.

The aircraft-engine case considered is a narrow-body type airframe operating with two lower thrust engines. This is a highly rated engine within its type, whose maintenance requirement is likely to be driven by the performance restoration requirement.

This engine is modelled in TURBOMATCH and the scheme implemented is represented schematically in Figure 7.2. It is a twin spool engine with a 1.55m fan diameter, a mass flow of 355kg/s and a pressure ratio of 32.8.

The aircraft-engine model verified by matching the payload range diagram generated by modelling the corners of the operating envelope against published data for the engine and aircraft type. The Payload Range diagram produced is presented in Figure 7.3.

8.0.1 Reference Mission

The reference mission for this engine aircraft combination conforms to the reference mission definition Table 4.2.

Flight Length (FL) 1.4 hours

Outside Air Temperature (OAT) $18°C$

Derate 10%

Performance modelling

The engine-aircraft modelling using HERMES and TURBOMATCH generates through mission parameters required as inputs by the subsequent steps in the methodology for both the overall engine (Figures 8.1, 8.2 and 8.3) and for the High Pressure Turbine (HPT) in particular (Figures 8.4, 8.5 and 8.6).

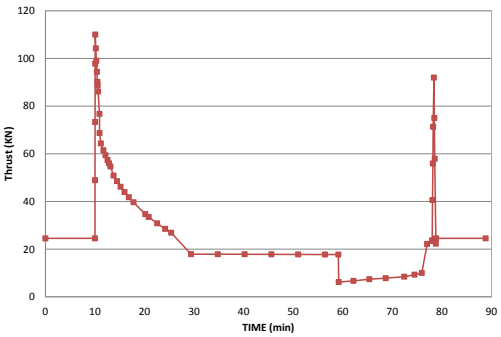

Figure 8.1: Thrust variation

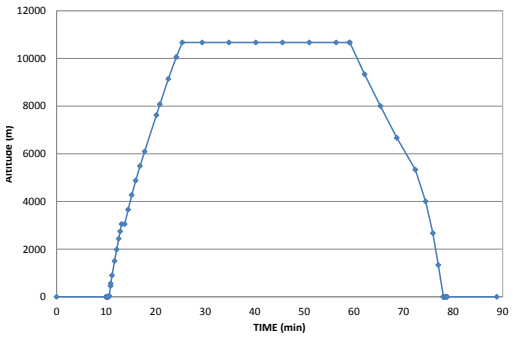

Figure 8.2: Altitude variation

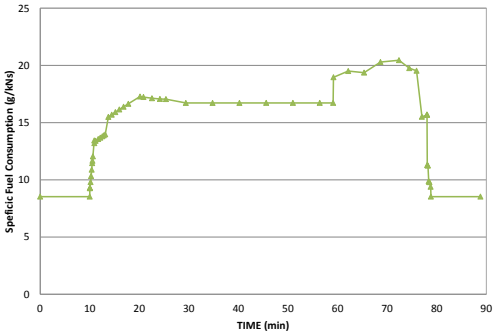

Figure 8.3: Specific Fuel Consumption

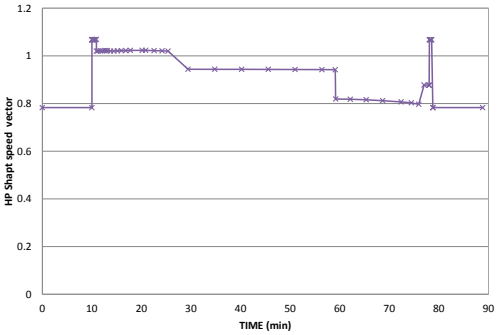

Figure 8.4: HP shaft speed

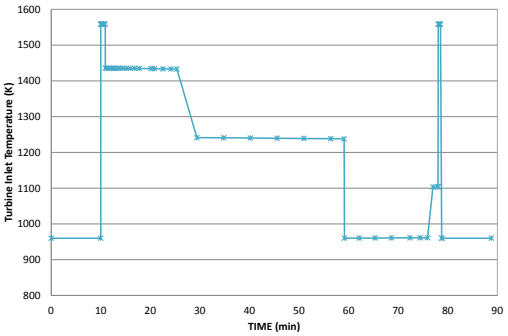

Figure 8.5: HPT Inlet Temperature

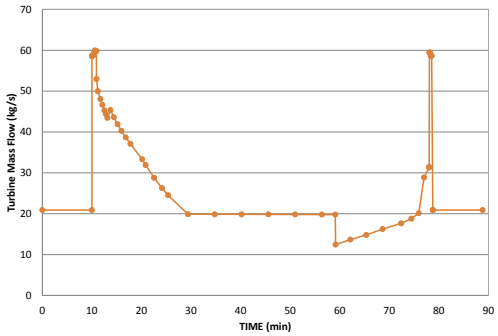

Figure 8.6: HPT Mass flow

Lifing and Aging

Finite Element (FE) modelling completed following the process established by Abdullahi [12]. Applying the heat transfer analysis described in subsection 4.3.2, the resulting radial temperature distributions were presented in Figure 7.4 and the heat transfer coefficient distribution in Figure 7.5.

The FE model produced is checked for appropriate Boundary Condition (BC) allocation as in Figure 7.7. The FE model outputs in the form of .rpt files are inputs to the lifing mechanism and severity models.

In parallel, the aging model is applied to generate an Exhaust Gas Temperature (EGT) margin deterioration curve. This follows Hanumanthan's [18] aging method presented in Figure 7.8(b) which uses a scaled deterioration pattern as

defined by Litt and Aylward [146] and presented in Table 8.1.

Degradation	EFC	Parameter	Fan	LPC	HPC	HPT	LPT
Moderate	3000	η %	-1.5	-1.46	-2.94	-2.63	-0.538
		$\dot{m}$ %	-2.04	-2.08	-3.91	1.76	0.2588
Severe	6000	η %	-2.85	-2.61	-9.40	-3.81*	-1.078*
		$\dot{m}$ %	-3.65	-4.00	-14.06	2.57*	0.4226*

$*$ extrapolated value

Table 8.1: Reference degradation values from Litt [146] attributed to Sallee [147]

The application of these deterioration patterns to the engine aircraft performance model EGT and shaft speeds for each deterioration set. These are then applied to a scaled Weibull curve to generate an aging curve, which combined with defined EGT red-line and margin restoration values [148] results in the Take-off Exhaust Gas Temperature Margin (EGTM) characteristic presented in Figure 8.7 . The performance intervals generated by this analysis are used as performance maintenance triggers in the workscoping methodology.

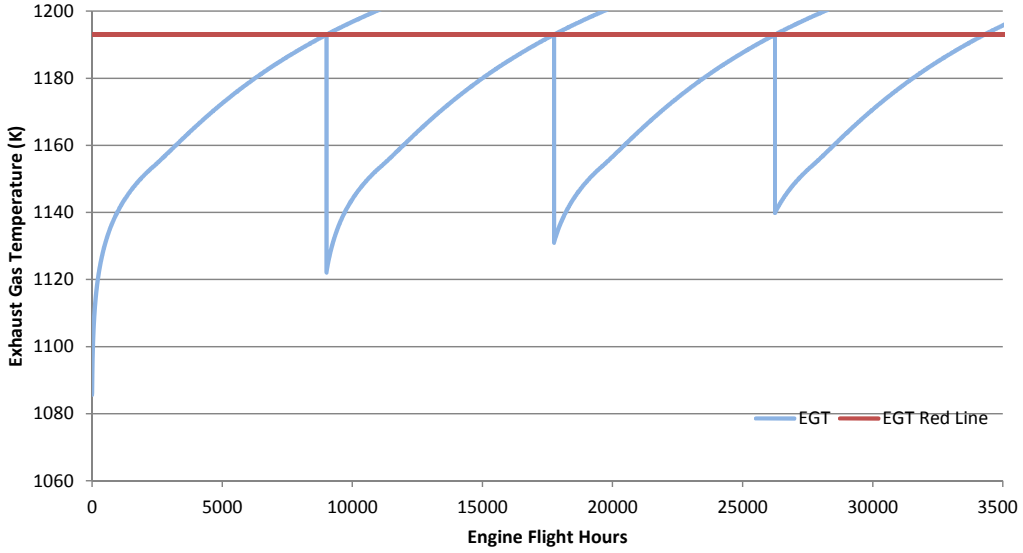

Figure 8.7: Take-Off EGT characteristic

Maintenance modelling

The workscoping method is applied to this engine. Following Hanumanthan [18], a working engine life of three shop visits is used as the calculation period.

The workscoping input for this engine includes 18 Life Limited Parts (LLPs) distributed into three LLP sets and four restoration actions. Due to its high thrust rating some restoration work is required at each shop visit (`level1core`), and higher levels of restoration requiring disassembly for each Quick Change Module (QCM) is completed when the linked LLP sets are replaced (`level2`). The engine input blocks for this case are reproduced in section E.1

The High rating of this engine and short flight durations lead to a high rate of deterioration. During the three shop visit interval period laid out by Hanumanthan [18], all shop visits are driven by performance deteriorations.

The three shop visits forming the through life workscope method output displayed in Listing 8.1 are all triggered by performance deterioration. As such the shop visit intervals are equal to the performance intervals determined by the deterioration and aging calculations. Due to the short performance maintenance intervals only the core LLP is changed.

The hourly attributable LLP cost per flying hour is calculated to be $26.86(\$/EFH)$. The stub life lost at replacement of the LLP set is 6%. While the remaining usable life of the LLP set at the end of the engine life is calculated to be 14250 cycles (or 71%), the cost of the LLP set is fully attributed to this engine. It is possible that in a fleet application this LLP set might be used in a different engine, or that this engine would in fact be run longer than the three maintenance cycle calculation period.

For comparison,the Engine Maintenance Cost Working Group (EMCWG) LLP

Listing 8.1: Workscoping Output

MAINTENANCE PLAN

SHOP VISIT	1	2	3	4
Trigger	deterioration	deterioration	deterioration	deterioration
Elapsed Engine Cycles	6433	12678	18744	24494
Elapsed Engine Hours	9006.20	17749.20	26241.60	34291.60
Elapsed Interval Cycles	6433	6245	6066	5750
Elapsed Interval Hours	9006.20	8743.00	8492.40	8050.00
fan&lpc	0.00	0.00	0.00	
core	0.00	0.00	921000.00	
lpt	0.00	0.00	0.00	
level1Core	1110000.00	1110000.00	1110000.00	
level2Core(TopUp)	0.00	0.00	435000.00	
level2fan&lpc	0.00	0.00	0.00	
level2lpt	0.00	0.00	0.00	
Rest Materials Cost ($)	900000.00	900000.00	1300000.00	
Rest Labour Cost ($)	210000.00	210000.00	245000.00	
Restoration Cost ($)	1110000.00	1110000.00	1545000.00	
LLP Cost ($)	0.00	0.00	921000.00	
Shop Visit Cost ($)	1110000.00	1110000.00	2466000.00	
Restoration DMC ($/EFH)	123.25	126.96	181.93	
LLP DMC ($/EFH)	0.00	0.00	108.45	
Shop DMC ($/EFH)	123.25	126.96	290.38	

MAINTENANCE SUMMARY

Useable Engine Life FC	24494
Restoration Cost ($)	3765000
LLP Cost ($)	921000
Shop Visit Cost ($)	4686000
Restoration DMC ($/EFH)	109.79
Shop DMC ($/EFH)	136.65

cost methods (Appendix B, section B.2 and B.2) are applied with the default calculation period, stub life, spares fraction and utilisation as defined in section B.2.

While the same number of LLP sets are replaced for the same cost in each of the three methods, three distinct attributable LLP costs are calculated:

Workscoping method $26.86(\$/EFH)$

EMCWG Hourly Method $22.92(\$/EFH)$

EMCWG Cyclic Cost method $36.55(\$/EFH)$

As discussed in section 6.4.1, the workscoping method makes the same assumption regarding the capitalisation of LLP sets as the EMCWG Hourly Method,

however, instead of being set inputs to the LLP cost calculation, the engine life and LLP stub lives are outputs of the model. In this case both are smaller than set in the EMCWG methods such that less LLP life is wasted in the workscoping model assessment than is assumed wasted in the EMCWG method, while the engine usable life is shorter. This is due to the interaction between the engine life and the performance deterioration driven shop visits and maximum shop visit number set, which is not accounted for by the EMCWG methods.

Considering the effect of engine maturity on shop visit costs

According to EMCWG method as described by Equation 5.12 the shop material cost is a function of engine maturity and mission severity. In this, the reference case, Operational Severity, given its definition as being damage relative to the reference case, is unity and is set in Listing E.4. The effect of maturity on the shop visit restoration cost can be considered by comparing the results of nominal workscoping calculation presented previously (Listing 8.1) with one of which considers the effect of maturity on restoration materials costs (Listing E.5). The effect of the maturity consideration is summarised in Figure 8.8.

The application of Equation 5.12 in the reference case has a severity equal to unity. It is considered that the application of the maturity factor the the shop material costs must be considered in the context of varying severity.

8.0.2 Effect of operating conditions

Two operating condition cases are considered. That of varying OAT in terms of an applied variation to standard atmosphere in the engine performance model, and, that of varying the flight length (in Hours).

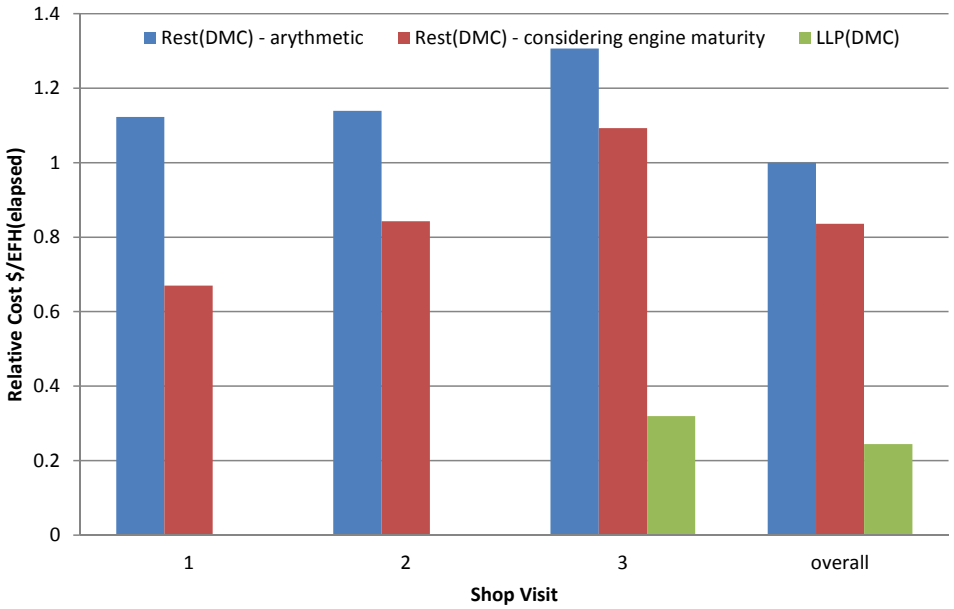

Figure 8.8: Restoration cost considering engine maturity

Outside Air Temperature

Changing the mission OAT would be expected to have several influences on the final costs of maintenance. As the OAT varies affecting the EGT margin available, the aging and deterioration profiles change. Increasing OAT would be expected to decrease the maximum performance based interval between shop visits.

Changing intervals can impact the scheduling of LLP replacements and therefore affect the stub lives lost and result in a variation of LLP costs per flying hour.

Increasing severity, linked with increasing OAT, would also be expected to increase restoration material costs.

EGT margin deterioration based aging curves are generated from engine and aircraft performance studies with varying mission OATs. Figure 8.7 is reproduced in Figure 8.9 with the addition of the equivalent performance EGT margin deterioration curves for 20$^{\circ}C$ and 25$^{\circ}C$.

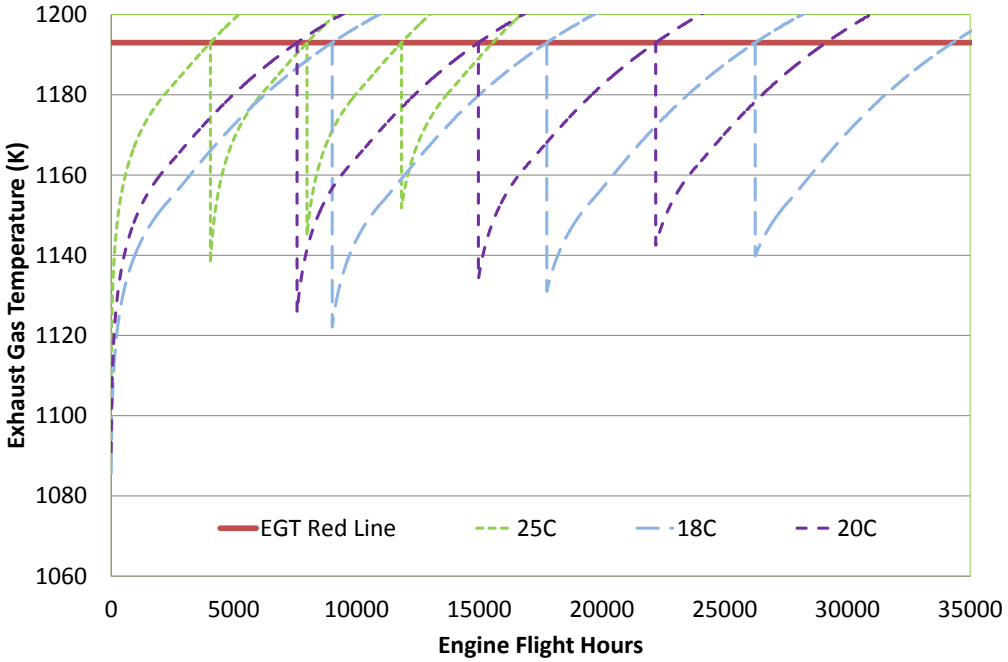

Figure 8.9: Effect of OAT on EGT characteristic

It is clear from Figure 8.9 that increasing OAT tends to reduce the performance based shop visit interval. It does so, not just by increasing the rate of deterioration, but also by reducing the initial EGTM between either the “new” or “restored” level and the red-line level. The effect of OAT on the shop visit interval, were this solely affected by performance interval, is considered in terms of Shop Visit Rates (SVRs) for the first interval and for the overall life (Mature), and these are presented graphically in Figure 8.10 and can also be considered relative to the reference case as in Figure 8.11.

For each LLP mission, a full workscope is calculated for each shop visit, these are summarised in Appendix E.

All shop visits are triggered by the performance deterioration mechanism, except for the $15^{\circ}C$ case where one of the shop visits is LLP triggered. This results in a lower level of wasted LLP stub life, but increases the maintenance cost per

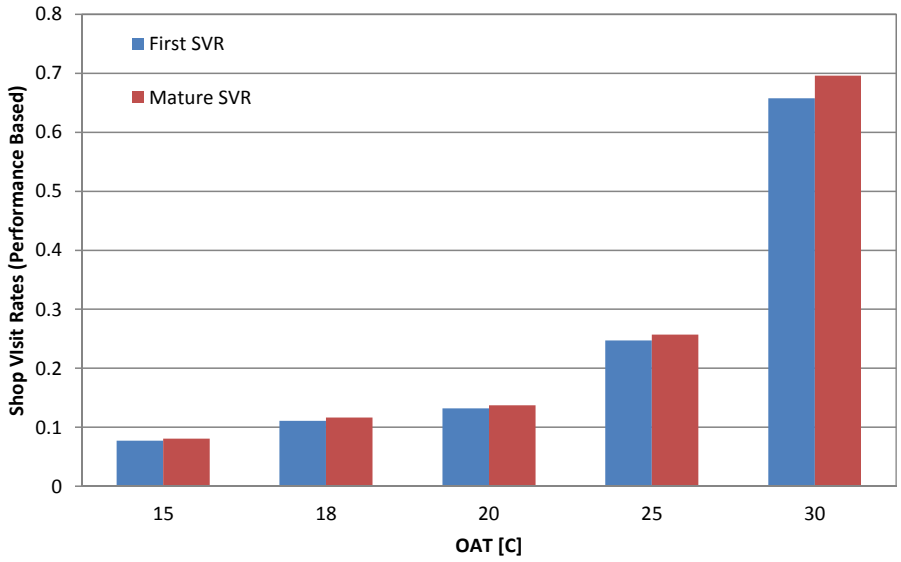

Figure 8.10: Effect of OAT on performance based maintenance maintenance intervals

flying hour as the time on wing interval has been reduced from the performance based limit previously calculated.

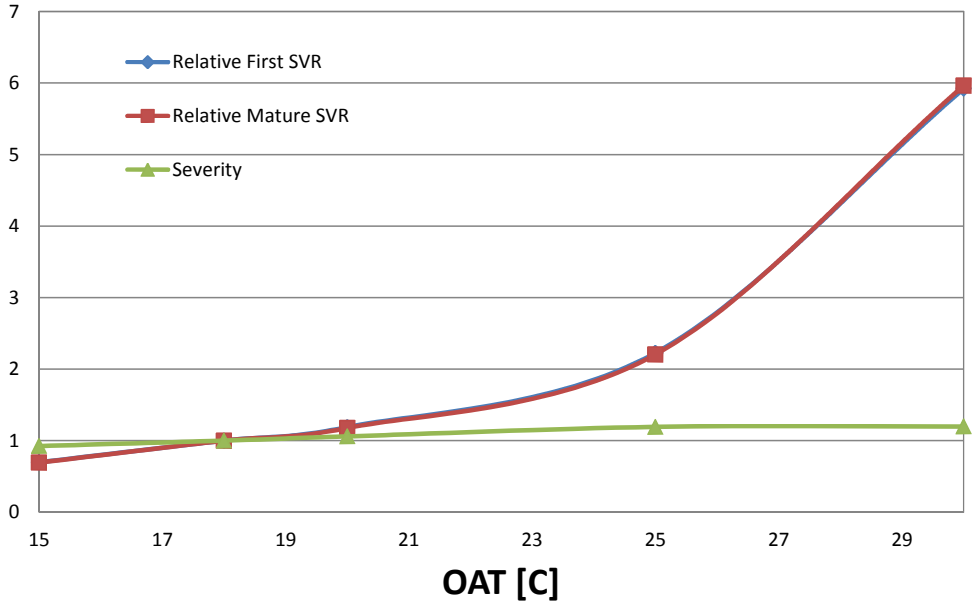

Figure 8.11: Effect of OAT on relative shop visit rates

Overall increasing outside air operating temperatures tend to increase the effective hourly cost of restoration.

The effect of three cost calculation choices described in subsection 6.2.6 is considered. These change the overall shop visit restoration cost rates in Figure 8.12, and therefore the total through life Shop Visit (SV) costs incurred.

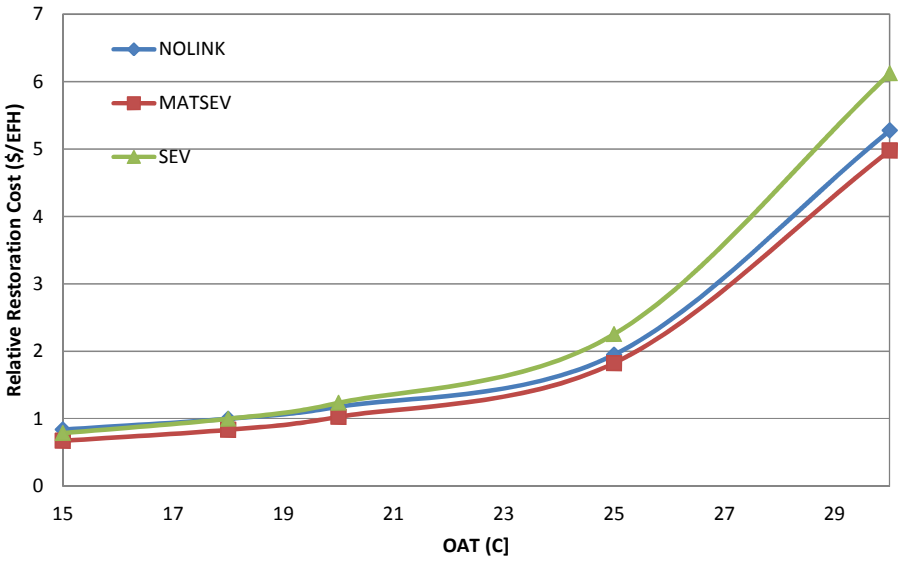

Figure 8.12: Effect of OAT on relative shop visit restoration cost rates

The most conservative approach, the Severity method is selected for use in the remainder of this analysis. it is considered that the effect of maturity is accounted for inherently by the time-cost effect of the workscoping method.

The effects of LLP on through life maintenance costs are summarised in Figure 8.13 and Figure 8.14 relative to the overall maintenance cost of the reference mission.

Considering total through life shop visit costs in isolation as presented in Figure 8.13 could result in the impression that increasing OAT reduces the maintenance cost incurred since at increased OAT no LLP sets are changed and there-

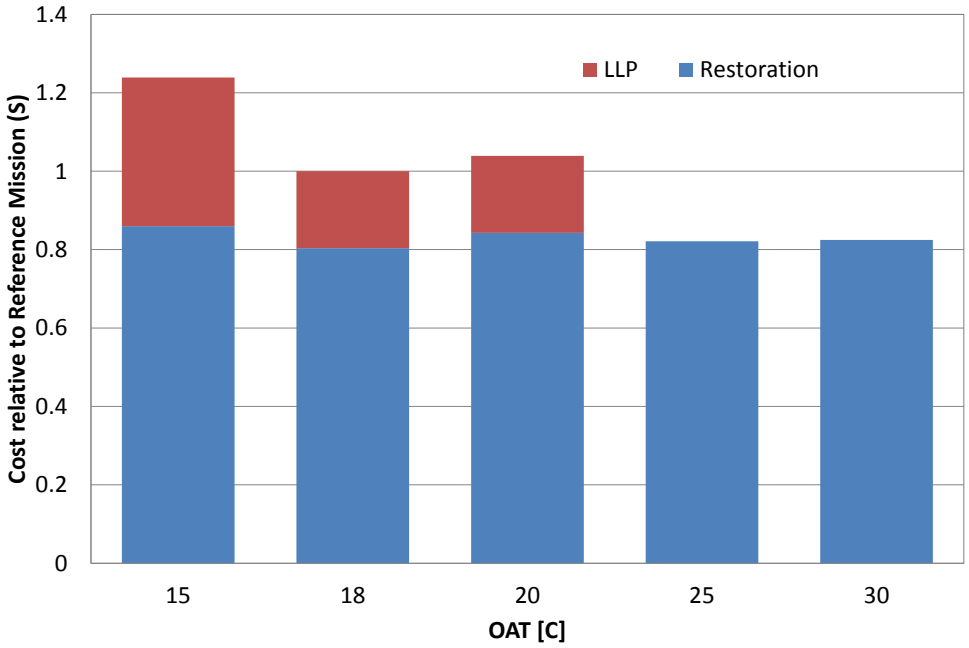

Figure 8.13: Effect of OAT on Total Shop Visit Costs ($)

fore the associated level-2 restoration tasks do not occur within the usable life defined by three Shop Visits (SVs) and the remaining period thereafter.

It is noted that the cost of restoration is not constant. In part this is due to materials cost of each restoration action completed increasing in line with severity driven by increasing OAT. It is also reducing, as the number of restoration actions reduces with increasing OAT.

However, when the coupled effect of OAT increasing which reduces the performance driven maintenance intervals is considered, the overall operating life available reduces.

It is observed in Figure 8.14 that the restoration DMC increases with OAT, as would generally be expected. This reflects not only the increasing cost of materials due to increasing operational severity, but also the coupled effect of reducing performance intervals which lead to lower usable engine lives which

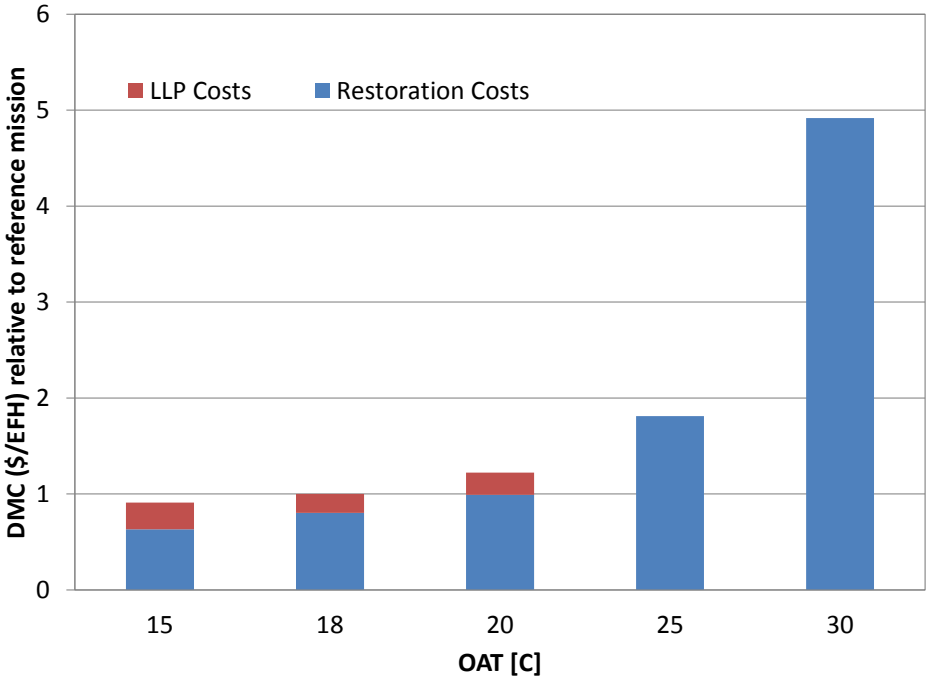

Figure 8.14: Effect of OAT on DMCs ($/EFH)

even for a constant restoration cost would drive increasing restoration DMC.

Conversely the effect of the reducing performance interval margins mean that at higher operating temperatures fewer or no LLP are replaced and therefore the associated level two restoration actions do not occur at higher OATs, therefore reducing both LLP costs and restoration cost at increased OAT. Whereas at lower OATs the total maintenance cost is increased by the LLP set replacements, but this outweighed when considered per flying hour by the increase in available usable life.

However, these relations are a function of the 3-SV usable life limit defined in the case as per Hanumanthan's application of EMCWG guidelines for the aging calculation. While this limit may appear reasonable for moderate temperature operations resulting in a usable life of over 11 years assuming 3000 FH/year at

$18°C$ it may not hold at elevated temperatures. The maintenance actions available in such cases (restoration tasks specifically) may be adapted to permit somewhat extended operations. But it is likely that in these high temperature applications, operations would be extended as far as replacing LLP sets near the end of and engine's usable life because of the elevated lost stub life that would result.

The concept of permanently elevated temperature operations is in itself primarily useful as a conservative framework within which the effect of OAT can be considered, since even if operated only on a route between two high temperature destinations, the actual operating temperatures would vary throughout the year with the seasons and daily with operations near dawn and after dusk benefiting from reduced temperatures.

Flight Duration

In this case, starting with the reference mission duration of 1.4 hours, the mission length is progressively increased to 6 hours.

Increasing mission length tends to increase steady state severities and decrease cyclic severities [7]. In this case, the severity remains near unity for the two hour trip, then increases (Figure 8.15). Since the reference case is set for all small engines, it is reasonable that it need not be the optimal trip length for all of them.

Applying the aging method generates a consecutive performance intervals due to EGT margin exhaustion. The effect of increasing flight length on the first performance interval is presented in Figure 8.16. Increasing trip length has a coupled effect on the EGT margin deterioration profile, in that longer trips (within the range of the engine) result in higher severities and reduced level of deteriora-

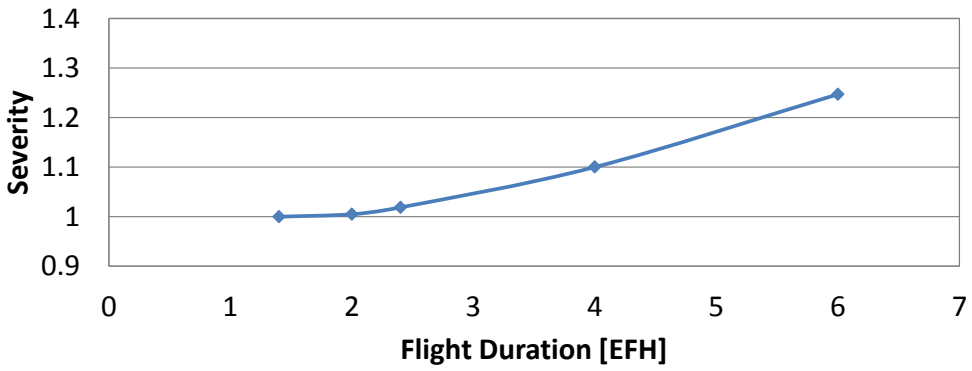

Figure 8.15: Effect of varying flight time on severity

tion, while additionally, the nature of the aging model, with deterioration defined on a per-cycle basis tends also to increase the available performance interval for longer trip lengths.

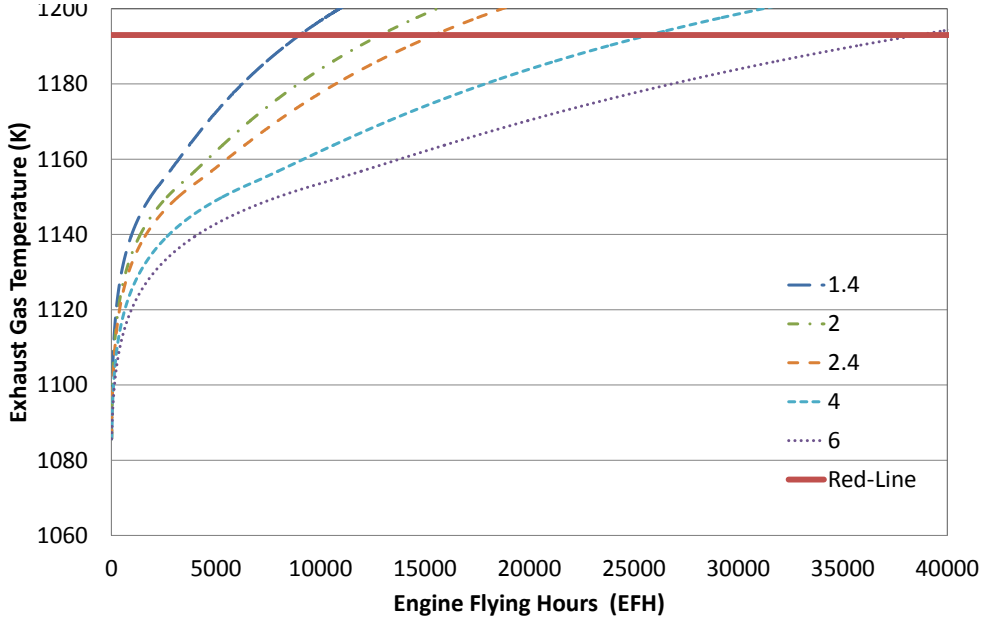

Figure 8.16: Variation in EGTM deterioration for first performance interval due to Flight Length

The effect of increasing trip length is presented in Figure 8.17 where the effect of trip length is presented for both the first SVR (1st performance interval) and

the mature SVR (over the complete usable engine life defined as previously by 3 Shop Visits) . It is noted that the performance based SVRs reduce with increasing trip length. Extended usable engine lives might therefore be expected for engines operating at longer trip lengths.

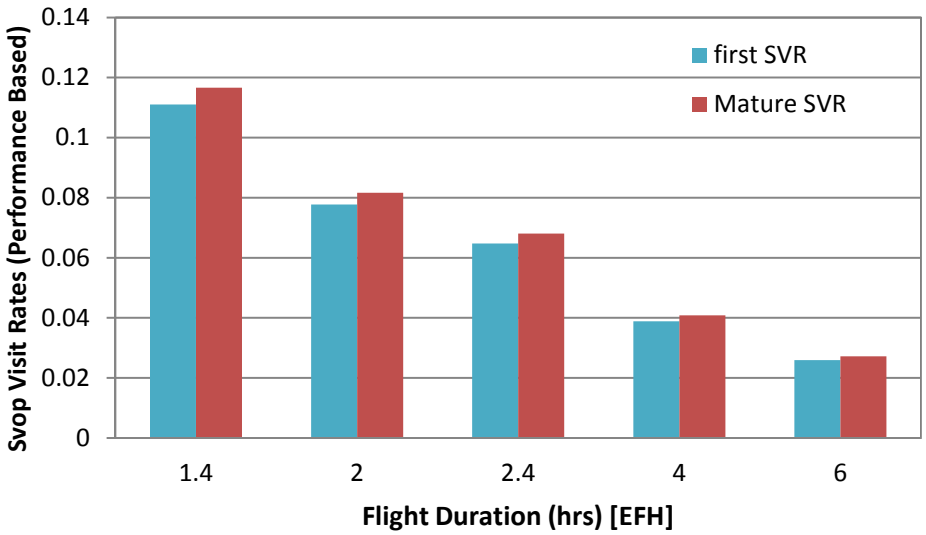

Figure 8.17: Effect of varying flight time on performance based maintenance requirements

In all the trip length cases, the pattern of maintenance is consistent as per the reference case presented in Listing 8.1, since increasing trip length, does not affect the cyclic LLP limits. All the shop visits are performance driven, and only the core LLP set is replaced at the final shop visit. Three methods for shop material cost calculation are assessed and the method which factors restoration maintenance cost with severity s retained as the most conservative (Figure 8.18).

This case is limited by the aging model assumption that the deterioration profiles are scaled by cycles to determine the EGT margin deterioration curve.

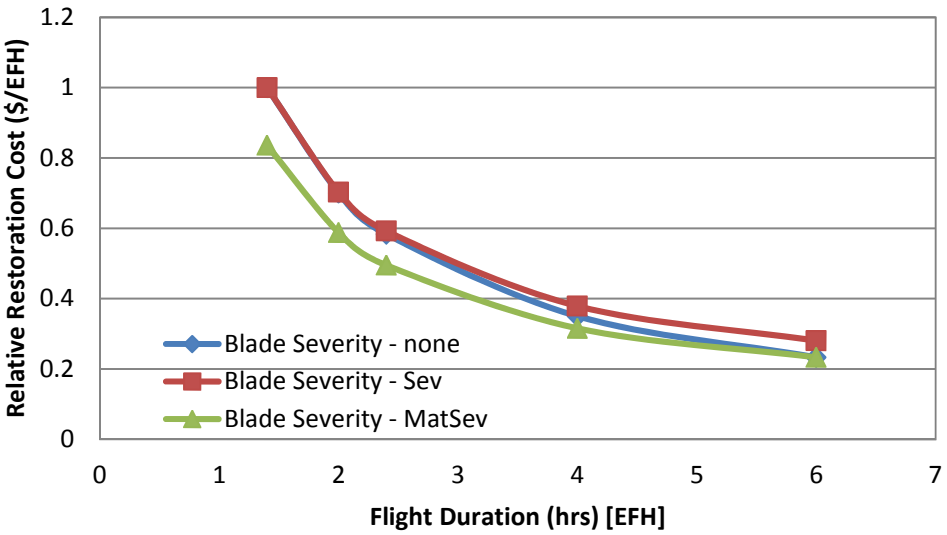

Figure 8.18: Effect of flight duration on relative shop visit restoration cost rates

The result of factoring Severity (Figure 8.15) into the material maintenance cost is considered as for the OAT case, is that while the maintenance actions remain constant with increasing trip length the total maintenance costs are seen to increase (Figure 8.19).

The balance of effects of the increasing severity (Figure 8.15) and reducing performance interval SVR (Figure 8.17) therefore determines the final effect of increasing flight interval on DMCs distributed per flying hour (Figure 8.20). Overall the influence of increased usable engine life in more significant than the increase in cost due to increasing severity and increasing trip lengths are found to reduce operating costs.

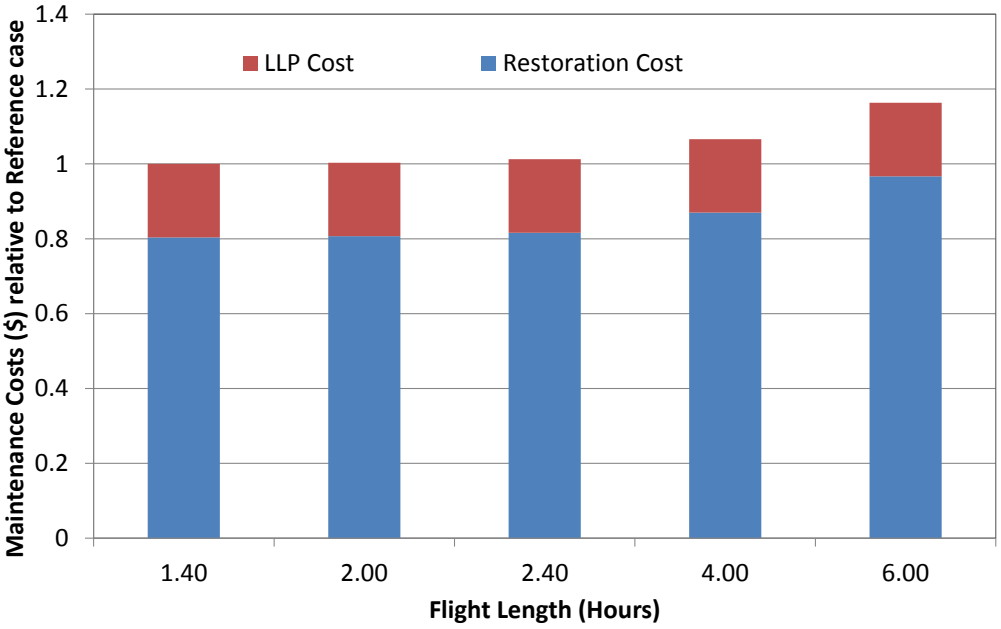

Figure 8.19: Effect of trip length on Total Shop Visit Costs ($)

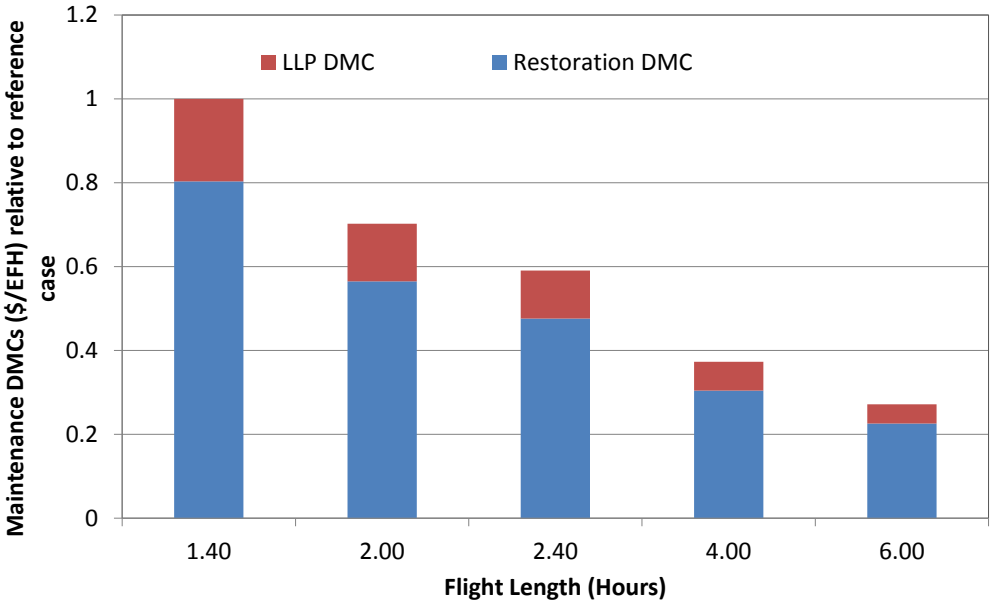

Figure 8.20: Effect of trip length on hourly maintenance costs ($/EFH)

8.0.3 Effect of operational decisions

Take-Off Derate

The effect of applying take-off derating is considered for this hight thrust narrow body engine.

The application of derate to an engine is considered an operation decision, as it is selected pre-flight in the cockpit. Airlines have different policies regarding its use, some requiring or requesting it's use by pilots whenever possible. It may not be possible to set a derated thrust at take off at higher ambient operating temperatures, high altitude airfields, or when the aircraft is fully loaded for longer range flights. This combinations of these conditions full thrust may be required for take-off and derate would not be used. However, as many aircraft operate habitually below maximum range and payload, derate is often possible.

The derate options available to pilots vary between manufacturers, on the whole two systems of derating are employed. A fixed take off derate, or a variable derate otherwise known as the assumed temperature method.

In this case we consider a fixed take off derate selection, with three options: off, 5% and 10% and compare these mission profiles at 15$^{\circ}C$ ambient air temperature with the reference mission defined in subsection 8.0.1.

Changes in thrust applied at take off has a direct impact on the maximum engine operating temperatures in the engine. Severity modelling results reflect the effect of increasing thrust and temperature on the relative damage to hot section components, as severity reduces with increasing derate Figure 8.21(a).

Reducing take off thrust also both increases the take off EGT margin available and reduces the rate of EGT margin deterioration, therefore increasing the time between performance based shop visit rates required (Figure 8.21(b)). The re-

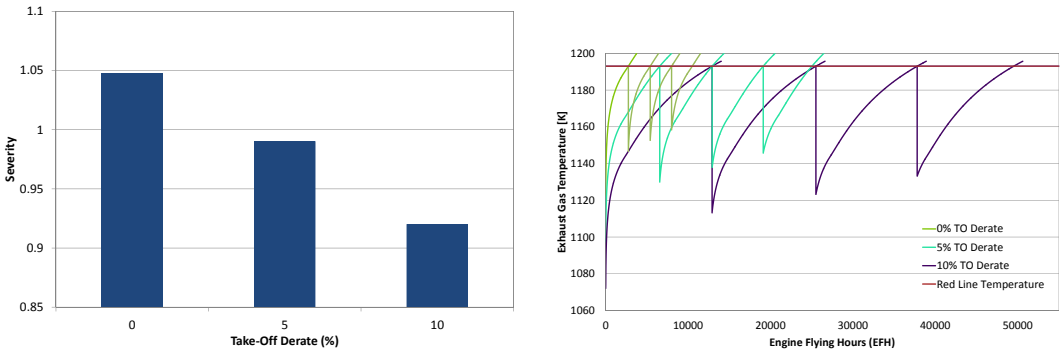

(a) Severity (b) Engine Aging

Figure 8.21: Effect of derating on engine life and aging

sulting performance based SVRs presented in Figure 8.22 can be seen to reduce significantly with increasing derate.

The sharp increase in shop visit rate and severity below 5% derate is particularly noticeable. It would be expected to have a significant knock on effect on the on the total maintenance costs (as severity is a factor in the) materials cost calculation.

As in previous case studies relating to this high thrust rated small engine, the predominant shop visit driver observed during the workscoping modelling is performance deterioration. When no derating is applied, or when only 5% derate is applied, performance deterioration is the only shop visit driver and no LLPs are replaced.

In the 10% derate case, for which the workscoping output is reproduced in Listing 8.2, LLPs are replaced at SVs two and three, with SV three being triggered by the Low Pressure Turbine (LPT) life limit. This results in a shorter Shop Visit Interval (SVI) between SVs two and three leading to some lost performance margin. Apart from this 10% derate case, the SVIs are driven by performance deterioration and conform to those presented in Figure 8.22. The 10% derate case at $15°C$ differs from the reference case at $18°C$ (also 10% derate) in that

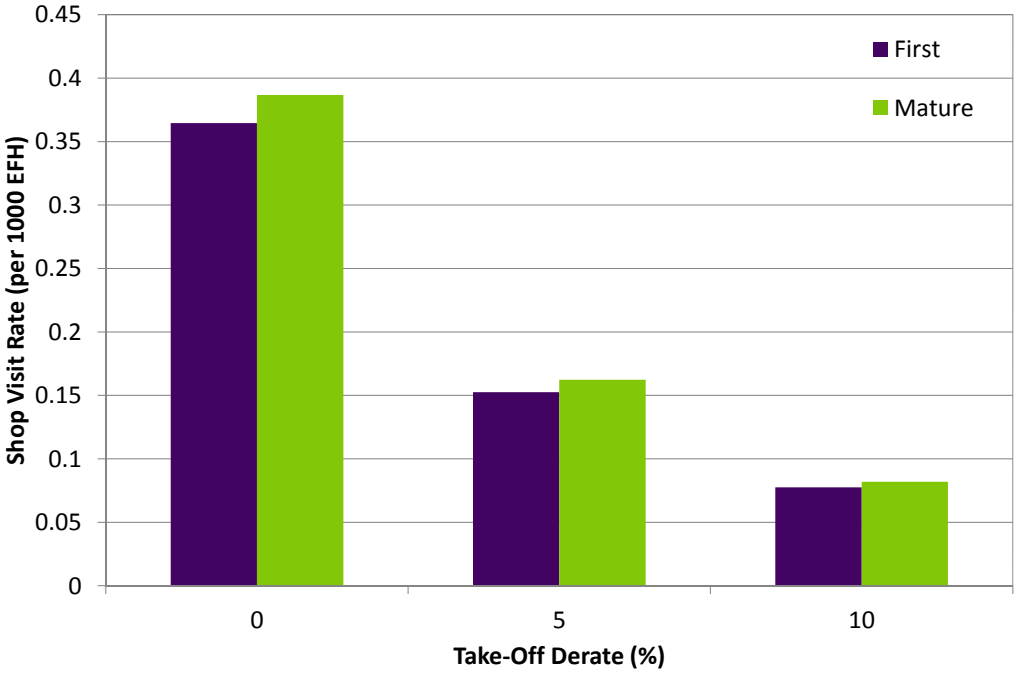

Figure 8.22: Effect of varying derate on performance based maintenance requirements

the 15°C case presented in Listing 8.2 requires all three LLP sets to be changed. Whereas, in the reference case, only the core LLP set is replaced. In the 5% and 0% derate cases, the SV intervals due to performance margin deterioration are so short that no LLP sets approach their life limits.

Therefore, one would expect the LLP costs and also restoration costs, to be higher fr the 10% derate case presented in Listing 8.2 than in the reference case. This is born out in Figure 8.23(a), however, it is also observed that the increased usable life available at 15°C compared to 18°C is sufficient to reduce the hourly DMCs Figure 8.23(b) for the 10% derate case at 15°C below those for the 18°C reference case.

Considering the higher rates cases (with lower or null derates), while the lack of LLP replacements converts to no cost contributions from LLP set replacements,

Listing 8.2: Workscoping for 10% Derated Mission at 15C

MAINTENANCE PLAN

SHOP VISIT	1	2	3	4
Trigger	deterioration	deterioration	lpt	deterioration
Elapsed Engine Cycles	9219	18221	25000	33365
Elapsed Engine Hours	12906.60	25509.40	35000.00	46711.00
Elapsed Interval Cycles	9219	9002	6779	8365
Elapsed Interval Hours	12906.60	12602.80	9490.60	11711.00
fan&lpc	0.00	0.00	356000.00	
core	0.00	921000.00	0.00	
lpt	0.00	0.00	499000.00	
level1Core	1038000.00	1038000.00	1038000.00	
level2Core(TopUp)	0.00	403000.00	0.00	
level2fan&lpc	0.00	0.00	160300.00	
level2lpt	0.00	0.00	339000.00	
Rest Materials Cost ($)	828000.00	1196000.00	1232800.00	
Rest Labour Cost ($)	210000.00	245000.00	304500.00	
Restoration Cost ($)	1038000.00	1441000.00	1537300.00	
LLP Cost ($)	0.00	921000.00	855000.00	
Shop Visit Cost ($)	1038000.00	2362000.00	2392300.00	
Restoration DMC ($/EFH)	80.42	114.34	161.98	
LLP DMC ($/EFH)	0.00	73.08	90.09	
Shop DMC ($/EFH)	80.42	187.42	252.07	

MAINTENANCE SUMMARY

Useable Engine Life FC	33365
Restoration Cost ($)	4016300.00
LLP Cost ($)	1776000.00
Shop Visit Cost ($)	5792300.00
Restoration DMC ($/EFH)	85.98
Shop DMC ($/EFH)	124.00

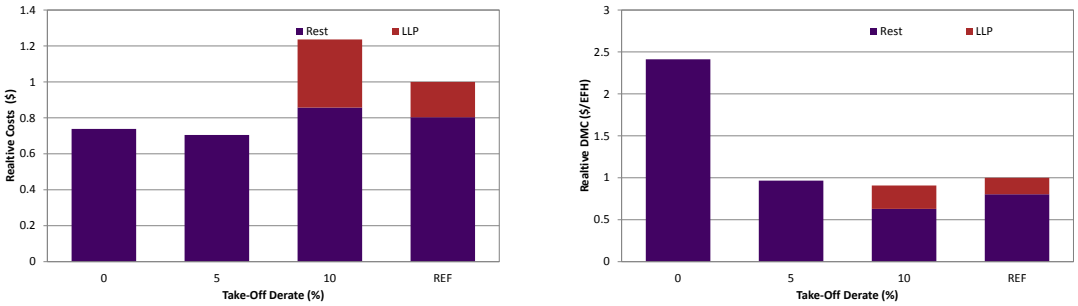

(a) Relative Costs ($) (b) Relative DMC ($/EFH)

Figure 8.23: Effect of varying derate on shop visit costs (Severity Cost Method)

in Figure 8.23(a) the small difference in cost between the 0% and 5% derate cases can be attributed to the severity component of the restoration cost calcula-

tion. Whereas, the large difference in hourly costs visible in Figure 8.23(b) reflect the heavily reduced available engine life (FH) in the 0% derate case.

The scale of the operational effects is quite marked. Considering the 10% derate and 15$^{\circ}C$ case as a starting point Figure 8.23(b), decreasing derate to 5% and increasing OAT by 3$^{\circ}C$, both increase SV DMC by less than 1%. Whereas the cost of operating (per flying hour) at zero derate is over 2.5 times that of operating at 10% derate. It is, considered unlikely that an aircraft would operate solely at Maximum Take Off Thrust. At many international airports, the runway lengths are sufficient for even heavily laden aircraft to apply some derate even on hot days.

Considering the impact of Severity measures

So far the case studies presented have applied Severities derived following Hanumanthan's [18] methodology presented in [7] (referred to here as Severity). At this stage it is considered of interest to demonstrate the integration of the workscoping method with Severity measures derived from the Thermo-mechanical fatigue (TMF) models implemented in this project after collaborative work between several students which was introduced in chapter 3 (referred to as S(TMF)). The effect of the two Operational Severity measures (each a relative damage term) are considered and presented in Figure 8.24.

It is noted that Figure 8.24 being a curve of derate-severity does not display the reference case, as each of these calculations was completed for 15$^{\circ}C$. It is noted that close to the reference case at 10% derate, the severity measures vary little, however at higher thrust ratings, though they both increase, the TMF based severity measure is much more sensitive. The impact of the S(TMF) severity measure on costs, is presented in Figure 8.25.

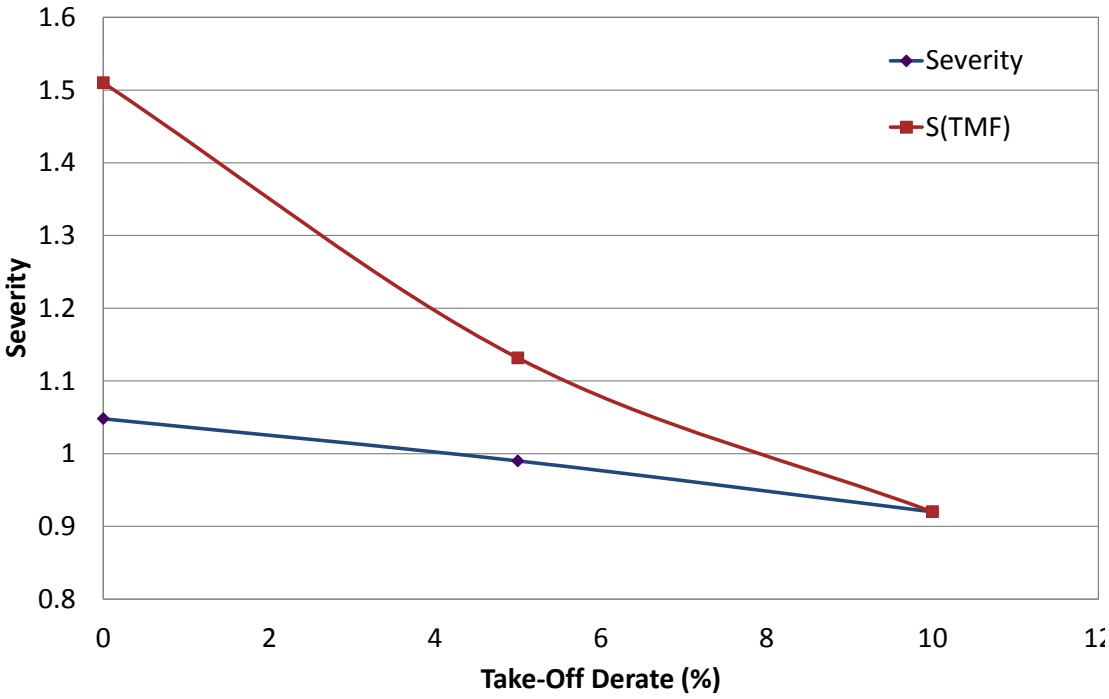

Figure 8.24: Two severity Measures considered

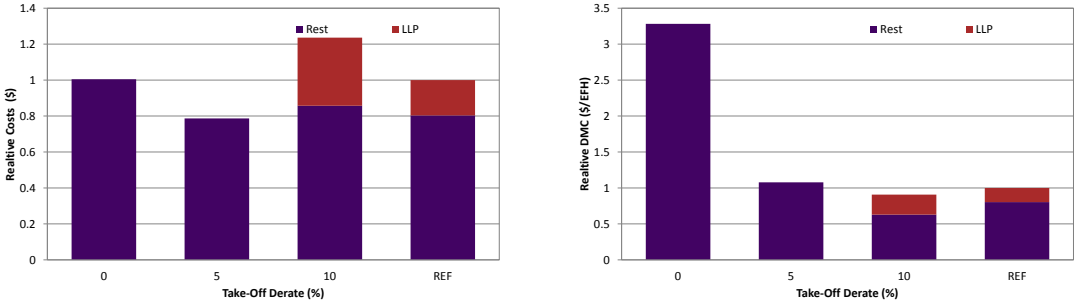

(a) Relative Costs ($)

(b) Relative DMC ($/EFH)

Figure 8.25: Effect of varying derate on shop visit costs (S(TMF))

The presence of LLP set replacements in the 10% derate case and the associated restoration actions mask the decrease in pure restoration costs with increasing derate in Figure 8.25(a), however, when the hourly costs of maintenance are considered in Figure 8.25 the effect of the S(TMF) measure is very

noticeable. Though it is hard to distinguish the effect of the increased S(TMF) severity measure from the effect of the performance intervals reducing available life.

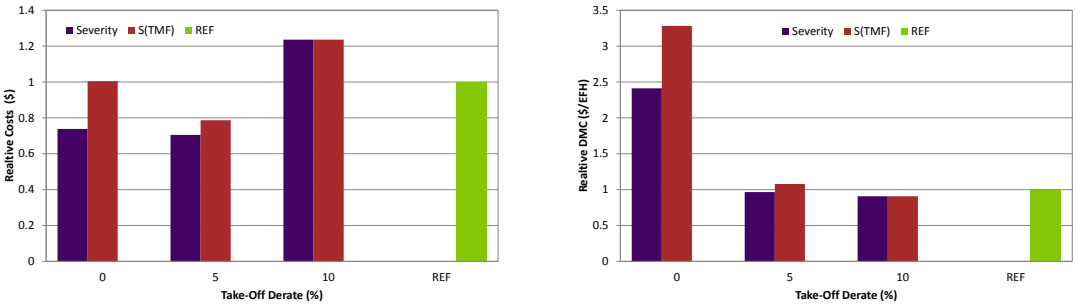

(a) Relative Costs ($) (b) Relative DMC ($/EFH)

Figure 8.26: Comparison of Severity Measure effects on Through life maintenance costs.

Figure 8.26 permits the comparison of the two severity measures. Interestingly, the balance of increased severity and increased restoration costs in the 0% derate S(TMF) case against LLP costs in the reference case is such that in terms of total through life maintenance costs Figure 8.26(a), they become equivalent varying only by 0.4%. This coincidence aside, for the lower derate cases, the S(TMF) derived severities produce greater through life costs. As both severity cases have the same applied performance deterioration intervals applied , the differences between them are only amplified when presented as hourly costs Figure 8.26(b).

This final set of graphs (Figure 8.26), serve to demonstrate several effects noted in the case studies:

- in (b) the reducing arc of DMC with increasing derate mirrors the effect of derate on mature SVR due to performance reflected in the aging curves.
- the relative size of the 10% derate case and the reference case in (a) and

(b) reflect the impact of reduced operating temperature ($3^{\circ}C$) which reduces severity (and therefore restoration costs) but also reduces the deterioration rate leading to increased performance intervals. These in turn result in increased LLP set changes, costs and associated restoration work which tend to increase the overall costs.

- the balance of pure restoration costs and LLP linked restoration tear down items visible in (a) when comparing the 10% derate case to the higher rated cases, since each case has the same level of base restoration actions (though their costs vary vary severity.

8.0.4 Summary

These cases have enabled the assessment of the relative impact of key operating parameters (OAT, Flight Length, Derate) on through life maintenance costs as determined by the workscoping method. Different applications of Severity and Maturity have been considered and compared.

Chapter 9

Conclusions and Opportunities

Contribution, commercial context and applicability

This research project was intended to provide a public-domain methodology and a coherent set of models to link engine and aircraft operation captured through physics-based performance modelling with through life engine maintenance costs; in effect to provide validation for an unpublished methodology. In this context the value of the methodology is not so much its accuracy when operating with the limited public data input sources used in the case studies presented, as the clarity with which the physics basis and physics-based cost drivers are established and linked. This can be considered both a strength and a weakness of the project design. The opportunities for verification and validation of the overall methodology are limited by the availability of data, but individual model components have been verified wherever feasible.

More generally this tool-set and methodology are capable of informing benchmarking studies comparing either engine and aircraft pairs, initial design decisions or mid-life design improvements, if not in their current format to determine

which of several options may be best, but to identify which avenues should be investigated further and which specific performance questions should be asked to understand better the cost implications of the various options.

The cases presented define usable life with respect to a fixed number of Shop Visits (SVs) thus linking costs per flying hour to SV intervals. This definition underlies the sometimes counter-intuitive relationships between operating conditions, operational decisions and costs per hour summarised above. Further cases using the current tool set and its existing capacity to define usable life in terms of a fixed input in terms of flying hours or cycles would enable these findings to be considered in a broader context.

Critical constraints

The workscoping methodology developed in this research is constrained by its dependence on operational severity and Exhaust Gas Temperature (EGT) margin deterioration rates as key physics-based inputs to the “virtual workshop” workscoping model for a given aircraft-engine pair. While the use of an operational severity measure in this way is common to several published cost models, the variations in definition, derivation and application of the concept of severity in each model limits the comparability of the models and their results. The use of a composite severity factor in this methodology though similar to other published models [149] means that in this method the varying effect of cyclic and steady state damage mechanisms cannot be distinguished in their effect on maintenance costs. The use of cost inputs relating to a specific engine type limits comparisons across engine-aircraft pairs and throughout the engine performance design space to analogue or parametric adjustments.

Key outcomes

- The workscoping model:
  - calculates the required performance interval from a published 'book' deterioration profile. Varying the applied deterioration profile changes the performance driven shop visit interval as expected from published reference case [14].
  - produces a through life maintenance plan for a published engine case. Varying the applied deterioration profile or planning build goal modify the through life maintenance plan and resulting usable life and costs as expected from published reference case.
  - calculates through life Life Limited Part (LLP) Direct Maintenance Cost (DMC) giving results within the range set by two published methods.
  - generates engine maintenance cost profiles which conform to published aging predictions [116].
- The workscoping methodology combines engine and aircraft performance models, Finite Element (FE) modelling, High Pressure Turbine (HPT) lifing severity, aging and maintenance workscoping and cost.
- Application of the workscoping methodology in the case studies shows that:
  - Reducing thrust at take-off (derating) reduces operational severity and lengthens the performance based shop visit intervals. More life limited part sets are therefore used during an engine's usable life. The overall shop visit costs increase, while increased operating life results in reduced costs per flying hour.

Comparison of the thermo-mechanical fatigue and the coupled creep-fatigue-oxidation measures of operational severity show them to be consistent for trends in total costs through life and costs per flying hour, although the thermo-mechanical fatigue measure is more sensitive.

– Operating at higher outside air temperatures increases operational severity and shortens performance based shop visit intervals. Performance deterioration becomes the primary trigger for shop visits. Fewer life limited part sets require replacement during the engine's usable life, resulting in lower overall costs. However, where shorter shop visit intervals result in a shorter usable life, costs per flying hour increase.

  Comparison of these case study results shows that in terms of maintenance cost per engine flying hour, the effect of operating at a higher outside air temperature (18$^{\circ}C$ against 15$^{\circ}C$) is equivalent to the effect of reducing take-off derate from 10% to 5%.

– Longer trips increase operational severity gradually. The nature of the aging method, which defines deterioration on a per-cycle basis, results in longer performance intervals for higher trip lengths. The moderate increase in overall shop visit costs with increasing trip length contrasts with a significant increase in usable engine life resulting in a reduction of costs per flying hour.

The workscoping model developed is constrained by the accuracy of its cost inputs and the choice and definition of maintenance actions selected by the user. However, even with limited input data, where the results are analysed conservatively focusing on the cost trends developed, the methodology is capable of usefully informing design, purchase or maintenance decisions. Wherever possi-

ble in the case studies presented, cost inputs were selected so as to be internally coherent as an input data set in terms of currency, source and year, and so limit the impact of inflation, foreign exchange and market on the cost trends. While these are important influences of maintenance cost, they are not physics-based and dependent on either the engine's design or operation, and were therefore considered outwith the scope of this research. A full set of accurate cost inputs would naturally improve the reliability of the model outputs.

Development opportunities

There is scope to conduct a variety of case studies using the workscoping methodology, limited only by the availability sufficient data to the user. Cases of particular interest might include benchmarking of technological development options based on their effect on the maintenance costs for the engine during its remaining usable life.

Key developments which would improve the physics-basis of the methodology include:

- Implementing a capability for the workscoping model to mix different mission definitions during each shop visit interval.
- Extending the aging model to account for time based deterioration as well as cyclic deterioration.
- Implementing a one off "upgrade" or 'acquisition" cost functionality to allow cost benefit analysis and enable comparisons for example between the operation of a cheaper engine in more severe conditions and a more expensive engine at less severe conditions.

- Implementing an alternative option for cost inputs allowing non-engine specific values potentially derived from existing Cost Estimating Relationship (CER) sets [128] adjusted to a suitable modern fleet [150].

- Replacing the composite severity factor with cyclic and steady state factors thus accounting for the effect of different lifing mechanisms on the maintenance required and its cost.

- Adding further component severities (eg. Fan, Low Pressure Turbine (LPT), Burner, High Pressure Compressor (HPC)) to the current severity measures based on HPT life, so that each component cost is factored by a representative component severity.

- Adding varying component lives sampled via Monte-Carlo methods [135] to the existing deterministic approach.

References

[1] J. Roskam. *Airplane design*, volume II & VIII. Roskam Aviation and Engineering Corporation, Ottawa, Kansas, 1990.

[2] D. A. Spera and S. J. Grisaffe. Life prediction of turbine components: Ongoing studies at the nasa lewis research center. Technical Report NASA-TM-X-2664, E-7158, NASA Lewis Research Center, Cleveland, OH, United States, Jan 1973. Unclassified; Publicly available; Unlimited.

[3] W.D. Callister. *Fundamentals of Materials Science and Engineering*. John Wiley & Sons, Inc, 2001.

[4] J.H. Frost and M.F. Ashby. *Deformation-mechanism maps- The plasticity and creep of metals and ceramics*. Pergamon Pres, Oxford, 1982.

[5] M. McLean. Creep-resistant super alloys. In J. Buschow, R. Cahn, M. Flemings, B. Ilschner, E. Kramer, and S. Mahajan, editors, *Encyclopedia of Materials - Science and Technology*, volume 2, pages 1845–1859. Elsevier, 2001. Online version available at: `http://app.knovel.com/hotlink/toc/id:kpEMSTV001/encyclopedia-materials`.

[6] R. G. Stabrylla and W. A. Troha. Effect of aircraft power plant usage on turbine engine relative durability/life. In *16th AIAA/SAE/ASME Joint Propul-*

sion Conference. General Electric Co., Evendale, USAF, Aero Propulsion Laboratory, Wright-Patterson AFB, AIAA, June 30-July 2, 1980 1980.

[7] H. Hanumanthan, A. Stitt, P. Laskaridis, and R. Singh. Severity estimation and effect of operational parameters for civil aircraft jet engines. *Proceedings of the Institution of Mechanical Engineers, Part G: Journal of Aerospace Engineering*, 226(12):1544–1561, 2012. Available online at: http://pig.sagepub.com/content/226/12/1544.abstract.

[8] E. Chiesa, P.and Macchi. A thermodynamic analysis of different ions to break 60% electric efficiency in combined cycle power plants. In *Proceedings of ASME Turbo Expo*, Amsterdam, Netherlands, June 2002. GT-2002-30663.

[9] S. Eshati. *An evaluation of operation and creep life of stationary gas turbine engine*. PhD thesis, School of Engineering, Cranfield University, Cranfield, Bedfordshire, UK, 2011.

[10] H. I. H. Saravanamuttoo, G. F. C. Rogers, and H. Cohen. *Gas turbine theory*. Prentice Hall, Harlow, 5th edition, 2001.

[11] S. Eshati, A.O. Abu, P. Laskaridis, and F. Khan. Influence of water-air ratio on the heat transfer and creep life of a high pressure gas turbine blade. *Applied Thermal Engineering*, 60(12):335 – 347, 2013. Available online at: http://www.sciencedirect.com/science/article/pii/S1359431113004869.

[12] A.O. Abu. *Integrated approach for physics based lifing of aero gas turbine blades*. Phd, School of Engineering, Cranfield University, Cranfield, Bedfordshire, UK, 2013.

[13] T. McMahon. Historical oil prices chart, March 2014. Available at: http://www.inflationdata.com/Inflation/Inflation_rate/Historical_Oil_Prices_Chart.asp, Accessed: 31/3/2014.

[14] S. Ackert. Engine maintenance concepts for financiers - elements of engine shop maintenance costs. Technical report, Macquarie AirFinance, March 2012.

[15] The efficiency of the engine shop visit process. *Aircraft Commerce*, 74, Feb/Mar 2011. Ref number: 36592910. Also available at http://www.aircraft-commerce.com.

[16] A. Stitt, P. Giannakakis, and P. Laskaridis. The effect of mission profile and rating strategies on the fuel and life consumption of commercial aircraft engines. Technical report, Department of Power and Propulsion, School of Engineering, Cranfield University, Cranfield, Bedfordshire, UK, Dec. 2009.

[17] ASCEND. An overview of engine values. In *Financing and Investing in EnginesInvesting in Engines Roundtable*. ASCEND, Airfinance Journal http://www.airfinancejournal.com/, April 2009.

[18] H. Hanumanthan. *Severity estimation and shop visit prediction of civil aircraft engines*. Phd, School of Engineering, Cranfield University, Cranfield, Bedfordshire, UK, 2009.

[19] N. T. Birch. 2020 Vision: the prospects for large civil aircraft propulsion. *The Aeronautical Journal*, 104(1038):347–352, August 2000.

[20] Yee Mey Goh, L.B. Newnes, A.R. Mileham, C.A. McMahon, and M.E. Saravi. Uncertainty in through-life costing -review and perspectives. *Engineering Management, IEEE Transactions on*, 57(4):689–701, Nov 2010.

[21] H. Wu, Y. Liu, Y. Ding, and J. Liu. Methods to reduce direct maintenance costs for commercial aircraft. *Aircraft Engineering and Aerospace Technology*, 76(1):15–18, 2004.

[22] J. R. Nelson. Life-cycle analysis of aircraft turbine engines. Technical Report R-2103-AF, RAND Corporation, Santa Monica, CA, 1977.

[23] J. R. Nelson. An approach to the life-cycle analysis of aircraft turbine engines. RAND Note N-1337-AF, RAND Corporation, Santa Monica, CA, 1979. Available online at: `http://www.rand.org/pubs/notes/N1337`.

[24] R. Stenger. The use of engine operating experience in the preliminary design of aircraft gas turbine combustion systems. In *17th AIAA/SAE/ASME Joint Propulsion Conference*. American Institute of Aeronautics and Astronautics, Jul 1981. AIAA-81-1399. Also available at `http://dx.doi.org/10.2514/6.1981-1399`.

[25] W. Willis. Advanced technology engine studies ATES - a status report. In *17th AIAA/SAE/ASME Joint Propulsion Conference*. American Institute of Aeronautics and Astronautics (AIAA), Jul 1981. AIAA-81-1502. Also available at `http://dx.doi.org/10.2514/6.1981-1502`.

[26] W. Willis and T. Sewall. The impact of engine usage on life cycle cost. In *19th AIAA/SAE/ASME Joint Propulsion Conference*. American Institute of Aeronautics and Astronautics (AIAA), Jun 1983. AIAA-83-1406. Also available at `http://dx.doi.org/10.2514/6.1983-1406`.

[27] W. Shoemaker. Life cycle cost as a tool in the detail design of advanced propulsion systems. In *16th AIAA/SAE/ASME Joint Propulsion Conference*. American Institute of Aeronautics and Astronautics (AIAA), Jun 1980. AIAA-80-1252. Also available at http://dx.doi.org/10.2514/6.1980-125.

[28] W. Willis. A methodology for planning a cost effective engine development. In *18th AIAA/SAE/ASME Joint Propulsion Conference*. American Institute of Aeronautics and Astronautics (AIAA), Jun 1982. AIAA-82-1140. Also available at http://dx.doi.org/10.2514/6.1982-1140.

[29] J. Janikovic. *Gas Turbine Transient Performance Modeling for Engine Flight Path Cycle Analysis*. Phd, School of Engineering, Cranfield University, Cranfield, Bedfordshire, UK, 2009.

[30] P. Giannakakis. *Design space exploration and performance modelling of advanced turbofan and open-rotor engines*. EngD, School of Engineering, Cranfield University, Cranfield, Bedfordshire, UK, June 2013.

[31] C. Eady. Modes of gas turbine component life consumption. In *Recommended Practices for Monitoring Gas Turbine Engine Life Consumption*, number RTO-TR-28 AC/323(AVT)TP/22 in "AVT-017 Task Group". Applied Vehicle Technology Panel (AVT) NATO Science and Technology Organization, April 2000. ISBN 92-837-1032-0.

[32] R. Kurz and K. Brun. Degradation in gas turbine systems. *Journal of Engineering for Gas Turbines and Power*, 123(1):70–77, January 2001 2001. Available online at: http://link.aip.org/link/?GTP/123/70/1.

[33] W. Brocks. Introduction to fracture and damage mechanics, five lectures at politecnico di milano, March 2012. Available online at http://www.tf.uni-kiel.de/matwis/instmat/departments/brocks/milano_lectures.pdf.

[34] R.W. Evans. Creep and constrant strain-rate deformation. In J. Buschow, R. Cahn, M. Flemings, B. Ilschner, E. Kramer, and S. Mahajan, editors, *Encyclopedia of Materials - Science and Technology*, volume 2, pages 1750–1757. Elsevier, 2001. Online version available at: http://app.knovel.com/hotlink/toc/id:kpEMSTV001/encyclopedia-materials.

[35] R. Viswanathan. Creep life prediction. In J. Buschow, R. Cahn, M. Flemings, B. Ilschner, E. Kramer, and S. Mahajan, editors, *Encyclopedia of Materials - Science and Technology*, volume 2, pages 1782–1788. Elsevier, 2001. Online version available at: http://app.knovel.com/hotlink/toc/id:kpEMSTV001/encyclopedia-materials.

[36] F. R. N. Nabarro. Creep mechanisms in crystalline solids. In J. Buschow, R. Cahn, M. Flemings, B. Ilschner, E. Kramer, and S. Mahajan, editors, *Encyclopedia of Materials - Science and Technology*, volume 2, pages 1788–1795. Elsevier, 2001. Online version available at: http://app.knovel.com/hotlink/toc/id:kpEMSTV001/encyclopedia-materials.

[37] W. Beres. Mechanisms of materials failure. In *Recommended Practices for Monitoring Gas Turbine Engine Life Consumption*, number RTO-TR-28 AC/323(AVT)TP/22 in ”AVT-017 Task Group”. Applied Vehicle Technology Panel (AVT) NATO Science and Technology Organization, April 2000. ISBN 92-837-1032-0.

[38] M.E. Kassner. *Fundamentals of creep in metals and alloys*. Elsevier Science, 2009.

[39] B. Dyson. Use of CDM in materials modeling and component creep life prediction. *Journal of Pressure Vessel Technology, Transactions of the ASME*, 122(3):281–296, 2000.

[40] F. R. Larson and J. Miller. A time-temperature relationship for rupture and creep stress. *Transactions of the ASME*, 74:765–775, July 1952. Manuscript received August 10, 1951. Paper No 51-A-36.

[41] R.A. Viswanathan. *Damage Mechanisms and Life Assessment of High-Temperature Components*. ASM International, 1989. Also available at `http://books.google.co.uk/books?id=JpZRAAAAMAAJ`.

[42] G.F. Harrison and T. Homewood. Application of the graham and walles creep equation to aeroengine superalloys. *Journal of Strain Analysis for Engineering Design*, 29(3):177–184, 1994.

[43] S. S. Manson, M. H. Hirschberg, and G. R. Halford. Creep-fatigue analysis by strain-range partitioning. NASA Technical Memorandum NASA TM X-67838, NASA, Cleveland,Ohio, 1971.

[44] G.R. Halford and S.S. Manson. Life prediction of thermal-mechanical fatigue using strainrange partitioning. *Thermal fatigue of materials and components, ASTM STP*, 612:239–254, 1976.

[45] V. P. Swaminathan, J. M. Allen, and G. L. Touchton. Temperature estimation and life prediction of turbine blades using post-service oxidation measurements. *Journal of engineering for gas turbines and power*, 119:922, 1997.

[46] W. H. Chang. Tensile embrittlement of turbine blade alloys after high temperature exposure. *Superalloys*, 5:V–1 to V–41, 1972.

[47] A. Izquierdo. A review of suitable oxidation models for aero gas turbine engines. Master's thesis, School of Engineering, Cranfield University, Cranfield, Bedfordshire, UK, September 2010.

[48] S. Corbo. Modelling and analysis of oxidation growth in turbine blades for life estimation of aero-gas turbines. Master's thesis, School of Engineering, Cranfield University, Cranfield, Bedfordshire, UK, September 2012.

[49] P. S. Liu, K. M. Liang, and S. R. Gu. Using theoretical formulae to calculate degradation life for an aluminide coating during high-temperature oxidation in air. *Surface and Coatings Technology*, 137(1):60–64, 2001.

[50] K. S. Chan, N. S. Cheruvu, and G. R. Leverant. Coating life prediction under cyclic oxidation conditions. *Journal of engineering for gas turbines and power*, 120:609, 1998.

[51] C.E. Lowell, C.A. Barrett, R.W. Palmer, J.V. Auping, and H.B. Probst. Cosp: A computer model of cyclic oxidation. *Oxidation of Metals*, 36(1):81–112, 1991.

[52] E. P. Busso, J. Lin, S. Sakurai, and M. Nakayama. A mechanistic study of oxidation-induced degradation in a plasma-sprayed thermal barrier coating system: Part I. Model formulation. *Acta materialia*, 49(9):1515–1528, 2001.

[53] E. P. Busso, J. Lin, S. Sakurai, and M. Nakayama. A mechanistic study of oxidation-induced degradation in a plasma-sprayed thermal barrier coating

system: Part II. Life prediction model. *Acta materialia*, 49(9):1529–1536, 2001.

[54] D.M. Nissley. Thermal barrier coating life modeling in aircraft gas turbine engines. *Journal of Thermal Spray Technology*, 6(1):91–98, 1997. Available online at: `http://dx.doi.org/10.1007/BF02646317`.

[55] S. M. Meier, D. M. Nissley, K. D. Sheffler, and T. A. Cruse. Thermal barrier coating life prediction model development. *Journal of Engineering for Gas Turbines and Power*, 114(2):258–263, April 1992.

[56] J. Harris. Fuzzy logic methods in fatigue and creep. *The Journal of Strain Analysis for Engineering Design*, 36(4):411–420, 2001.

[57] J. E. Heine, J. R. Warren, and B. A. Cowles. Thermal mechanical fatigue of coated blade materials. Technical report, DTIC Document, 1989.

[58] W. Z. Zhuang and N. S. Swansson. Thermo-mechanical fatigue life prediction: A critical review. Technical report, DTIC Document, 1998.

[59] A. Blanchard. Review of thermomechanical fatigue models for aero-engines. Master's thesis, School of Engineering, Cranfield University, Cranfield, Bedfordshire, UK, September 2011.

[60] G. F. Harrison, P. H. Tranter, S. J. Williams, and Rolls-Royce plc (United Kingdom);. Modelling of thermomechanical fatigue in aero engine turbine blades. *ROLLS ROYCE PLC-REPORT-PNR*, 1996.

[61] T. Beck, P. Hähner, H-J. Kühn, C. Rae, E. E. Affeldt, H. Andersson, A. Köster, and M. Marchionni. Thermo-mechanical fatigue–the route to

standardisation (tmf-standard project). *Materials and corrosion*, 57(1):53–59, 2006.

[62] G. R. Halford, M. J. Verrilli, S. Kalluri, F. J. Ritzert, R. E. Duckert, and F. A. Holland. Thermomechanical and bithermal fatigue behavior of cast b1900+ hf and wrought haynes 188. In Michael R Mitchell and Ronald W Landgraf, editors, *Advances in fatigue lifetime predictive techniques*, volume 1, pages 120–142. ASTM International, 1992.

[63] S. D. Antolovich, R. L. Amaro, R. W. Neu, and A. Staroselsky. On the development of physically based life prediction models in the thermo mechanical fatigue of Ni-base superalloys. *Key Engineering Materials*, 465:47–54, 2011.

[64] J. Ziebs, J. Meersmann, H-J. Kühn, and H. Klinglehöffer. Multiaxial thermomechanical deformation behavior of IN 738 LC and SC 16. In H. Sehitoglu and H. J. Maiers, editors, *Thermo-Mechanical Fatigue Behavior of Materials*, volume 3, pages 257–278. ASTM International, 2000. 1371.

[65] S. Kalluri and P. J. Bonacuse. An axial-torsional, thermomechanical fatigue testing technique. In S. Kalluri and P. J. Bonacuse, editors, *Multi Axial Fatigue and Deformation Testing Techniques*, pages 184–207. American Society for Testing and Materials, 1997. 1280.

[66] J. M. Martinez-Esnaola, M. Arana, J. Bressers, J. Timm, A. Martin-Meizoso, A. Bennett, and E. E. Affeldt. Crack initiation in an aluminide coated single crystal during thermomechanical fatigue. ASTM special technical publication 1263, American Society for Testing and Materials, 1996.

[67] S. Kraft, R. Zauter, and H. Mughrabi. Aspects of high-temperature low-cycle thermomechanical fatigue of a single crystal nickel-base superalloy. *Fatigue & fracture of engineering materials & structures*, 16(2):237–253, 1993.

[68] R. L. Amaro, S. D. Antolovich, R. W. Neu, and A Staroselsky. On thermo-mechanical fatigue in single crystal Ni-base superalloys. *Procedia Engineering*, 2(1):815 – 824, 2010. Fatigue 2010. Also available online at: `http://www.sciencedirect.com/science/article/pii/S1877705810000895`.

[69] L. Rémy. *Comprehensive structural integrity ; vol 5*, volume 5, chapter Thermal-mechanical fatigue (including thermal shock), pages 113–199. Elsevier, 2003.

[70] R. W. Neu and H. Sehitoglu. Thermomechanical fatigue, oxidation, and creep: Part i. Damage mechanisms. *Metallurgical Transactions A*, 20(9):1755–1767, 1989.

[71] R. W. Neu and H. Sehitoglu. Thermomechanical fatigue, oxidation, and creep: Part ii. Life prediction. *Metallurgical Transactions A*, 20(9):1769–1783, 1989.

[72] D. A. Boismier and H. Sehitoglu. Thermo-mechanical fatigue of Mar-M247: Part 1 Experiments. *Journal of Engineering Materials and Technology*, 112(1):68–79, 1990.

[73] H. Sehitoglu and D. A/ Boismier. Thermo-mechanical fatigue of Mar-M247: Part 2Life Prediction. *Journal of Engineering Materials and Technology*, 112(1):80–89, 1990.

[74] M. Sapsard and ”AVT-017 Task Group”, editors. *Recommended Practices for Monitoring Gas Turbine Engine Life Consumption*. Number RTO-TR-28 AC/323(AVT)TP/22 in ”AVT-017 Task Group”. Applied Vehicle Technology Panel (AVT) NATO Science and Technology Organization, April 2000. ISBN 92-837-1032-0.

[75] M. Sapsard. Introduction to engine usage monitoring. In *Recommended Practices for Monitoring Gas Turbine Engine Life Consumption*, number RTO-TR-28 AC/323(AVT)TP/22 in ”AVT-017 Task Group”. Applied Vehicle Technology Panel (AVT) NATO Science and Technology Organization, April 2000. ISBN 92-837-1032-0.

[76] T. Tinga, W. P. J. Visser, W. B. de Wolf, and M. J. Broomhead. Integrated lifing analysis tool for gas turbine components. Technical Report NLR-TP-2000-049, National Aerospace Laboratory NLR, February 2000 2000.

[77] R. Holmes. Civil and military practices. In *Recommended Practices for Monitoring Gas Turbine Engine Life Consumption*, number RTO-TR-28 AC/323(AVT)TP/22 in ”AVT-017 Task Group”. Applied Vehicle Technology Panel (AVT) NATO Science and Technology Organization, April 2000. ISBN 92-837-1032-0.

[78] O. Davenport. Maintenance policies and procedures. In *Recommended Practices for Monitoring Gas Turbine Engine Life Consumption*, number RTO-TR-28 AC/323(AVT)TP/22 in ”AVT-017 Task Group”. Applied Vehicle Technology Panel (AVT) NATO Science and Technology Organization, April 2000. ISBN 92-837-1032-0.

[79] F. P. Grooteman. A fully stochastic approach to determine the lifetime and inspectionscheme of aircraft components. Technical Report NLR-TP-2004-131, National Aerospace Laboratory NLR, April 2004. Available online at: `http://www.nlr.nl/smartsite.dws?id=2816`.

[80] J. Crocker. Effectiveness of maintenance. *Journal of Quality in Maintenance Engineering*, 5(4):307–314, 1999. Available online at: `http://www.emeraldinsight.com/10.1108/13552519910298064`.

[81] S. Vittal, P. Hajela, and A. Joshi. Review of approaches to gas turbine life management. In *Collection of Technical Papers - 10th AIAA/ISSMO Multidisciplinary Analysis and imization Conference*, volume 2, pages 876–886, September 2004. Conference code: 65014.

[82] F. E. Wu. *Aero Engine's Life evaluated for combined creep and fatigue, and extended by trading-off excess thrust*. PhD thesis, School of Engineering, Cranfield University, Cranfield, Bedfordshire, UK, 1994.

[83] M. Koehl. Algorithmic aero engine life usage monitoring based on reference analysis of design mission, Aug 2013. Available online at: `http://www.mtu.de/en/technologies/engineering_news/development/Koehl_Algorithmic_aero_engine_en.pdf`.

[84] R. S. J. Corran and S. J. Williams. Lifing methods and safety criteria in aero gas turbines. *Engineering Failure Analysis*, 14(3):518–528, 2007.

[85] M. Naeem, R. Singh, and D. Probert. Consequences of aero-engine deteriorations for military aircraft. *Applied Energy*, 70(2):103–133, 2001.

[86] M. Naeem, R. Singh, and D. Probert. Implications of engine deterioration for creep life. *Applied Energy*, 60(4):183–223, 1998.

[87] O. V. Suria. A flexible lifing model for gas turbines:creep and low cycle fatigue approach. Master's thesis, School of Engineering, Cranfield University, Cranfield, Bedfordshire, UK, 2006.

[88] J. Z. Gyekenyesi, P. L. N. Murthy, and S. K. Mital. Nasalife–component fatigue and creep life prediction program. Technical Report NASA-TM2005-213887, NASA Glenn Research Center, Cleveland, Ohio: National Aeronautics and Space Administration, Glenn Research Center, 2005.

[89] J. B. Conway. *Stress-Rupture Parameters: Origin, Calculation and Use*. Gordon and Breach Science Publishers, New York, NY, 1969.

[90] M. Zuo, S. Chiovelli, and Y Nonaka. Fitting creep-rupture life distribution using accelerated life testing data. In *Transactions of ASME*, volume 122, Nov 2000.

[91] S. M. Bagnall, D. L. Shaw, and J. C. Mason-Flucke. Implications of 'power by the hour' on turbine blade lifing. In *Design for Low Cost Operation and Support*, volume Applied Vehicle Technology Panel (AVT) Specialists Meeting, Ottawa, Canada, October 1999. NATO RTO, RTO. RTO-MP-037-12.

[92] H. Sehitoglu. Thermo-mechanical fatigue life prediction methods. *Advances in Fatigue Lifetime Predictive Techniques*, pages 47–76, 1992.

[93] M.P. Miller, D.L. McDowell, R.L.T. Oehmke, and S.D. Antolovich. Life prediction model for thermomechanical fatigue based on microcrack propagation. *ASTM Special Technical Publication*, pages 35–49, 1993. 1186.

[94] H.-J. Christ, A. Jung, H.J. Maier, and R. Teteruk. Thermomechanical fatigue-damage mechanisms and mechanism-based life prediction methods. *Sadhana*, 28(1-2):147–165, 2003.

[95] G. Harrison. Translation of service usage into component life consumption. In *Recommended Practices for Monitoring Gas Turbine Engine Life Consumption*, number RTO-TR-28 AC/323(AVT)TP/22 in "AVT-017 Task Group". Applied Vehicle Technology Panel (AVT) NATO Science and Technology Organization, April 2000. ISBN 92-837-1032-0.

[96] T. Tinga, W.B. de Wolf, W.P.J. Visser, and S. Woldendorp. Integrated lifing analysis of a film-cooled turbine blade. NLR Technical Publication NLR-TP-2001-402, National Aerospace Laboratory NLR, 2001. Also available at `http://hdl.handle.net/10921/783`.

[97] E. L. Suarez, M. J. Duffy, D. Seto, and S. M. Cote. Advanced life prediction systems for gas turbine engines. In *Proceedings of the 39th Joint Propulsion Conference and Exhibit*, number AIAA 2003-4985 in AIAA/ASME/SAE/ASEE, Huntsville, Alabama, July 2003. American Institute of Aeronautics and Astronautics.

[98] E. Suarez, J. Hansen, M. Duffy, and P. Gatlin. New approach to tracking engine life. In *Proceedings of the 33rd Joint Propulsion Conference and Exhibit*, number AIAA 1997-2900 in AIAA/ASME/SAE/ASEE. American Institute of Aeronautics and Astronautics, July 1997.

[99] P. P. Walsh and P. Fletcher. *Gas turbine performance*. Blackwell Science, Oxford, 2nd edition, 2004. Also available at `http://www.knovel.com/knovel2/Toc.jsp?BookID=1382`.

[100] A. S. Haslam. Mechanical design of turbomachinery. Course Notes MSc Thermal Power, 2009.

[101] Rubini. Turbine blade cooling. MSc Course Lecture Notes, Cranfield University, 2008.

[102] J.H. Horlock. Heat exchanger performance with water injection (with relevance to evaporative gas turbine (EGT) cycles). *Energy Conversion and Management*, 39(16-18):1621–1630, 1998.

[103] D. G. Ainley. Internal air-cooling for turbine blades: A general design survey. Technical report, Aeronautical Research Council (Great Britain), 1957.

[104] M. J. Holland and T. F. Thake. Rotor blade cooling in high pressure turbines. *Journal of Aircraft*, 17(6):412–418, June 1980.

[105] S. Consonni. *Performance Prediction of GasSteam Cycles for Power Generation*. PhD thesis, Mechanical and Aerospace Engineering Dept., Princeton University, Princeton, NJ, 1992. No. 1893- T.

[106] J.B. Young and R.C. Wilcock. Modeling the air-cooled gas turbine: Part 1 - General thermodynamics. *Journal of Turbomachinery*, 124(2):207–213, 2002.

[107] J.B. Young and R.C. Wilcock. Modeling the air-cooled gas turbine: Part 2 - Coolant flows and losses. *Journal of Turbomachinery*, 124(2):214–221, 2002.

[108] L. Torbidoni and J.H. Horlock. A new method to calculate the coolant requirements of a high-temperature gas turbine blade. *Journal of Turbomachinery*, 127(1):191–199, 2005.

[109] J.H. Horlock, D.T. Watson, and T.V. Jones. Limitations of gas turbine performance imposed by large turbine cooling flows. *Journal of Engineering for Gas Turbines and Power*, 123(3):487–494, 2001.

[110] M.J. Jones, S.J. Bradbrook, and K. Nurney. A preliminary engine design process for an affordable capability. In *Reduction of Military Vehicle Acquisition Time and Cost through Advanced Modelling and Virtual Simulation RTO-MP-089*, RTO AVT Symposium, Paris, France, April 2002. NATO RTO.

[111] A.O. Abu, W. Eshati, P. Laskaridis, and R. Singh. Aero-engine turbine blade life assessment using the neu/sehitoglu damage model. *International Journal of Fatigue*, 61:160 – 169, 2014. Available online at: `http://www.sciencedirect.com/science/article/pii/S0142112313003307`.

[112] P. Alia. Sensitivity of turbine blade materials to thermomechanical fatigue using a simplified model of a turbine blade. MSc, School of Engineering, Cranfield University, Cranfield, Bedfordshire, UK, Sept. 2012.

[113] R. D. Schaufele. *The Elements of Aircraft Preliminary Design*. Aries Publications, 2000.

[114] J. Markish. Valuation techniques for commercial aircraft program design. Master's thesis, MIT, June 2002.

[115] S. Sefarty. Engine operating cost reduction An OEM perspective. In *IATA Executive financial summit*, 2007.

[116] M. C. Dixon. The maintenance costs of aging aircraft: Insights from commercial aviation. Monograph, RAND Corporation, 2006.

[117] M. C. Dixon. *The Costs of Aging Aircraft: Insights from Commercial Aviation*. PhD thesis, Pardee RAND Graduate School., 2005.

[118] D. J. Pickerell. The design of future commercial propulsion systems for minimum direct operating cost. In *Key trends in airworthyness, maintenance and related economics*, pages 4.1–4.27. The Royal Aeronautical Society (RAeS), Nov. 1988.

[119] P. Duplace. How to compare two engines? In *Financing, managing and maintaining engines: Roundtable Summit for financiers*. CFMI, Airfinance Journal `http://www.airfinancejournal.com/`, May 2008.

[120] F-X. Hussenet. The CFM solution. In *Financing & Investing in Engines: Roadshow*, New York, USA, April 2007. CFMI, Airfinance Journal `http://www.airfinancejournal.com/`.

[121] J. Chausse. Building and maintaining engine value. In *Financing & Investing in Engines: Roadshow*, New York, USA, April 2007. GE - Aviation, Airfinance Journal `http://www.airfinancejournal.com/`.

[122] J. Marrero. Study into the maintenance costs of aero engines. Master's thesis, School of Engineering, Cranfield University, Cranfield, Bedfordshire, UK, September 2010.

[123] G. Poupeau. Direct operating cost estimation for aircraft engines. Master's thesis, School of Engineering, Cranfield University, Cranfield, Bedfordshire, UK, September 2011.

[124] J. Tronchi. Direct operating cost estimation method for civil aircraft engine. MSc, School of Engineering, Cranfield University, Cranfield, Bedfordshire, UK, Sept. 2012.

[125] J. J. Eden, D.C.Ae., Dipl.Ing., B.Sc.(Int.), A.F.R.Ae.S., P.Eng., and M.C.A.I. Overhaul life development and early failure detection of aircraft gas turbines: A description of the methods by which scheduled and unscheduled engine removals may be minimized based on the techniques aded by transcanada airlines for use with rolls-royce tyne, conway and dart engines. *Aircraft Engineering and Aerospace Technology*, 34(10):288–292, 1962. Available online at: `http://www.emeraldinsight.com/10.1108/eb033621`.

[126] W. C. Mentzer. Some economic aspects of transport airplane performance. part i. *Journal of the Aeronautical Sciences*, 7(6):227–234, April 1940.

[127] W. C. Mentzer. Some economic aspects of transport airplane performance. parts ii and iii. *Journal of the Aeronautical Sciences*, 7(7):302–308, May 1940.

[128] G.P. Sallee. Economic effects of propulsion system technology on existing and future transport aircraft. Technical report, American Airlines, Inc., New York, NY, 1974.

[129] W. Port. Formulae for calculation of direct operating costs of civil aircraft. Technical report, Supersonic Transport Committee, Royal Aeronautical Establishment (RAE), UK, 1958.

[130] E. Thomas. ATA direct operating cost formula for transport aircraft. Technical report, Air Transport Association of America (ATA), USA, 1967.

[131] M. R. Hayes. An analysis of standard methods for estimating direct operating costs with reference to V/STOL aircraft. Master's thesis, School of Engineering, Cranfield University, Cranfield, Bedfordshire, UK, 1972.

[132] R. H. Liebeck. Advanced subsonic airplane design and economic studies. Technical report, National Aeronautics and Space Administration (NASA), 1994.

[133] H. Ekstrand, R. Avellán, and T. Grönstedt. Minimizing direct operating costs (DOC) for a small european airline. In *Proceedings of the 18th International Society of Air Breathing Engines (ISABE) Conference*, Beijing, CH, 2007. American Institute of Aeronautics and Astronautics (AIAA). Paper No. ISABE-2007-1105.

[134] M.H. Eres and J.P. Scanlan. A hierarchical life cycle cost model for a set of aero-engine components. In *Collection of Technical Papers - 7th AIAA Aviation Technology, Integration, and Operations Conference*, volume 1, pages 41–46. 2007.

[135] M.A. Burkett. DMTrade - a Rolls-Royce tool to model the impact of design changes and maintenance strategies on lifetime reliability and maintenance cost. *Proceedings of the ASME Turbo Expo*, 2:11–23, 2006.

[136] J-M. Wu, H-F. Zuo, and Y. Chen. An estimation method for direct maintenance cost of aircraft components based on particle swarm optimization with immunity algorithm. *Journal of Central South University of Technology*, 12(2):95–101, 2005.

[137] M. Glade, J. Longere, and P. Lyonnet. Design of parametric maintenance cost models. In *International conference on man system and cybernetics*, volume 7, Sept. 2002.

[138] Understanding maintenance costs for new and existing aircfraft. *Airline fleet & asset management*, 2001(5):56–62, September - October 2001.

[139] P. R. Lacey. Uses and misuses of CAB Form 41 data in determination of airplane operating economics. In *Transportation Research Circular*, pages 4–5. Transportation Research Board, DC, USA, Jan 1981. No. 239.

[140] G. G. Hildebrandt and M-B. Sze. An estimation of USAF aircraft operating and support cost relations. Note, RAND Corporation, 1990.

[141] Protecting the asset: maintenance reserves and redelivery conditions. *Airline fleet & network management.*, 2006(5):60–62, September - October 2006.

[142] R.H. Liebeck and Lewis Research Center. *Advanced Subsonic Airplane Design & Economic Studies*. National Aeronautics and Space Administration, Lewis Research Center, 1995.

[143] Cost estimation BEA technical notes. Technical report, British European Airways (BEA), UK, 1971.

[144] Assessing engine maintenance costs - there's more to it than meets the eye. *Airline fleet & asset management*, 2001:40–47, Jan - Feb 2001.

[145] R. Pyles. Aging aircraft: Implications for programmed depot maintenenace and engine support costs. Statement of Dr. Raymond A. Pyles before the

procurement subcommittee of the house armed services committee., Feb 1999. CT-149.

[146] J. S. Litt and E. M. Aylward. Adaptive detuning of a multivariable controller in response to turbofan engine degradation. NASA/TM 2003-212723, National Aeronautics and Space Administration, Glenn Research Center, October 2003. ARL-TR-3091. Available online at: http://gltrs.grc.nasa.gov.

[147] G.P. Sallee. Performance deterioration based on existing (historical) data; JT9D jet engine diagnostics program, 1978. Available online at: http://ntrs.nasa.gov/archive/nasa/casi.ntrs.nasa.gov/19800013837.pdf.

[148] Our Consultancy Philosophy. Technical report, JetEngine Consulting, 2006.

[149] C. Justin and D. N. Mavris. Option-based approach to value engine maintenance cost guarantees and engine maintenance contracts. In *AIAA Aviation Technology, Integration, and Operations Conference*, 2011.

[150] M. Kang, S. Ogaji, P. Pilidis, and C. Kong. An approach to maintenance cost estimation for aircraft engines. In *ASME Turbo Expo 2008: Power for Land, Sea, and Air*, pages 71–79. American Society of Mechanical Engineers, 2008.

[151] Owners & operators guide: CFM56-7B. *Aircraft Commerce*, 58, June/July 2008. Ref number: 36582705. Also available at http://www.aircraft-commerce.com.

Appendix A

Workscoping model detail

A.1 Inputs

A.1.1 Maintenance Actions

Restoration actions

A restoration maintenance input block as that shown in Listing A.1 must be defined for each restoration action. Each block should be numbered sequentially as `REST(n)` where `n` is the block number. Restoration items are assigned a name through the `REST(n).type` item. This name is displayed on the summary output files and should be meaningful and declared as a string.

Listing A.1: Example of restoration maintenance item input block

```
1  REST(n).type = 'restoreName';
2  REST(n).isLinkedWith.type = ;
3  REST(n).isLinkedWith.rule = ;
4  REST(n).manHours.shop = ;
5  REST(n).manHours.subcontract = ;
6  REST(n).materials.dollars = ;
7  REST(n).subContract.dollars = ;
```

The cost for each restoration maintenance item is defined in terms of labour

(`REST(n).manHours`), materials (`REST(n).materials.dollars`) and subcontracted work (`REST(n).subcontract.dollars`). The labour inputs are further subdivided into `shop` and `subcontract` items.

Life Limited Part (LLP)

LLP input block like that the example in Listing A.2 are assigned individual sequential numbers `LLP(n)` and a name through the `LLP(n).moduleName` item. This name is displayed in the summary output and also used to link LLP actions with restoration actions where desired.

Listing A.2: Example of LLP maintenance item input block

```
1  LLP(n).moduleName='LLPname';
2  LLP(n).replacementCost.dollars=;
3  LLP(n).lifeLimit.cycles=;
```

A.2 Case Inputs

Engine

The `Engine` input block defined the deterioration intervals and margins applied to an engine case. An input file can have several `Engine` blocks, each must be assigned a reference number `Engine(n)` and name using the `Engine(n).type` item. Different options are available for defining deterioration rates these are described later under section A.3.

Listing A.3: Example of `Engine` input block with “book” deterioration inputs

```
1  Engine(n).type = 'name';
2  Engine(n).rating.lbs = ;
3  Engine(n).EGT(1).OATdegC=;
4  Engine(n).EGT(1).margin=;
5  Engine(n).EGT(2).OATdegC=;
6  Engine(n).EGT(2).margin= ;
7  Engine(n).EGT(1).deterioration=[ , , ];  ...
8  Engine(n).EGT(2).deterioration=[ , , ];  ...
```

Listing A.4: Optional EGTM variation with OAT in `Engine` input block

```
1  Engine(n).EGT(a).varying.OATdegC=[ , , , , ] ;  ...
2  Engine(n).EGT(a).varying.margin=[ , , , , ];  ...
```

Listing A.5: Optional aging input in `Engine` input block

```
1  Engine(n).aging.limits=[, , , ];  ...
```

Case definition

The case definition input block `Inputs` contains a mix of descriptive and functional inputs. The descriptive inputs are used to ensure that the outputs are human readable and ensure that the user has an opportunity to verify their inputs are coherent.

Listing A.6: Case `Inputs` block

```
1  Inputs.mission.EFH.hours=;
2  Inputs.mission.OAT.degreesC=;
3  Inputs.mission.rating.derate=;
4  Inputs.cost.labourRate.dollars=;
5  Inputs.cost.dollars.year=;
6  Inputs.planning.limit.type=;
7  Inputs.planning.limit.rule.max=;
8  Inputs.aging=;
9  Inputs.severity=;
10 Inputs.costAjust=;
11 Inputs.case.engine=;
12 Inputs.case.intervalMargin=;
```

A.3 Performance Restoration Functionality

Restoration maintenance items can be triggered in several ways and is controlled by the `REST(n).isLinkedWith` items in the restoration input block. Three options exist within `islinkedWith`, where `isLinkedWith.rule =`

0 restoration is not linked and only triggered by an exhausted performance margin as in Listing A.7. In this case the input `isLinkedWith.type` is not used and can be omitted. The performance margin, and deterioration are defined as part of the `Engine` input block section A.2.

1 links restoration to an LLP replacement action such that when the linked LLP part/module is replaced the restoration action will be included in the same shop visit. The link LLP is selected using the name string of the desired LLP module set in the LLP input block as `LLP(n).moduleName` as the `isLinkedWith.type` parameter.

2 links the restoration to a specific shop visit in two possible ways. The link is selected using the `isLinkedWith.type` using the number of the related shop visit such that where `isLinkedWith.type`:

a restoration item will occur only on shop visit number **a**

-a restoration item will occur at all shop visits other than **a**

Listing A.7: Example of un-linked performance based restoration item

```
1  REST(n).type = 'restorePerf';
2  REST(n).isLinkedWith.rule = 0;
```

This functionality has been developed to be representative of current maintenance trends.

Some restoration is only possible on module tear-down. As module tear-down can be expensive in terms of time and materials, in some engines module tear-down only takes place on LLP replacement. When this is the case, costs associated with the restoration can be attributed to restoration rather than LLP change by using the `isLinkedWith LLP` rule described above. In the presented in Listing A.8, `'restoreHPT'` will only occur when LLP module `'hpt'` is replaced.

Listing A.8: Example of restoration `isLinkedWith` a given `LLP`

```
1  REST(n).type = 'restoreHPT';
2  REST(n).isLinkedWith.type = 'hpt';
3  REST(n).isLinkedWith.rule = 1;
```

Some engine maintenance specifications distinguish between “new” and “mature” restoration tasks and costs. When this is the case using the `isLinkedWith SV` rule described above can be useful. Definitions of “new” and “mature” vary for example “new” could be either (a) the first shop visit or (b)the first shop visit at which restoration takes place. When

(a) restoration at the first shop visit is different to restoration at subsequent shop visits, the `isLinkedWith SV` functionality should be implemented for two `REST(n)` items as in Listing A.9 and Listing A.10.

(b) where restoration “maturity” is determined by the first shop visit at which restoration occurs, a first workscoping run should be conducted using `isLinkedWith.rule = 0` to identify the shop visit number `n` at which restoration occurs, and a second workscoping run should be conducted using two `REST` blocks with `isLinkedWith.rule = 2` setting `isLinkedWith type ... = n` or `= −n`. Because this is a two-step implementation, it is not at present usable when the workscoping model is operating in case mode.

Listing A.9: Example of restoration `isLinkedWith` a given `SV`

```
1  REST(n).type = 'restoreNew';
2  REST(n).isLinkedWith.type = 1;
3  REST(n).isLinkedWith.rule = 2;
```

Listing A.10: Example of restoration `isLinkedWith` all but a given `SV`

```
1  REST(n).type = 'restoreMature';
2  REST(n).isLinkedWith.type = -1;
3  REST(n).isLinkedWith.rule = 2;
```

Where restoration is triggered by performance deterioration two options are available:

1. if "book" restoration is applied the Exhaust Gas Temperature Margin (EGTM) and deterioration rates are inputs to the `Engine` data block for both `first-run` and `mature run engines`. Each EGTM is defined by a margin and a temperature at which that margin applies. The effect of Outside Air Temperature (OAT) varying EGTM can be captured either by the inclusion of varying margins for different temperatures or can be calculated by the workscoping code assuming a standard variation of 3.2$^{\circ}C$ margin per $^{\circ}C$ OAT change.

2. alternately, performance interval margin can be calculated externally using Hanumanthan's [18] aging method and input as a comma separated list of intervals (in FH). It is essential that at least one more interval in input in this case than the maximum number of shop visits set in the `Inputs.planning.limit.rule` block.

Appendix B

Engine Maintenance Cost Working Group (EMCWG) cost models

B.1 Shop Visit (SV)

$$\text{Shop material cost} = \text{Maturity factor} * \text{Severity Factor} * (\$/EFH) \tag{B.1}$$

$$\text{Shop labour cost} = \text{Labour rate} * \text{Shop labour factor} * \text{Number of engines} \tag{B.2}$$

$$\text{Shop visit rate}(SVR) = (\text{Number of shop visits}/\text{Total engine flying hours}) * 1000 \tag{B.3}$$

$$\text{Mature shop visit rate} = SVR * \text{Severity Factor} \tag{B.4}$$

B.2 Life Limited Parts (LLPs)

These methods asses the attribution of cost for each LLP set replacement.

Required inputs:

Calculation Period $Tcalculation$(years) - usually 25 years is used

Spare Allocation $frac_{spare}$(%) usually 15%

Stub time $frac_{stub}$(%) usually 10%

Utilisation FH/y (flying hours per year) usually 3180 hours per year

LLP set life $Life_{LLP}$ (Flight Cycles (FCs))

LLP set cost C_{set} ($)

Cycle Flying Hours (FH) to calculate EFH/EFC

Engine Maintenance Cost Working Group (EMCWG) Hourly Method assumes the LLPs are fully capitalised when the engine is new and that LLPs have residual value proportional to stub life upon retirement of the engine.

Engine usable time T_{usable} is calculated, using

$$T_{usable} = Life_{LLP} * EFH/EFC * (1 - frac_{stub})$$

Utilisation of engine accounting for spare use,

$$T_{utilised} = FH/y/(1 + frac_{spare})$$

Retirement of initial LLP set will occur after $T_{retirement}$ years use

$$T_{retirement} = T_{usable}/T_{utilised}$$

Number of sets required for calculation period

$$N_{sets} = Tcalculation/T_{retirement} - 1$$

Total engine hours expected during calculation period

$$T_{EFH} = Tcalculation * T_{utilised}$$

Total cost of LLP sets

$$TC_{LLP} = N_{sets} * C_{set}$$

Hourly Cost of LLP distributed over calculation period $(\$/EFH)$

$$HC_{LLP}^{hourlymethod} = TC_{LLP}/T_{EFH}$$

EMCWG Cyclic Cost method considers that the initial LLP set is not fully capitalised and aims to calculate the cost of LLP usage for the purpose of establishing the correct LLP reserve.

$$HC_{LLP}^{cyclicmethod} = \frac{C_{set}}{(1 - frac_{stub}) * Life_{LLP}} * \frac{1}{EFH/EFC}$$

This results in a cost per engine flying hour that can be significantly different to that derived using the hourly method.

Appendix C

Initial verification Cases

Engine Base Information				Engine Severity Factors Table						Engine LLPs		
Base Point :	1.000	First-Run RSVR:	0.0500	FL	0%	5%	10%	15%	20%	Module	Cost	FC Limit
Rating :	27,00 Lbs	Mature-Run RSVR :	0.0625	1.0	1.850	1.750	1.650	1.550	1.450	FAN	$400K	30,000
Annual FH :	3,000	First-Run Rest $:	$1.6M	1.5	1.350	1.250	1.200	1.150	1.100	HPC	$500K	20,000
Annual FL :	2.0	Mature-Run Rest $:	$1.8M	2.0	1.100	1.050	1.000	0.950	0.850	HPT	$500K	20,000
Derate :	10%	Environment	Factor	2.5	0.980	0.930	0.880	0.830	0.780	LPT	$600K	25,000
Environment :	Temperate	Temperate	**1.000**	3.0	0.900	0.850	0.800	0.780	0.735			
		Hot / Dry	**1.100**	3.5	0.825	0.800	0.775	0.750	0.725			
		Erosive	**1.200**	4.0	0.800	0.775	0.750	0.725	0.715			

Table C.1: Case engine metrics reproduced from Ackert [14, p.23]

C.1 Restoration interval verification

C.1.1 Input Blocks

Listing C.1: Engine Input Block minDet

```
1  Engine(1).type = 'minDet';
2  Engine(1).rating.lbs = 27000;
3  Engine(1).EGT(1).OATdegC=0;
4  Engine(1).EGT(1).margin=85;
5  Engine(1).EGT(2).OATdegC=0;
6  Engine(1).EGT(2).margin=85;
7  Engine(1).EGT(1).deterioration=[1000, 10, 0.004];
8  Engine(1).EGT(2).deterioration=[1000, 10, 0.004];
```

Listing C.2: Engine Input Block maxDet

```
1  Engine(2).type = 'maxDet';
2  Engine(2).rating.lbs = 27000;
3  Engine(2).EGT(1).OATdegC=0;
4  Engine(2).EGT(1).margin=85;
5  Engine(2).EGT(2).OATdegC=0;
6  Engine(2).EGT(2).margin=85;
7  Engine(2).EGT(1).deterioration=[1000, 15, 0.005];
8  Engine(2).EGT(2).deterioration=[1000, 15, 0.005];
```

C.1.2 Results

The results for “maxDet” case are presented in Listing 6.3.

Listing C.3: Results minDet with 10000FC Build Goal

```
ENGINE SPEC
-----------------------------------
type      ::            minDet
rating    ::       27000 lbs
-----------------------------------
MISSION
-----------------------------------
EFH:EFC   ::         2.00
-----------------------------------
Planning Mode
-----------------------------------
Rule      ::       buildGoal
Limit     ::           10000
(SV)      ::               4
-----------------------------------

MAINTENANCE PLAN
-------------------------------------------------------------------------------------
SHOP VISIT                          1            2            3            4
-------------------------------------------------------------------------------------
Trigger                    deterioration   Build Goal          HPC   Build Goal
Elapsed Engine Cycles           19750        29750        39750        49750
Elapsed Interval Cycles         19750        10000        10000        10000
-------------------------------------------------------------------------------------
FAN                                 0       400000            0            0
HPC                            500000            0       500000            0
HPT                            500000            0       500000            0
LPT                            600000            0       600000            0
-------------------------------------------------------------------------------------
firstRun                       1600000            0            0            0
matureRun                            0      1800000      1800000      1800000
-------------------------------------------------------------------------------------
Restoration Cost     ($)       1600000      1800000      1800000      1800000
LLP Cost             ($)       1600000       400000      1600000            0
-------------------------------------------------------------------------------------
Shop Visit Cost      ($)       3200000      2200000      3400000      1800000
-------------------------------------------------------------------------------------
Restoration DMC ($/EFH)          40.51        90.00        90.00        90.00
LLP DMC         ($/EFH)          40.51        20.00        80.00         0.00
Shop DMC        ($/EFH)          81.01       110.00       170.00        90.00
-------------------------------------------------------------------------------------

MAINTENANCE SUMMARY
-----------------------------------
Useable Engine Life  FC      59750
-----------------------------------
Restoration Cost     ($)     7000000
LLP Cost             ($)     3600000
-----------------------------------
Shop Visit Cost      ($)    10600000
-----------------------------------
Restoration DMC ($/EFH)          58.58
Shop DMC        ($/EFH)          88.70
-----------------------------------
```

C.2 Through life maintenance case

The through life maintenance verification case chosen is that presented by Ackert as Example 8 Scenario B, and is reproduced in Figure C.1 However, this case

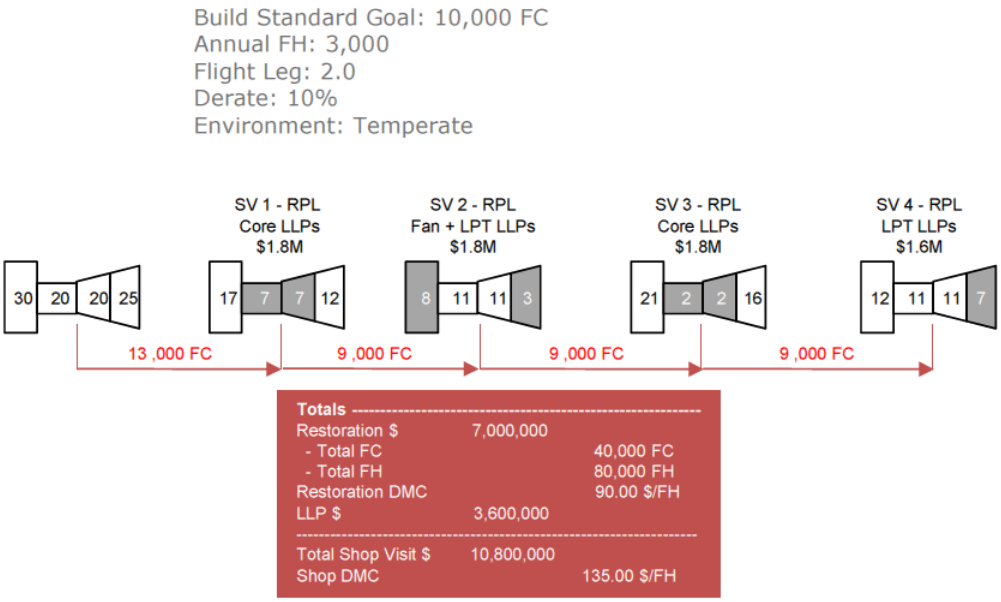

Figure C.1: Through life maintenance case benchmark reproduced from Ackert [14, p.27]

description is noted to contain a few typographical errors:

- The case description prescribes a 10,000FC build goal whereas the case demonstration result describes a case with a 9,000 FC build Goal.
- Ackert [14, p.23] establishes that the minimum Time On Wing (TOW) due to performance deterioration is 15,000 FC. Whereas the case demonstration uses 13,000 FC as the initial performance drive shop visit interval.
- The case demonstration has inverted the restoration costs applied to the first and final shop visits when compared with the engine metric definition Table C.1

- The total shop visit cost is shown as $10,800,000 whereas the sum of the Life Limited Part (LLP) and restoration costs is actually $10,600,000

Correcting these typographical errors leads to two possible cases with 10,000 and 9,000 FC build goals respectively. The corrected benchmark results for these cases are presented in Figure C.2 and Figure C.3.

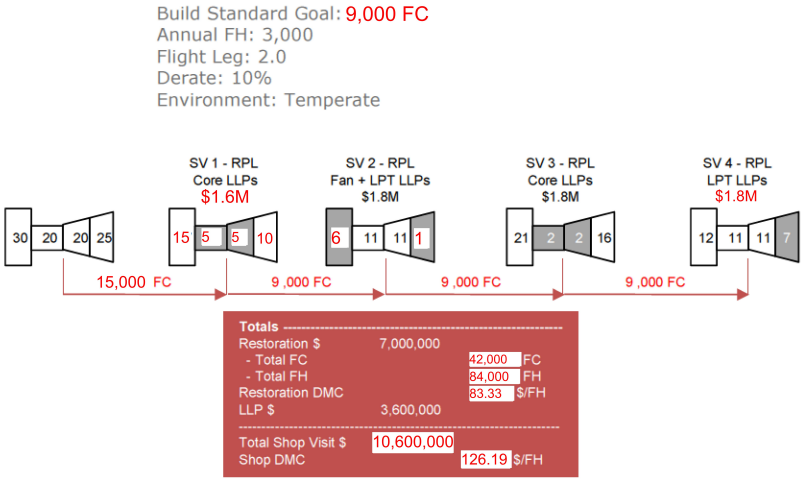

Figure C.2: 9000 FC build goal

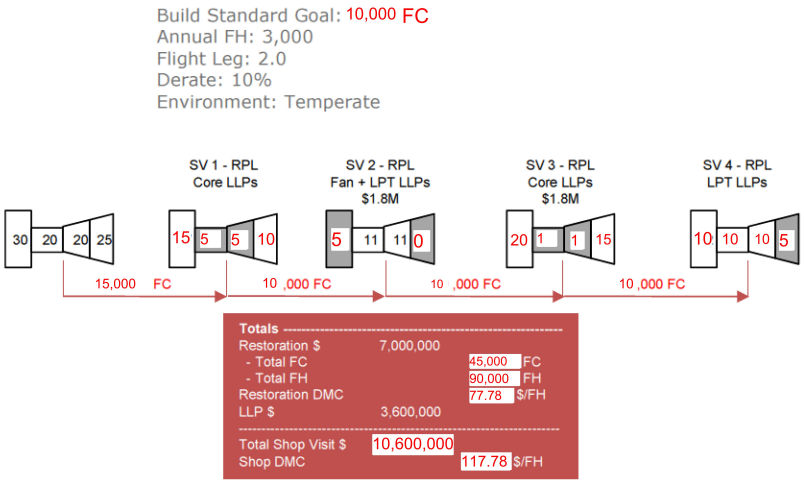

Figure C.3: 10000 FC build goal

C.2.1 Results

Listing C.4: Results maxDet with 9000FC Build Goal

ENGINE SPEC

type	maxDet
rating	27000 lbs

MISSION

EFH:EFC	2.00

Planning Mode

Rule	buildGoal
Limit	9000
(SV)	4

MAINTENANCE PLAN

SHOP VISIT	1	2	3	4
Trigger	deterioration	Build Goal	Build Goal	Build Goal
Elapsed Engine Cycles	15000	24000	33000	42000
Elapsed Interval Cycles	15000	9000	9000	9000
FAN	0	400000	0	0
HPC	500000	0	500000	0
HPT	500000	0	500000	0
LPT	0	600000	0	600000
firstRun	1600000	0	0	0
matureRun	0	1800000	1800000	1800000
Restoration Cost ($)	1600000	1800000	1800000	1800000
LLP Cost ($)	1000000	1000000	1000000	600000
Shop Visit Cost ($)	2600000	2800000	2800000	2400000
Restoration DMC ($/EFH)	53.33	100.00	100.00	100.00
LLP DMC ($/EFH)	33.33	55.56	55.56	33.33
Shop DMC ($/EFH)	86.67	155.56	155.56	133.33

MAINTENANCE SUMMARY

Useable Engine Life FC	51000
Restoration Cost ($)	7000000
LLP Cost ($)	3600000
Shop Visit Cost ($)	10600000
Restoration DMC ($/EFH)	68.63
Shop DMC ($/EFH)	103.92

The results for the 10,000 FC case are listed in Listing 6.3

C.3 Build Goal Cases

Listing C.5: Maintenance summaries for minDet engine with varying build goals (Part 1)

ENGINE TYPE		minDet	minDet	minDet	minDet
PLANNING RULE		buildGoal 5000 4	buildGoal 6000 4	buildGoal 7000 4	buildGoal 8000 4
Number of Shop Visits		4	4	4	4
OAT	degC	0	0	0	0
Useable Engine Life	FC	39750	43750	47750	51750
Restoration Cost	($)	7000000	7000000	7000000	7000000
LLP Cost	($)	2000000	3000000	3600000	3600000
Shop Visit Cost	($)	9000000	10000000	10600000	10600000
Restoration DMC	($/EFH)	88.05	80.00	73.30	67.63
Shop DMC	($/EFH)	113.21	114.29	110.99	102.42

Listing C.6: Maintenance summaries for minDet engine with varying build goals (Part 2)

ENGINE TYPE		minDet	minDet	minDet	minDet
PLANNING RULE		buildGoal 9000 4	buildGoal 10000 4	buildGoal 11000 4	buildGoal 12000 4
Number of Shop Visits		4	4	4	4
OAT	degC	0	0	0	0
Useable Engine Life	FC	55750	59750	63750	67750
Restoration Cost	($)	7000000	7000000	7000000	7000000
LLP Cost	($)	3600000	3600000	6000000	6000000
Shop Visit Cost	($)	10600000	10600000	13000000	13000000
Restoration DMC	($/EFH)	62.78	58.58	54.90	51.66
Shop DMC	($/EFH)	95.07	88.70	101.96	95.94

Listing C.7: Maintenance summaries for maxDet engine with varying build goals (Part 1)

ENGINE TYPE		maxDet	maxDet	maxDet	maxDet
PLANNING RULE		buildGoal 5000 4	buildGoal 6000 4	buildGoal 7000 4	buildGoal 8000 4
Number of Shop Visits		4	4	4	4
OAT	degC	0	0	0	0
Useable Engine Life	FC	35000	39000	43000	47000
Restoration Cost	($)	7000000	7000000	7000000	7000000
LLP Cost	($)	2000000	3000000	3000000	3000000
Shop Visit Cost	($)	9000000	10000000	10000000	10000000
Restoration DMC	($/EFH)	100.00	89.74	81.40	74.47
Shop DMC	($/EFH)	128.57	128.21	116.28	106.38

Listing C.8: Maintenance summaries for maxDet engine with varying build goals (Part 2)

ENGINE TYPE		maxDet	maxDet	maxDet	maxDet
PLANNING RULE		buildGoal 9000 4	buildGoal 10000 4	buildGoal 11000 4	buildGoal 12000 4
Number of Shop Visits		4	4	4	4
OAT	degC	0	0	0	0
Useable Engine Life	FC	51000	55000	59000	63000
Restoration Cost	($)	7000000	7000000	7000000	7000000
LLP Cost	($)	3600000	3600000	6000000	6000000
Shop Visit Cost	($)	10600000	10600000	13000000	13000000
Restoration DMC	($/EFH)	68.63	63.64	59.32	55.56
Shop DMC	($/EFH)	103.92	96.36	110.17	103.17

Appendix D

Lower Thrust Engine Verification Cases

D.1 Workscoping inputs

All inputs for these cases are from Aircraft Commerce and are set in 2006 Dollars. Seven maintenance actions (Life Limited Part (LLP) and restoration) are considered.

D.1.1 LLP definitions

Nineteen life limited part types are distributed into three LLP sets are considered, one high pressure core set, a fan & booster set and an Low Pressure Turbine (LPT) set.

Listing D.1: The fan & booster LLP set inputs

```
1 LLP(1).moduleName='fan&booster';
2 LLP(1).replacementCost.dollars=305000;
3 LLP(1).lifeLimit.cycles=30000;
```

Listing D.2: The core LLP set inputs accounting for components in the HPC and HPT

```
1 LLP(2).moduleName='hpc&hpt';
2 LLP(2).replacementCost.dollars=755000;
3 LLP(2).lifeLimit.cycles=20000;
```

Listing D.3: The LPT LLP set inputs

```
1 LLP(3).moduleName='lpt';
2 LLP(3).replacementCost.dollars=485000;
3 LLP(3).lifeLimit.cycles=25000;
```

D.1.2 Restoration actions

Four restoration actions are implemented, they are each linked with a relevant LLP action such that :

- replacement of the fan and booster LLP set triggers fan and booster overhaul (Listing D.7)
- replacement of the core LLP set triggers core overhaul (Listing D.5)
- replacement of the LPT LLP set triggers LPT overhaul (Listing D.6)

Additionally a lower level of core restoration (Listing D.4) is completed at each shop visit that the core is not overhauled.

Listing D.4: The core restoration inputs

```
1  REST(1).type = 'restoreHP';
2  REST(1).isLinkedWith.LLP = 'hpc&hpt';
3  REST(1).isLinkedWith.rule = 0;
4  REST(1).manHours.shop = 1500;
5  REST(1).manHours.subcontract = 1500;
6  REST(1).materials.dollars = 550000;
7  REST(1).subContract.dollars = 100000;
```

Listing D.5: The core overhaul inputs

```
1  REST(2).type = 'overhaulHp';
2  REST(2).isLinkedWith.LLP = 'hpc&hpt';
3  REST(2).isLinkedWith.rule = 1;
4  REST(2).manHours.shop = 1500;
5  REST(2).manHours.subcontract = 2000;
6  REST(2).materials.dollars = 550000;
7  REST(2).subContract.dollars = 300000;
```

Listing D.6: The LPT overhaul inputs

```
1  REST(3).type = 'overhaulLpt';
2  REST(3).isLinkedWith.LLP = 'lpt' ;
3  REST(3).isLinkedWith.rule = 1;
4  REST(3).manHours.shop = 325;
5  REST(3).manHours.subcontract = 750;
6  REST(3).materials.dollars =100000 ;
7  REST(3).subContract.dollars = 50000;
```

Listing D.7: The fan & booster overhaul inputs

```
1  REST(4).type = 'overhaulf&b';
2  REST(4).isLinkedWith.LLP = 'fan&booster';
3  REST(4).isLinkedWith.rule = 1;
4  REST(4).manHours.shop = 250;
5  REST(4).manHours.subcontract = 150;
6  REST(4).materials.dollars = 50000;
7  REST(4).subContract.dollars = 20000;
```

D.1.3 Engine definitions

Four engine types are defined in terms of rating, Outside Air Temperature (OAT) margin and book deterioration profiles.

Listing D.8: E1 definition

```
Engine(1).type = 'B1';
Engine(1).rating.lbs = 18500;
Engine(1).EGT(1).OATdegC=30;
Engine(1).EGT(1).margin=115 ;
Engine(1).EGT(2).OATdegC=30;
Engine(1).EGT(2).margin=90 ;
Engine(1).EGT(1).deterioration=[5000, 7.5, 0.0015];
Engine(1).EGT(2).deterioration=[2000, 9, 0.003];
```

Listing D.9: E2 definition

```
Engine(2).type = 'B1&C1';
Engine(2).rating.lbs = 20000;
Engine(2).EGT(1).OATdegC=30;
Engine(2).EGT(1).margin=90 ;
Engine(2).EGT(2).OATdegC=30;
Engine(2).EGT(2).margin=80 ;
Engine(2).EGT(1).deterioration=[5000, 8.75, 0.0015];
Engine(2).EGT(2).deterioration=[2000, 14, 0.003];
```

Listing D.10: E3 definition

```
Engine(3).type = 'B2&C1';
Engine(3).rating.lbs = 22000;
Engine(3).EGT(1).OATdegC=30;
Engine(3).EGT(1).margin=60 ;
Engine(3).EGT(2).OATdegC=30;
Engine(3).EGT(2).margin=40 ;
Engine(3).EGT(1).deterioration=[5000, 5, 0.0024];
Engine(3).EGT(2).deterioration=[2000, 16, 0.004];
```

Listing D.11: E4 definition

```
Engine(4).type = 'C1';
Engine(4).rating.lbs = 23500;
Engine(4).EGT(1).OATdegC=30;
Engine(4).EGT(1).margin=40 ;
Engine(4).EGT(2).OATdegC=30;
Engine(4).EGT(2).margin=30 ;
Engine(4).EGT(1).deterioration=[4000, 11, 0.003];
Engine(4).EGT(2).deterioration=[2000, 18, 0.004];
```

D.2 Aging Verification Case Results

Listing D.12: Maintenance Summary E1 20 OAT

RUN SUMMARY tputCaseE1VarOAT20

ENGINE SPEC

type	::	B1
rating	::	18500 lbs

MISSION

EFH:EFC	::	1.40
OAT	::	20 degreesC

MAINTENANCE PLAN

SHOP VISIT	1	2	3	4
Trigger	hpc&hpt	lpt	fan&booster	fan&booster
Elapsed Engine Cycles	20000	25000	30000	35000
Elapsed Interval Cycles	20000	5000	5000	5000
fan&booster	0	0	305000	305000
hpc&hpt	755000	0	0	0
lpt	0	485000	485000	485000
restoreHP	0	860000	860000	860000
overhaulHp	1095000	0	0	0
overhaulLpt	0	225250	225250	225250
overhaulf&b	0	0	98000	98000
Restoration Cost ($)	1095000	1085250	1183250	1183250
LLP Cost ($)	755000	485000	790000	790000
Shop Visit Cost ($)	1850000	1570250	1973250	1973250
Restoration DMC ($/EFH)	39.11	155.04	169.04	169.04
LLP DMC ($/EFH)	26.96	69.29	112.86	112.86
Shop DMC ($/EFH)	66.07	224.32	281.89	281.89

MAINTENANCE SUMMARY

Useable Engine Life	FC	40000
Restoration Cost	($)	4546750
LLP Cost	($)	2820000
Shop Visit Cost	($)	7366750
Restoration DMC	($/EFH)	81.19
Shop DMC	($/EFH)	131.55

Listing D.13: Maintenance Summary E3 35 OAT

RUN SUMMARY CaseE3VarOAT35

ENGINE SPEC

type	::	B2&C1
rating	::	22000 lbs

MISSION

EFH:EFC	::	1.40
OAT	::	35 degreesC

MAINTENANCE PLAN

SHOP VISIT	1	2	3	4
Trigger	hpc&hpt	deterioration	deterioration	deterioration
Elapsed Engine Cycles	20000	24000	28000	32000
Elapsed Interval Cycles	20000	4000	4000	4000
fan&booster	0	0	305000	305000
hpc&hpt	755000	0	0	0
lpt	0	485000	485000	485000
restoreHP	0	860000	860000	860000
overhaulHp	1095000	0	0	0
overhaulLpt	0	225250	225250	225250
overhaulf&b	0	0	98000	98000
Restoration Cost ($)	1095000	1085250	1183250	1183250
LLP Cost ($)	755000	485000	790000	790000
Shop Visit Cost ($)	1850000	1570250	1973250	1973250
Restoration DMC ($/EFH)	39.11	193.79	211.29	211.29
LLP DMC ($/EFH)	26.96	86.61	141.07	141.07
Shop DMC ($/EFH)	66.07	280.40	352.37	352.37

MAINTENANCE SUMMARY

Useable Engine Life	FC	36000
Restoration Cost	($)	4546750
LLP Cost	($)	2820000
Shop Visit Cost	($)	7366750
Restoration DMC	($/EFH)	90.21
Shop DMC	($/EFH)	146.17

D.3 OAT Verification Case Results

Maintenance Summary E1

Listing D.14: Maintenance Summary E1 (Part 1)

CASE RUN SUMMARY CaseE1VarOAT

ENGINE TYPE		B1	B1	B1	B1	B1
ENGINE RATING		18500	18500	18500	18500	18500
		lbs	lbs	lbs	lbs	lbs
Number of Shop Visits		4	4	4	4	4
OAT	degC	0	5	10	15	20
Useable Engine Life	FC	40000	40000	40000	40000	40000
Restoration Cost	($)	4546750	4546750	4546750	4546750	4546750
LLP Cost	($)	2820000	2820000	2820000	2820000	2820000
Shop Visit Cost	($)	7366750	7366750	7366750	7366750	7366750
Restoration DMC	($/EFH)	81.19	81.19	81.19	81.19	81.19
Shop DMC	($/EFH)	131.55	131.55	131.55	131.55	131.55

Listing D.15: Maintenance Summary E1 (Part 2)

ENGINE TYPE		B1	B1	B1	B1
ENGINE RATING		18500	18500	18500	18500
		lbs	lbs	lbs	lbs
Number of Shop Visits		4	4	4	4
OAT	degC	25	30	35	40
Useable Engine Life	FC	40000	40000	40000	40000
Restoration Cost	($)	4546750	4546750	4546750	4546750
LLP Cost	($)	2820000	2820000	2820000	2820000
Shop Visit Cost	($)	7366750	7366750	7366750	7366750
Restoration DMC	($/EFH)	81.19	81.19	81.19	81.19
Shop DMC	($/EFH)	131.55	131.55	131.55	131.55

Maintenance Summary E2

Listing D.16: Maintenance Summary E2 (Part 1)

CASE RUN SUMMARY CaseE2VarOAT

ENGINE TYPE		B1&C1	B1&C1	B1&C1	B1&C1	B1&C1
ENGINE RATING		20000	20000	20000	20000	20000
		lbs	lbs	lbs	lbs	lbs
Number of Shop Visits		4	4	4	4	4
OAT	degC	0	5	10	15	20
Useable Engine Life	FC	40000	40000	40000	40000	40000
Restoration Cost	($)	4546750	4546750	4546750	4546750	4546750
LLP Cost	($)	2820000	2820000	2820000	2820000	2820000
Shop Visit Cost	($)	7366750	7366750	7366750	7366750	7366750
Restoration DMC	($/EFH)	81.19	81.19	81.19	81.19	81.19
Shop DMC	($/EFH)	131.55	131.55	131.55	131.55	131.55

Listing D.17: Maintenance Summary E2 (Part 2)

ENGINE TYPE		B1&C1	B1&C1	B1&C1	B1&C1
ENGINE RATING		20000	20000	20000	20000
		lbs	lbs	lbs	lbs
Number of Shop Visits		4	4	4	4
OAT	degC	25	30	35	40
Useable Engine Life	FC	40000	40000	40000	40000
Restoration Cost	($)	4546750	4546750	4546750	4546750
LLP Cost	($)	2820000	2820000	2820000	2820000
Shop Visit Cost	($)	7366750	7366750	7366750	7366750
Restoration DMC	($/EFH)	81.19	81.19	81.19	81.19
Shop DMC	($/EFH)	131.55	131.55	131.55	131.55

Maintenance Summary E3

Listing D.18: Maintenance Summary E3 (Part 1)

CASE RUN SUMMARY CaseE3VarOAT

ENGINE TYPE		B2&C1	B2&C1	B2&C1	B2&C1	B2&C1
ENGINE RATING		22000	22000	22000	22000	22000
		lbs	lbs	lbs	lbs	lbs
Number of Shop Visits		4	4	4	4	4
OAT	degC	0	5	10	15	20
Useable Engine Life	FC	40000	40000	40000	40000	40000
Restoration Cost	($)	4546750	4546750	4546750	4546750	4546750
LLP Cost	($)	2820000	2820000	2820000	2820000	2820000
Shop Visit Cost	($)	7366750	7366750	7366750	7366750	7366750
Restoration DMC	($/EFH)	81.19	81.19	81.19	81.19	81.19
Shop DMC	($/EFH)	131.55	131.55	131.55	131.55	131.55

Listing D.19: Maintenance Summary E3 (Part 2)

ENGINE TYPE		B2&C1	B2&C1	B2&C1	B2&C1
ENGINE RATING		22000	22000	22000	22000
		lbs	lbs	lbs	lbs
Number of Shop Visits		4	4	4	4
OAT	degC	25	30	35	40
Useable Engine Life	FC	40000	40000	36000	14583
Restoration Cost	($)	4546750	4546750	4546750	3440000
LLP Cost	($)	2820000	2820000	2820000	0
Shop Visit Cost	($)	7366750	7366750	7366750	3440000
Restoration DMC	($/EFH)	81.19	81.19	90.21	168.49
Shop DMC	($/EFH)	131.55	131.55	146.17	168.49

Maintenance Summary E4

Listing D.20: Maintenance Summary E4 (Part 1)

CASE RUN SUMMARY CaseE4VarOAT

ENGINE TYPE		C1	C1	C1	C1	C1
ENGINE RATING		23500	23500	23500	23500	23500
		lbs	lbs	lbs	lbs	lbs
Number of Shop Visits		4	4	4	4	4
OAT	degC	0	5	10	15	20
Useable Engine Life	FC	40000	40000	40000	40000	40000
Restoration Cost	($)	4546750	4546750	4546750	4546750	4546750
LLP Cost	($)	2820000	2820000	2820000	2820000	2820000
Shop Visit Cost	($)	7366750	7366750	7366750	7366750	7366750
Restoration DMC	($/EFH)	81.19	81.19	81.19	81.19	81.19
Shop DMC	($/EFH)	131.55	131.55	131.55	131.55	131.55

Listing D.21: Maintenance Summary E4 (Part 2)

ENGINE TYPE		C1	C1	C1	C1
ENGINE RATING		23500	23500	23500	23500
		lbs	lbs	lbs	lbs
Number of Shop Visits		4	4	4	1
OAT	degC	25	30	35	40
Useable Engine Life	FC	39000	33666	12333	3000
Restoration Cost	($)	4546750	4693500	3440000	860000
LLP Cost	($)	2820000	3540000	0	0
Shop Visit Cost	($)	7366750	8233500	3440000	860000
Restoration DMC	($/EFH)	83.27	99.58	199.23	204.76
Shop DMC	($/EFH)	134.92	174.69	199.23	204.76

Appendix E

Small Engine Case

E.1 Workscoping model Inputs

All costs in the small engine case are defined in 2008 US Dollars and are sources from Aircraft Commerce [151].

Listing E.1: LLP set inputs

```
1  %there are 18 LLP in the 56-7b27
2  LLP(1).moduleName='fan&lpc';%3LLPs those with shorter lives do not require dissasenbly
3  LLP(1).replacementCost.dollars=356000;%2008 dolalrs US LIST PRICE
4  LLP(1).lifeLimit.cycles=30000;
5
6
7  LLP(2).moduleName='core';%9LLPs HPC and HPT
8  LLP(2).replacementCost.dollars=921000;
9  LLP(2).lifeLimit.cycles=20000;% 6 items 20000 2 times 17300 one item 19200
10
11
12
13 LLP(3).moduleName='lpt';%6LLPs
14 LLP(3).replacementCost.dollars=499000;
15 LLP(3).lifeLimit.cycles=25000;%4 items 25000, 1 item 23900 and one item 16300
```

Listing E.2: Restoration inputs

```
REST(1).type = 'level1Core';
REST(1).isLinkedWith.rule = 0;%TRUE flag this REST() occurs when linked LLP is changed
REST(1).manHours.shop = 3000;
REST(1).manHours.subcontract = 0;
REST(1).materials.dollars = 650000;
REST(1).subContract.dollars = 250000;

REST(2).type = 'level2Core(TopUp)';%TopUps required to Level 1 core
REST(2).isLinkedWith.type = 'core';
REST(2).isLinkedWith.rule = 1;%TRUE flag this REST() occurs when linked LLP is changed
REST(2).manHours.shop = 500;%3500
REST(2).manHours.subcontract = 0;%
REST(2).materials.dollars = 250000;%900
REST(2).subContract.dollars = 150000;%400

REST(3).type = 'level2fan&lpc';
REST(3).isLinkedWith.type = 'fan&lpc' ;
REST(3).isLinkedWith.rule = 1;
REST(3).manHours.shop = 450;
REST(3).manHours.subcontract = 0;
REST(3).materials.dollars =100000 ;
REST(3).subContract.dollars = 40000;

REST(4).type = 'level2lpt';
REST(4).isLinkedWith.type = 'lpt';
REST(4).isLinkedWith.rule = 1;
REST(4).manHours.shop = 900;
REST(4).manHours.subcontract = 0;
REST(4).materials.dollars = 250000;
REST(4).subContract.dollars = 50000;
```

Listing E.3: Engine inputs

```
Engine(1).type = 'B27';
Engine(1).rating.lbs = 27300;
Engine(1).EGT(1).OATdegC=30;
Engine(1).EGT(1).margin=55 ;%
Engine(1).EGT(2).OATdegC=30;
Engine(1).EGT(2).margin=40 ;%39-44
Engine(1).EGT(1).deterioration=[1000, 15, 0.004];
Engine(1).EGT(2).deterioration=[1000, 11, 0.004];
Engine(1).aging.limits=[12906.6, 12608.4, 12299, 12299]
```

Listing E.4: Case inputs

```
Inputs.mission.EFH.hours=1.4;
Inputs.mission.OAT.degreesC=18;
Inputs.mission.rating.derate=10;
Inputs.cost.labourRate.dollars=70;%dollars per hour
Inputs.cost.dollars.year=2008;
Inputs.planning.limit.type='nSV';
Inputs.planning.limit.rule.max=3;
Inputs.aging='aging';%'book'=published book deterioration- or -`aging' inputs from aging model
Inputs.severity=1;
Inputs.costAjust='Sev';%'MatSev','Sev','none'
```

E.2 Results

Listing E.5: Workscoping output for REF case including Maturity

MAINTENANCE PLAN

SHOP VISIT	1	2	3	4
Trigger	deterioration	deterioration	deterioration	deterioration
Elapsed Engine Cycles	6.433000e+003	12678	18744	24494
Elapsed Engine Hours	9006.20	17749.20	26241.60	34291.60
Elapsed Interval Cycles	6.433000e+003	6245	6066	5750
Elapsed Interval Hours	9006.20	8743.00	8492.40	8050.00
fan&lpc	0.00	0.00	0.00	
core	0.00	0.00	921000.00	
lpt	0.00	0.00	0.00	
level1Core	662795.64	980010.90	1082230.31	
level2Core(TopUp)	0.00	0.00	422657.92	
level2fan&lpc	0.00	0.00	0.00	
level2lpt	0.00	0.00	0.00	
Rest Materials Cost ($)	452795.64	770010.90	1259888.23	
Rest Labour Cost ($)	210000.00	210000.00	245000.00	
Restoration Cost ($)	662795.64	980010.90	1504888.23	
LLP Cost ($)	0.00	0.00	921000.00	
Shop Visit Cost ($)	662795.64	980010.90	2425888.23	
Restoration DMC ($/EFH)	73.59	112.09	177.20	
LLP DMC ($/EFH)	0.00	0.00	108.45	
Shop DMC ($/EFH)	73.59	112.09	285.65	

MAINTENANCE SUMMARY

Useable Engine Life	FC	24494
Restoration Cost	($)	3147694.76
LLP Cost	($)	921000.00
Shop Visit Cost	($)	4068694.76
Restoration DMC	($/EFH)	91.79
Shop DMC	($/EFH)	118.65

Listing E.6: Effect of OAT with Arithmetic Materials Costs

OAT	degC	15	18	20	25	30
Severity		0.92	1.00	1.06	1.19	1.20
Rest Mat		none	none	none	none	none
Useable Engine Life	FC	33365	24494	20805	11107	4106
Rest Mterials Cost	($)	3540000.00	3100000.00	3100000.00	2700000.00	2700000.00
Rest Labour Cost	($)	759500.00	665000.00	665000.00	630000.00	630000.00
Restoration Cost	($)	4299500.00	3765000.00	3765000.00	3330000.00	3330000.00
LLP Cost	($)	1776000.00	921000.00	921000.00	0.00	0.00
Shop Visit Cost	($)	6075500.00	4686000.00	4686000.00	3330000.00	3330000.00
Restoration DMC	($/EFH)	92.04	109.79	129.26	214.15	579.29
Shop DMC	($/EFH)	130.07	136.65	160.88	214.15	579.29

Listing E.7: Effect of OAT with Maturity and Severity dependent Materials Costs

OAT	degC	15	18	20	25	30
Severity		0.92	1.00	1.06	1.19	1.20
Rest Mat		MatSev	MatSev	MatSev	MatSev	MatSev
Useable Engine Life	FC	33365	24494	20805	11107	4106
Rest Mterials Cost	($)	2689557.22	2482694.76	2620621.67	2487277.84	2512702.31
Rest Labour Cost	($)	759500.00	665000.00	665000.00	630000.00	630000.00
Restoration Cost	($)	3449057.22	3147694.76	3285621.67	3117277.84	3142702.31
LLP Cost	($)	1776000.00	921000.00	921000.00	0.00	0.00
Shop Visit Cost	($)	5225057.22	4068694.76	4206621.67	3117277.84	3142702.31
Restoration DMC	($/EFH)	73.84	91.79	112.80	200.47	546.71
Shop DMC	($/EFH)	111.86	118.65	144.42	200.47	546.71

Listing E.8: Effect of OAT with Severity dependent Materials Costs

OAT	degC	15	18	20	25	30
Severity		0.92	1.00	1.06	1.19	1.20
Rest Mat		Sev	Sev	Sev	Sev	Sev
Useable Engine Life	FC	33365	24494	20805	11107	4106
Rest Mterials Cost	($)	3270573.51	3100000.00	3283436.15	3218871.01	3233325.60
Rest Labour Cost	($)	759500.00	665000.00	665000.00	630000.00	630000.00
Restoration Cost	($)	4030073.51	3765000.00	3948436.15	3848871.01	3863325.60
LLP Cost	($)	1776000.00	921000.00	921000.00	0.00	0.00
Shop Visit Cost	($)	5806073.51	4686000.00	4869436.14	3848871.01	3863325.60
Restoration DMC	($/EFH)	86.28	109.79	135.56	247.52	672.07
Shop DMC	($/EFH)	124.30	136.65	167.18	247.52	672.07